APPENDIX F

Oil Spill Trajectory Model

CHEVRON CANADA LIMITED WEST FLEMISH PASS EXPLORATION DRILLING PROJECT 2021-2030 19-P-202035

Oil Spill Trajectory and Fate Assessment

Oil Spill Risk Assessment
Chevron Canada Limited
West Flemish Pass
Exploration Drilling Project
2021-2030
19-P-202035
Final
June 25, 2019

www.rpsgroup.com

Document Status

Version	Purpose of document	Authored by	Reviewed by	Approved by	Review date
Final	Oil Spill Trajectory and Fate Assessment: Technical Report	LM, ST, JZ, DT, MM, TT, MF, JD, MH	MH following Chevron review comments	MH	June 25, 2019
Draft	Oil Spill Trajectory and Fate Assessment: Technical Report	LM, ST, JZ, DT, MM, TT, MF, JD, MH	MH	MH	May 28, 2019

Approval for issue

<Original signed by>

Matt Horn 2019-06-25

This report was prepared by RPS Group, Inc. ('RPS') within the terms of its engagement and in direct response to a scope of services. This report is strictly limited to the purpose and the facts and matters stated in it and does not apply directly or indirectly and must not be used for any other application, purpose, use or matter. In preparing the report, RPS may have relied upon information provided to it at the time by other parties. RPS accepts no responsibility as to the accuracy or completeness of information provided by those parties at the time of preparing the report. The report does not take into account any changes in information that may have occurred since the publication of the report. If the information relied upon is subsequently determined to be false, inaccurate or incomplete then it is possible that the observations and conclusions expressed in the report may have changed. RPS does not warrant the contents of this report and shall not assume any responsibility or liability for loss whatsoever to any third party caused by, related to or arising out of any use or reliance on the report howsoever. No part of this report, its attachments or appendices may be reproduced by any process without the written consent of RPS. All enquiries should be directed to RPS.

Prepared by:

RPS Group, Inc.

Lisa McStay, Steven Tadros, Joseph Zottoli, Daniel Torre, Mahmud Monim, Tayebeh Tajalli Bakhsh, Matthew Frediani, Jenna Ducharme

Project Lead & Senior Scientist:
Matt Horn, PhD
Director
55 Village Square Drive
South Kingstown, RI 02879

T 401-789-6224
E matt.horn@rpsgroup.com

Prepared for:

Stantec

Ellen Tracy
Senior Associate, Environmental Management

141 Kelsey Drive
St. John's NL A1B 0L2

T **709 576-1458**
E **Ellen.Tracy@stantec.com**

EXECUTIVE SUMMARY

Study Summary

Oil spill trajectory and fate modelling was performed to support an Environmental Assessment (EA) for the Chevron Canada Limited West Flemish Pass Exploration Drilling Project 2021-2030. Hypothetical releases were modelled at two locations in the West Flemish Pass Project Area, located approximately 375 km northeast of St. John's, Newfoundland. Two hypothetical subsurface blowout scenarios were developed within the Project Area to capture both shallow (500 m) and deep (1,500 m) releases. Releases were modelled as unmitigated subsurface blowouts of West Flemish Pass Light Oil (WFPLO). At the deep site, West Flemish 1, the subsurface blowouts were simulated as continuous 30- and 123- day releases, with a total simulation time of 160 days. At the shallow site, West Flemish 2, the subsurface blowouts were simulated as continuous 27- and 135-day releases, again with a total simulation time of 160 days. The 123- and 135-day releases represent the anticipated time to shut in a well by mobilizing a drilling platform and drilling a relief well, while the 27- and 30-day release represents the successful mobilization and implementation of a capping stack to contain the release. The estimated release rates of hydrocarbons simulated in the subsurface blowout scenario were conservative (i.e., high) based on the current knowledge of the reservoir and other subsurface properties associated with the blowout scenario. In addition, one shorter duration and smaller volume marine diesel batch release was modelled at West Flemish 1.

Study Goals

There were several goals of the modelling study. A stochastic assessment was used to provide an understanding of the probability and minimum time to exposure from unmitigated releases of oil. Separate highly conservative thresholds were investigated for oil on the water surface, concentrations of hydrocarbons in the water column, and oil on shorelines. The goal was to identify the areas that may be susceptible to contamination as well as the associated minimum time to exposure based upon variable environmental conditions (i.e. seasonal and interannual variability was assessed using >100 simulated releases). To conservatively determine the approximate magnitude of potential contamination from a single credible "worst-case" scenario (i.e., with spatially- and temporally-varying concentrations, rather than simply the knowledge of a threshold exceedance), three individual deterministic scenarios were selected from each stochastic simulation to represent 95th percentile maximum potential effects within each environmental compartment. These highly conservative 95th percentile scenarios were identified from the area of surface oil, volume of oil in the water column, and the length of shoreline oiled.

Models

In order to reproduce the dynamic and complex processes associated with deep subsea blowout releases, two models developed and maintained by RPS were used. The near-field model OILMAPDeep was used to characterize the dynamics of the jet and buoyant-plume phases of a subsurface blowout. It contains two sub-models, a plume model and a droplet size model. The plume model predicts the evolution of plume position, geometry, centerline velocity, and oil and gas concentrations until the plume either surfaces or reaches a terminal height, at which point the plume is trapped. The droplet size model was used to characterize the size and distribution of oil droplets, including the associated mass of oil being released at specific water depths, where the oil jet and buoyant plume traps as an intrusion and the droplets rise by buoyancy alone. The output

data from OILMAPDeep was then used to initialize the SIMAP model, which simulated the far-field trajectory, fate, and potential exposure of various environmental compartments within the marine environment following a release.

Geographical Data

Geographical data including habitat mapping and shoreline identification and classification were obtained from multiple data sources. For Canadian areas, province-specific data from the New Brunswick Department of Natural Resources and Nova Scotia Department of Natural Resources were used, as well as high-resolution data covering Canadian shorelines from Environment and Climate Change Canada. For the U.S. shoreline, the U.S. National Oceanic and Atmospheric Administration's Environmental Sensitivity Index and Maine Department of Environmental Protection's Environmental Vulnerability Index were used. Bathymetry was characterized using databases provided by NOAA National Geophysical Data Center and GEBCO (General Bathymetric Chart of the Oceans).

Wind and Currents

Wind data for this study were obtained from the U.S. National Centers for Environmental Prediction (NCEP) Climate Forecast System Reanalysis (CFSR) and Climate Forecast System Version 2 (CFSv2) models. Currents for the North Atlantic region were acquired from the U.S. Navy Global HYCOM (HYbrid Coordinate Ocean Model) circulation model. All data were acquired and used for the period between January 2006 and December 2012. This corresponded with the most recent long term (7 year) reanalysis period, meaning the same code-base (which is updated regularly) was used to drive a hind-cast of the coupled hydrodynamic and wind model. In essence, variability within this dataset would be associated with natural environmental variability and not any changes to the way the met-ocean modelling was conducted.

Stochastic Analysis

A stochastic analysis was conducted for each hypothetical release location, consisting of 171 individual modelled simulations within each stochastic scenario. Each simulation was initialized with a different start date/time between 2006-2012 to sample a range of environmental conditions. The dates and times were selected randomly from within each 14-day interval spanning the entire seven years of data. Results of the stochastic analysis included probability footprints above specified highly conservative thresholds for surface, water column, and shoreline contact and minimum time to oil exposure. Because each set of stochastic simulations spanned seven full years and included the associated seasonal variability, the complete set was referred to as annual summaries. To investigate seasonality, results from stochastic analyses were broken into two seasons depending on the majority of modelled days falling within either ice free conditions (i.e. summer) from May through October or periods with ice-cover (i.e. winter) from November through April.

It is important to note that although large footprints of oil are depicted for stochastic analyses, they are not the expected distribution of oil from any single release. These maps do not provide any information on the quantity of oil in a given area. They simply denote the probability of oil exceeding the specific threshold passing through each grid cell location in the model domain at any point over the entire model duration (160 days), based on the entire ensemble of simulations (171 individual releases). Only probabilities of 1% or greater were included in the map output, as lesser probabilities represent random variability in the set of 171 trajectories. Stochastic maps of water column exposure depict the likelihood that dissolved and total hydrocarbon concentrations are predicted to exceed the identified threshold at any depth within the water column (i.e., vertical maximum).

However, these figures do not specify the depth at which this threshold exceedance occurs and do not imply that the entire water column (i.e., from surface to bottom) will experience a concentration above the identified threshold.

Deterministic Analysis

Representative deterministic scenarios (i.e., single trajectory) were identified from each set of stochastic results of subsurface blowouts. Individual scenarios were selected based upon the size of the surface oil footprint, the concentration of dissolved hydrocarbons in the water column, and the length of shoreline contacted with oil, contingent upon a set of highly conservative socio-economic thresholds:

- Surface oil average thickness >0.04 µm,
- Subsurface (within the water column) dissolved hydrocarbon concentrations >1.0 µg/L,
- Shore oil average concentration >1.0 g/m^2.

The selected cases for deterministic analysis included the identified 95th percentile scenarios for surface oil footprint (by area), water column concentration (by volume), and shoreline oil length predicted to be affected by releases at West Flemish 1 and 2. In addition to these deterministic scenarios, one batch spill of marine diesel was modelled at West Flemish 1 with a release volume of 1,000 L, representing a potential spill that could occur during bunkering operations.

Results

Stochastic results are useful in planning for oil spill response as well as environmental assessments, as they characterize the probability that regions may experience oil exposure above specified thresholds, taking into account the environmental variability that is expected. Many release scenarios were simulated over multiple years to capture the different environmental forcing (e.g., variable wind and current speed and direction) that may be possible. For both release sites, West Flemish 1 and 2, stochastic analyses demonstrated that the highest potential likelihood (>90%) to exceed thresholds of potential surface oil exposure and water column contamination by dissolved hydrocarbons primarily occurred to the east, up to 2,000 km from the release site. In essence, prevailing winds and currents were most likely to force released oil to the east, away from Canadian shorelines. Water column probability footprints were smaller than surface oil footprints, where the probability of threshold exceedance decreased as distance from the release site increased. In nearly all stochastic scenarios, lower probabilities of threshold exceedance are predicted for surface and water column oil contamination to the north and south, while generally <25% of releases have the potential to exceed thresholds >100 km to the west of the Project Area.

Due to the predominantly eastward transport of oil and the distance of West Flemish 1 and 2 to Canadian shorelines (375 km), the average probability of shoreline oiling above the threshold was low, with a maximum probability of 8.7% for a single point. The currents in the region, due primarily to the bathymetric steering along the continental shelf, were predicted to further reduce the potential for Canadian shoreline exposure to oil. As the Labrador Current flows southward along the continental shelf, it transports entrained oil parallel to the coast. However, this trend is generally absent in the surface oil predictions, as wind forcing typically transported oil to the east, further out to sea. Oil that does make its way to Canadian shorelines would likely be patchy and discontinuous due to the considerable weathering that would take place over the span of weeks to months. Predicted minimum time to shoreline threshold exceedance is 10.9-32 days along southeastern Newfoundland

and 50-100 days along the northern shores of the Newfoundland, eastern Gulf of St. Lawrence, and southeastern Labrador.

For most representative credible “worst-case” deterministic scenarios at West Flemish 1 and West Flemish 2, natural degradation processes (evaporation and biological degradation) weathered the majority of oil over the 160-day model simulations. The highly volatile nature and large proportion of lower molecular weight compounds in the WFPLO led to large percentages of evaporated (46-49%) and degraded (28-41%) oil, accounting for >75% of each modelled release. The amount of oil predicted to remain on the water surface or within the water column totaled 1-14%, understanding that entrainment and resurfacing can result in surface and entrained oil “see-sawing” between the two environmental compartments based upon wind/wave conditions on hourly time-scales. Between 3.6-21.2% of oil (predominantly persistent surface oil) was predicted to be transported by winds outside the model domain (to the east) over the 160-day simulation. Shoreline contact made up a very small proportion of released oil for these simulations with a maximum value of 0.4% of the released oil making contact with shorelines and the 95th percentile shoreline-contact cases predicted to have ≤0.1% of the released oil reaching shorelines. Oil transported to the sediment was not a major fate pathway for these completely unmitigated offshore subsurface blowouts with <0.1 percent predicted to settle on sediments. Note that all scenarios assume a completely unmitigated release, which is an unlikely situation, as emergency response tactics would typically be employed in the event of a spill within hours to days of the release.

At West Flemish 1, the 1,000 L marine diesel batch release was predicted to result in a patchy and discontinuous distribution of colorless or silver sheen of oil <0.0001 mm (0.1 µm), where the total area that was predicted to be affected by oil >0.04 µm over the entire 30 day simulation totaled 8 km^2. Due to the small release volume, low entrainment during modelled calm wind conditions, and size of the concentration gridding, predicted concentrations of dissolved or total hydrocarbons in the water column were not predicted to exceed concentrations above the identified threshold (1ppb). Oil was not predicted to reach any shorelines from the modelled batch spill.

Document Summary

This report includes an introduction describing the region, the modelling approach, the methodology, and finally the predicted modelling results of the study. The model results are summarized in figures and tables in the main body of this document, describing the potential for oil exposure on the water surface, within the water column, and along shorelines. This document is broken down into several sections.

- Section 1 – Introduction
- Section 2 – Background and Scenarios, including description of Regional Area and Project Area, modelling approach with the OILMAPDeep and SIMAP models, scenarios, and uncertainty
- Section 3 – Model Input Data
- Section 4 – Model Results, including both stochastic and deterministic oil trajectory and fate simulations
- Section 5 – Discussion and Conclusions
- Section 6 – References

Appendix A – additional information including a detailed description of the OILMAPDeep and SIMAP models, fate processes, and algorithms used.

Contents

Tables

Figures

1 INTRODUCTION

RPS conducted trajectory and fate modelling to support an Environmental Assessment for the Chevron Canada Ltd. West Flemish Pass Exploration Drilling Project 2021-2030. Hypothetical releases were modelled at two locations in the West Flemish Pass Project Area, located approximately 375 km northeast of St. John's, Newfoundland, in water depths of 500 and 1,500 m. Major currents, including the Labrador Current and the Gulf Stream, influence the circulation and biological productivity in this region.

This modelling was conducted to evaluate hypothetical unmitigated release events associated with exploration drilling within the West Flemish Pass release location within Exploration License (EL) 1138. Modelling included large-scale, long-duration, deep-water blowouts of a light crude oil (known as West Flemish Pass Light Oil or WFPLO) from the wellhead at the seafloor and a smaller scale surface batch spill of marine diesel. All release were modelled as completely unmitigated, implying that no response efforts were undertaken during the modelled time period. Three-dimensional (3D) oil spill trajectory and fate modelling and analyses were performed to support evaluation of the potential movement and behavior of oil following hypothetical releases into the Northwest Atlantic Ocean near Newfoundland, with the goal to determine the magnitude and extent of potential for surface oil, subsurface contamination, and shoreline oiling. The nearfield OILMAPDeep blowout model and the far-field Spill Impact Model Application Package (SIMAP) oil trajectory, fate, and potential effects model were used. These state-of-the-art models were developed and are maintained by RPS. This report provides a description of the Project Area, modelled hypothetical release scenarios, an overview of the modelling approach, details about the model input data that were used, and a presentation and discussion of the predicted model results.

2 BACKGROUND AND SCENARIOS

2.1 Project Area

Newfoundland is comprised of a series of islands off the east coast of Canada, and along with Labrador forms the easternmost Canadian province. The relatively shallow waters of the continental shelf extend eastward into the Northwest Atlantic Ocean, up to 500 km off the Newfoundland coast. The hypothetical modelled release location is within the West Flemish Pass Project Area, located approximately 375 km northeast of St. John's, Newfoundland (Figure 2-1). This biologically productive region sits atop substantial petroleum resources, with the Hibernia and White Rose fields approximately 150-200 km to the southwest. Bathymetry within the Project Area ranges between 300 and 2,500 m, however regions within the model domain do exceed 4,500 m deep, in regions such as the Laurentian Basin, Bonnition Basin, and the abyssal plain east of the Flemish Cap. The model domain extends from 42°N to 57°N and 72°W to 28°W, encompassing Canadian, U.S., French, Portuguese (the Azores), Greenland (Denmark), and International waters. This modelled extent is much larger than the Project Area, as hypothetical releases of oil were to be tracked for long periods of time (160 days).

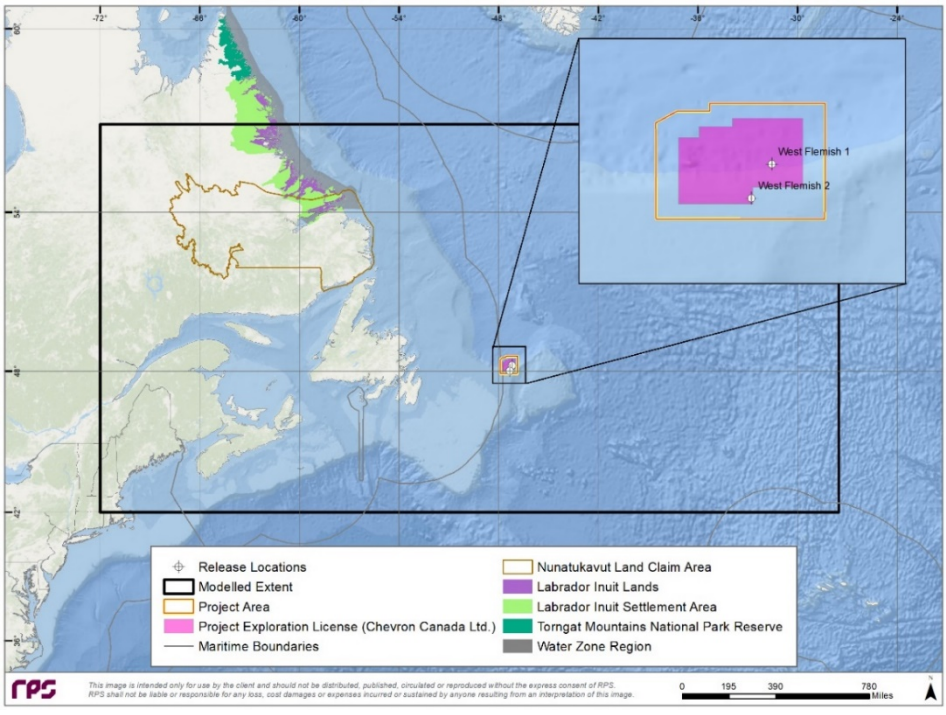

Figure 2-1. Project Area, including the two hypothetical release locations for the subsurface blowouts (West Flemish 1 and West Flemish 2). The black bounding box represents the modelled extent, while the smaller orange box represents the Project Area.

2.2 Modelling Approach

This modelling study employed a combined stochastic and deterministic approach to determine the potential trajectory and fate of hypothetical hydrocarbon releases from two sites east of Newfoundland (Table 2-1). Stochastic modelling provides a probabilistic view of the likelihood that a given region might be exposed to released hydrocarbons over specified thresholds as well as the minimum time it may take for those threshold exceedances. Because stochastic analyses include >100 simulated releases with different start dates throughout a year and over multiple years, they provide a range of possible trajectories based upon variable environmental conditions. Deterministic analyses provide views of the time-history of individual releases including the spatially- and temporally-varying movement and behavior of released oil from specified individual releases (i.e., representative credible "worst cases"). Deterministic scenarios provide an understanding of the predicted spatial and temporal variability in thicknesses, concentrations, and mass within each environmental compartment. Together, these methods provide a more complete view of the likelihood, timing, and degree or magnitude of potential exposure.

Predicted surface oil thickness, dispersed oil in the water column, and shoreline oil mass exceeding specified thresholds for the full year (i.e., annual) are provided along with seasonal breakdowns associated with variable ice-cover conditions (i.e., summer/ice-free and winter/ice-covered). Individual deterministic trajectories that characterize single release scenarios are also presented associated with representative credible "worst-case" scenarios (i.e. 95th percentile "worst-case" for surface oil, subsurface contamination, and shoreline oiling). Stochastic analysis of hypothetical blowouts were modelled using the physical-chemical properties of WFPLO and seven years of variable environmental data, which are discussed further in Section 3. The hypothetical spill sites are located within the West Flemish Pass Project Area (Figure 2-1). A total of 171 individual oil spill trajectories were modelled as unmitigated subsurface releases with randomized start dates/times within each two-week time period making up the seven-years modelled here (Table 2-1). The releases included 82 winter and 89 summer scenarios. The duration of each simulation within the stochastic scenario was 160 days.

In addition, a single representative deterministic release (1,000 L) was analyzed to evaluate a potential discharge of marine diesel on the surface associated with a batch spill that could occur from vessels, unloading hoses, or a tank.

Table 2-1. Site and release information used for the stochastic and deterministic approaches.

Modelling Approach	Release Location	Depth of Release	Release Duration	Model Duration	Number of Simulations	Released Product	Release Type	Release Volume
Stochastic and Deterministic*	West Flemish 1 (48.22°N, 47.18°W)	1,500 m	30 d	160 d	171	WFPLO	Subsurface Blowout	679,200 m^3
			123 d					2,784,720 m^3
	West Flemish 2 (48.02°N, 47.31°W)	500 m	27 d					545,130 m^3
			135 d					2,725,650 m^3
Deterministic	West Flemish 1 (48.22°N, 47.18°W)	Surface	Inst.	30 d	1	Marine Diesel	Surface Batch Spill	1,000 L

*The 95th percentile "worst-case" scenarios for surface, water column, and shoreline were identified from each of the four stochastic scenarios and modelled as three separate deterministic simulations per stochastic scenario.

2.2.1 Modelling Tools

Hypothetical release scenarios were simulated using the OILMAPDeep blowout model and the SIMAP oil trajectory, fate, and effects model, both developed and maintained by RPS. OILMAPDeep was used to define the near-field dynamics of the subsurface blowout plume, which was then used to initialize the far-field modelling conducted in SIMAP. The near-field plume dynamics are modelled to predict the mass, location, and droplet size distribution of the subsurface oil droplets at the termination (i.e., trap) height, where the oil jet and buoyant oil and gas plume are "trapped" and form an intrusion. The depth of the trap height is dependent upon the environmental conditions, the specific chemical and physical properties of the oil, and other release parameters. Typically, the near-field model considers timescales of seconds and length scales of hundreds of meters, whereas the far-field model considers many days and months (at 30 minute time steps) and length scales of tens, hundreds, and even thousands of kilometers.

OILMAPDeep Model

The OILMAPDeep model incorporates the basic dynamics of a subsurface oil and gas plume and the associated complexities of increased hydrostatic pressure at depths deeper than 200 m. It contains two sub-models, a plume model and a droplet size model. The plume model predicts the evolution of the plume position, geometry, centerline velocity, and oil and gas concentrations until the plume either surfaces or reaches a terminal height (i.e., trap height). During a subsea blowout in deep water, an oil jet and buoyant plume carries oil and gas upwards to a water depth (or depths) where, due to the ambient density gradient in the ocean, the buoyant plume is arrested, or "trapped" and forms an intrusion (Socolofsky et al. 2011, 2015). Oil droplets are released from the intrusion to the water column above, where they subsequently rise (buoyancy) and are

transported by ambient currents. The trap height is typically a few hundred meters above the release depth (Socolofsky et al. 2015). The jet created by the blowout is modelled by considering the momentum of the oil discharge, the density difference between the expanding gas bubbles in the plume and the receiving water, the entrainment of water into the plume, the mixing by turbulence within the plume, the hydrate formation, and the transport by local ambient currents. The droplet size model predicts the size and volume (mass) distribution of the oil droplets in the release at the trap height or at the water surface, which influences trajectory and fate processes, such as oil rise velocity and dissolution.

For oil discharged during a deep-water blowout, the oil droplet size distribution profoundly effects how oil is transported and behaves after the initial release as a buoyant plume. The size of the individual droplets dictates buoyancy, which controls rise rate and the associated length of time that oil will remain within the water column before surfacing. Large oil droplets surface faster than small ones, thus large droplets more quickly generate a floating oil slick, which may be transported by winds and surface currents. Small droplets remain in the water column longer than large droplets (due to less buoyancy and increased drag) and are subjected to subsurface advection-diffusion processes. The small droplets are therefore transported within the water column for a longer period of time. As oil is transported by subsurface currents away from the release location, natural dispersion and degradation of the oil droplets will reduce concentrations within the water column. However, the lower rise velocities associated with smaller oil droplets correspond to longer residence times of oil suspended in the water column, which can increase the dissolution of soluble components and potentially result in larger volumes of water being affected. The surface area to volume ratio of smaller droplets is much larger than that of larger droplets. Therefore, with such a large exchange interface, a larger portion of the soluble fraction of hydrocarbons within the smaller droplets will dissolve into the water column and at a higher rate than that of larger oil droplets. Details of the OILMAPDeep model background theory, inputs, algorithms, and outputs can be found in Appendix A.

SIMAP Model

The SIMAP model is a state-of-the-art oil trajectory, fate, and effects model that was developed by RPS and is constantly being updated/maintained based upon the growing body of field and laboratory data associated with releases of oil in many different environments. The SIMAP model originated from the oil fate sub-model within the Natural Resource Damage Assessment Models for Coastal and Marine Environments (NRDAM/CME). RPS (previously Applied Science Associates) developed the NRDAM/CME in the early 1990s for the U.S. Department of the Interior for use in “type A” Natural Resource Damage Assessment (NRDA) regulations under the Comprehensive Environmental Response, Compensation and Liability Act of 1980 (CERCLA). The most recent version of the type A models, the NRDAM/CME (Version 2.4, April 1996) was published as part of the CERCLA type A NRDA Final Rule (Federal Register, May 7, 1996, Vol. 61, No. 89, p. 20559-20614). The technical documentation for the NRDAM/CME is in French et al. (1996). While the NRDAM/CME was developed for simplified NRDAs of small releases in the U.S., SIMAP was further developed to evaluate fate and exposure of both real and hypothetical releases in marine, estuarine, and freshwater environments worldwide. Additions and modifications to SIMAP include increasing model resolution, allowing site-specific input data, incorporating spatially and temporally varying current data, evaluating subsurface releases and movements of subsurface oil, tracking multiple chemical components of the oil, enabling stochastic modelling, and facilitating analysis of results.

The 3D physical fates model estimates the distribution of whole oil and oil components on the water surface, on shorelines, in the water column, and in sediments as both mass and concentration. Because oil contains many chemicals with varying physical and chemical properties, and the environment is spatially and temporally variable, the oil rapidly separates into different environmental compartments through multiple fate processes. Oil fate processes included in SIMAP are spreading (gravitational and by shearing), evaporation, transport, randomized dispersion, emulsification, entrainment (natural and facilitated by dispersant), dissolution of the soluble fraction of oil into the water column, volatilization of dissolved hydrocarbons from the surface water, adherence of oil droplets to suspended sediments, adsorption of soluble and sparingly-soluble aromatics to suspended sediments, sedimentation, and degradation. Oil trajectory and weathering endpoints include surface oil, emulsified oil (mousse), tar balls, suspended oil droplets, oil adhered to particulate matter, dissolved hydrocarbon compounds in the water column and pore water, and oil on and in bottom sediments and shoreline surfaces. Details of the SIMAP model background theory, inputs, algorithms, and outputs can be found in Appendix A.

2.2.2 Stochastic Approach

A stochastic approach was employed to determine the footprint and probability of areas that are at increased risk of oil exposure based upon the variability of meteorological and hydrodynamic conditions that might prevail during and after a release. A stochastic scenario is a statistical analysis of results generated from many (>100) different individual trajectories of the same release scenario, with each trajectory starting at a randomized time from a relatively long-term window. For this project, individual trajectory start dates were selected randomly every 14 days throughout the window of environmental data coverage (2006-2012) to ensure that the data was adequately sampled. This stochastic approach allowed for the same type of release to be analyzed under varying environmental conditions (e.g., summer vs. winter or one year to the next). The results provide the probable behavior of the potential releases based upon this environmental variability.

To reproduce the natural variability of winds and currents, the model requires both spatially- and temporally-varying datasets. Historical observations and models of multiple-year wind and current records were used to perform the simulations within the coinciding time period. These datasets allow for reproduction of the natural variability of the wind and current speeds and directions. Optimally, the minimum time window for stochastic analysis is at least five years, so that various weather patterns from year to year are represented. Seven years of environmental data were used for this modelling study, including 2006-2012. Using wind and current data from throughout this period, a sufficient number of model simulations will adequately sample the variability in wind and current speeds and directions in the region over time and will result in a prediction of the probable oil pathways for releases at the prescribed location.

Stochastic analyses provide two types of information: 1) the areas associated with the probability of oil exposure at some time during or after a release, and 2) the shortest time required for oil above a specified threshold to reach any point within the modelled areas. The left panel of Figure 2-2 depicts four individual trajectories predicted by SIMAP for a generic example scenario. Because these trajectories were started on different dates and times, they experienced different environmental conditions, and thus traveled in different directions. To compute the stochastic results in this study, 171 individual trajectories were overlaid upon one another, like the four depicted below. The number of times that each given location throughout the modelled domain (i.e. grid cell) was intersected by a trajectory that exceeded the specified threshold was then quantified and used to

calculate the probability of oil exposure for each specific location. This process is illustrated by the stacked simulations in the right panel of Figure 2-2. The predicted footprint is the cumulative oil-exposed area for all of the 171 individual releases combined. The color-coding represents a statistical analysis of all the individual trajectories to predict the probability of oil at each point in space, based upon the environmental variability. The footprint of any single release of oil, be it modelled or real, would likely be much smaller than the cumulative footprint of all the simulations used in the stochastic analysis. Similarly, the footprint of oil from any individual release at a single time step (snapshot in time) would be even smaller than the cumulative swept area depicted here.

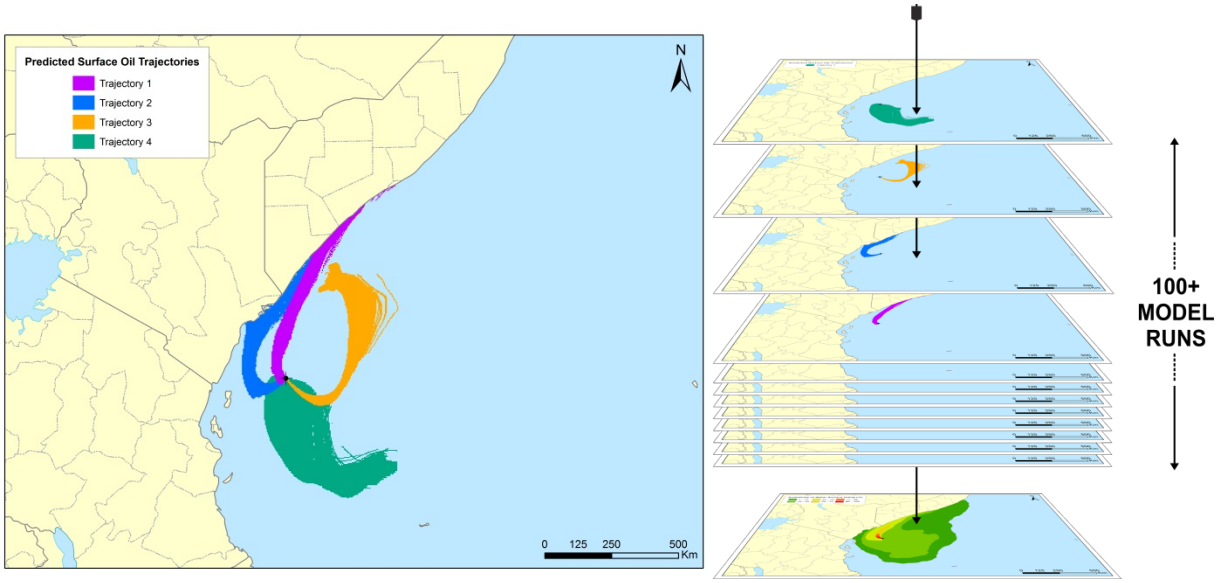

Figure 2-2. Example of four individual release trajectories predicted by SIMAP for a generic release scenario at a generic location simulated with different start dates and therefore environmental conditions. In a stochastic analysis, over one hundred individual trajectories are overlaid (shown as the stacked simulations on the right) and the frequency of threshold exceedance at each location is used to calculate the predicted probability following a release.

The number of individual trajectories and the timeframe of a given stochastic analysis play roles in the spatial extent of the resulting stochastic footprints. More individual simulations may incorporate greater environmental variability, which may result in larger footprints. As the number of trajectories modelled increases, the confidence and resolution of reported probabilities also increase. However, there is a “law of diminishing returns” and thousands of scenarios are not necessary to capture the environmental variability within the system. Annual stochastic model simulations resulted in the largest footprint, encompassing all environmental variability throughout the years. Seasonal footprints may be smaller, encompassing only the environmental variability expected within the smaller time period (e.g., prevailing winds, seasonal patterns, etc.). It is important to note that a single trajectory encounters only a small portion of an overall stochastic probability footprint (i.e., an individual trajectory may be less than 10% of an annual stochastic footprint). Maps of probability and minimum time to oil exceeding identified thresholds are provided in Section 4.1.

2.2.3 Thresholds of Interest

In a stochastic analysis, multiple model simulations (over one hundred releases) are overlaid upon one another to create a cumulative footprint of the potential trajectories. When combined with one another, the many individual deterministic footprints can be used to generate an area of probability that describes the potential areas that may be exposed to oil from the entire suite of modelled conditions. To determine the probability or likelihood of potential exposure, specific thresholds for surface oil thickness, oil on shorelines and sediments, and in-water concentrations were required (Table 2-2). Above these conservative socio-economic thresholds, previous studies identified that there is the potential for negative effects to occur. Figures and further analyses in this study include the more conservative lower socio-economic thresholds of concern calculated from stochastic results. The use of such conservative thresholds serves as more of a binary “yes/no” question of whether any oil passed through each identified area, as opposed to an ecological threshold that may indicate the potential for acute mortality. Should a higher, less conservative stochastic threshold be used (e.g., ecological threshold), the predicted probability footprint would be much smaller.

Floating surface oil is expressed as mass per unit area, averaged over a defined (grid cell) area. If the oil is evenly distributed in that area, it would be equivalent to a mean thickness, where 1 micron (µm) corresponds to a layer of oil that has a mass concentration of approximately 1 g/m^2. Surface oil thickness is typically associated with visual appearance by aerial observation for responders (NRC, 1985; Bonn Agreement, 2009, 2011; NOAA, 2016b; Table 2-3). As an example, barely visible sheens may be observed above 0.04 µm and silver sheens correspond with surface oil thickness of approximately 0.3 µm. Crude and heavy fuel oils greater than 1 mm thick typically appear as black oil, while light fuels and diesels that are greater than 1 mm thick may appear brown or reddish. Because of the differences between oils and their degree of weathering, as well as the weather conditions and sea state at the time of observations, floating oil will not always have the same appearance. As oil weathers, it may be observed in the form of scattered floating tar balls and tar mats where currents converge. Typically, oil slicks in the environment would be observed as patchy and discontinuous with a range of visual appearances including silver sheen, rainbow sheen, and metallic areas simultaneously, as a combination of thicknesses may be present (Table 2-3). Thus, a model result presented as average oil mass per unit area or “thickness” is actually a region with patches of oil of varying thickness, which when distributed evenly in the area of interest, would be on average a certain thickness.

Table 2-2. Thresholds used to define areas and volumes exposed above levels of concern.

Threshold Type	Cutoff Threshold*	Rationale/Comments (Socio-economic, Response, Ecological)	Visual Appearance	References
Oil Floating on Water Surface	0.04 g/m^2 (0.04 µm on average over grid cell)	**Socio-economic:** A conservative threshold used in several risk assessments to determine effects on socio-economic resources (e.g., fishing may be prohibited when sheens are visible on the sea surface). Socio-economic resources and uses that would be affected by floating oil include commercial, recreational and subsistence fishing; aquaculture; recreational boating, port concerns such as shipping, recreation, transportation, and military uses; energy production (e.g., power plant intakes, wind farms, offshore oil and gas); water supply intakes; and aesthetics.	Fresh oil at this minimum threshold corresponds to a slick being barely visible or scattered sheen (colorless or silvery/grey), scattered tarballs, or widely scattered patches of thicker oil.	French McCay et al., 2011; French McCay et al., 2012; French McCay, 2016; Lewis, 2007, Bonn Agreement
	10 g/m^2 (10 µm on average over grid cell)	**Ecological:** Mortality of birds on water has been observed at and above this threshold. Sublethal effects on marine mammals, sea turtles, and floating Sargassum communities are of concern.	Fresh oil at this threshold corresponds to a slick being a dark brown or metallic sheen.	French et al., 1996; French McCay, 2009 (based on review of Engelhardt, 1983, Clark, 1984, Geraci and St. Aubin 1988, and Jenssen 1994 on oil effects on aquatic birds and marine mammals); French McCay et al., 2011; French McCay et al., 2012; French McCay, 2016
Shoreline Oil	1.0 g/m^2 (1 µm on average over grid cell)	**Socio-economic/Response:** A conservative threshold used in several risk assessments. This is a threshold for potential effects on socio-economic resource uses, as this amount of oil may trigger the need for shoreline cleanup on amenity beaches and affect shoreline recreation and tourism. Socio-economic resources and uses that would be affected by shoreline oil include recreational beach and shore use, wildlife viewing, nearshore recreational boating, tribal lands and subsistence uses, public parks and protected areas, tourism, coastal dependent businesses, and aesthetics.	May appear as a coat, patches or scattered tar balls, stain	French-McCay et al., 2011; French McCay et al., 2012; French McCay, 2016
	100 g/m^2 (100 µm on average over grid cell)	**Ecological:** This is a screening threshold for potential ecological effects on shoreline flora and fauna, based upon a synthesis of the literature showing that shoreline life has been affected by this degree of oiling. Sublethal effects on epifaunal intertidal invertebrates on hard substrates and on sediments have been observed where oiling exceeds this threshold. Assumed lethal effects threshold for birds on the shoreline.	May appear as black opaque oil.	French et al., 1996; French McCay, 2009; French McCay et al., 2011; French McCay et al., 2012; French McCay, 2016
In Water Concentration	1.0 ppb (µg/L) of dissolved PAHs; corresponds to ~100 ppb (µg/L) of whole oil (THC) in the water column (soluble PAHs are approximately 1% of the total mass of fresh oil)	Water column effects for both **ecological** and **socio-economic** (e.g., seafood) resources may occur at concentrations exceeding 1 ppb dissolved PAH or 100 ppb whole oil; this threshold is typically used as a screening threshold for potential effects on sensitive organisms.	N/A	Trudel et al. 1989; French-McCay 2004; French McCay 2002; French McCay et al. 2012

*Thresholds used in supporting stochastic results figures. For comparison, a bacterium is 1-10 µm in size, a strand of spider web silk is 3-8 µm, and paper is 70-80 µm thick. Oil averaging 1 g/m^2 is roughly equivalent to 1 µm.

Table 2-3. Oil Appearances based on NOAA JobAid (2016b) and BAOAC.

Code	Description	Layer-Thickness		Concentration	
		microns (µm)	Inches (in.)	m^3 per km^2	bbl/acre
S	Silver Sheen	0.04 - 0.30	1.6×10^{-6} - 1.2×10^{-5}	0.04 - 0.30	1×10^{-3} - 7.8×10^{-3}
R	Rainbow Sheen	0.30 - 5.0	1.2×10^{-5} - 2.0×10^{-4}	0.3 - 5.0	7.8×10^{-3} - 1.28×10^{-1}
M	Metallic Sheen	5.0 - 50	2.0×10^{-4} - 2.0×10^{-3}	5.0 - 50	1.28×10^{-1} - 1.28
T	Transitional Dark (or true) Color	50 - 200	2.0×10^{-3} - 8×10^{-3}	50 - 200	1.28 - 5.1
D	Dark (or true) Color	> 200	> 8×10^{-3}	> 200	> 5.1
E	Emulsified	Thickness range is very similar to that of dark oil.			

* Chart from Bonn Agreement Oil Appearance Code (BAOAC) May 2, 2006, modified by A. Allen

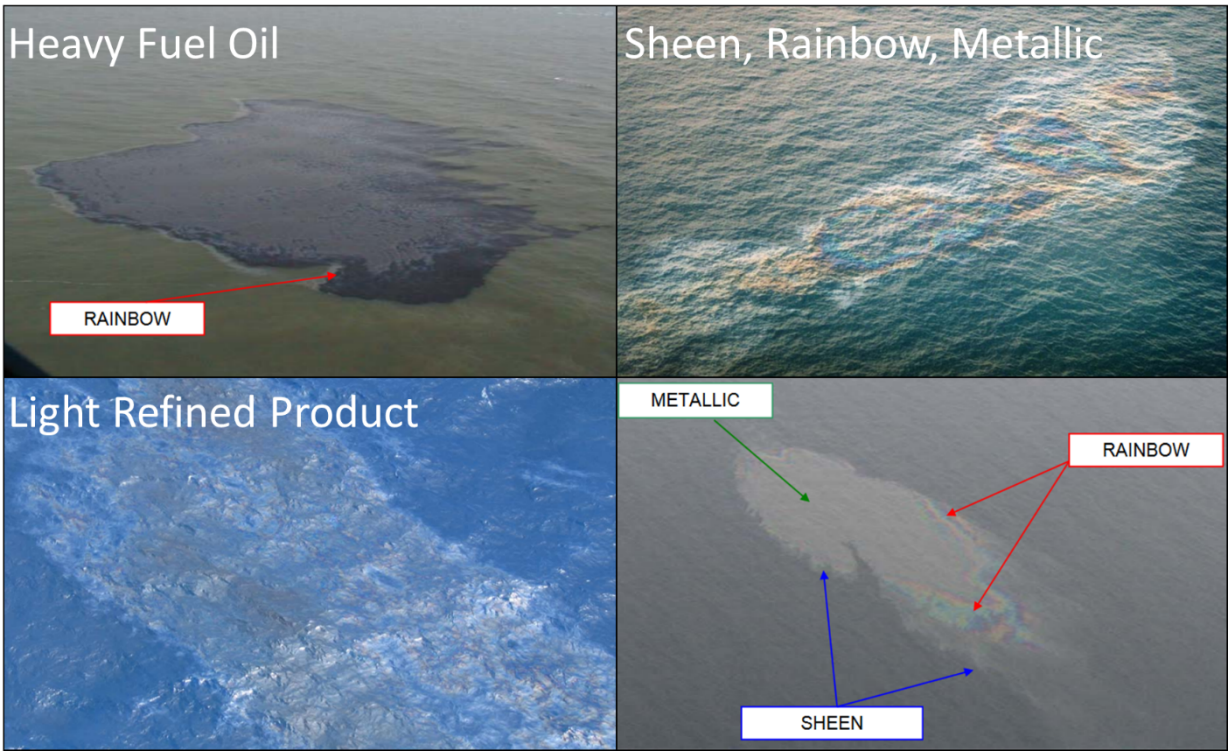

Figure 2-3. Aerial surveillance images of released oil in the environment as examples of different visual appearances based on surface oil thickness and product type (Bonn Agreement, 2011).

2.2.4 Deterministic Approach

Individual trajectories of interest were identified and selected from the stochastic ensemble of results for the deterministic analysis. The deterministic trajectory and fate simulations provided an estimate of the oil's transport and fate through the environment as well as its physical and chemical behavior for a specific set of environmental conditions. While the stochastic analysis provides insight into the probable behavior of oil spills given historic wind and current data for the Project Area, the deterministic analysis provides individual trajectory, oil weathering information, expected concentrations of oil contamination, mass balance, and other information related to a single release at a given location and time.

Each single deterministic simulation within a stochastic analysis represents a specific set of wind and current conditions for the modelled time period. When analyzed together, over one hundred simulations within a stochastic scenario provide a range of expected exposures. The exposures between cases may differ as the trajectory and fate of each individual modelled release is unique. Therefore, the movement and behavior, as well as the resulting areas and magnitudes of predicted contamination for surface, water column, and shoreline oil will be different for each modelled simulation. The 95th percentile "worst-case" exposure for surface, in-water concentration, and shoreline were identified based upon the area, volume, or length of oil that was predicted in each environmental compartment of interest (i.e., water surface area, volume in the water column, or shoreline length).

In addition, a deterministic analysis of a single batch spill release of marine diesel was modelled at the West Flemish Pass 1 with a release volume of 1,000 L. The modelled batch spill volume evaluated a potential discharge on the surface associated with marine diesel spills that could occur from a vessel, unloading hose, or tank. Scenarios were assumed to occur during the calmest wind-speed period during the summer/ice-free conditions, as they would result in the largest amount of oil on the surface. The simulation includes its own spatially and temporally variable trajectory, mass balance, surface oil thickness, in-water concentration of dissolved hydrocarbons, etc. reported individually.

The results of each deterministic simulation provides a time history of the fate and weathering of oil over the duration of the release (mass balance), expressed as the percentage of released oil on the water surface, on the shoreline, evaporated, entrained in the water column, and degraded, as well as the portion that was transported outside of the model domain. In addition, cumulative footprints of the individual trajectories over the course of the entire modelled duration will depict the cumulative path of floating surface oil, the mass of oil on shorelines, and the maximum concentrations of dissolved hydrocarbons in the water column at any instant in time. These results are a way to simplify the 4-dimensional nature of 3D model predictions through time with spatially and temporally variable magnitudes and are presented in figures in Section 4.2.

2.3 Modelled Scenarios

Two hypothetical release locations were used for subsurface blowout modelling, representative of both deep (1,500 m) and shallow (500 m) locations in the West Flemish Pass Project Area (Table 2-1 and Table 2-4). A surface batch spill was also modelled from the deeper West Flemish 1 location. Subsurface blowouts near the seafloor were modelled separately in a stochastic analysis that included 171 individual model simulations per

location per scenario. This analysis investigated the influence of environmental variability throughout the year over multiple years, on the trajectory and fate of released oil (Table 2-4). The estimated volume of hydrocarbons released in the subsurface blowout scenarios represent the best technical estimate of the release rates from the wells. In essence, these blowout rates represent credible “worst-case” release volumes given realistic inputs and hypothetical releases.

Table 2-4. Hypothetical subsurface release location, parameters, and stochastic scenario information.

Scenario Parameter	Release Locations of Subsurface Blowout Scenarios			
Block	EL 1138			
Release Location	West Flemish 1		West Flemish 2	
Latitude	48°13'20" N		48°01'00" N	
Longitude	47°11'00" W		47°18'23" W	
Water Depth of Release	1,500 m		500 m	
Released Product	West Flemish Pass Light Oil (WFPLO)			
Gas to Oil Ratio	1,500 scf/bbl			
Pipe Diameter	21.6 cm (8.5 in.)			
Oil Discharge Temperature	127°C			
Release Duration	30 d	123 d	27 d	135 d
Release Rate	22,640 m^3/d		20,190 m^3/d	
Total Released Volume	679,200 m^3	2,784,720 m^3	545,130 m^3	2,725,650 m^3
Model Duration	160 d			
Number of Simulations within Stochastic Analysis*	171 annual (82 winter & 89 summer) for each scenario			

*A total of 684 individual subsurface releases were modelled within the stochastic analyses.

Table 2-5. Selected representative deterministic scenarios.

Scenario Parameter	Release Parameters for Representative 95th Percentile Deterministic Scenarios											
	30 d Subsurface Release			**123 d Subsurface**			**27 d Subsurface Release**			**135 d Subsurface**		
Representative Scenario	Surface Oil Exposure Area	Water Column Oil Volume	Shoreline Contact Length	Surface Oil Exposure Area	Water Column Oil Volume	Shoreline Contact Length	Surface Oil Exposure Area	Water Column Oil Volume	Shoreline Contact Length	Surface Oil Exposure Area	Water Column Oil Volume	Shoreline Contact Length
Block Release Site	EL 1138 West Flemish 1						EL 1138 West Flemish 2					
Release Type	Subsurface Blowout											
Water Depth of Release	1,500 m						500 m					
Released Product	WFPLO											
Release Duration	30 d			123 d			27 d			135 d		
Release Rate	22,640 m^3/d						20,190 m^3/day					
Total Released Volume	679,200 m^3			2,784,720 m^3			545,130 m^3			2,725,650 m^3		
Model Duration	160 d											
Modelled Start Date and Season	Jan. 17, 2010 Winter	Sep. 8, 2011 Winter	Dec. 25, 2009 Winter	Aug. 16, 2010 Winter	Jun. 1, 2008 Summer	Jan. 7, 2010 Winter	Mar. 3, 2010 Summer	Jun. 21, 2012 Summer	Sep. 13, 2010 Winter	Feb. 8, 2010 Winter	Jan. 17, 2010 Winter	Jul. 26, 2010 Summer

2.4 Model Uncertainty and Validation

The SIMAP model has been developed over several decades to include past and recent information from laboratory-based experiments and real-world releases to simulate the trajectory and fate of discharged oil. However, there are limits to the complexity of processes that can be modelled, as well as gaps in knowledge regarding the affected environment. Assumptions based on available scientific information and professional judgment were made in the development of the model, which represent a best assessment of the processes and potential exposures that could result from oil releases.

The major sources of uncertainty in the oil fate model are:

- Oil contains thousands of chemicals with differing physical and chemical properties that determine their fate in the environment. The model must, out of necessity, treat the oil as a mixture of a limited number of components, grouping chemicals by physical and chemical properties.
- The fate model contains a series of algorithms that are simplifications of complex physical-chemical processes. These processes are understood to varying degrees.
- The model treats each release as an isolated, singular event and does not account for any potential cumulative exposure from other sources.
- Several physical parameters, including but not limited to, hydrodynamics, water depth, total suspended solids concentration, and wind speed were not sampled extensively throughout the entire modelled domain. However, the data that did exist was sufficient for this type of modelling. When data was lacking, professional judgment and previous experience was used to refine the model inputs.

SIMAP has been validated against many real-world releases including the Deepwater Horizon oil spill, where it was used in the US Government's Natural Resource Damage Assessment. In this specific example, a small portion of the released oil may have sunk as a result of the interaction of released oil with sediments, drilling muds, and other material used in response efforts such as procedures used to seal a leaking well. These are currently areas of active research. While there are additional fate processes that may result in slight differences in the ultimate fate of oil, these processes are known to have relatively lower effects on the total volume of oil in each environmental compartment (on the order of single percentages different, depending on the release and receiving environment) as compared to the fate processes such as entrainment, which are already being modelled. The science and algorithms that may be used to model these processes have not been developed in the scientific community to the point of a consensus or use in modelling. Ongoing research topics currently underway include the formation of marine oil snow (MOS), photo-degradation, droplet size distributions, and other research areas. These and other multi-year research projects are considered for incorporation in modelling nearly constantly. Due to these topics being in the research phase, without scientific consensus, they have not been included in this analysis.

In the unlikely event of an actual release of oil, the trajectory and fate will be strongly determined by the specific environmental conditions, the precise location, and a myriad of details related to the event and specific timeframe of the release. Modelled results are a function of the scenarios simulated and the accuracy of the input data used. The goal of this study was not to forecast every detail that could potentially occur, but to

describe a range of possible consequences and exposures of oil releases under various representative release scenarios.

3 MODEL INPUTS DATA

3.1 Oil Characterization

Two hydrocarbon products (WFPLO and Marine Diesel) were modelled for this hypothetical release study. The physical and chemical data used to characterize WFPLO was provided by Chevron Canada Ltd. WFPLO is a light crude oil that has a low viscosity and a high volatile content (Table 3-1 and Table 3-2). Chevron noted that WFPLO is predicted to have a high (94%) maximum water content compared to most oils and specifically other light crudes with similar properties. The high maximum water content of this oil would result in the increased potential to form emulsions, which would rapidly increase the viscosity of the oil. Increased viscosity would be expected to limit entrainment, decrease the rate and extent of spreading, slow weathering processes, and ultimately affect the trajectory and fate of the oil. The characteristics of this oil will provide highly conservative approximations of anticipated surface oil concentrations following a release, as the oil would be more persistent than other light crude oils,

Marine diesel was modelled for the surface batch spill at the West Flemish 1 site. The marine diesel modelled is a standard diesel (light fuel oil with very little residual fraction) that has a low viscosity and high content of volatile hydrocarbons. Thus, marine diesel is expected to weather (i.e. evaporate) rapidly and be nearly completely on the water surface (Table 3-2). The physical and chemical data used to characterize these oils was provided by Chevron Canada, with additional information taken from Environment Canada's oil database (ECCC, 2001).

Table 3-1. Physical properties for the oil products used in the modelling.

Physical Property	WFPLO	Marine Diesel
Density (g/cm^3)	0.825 @16°C	0.83100 @25°C
Viscosity (cP)	4.0 @ 25°C	2.76 @15°
API Gravity	40.0	38.8
Pour Point (°C)	-2.0	-50
Interface Tension (dyne/cm)	30.2	27.5
Emulsion Maximum Water Content (%)	94%	0

Table 3-2. Fraction of the whole oil comprised of different distillation cuts for the modelled oil product. Note that the total hydrocarbon concentration (THC) is the sum of the aromatic (AR) and aliphatic (AL) groups. Numbers of carbons (C#) in the included compounds are listed.

Distillation Cut[1]	Boiling Point (°C)	Description	WFPLO	Marine Diesel
AR1	< 180	highly volatile and soluble monoaromatic hydrocarbons (BTEX[2] and MAHs C6-C9)	3.93	1.93
AR2	180 - 264	semi-volatile and soluble 2-ring aromatics (MAHs and PAHs C10-C12)	1.02	1.14
AR3	265 - 380	low volatility and solubility 3-ring aromatics (PAHs C13-C18)	0.18	1.56
AL1	< 180	highly volatile aliphatics (C4-C8)	17.07	14.46
AL2	180 - 280	semi-volatile aliphatics (C9-C16)	37.28	47.86
AL3	280 - 380	low volatility aliphatics (C17-C23)	3.22	30.32
THC1	< 180	total hydrocarbon fraction 1 (sum of AR1 and AL1)	21.00	16.40
THC2	180 - 280	total hydrocarbon fraction 2 (sum of AR2 and AL2)	38.30	49.01
THC3	280 - 380	total hydrocarbon fraction 3 (sum of AR3 and AL3)	3.40	31.89
Residuals	> 380	aromatics ≥ 4 rings and aliphatics > C20 that are neither volatile nor soluble	37.30	2.70

Numerous data sources and dozens of analyses are used to classify the different chemical and physical characteristics of the oil. As an example, this would include but not be limited to physical testing, distillation studies, weathering studies, measurements of chemicals (e.g. GCMS, PAH, alkanes, saturates, aromatics,

[1] Note that the terms “aromatic” and “aliphatic” are used in a modelling context. “Aromatic” refers to all soluble and volatile hydrocarbons and may include actual aliphatic compounds (by chemical definition) that are soluble. In the modelling context, “aliphatic” refers to insoluble and volatile hydrocarbons. Note that Σ(AR) + Σ(AL) + residuals = Σ(THC) + residual = total hydrocarbon composition

[2] BTEX (benzene, toluene, ethylbenzene, xylene), MAHs (monocylic aromatic hydrocarbons), and PAHs (polycyclic aromatic hydrocarbons) are the more soluble, bioavailable, and potentially toxic components in oil.

resins, asphaltenes, etc.), emulsification studies, degradation studies, etc. All available data is used to classify each oil. When advanced analyses are not available, surrogate oils with more information are used to fill in data gaps and professional judgement and previous experience are used to further refine the oil characterization model inputs.

The “pseudo-component” approach is used to simplify the tracking of thousands of chemicals comprising oil for modelling (Payne et al., 1984; 1987; French et al., 1996; Jones, 1997; Lehr et al., 2000). Chemicals in the oil mixture are grouped by physical-chemical properties, and the resulting component category behaves as if it were a single chemical with characteristics typical of the chemical group. In this component breakdown, aromatic (AR) groups are treated as both soluble (i.e., dissolve into the water column) and volatile (i.e., evaporate to the atmosphere), while the aliphatic (AL) groups are only volatile. The total hydrocarbon concentration (THC) within the boiling range of volatile components is the sum of all AR and AL components. The remainder of the oil is considered to be residual oil, which does not dissolve or volatilize but will degrade over time.

Degradation rates for each component and compartment (surface, upper water column, lower water column, and sediments) were based on biodegradation rates obtained from literature reviews that included estimates for compounds and/or components of crude oil generally (French McCay et al., 2018a: Annex C to Appendix II). For the semi-volatile components, degradation in floating oil would be considerably slower than volatilization. The rates for residual oil are consistent with studies by Zahed et al. (2011) and Atlas and Bragg (2009).

Through the modelled processes, the density and viscosity of the oil tend to increase as the oil weathers. It is possible for the weathered oil, especially in the presence of suspended particulate matter in the water column, to become denser than water and sink. In addition, the oil (including the residual fraction) does continue to degrade over time within the model. In addition, one must consider that the hypothetical long-term releases of oil (many months) continues to add fresh oil, which will increase the total amount of oil through time that will degrade. As time progresses, residual oil is all that remains of the early portions of the release while whole fresh oil continues to be released in later stages. In total, this may appear as though degradation rates are increasing, but it is rather a function of the static degradation rate and the increasing amount of oil (a portion fresh oil) through time.

A recent comprehensive model update with literature review of over a dozen of the most recent studies on oil degradation rates validating the use of modelled SIMAP degradation rates was conducted for work following the Deepwater Horizon Natural Resource Damage Assessment (French et al., 2015) as well as for the United States Bureau of Ocean Energy Management (BOEM) (French McCay et al., 2018b,c).

The long-term weathering and degradability of an oil (including microbial degradation, photo-oxidation, and other processes that may break down compounds or components of oil) may increase the tendency of an oil to sink. These processes are highly dependent upon the type of oil released and the environmental conditions of the receiving environment. A large amount of work is currently being undertaken to develop scientific consensus in this area; however, it is understood that compounds with a boiling temperature >380°C degrade slowly and that these compounds are difficult to measure. The modelled bulk disappearance is quite slow and would conservatively overestimate the effects following a release as oil would remain in the modelled system. The inclusion of compound-specific degradation would increase the degradation and reduce the amount of oil remaining in the model, therefore potentially skewing results towards less effects.

3.2 Geographic and Habitat Data

For geographical reference, SIMAP uses rectilinear grids to designate the location of the shoreline, the water depth (bathymetry), and the shore or habitat type. The grids were generated from a digital shoreline using ESRI geoprocessing and Spatial Analyst Extension tools. The cells were coded for depth and habitat type. Geographical data were obtained from multiple international sources to provide the geographic and environmental information required for modelling (Table 3-3). Habitat data were used to define the bottom type and vegetation found in subtidal areas, areas of extensive mud flats and wetlands, and the shoreline type (e.g., sandy beach, rocky shoreline, etc.).

The SIMAP model used these grids to identify the location of the shoreline and amount of oil that may adhere once oil contacted the shoreline (Figure 3-1). Retention of oil on a shoreline depends on the shoreline type, physical and chemical properties (e.g., viscosity) of the oil, tidal amplitude in estuarine areas, and wave energy. The resolution of the habitat grid was approximately 1.8 km north-south by 2.5 km east-west (0.02225° on each side). Bathymetry data define the water depths within the modelled extent. The General Bathymetric Chart of the Oceans (GEBCO) one arc-minute interval grid was used but was resampled into a grid with the same resolution as the habitat grid (Figure 3-1).

Table 3-3. Sources for habitat, shoreline, and bathymetry data.

Data Type	Data Source	Geographic Location	Reference
Habitat/Shoreline	Environment and Climate Change Canada	Canada	Therrien, A. 2017
	National Oceanic and Atmospheric Administration Environmental Sensitivity Index	United States (except Maine)	NOAA 2016a
	Maine Environmental Vulnerability Index	United States - Maine	MDEP 2016
	New Brunswick Department of Natural Resources	New Brunswick	NBDNR 2013
	Nova Scotia Department of Natural Resources	Nova Scotia	NSDNR 2013
Bathymetry	General Bathymetric Chart of the Oceans Digital Atlas	Global	GEBCO 2003

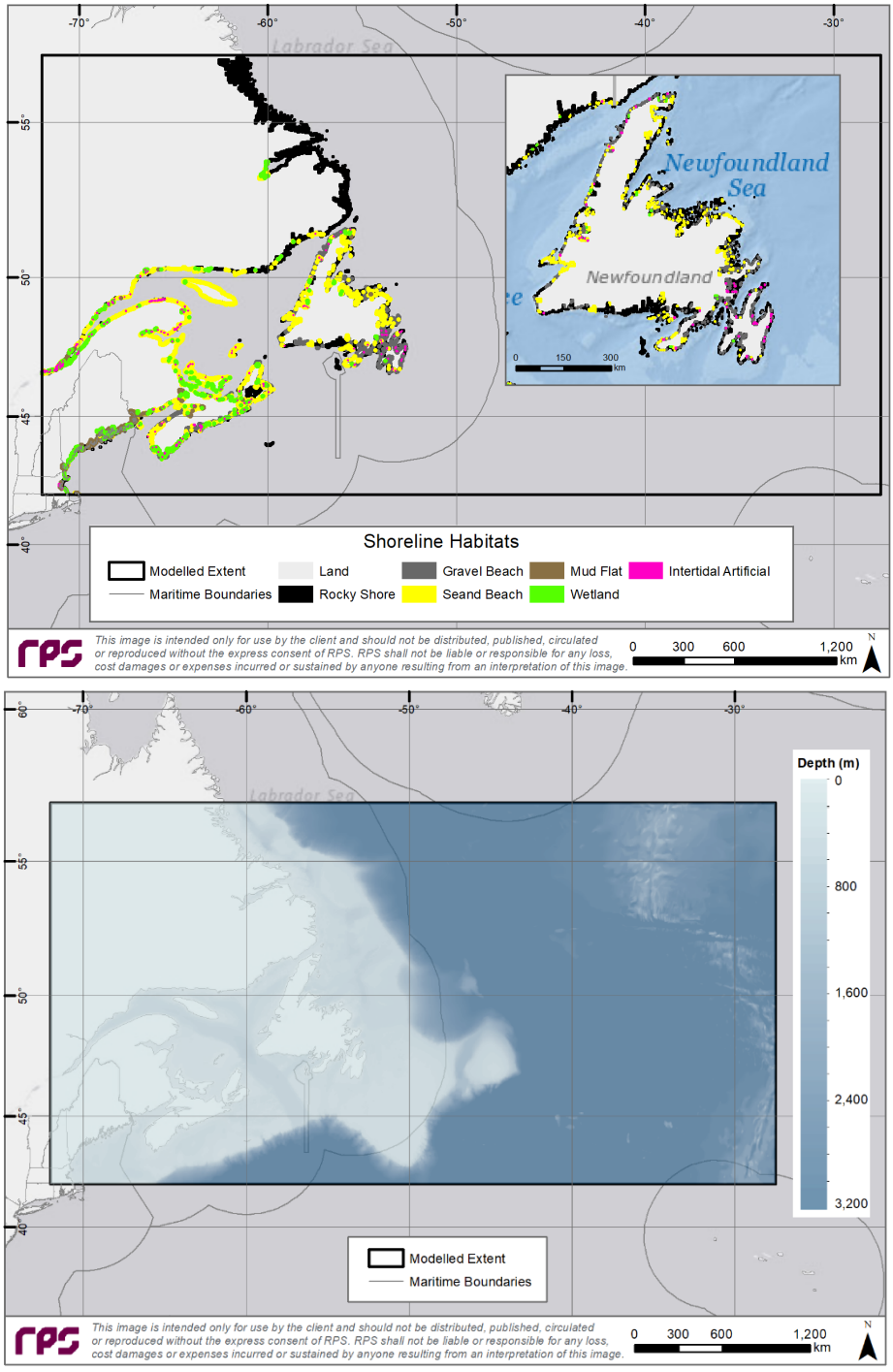

Figure 3-1. Shoreline habitat data (top) and depth (bottom) through modelled domain. The black box represents the modelled extent.

3.3 Ice Cover

Sea-ice is formed in the autumn in the Arctic and sub-Arctic regions of the world. The growth rate of sea-ice depends on surface temperature and the heat flux in the underlying water. The formation and development of sea-ice follows a progression of stages. The exact timing of these stages at any location is not the same from year to year because of subtle differences in climatic conditions. In the Northern Hemisphere during September and October, the air temperature lowers sufficiently to form a thin sheet of ice on the sea surface. The freezing temperature for average ocean salt water with a salinity of 35 parts per thousand (PPT) is about -2°C (NOAA, 2014).

The movement and behavior of released oil is greatly affected by the presence of sea-ice (Figure 3-2). Oil trapped in or under sea-ice will weather more slowly than oil released in open water. Algorithms in SIMAP for modelling the movement and behavior of oil in the presence of sea-ice are based on the percent of ice coverage (also commonly referred to as ice concentration) and an extensive review of the literature (French McCay et al., 2014, French McCay et al., 2016, French McCay et al., 2017a, French McCay et al., 2017b, French McCay et al., 2018a, Wilson et al., 2018). From 0 to ~30% coverage, the sea-ice has no effect on the advection or weathering of surface floating oil. From approximately 30 to 80% ice coverage, oil advection is forced to the right of sea-ice motion in the Northern Hemisphere. Surface oil thickness generally increases due to ice-restricted spreading, and evaporation and entrainment are both reduced by damping/shielding the water surface from wind and waves. Above 80% sea-ice coverage, surface oil moves with the sea-ice, and evaporation and entrainment cease.

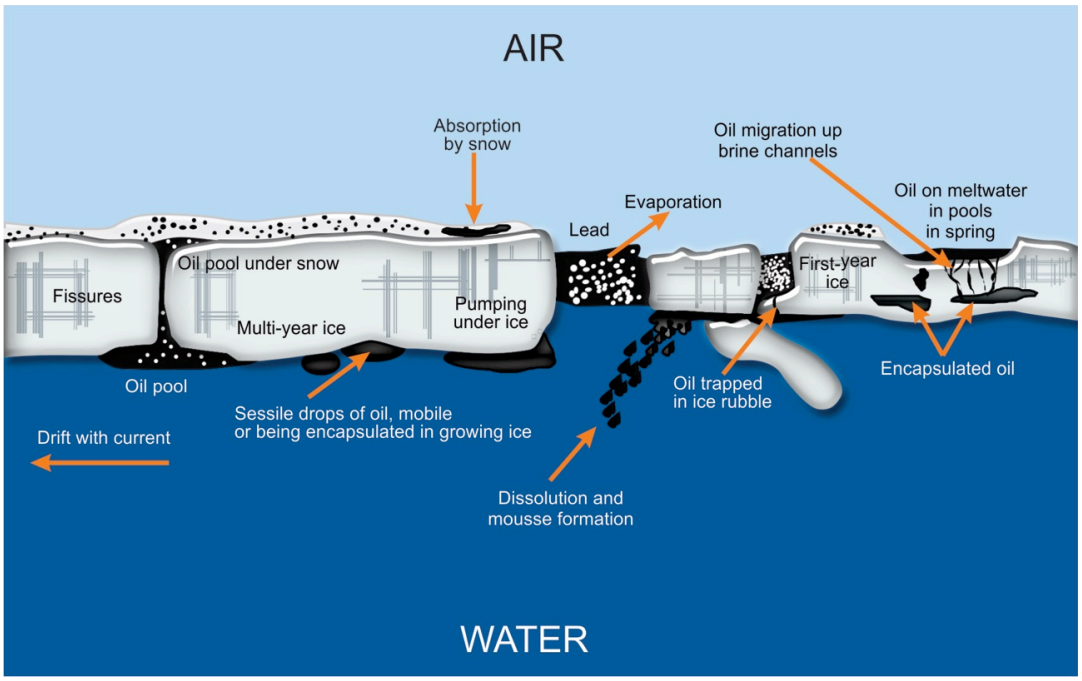

Figure 3-2. Oil and ice interactions at the water surface (RPS 2017, modified by Alan A. Allen from original, DF Dickins Associates Ltd, 2004).

The sea-ice thickness and concentration can vary greatly based upon prevailing weather conditions. If oil is released under sea-ice, water column exposures can be greater, due to the "capping" effect of the ice. Sea-ice cover limits or prevents evaporative losses and could result in substantially greater dissolution of hydrocarbons into the water column.

Sea-ice data used as modelling inputs were obtained from the Canadian Ice Service (CIS; ECCC, 2017) in weekly files spanning from January 2006 to December 2012. These data were in the form of polygon data, with information on total sea-ice concentration and stage of development. For each ice polygon, concentration codes were converted to concentration percentages. Average sea-ice thickness was calculated based on the proportional concentration of the various stages of sea-ice present for each week of the season over seven years. The CIS data provides a range of thicknesses for each sea-ice category and stage of development. In most cases, the mid-point of those ranges was used in the calculation of average sea-ice thickness. If the stage was not identified, but there were concentrations provided, then sea-ice stage was assumed to be first-year medium ice (Table 3-4). The sea-ice data was gridded at a resolution matching the habitat grid (0.02225°). A representative map depicting percentage of sea-ice coverage and thickness for the first week of February 2010 is presented (Figure 3-3).

Table 3-4. Sea-ice thickness used in the modelling characterized by CIS stage of development.

CIS Sea-Ice Category or Sea-Ice Stage	Concentration	CIS Thickness Range (cm)	Model Applied Thickness (cm)
Ice Free	0%	n/a	n/a
Open Water	30%	n/a	50
Land fast Ice	100%	n/a	assumed full water depth
First year thick ice	Total concentration converted from tenths to percent ice cover	> 120	120
First year medium ice*		70 – 120	95
First year thin ice		30 – 70	50
Young ice		10 – 30	20
Grey white ice		15 – 30	22.5
Grey ice		10 – 15	12.5
New ice		< 10	5
Icebergs		unknown	100

*Default sea-ice stage assumed when none was identified in the data.

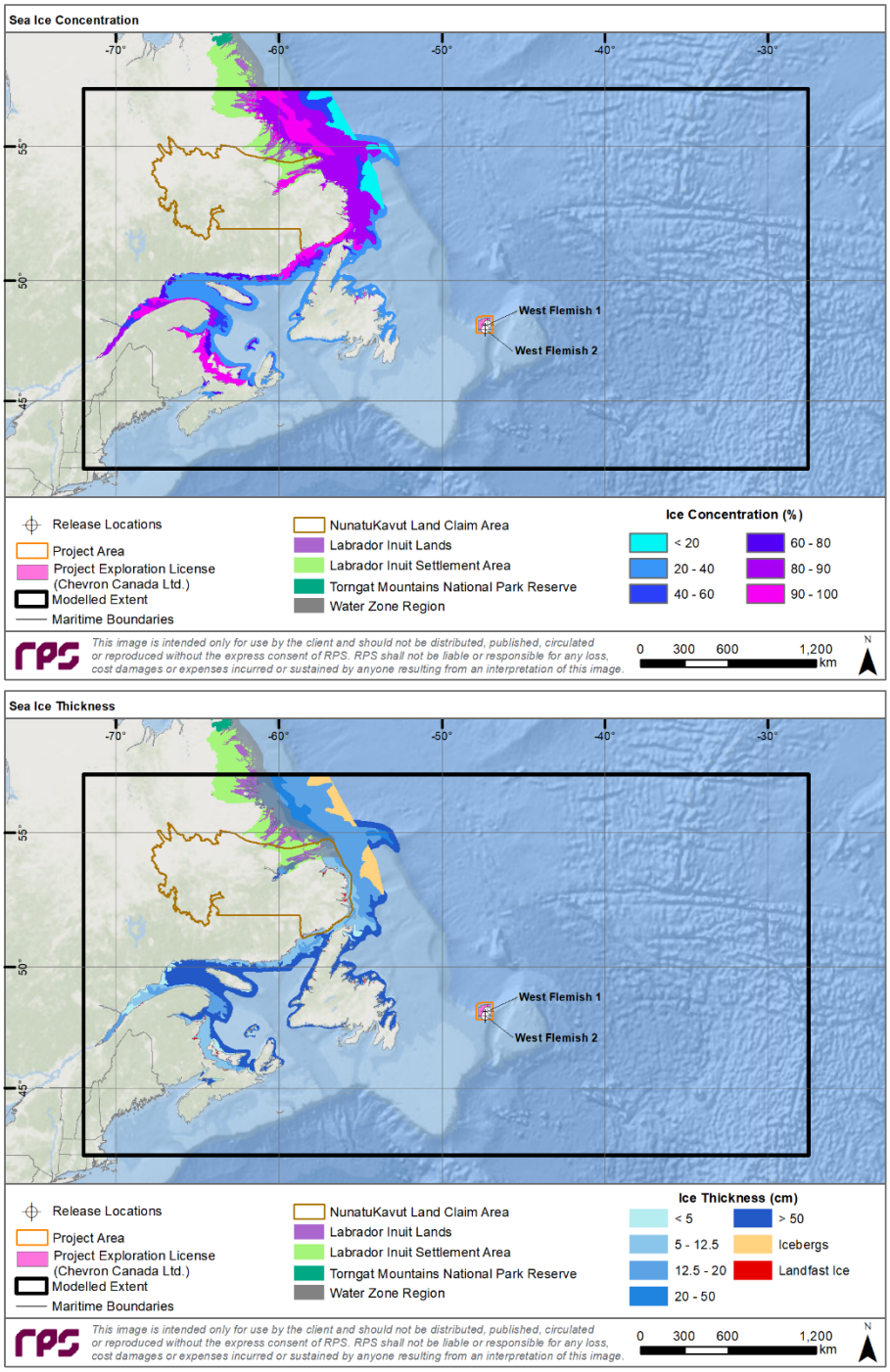

Figure 3-3. Representative percentage sea-ice coverage (top) and corresponding thickness (bottom) for the first week of February 2008.

3.4 Wind Data

Winds are one of the main physical forcings of oil transport on the water surface, thus wind speed and direction at the water surface are driving factors of a transport simulation. To effectively model this phenomenon, the wind velocity components data must encompass a large geographic area in order to capture the spatial extent and any spatial variability in potential transport that may occur. The SIMAP model uses time-varying wind speeds and directions over the area for the period which each release was simulated. A multi-year dataset of wind velocity components was used to capture the variability that occurs over the model domain for the multiple years that were modelled (2006-2012). Simulated oil release trajectories using these long-term wind datasets are representative of possible wind conditions at each hypothetical release site. Oil released over long periods of time (e.g., the 135-day blowouts modelled here for 160 days) has the potential to travel long distances by wind transport.

Wind data for this study were obtained for the entire model domain (Figure 2-1) from the National Centers for Environmental Prediction (NCEP) Climate Forecast System Reanalysis (CFSR) product for 2006 through 2010 (Saha et al., 2010). Another two years (2011-2012) of wind data were added to the analysis from CFSv2, which uses the same model that was used to create CFSR and thus works as an extension of CFSR (Saha et al., 2014). The CFS was designed and executed as a global, high-resolution, coupled atmosphere-ocean-land surface-sea-ice system to provide the best estimate of the state of these coupled domains (Saha et al., 2010). The CFS includes coupling of atmosphere and ocean, as well as assimilation of satellite radiances. The CFS global atmospheric resolution is ~38 km, with 64 vertical levels extending from the surface to 0.26 hPa. CFS winds are one of the main driving forces in the HYCOM hydrodynamic dataset which also is used for this oil spill modelling study (see Section 3.5). The CFS dataset acquired for and used in this study has 0.5-degree horizontal resolution and 6-hourly intervals.

Averaged annual wind data at the West Flemish 1 and West Flemish 2 sites are most frequently from the west-southwest direction (Figure 3-4) as part of prevailing Westerlies wind patterns. As the two sites are in close proximity to one another, they have similar environmental conditions and metocean figures have been provided for West Flemish 1 only. These winds would be expected to transport oil generally to the east, away from nearby shorelines and further into the open ocean. Winter season winds are most frequently from the west and northwest with higher velocity than summer season winds, which typically come from the southwest (Figure 3-5). Spring and fall months are more dynamic transitional periods between summer and winter wind regimes. Low pressure systems, tropical, and extra-tropical storms pass through the Grand Banks on a regular basis generating substantial wind speeds for short periods of time. However, winds throughout the year predominantly come from the west, northwest, and southwest, which would force oil further into the open ocean. Monthly average wind speeds varied between 7 and 12 m/s while the 95th percentile wind ranged from 12 to 20 m/s throughout the year (Figure 3-6). The highest wind speeds occurred during winter months (November-March) and lowest speeds during summer months (June-August). Resulting significant wave heights, induced by winds at the surface of the ocean, are typically highest from November – February, in regions with no ice (C-NLOPB, 2014).

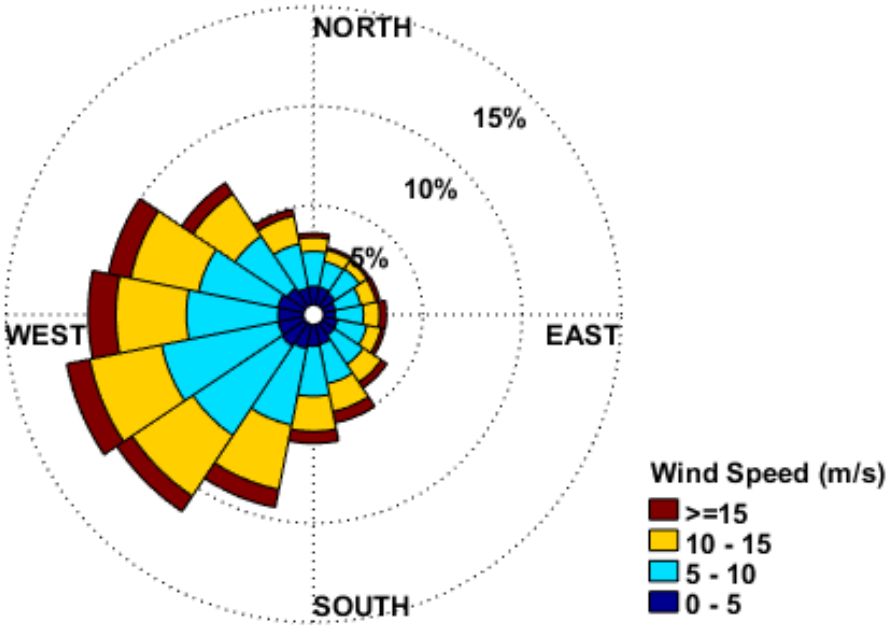

Figure 3-4. Annual CFS wind rose near the West Flemish 1 site. Wind speeds are presented in m/s, using meteorological convention (i.e., direction wind is coming from).

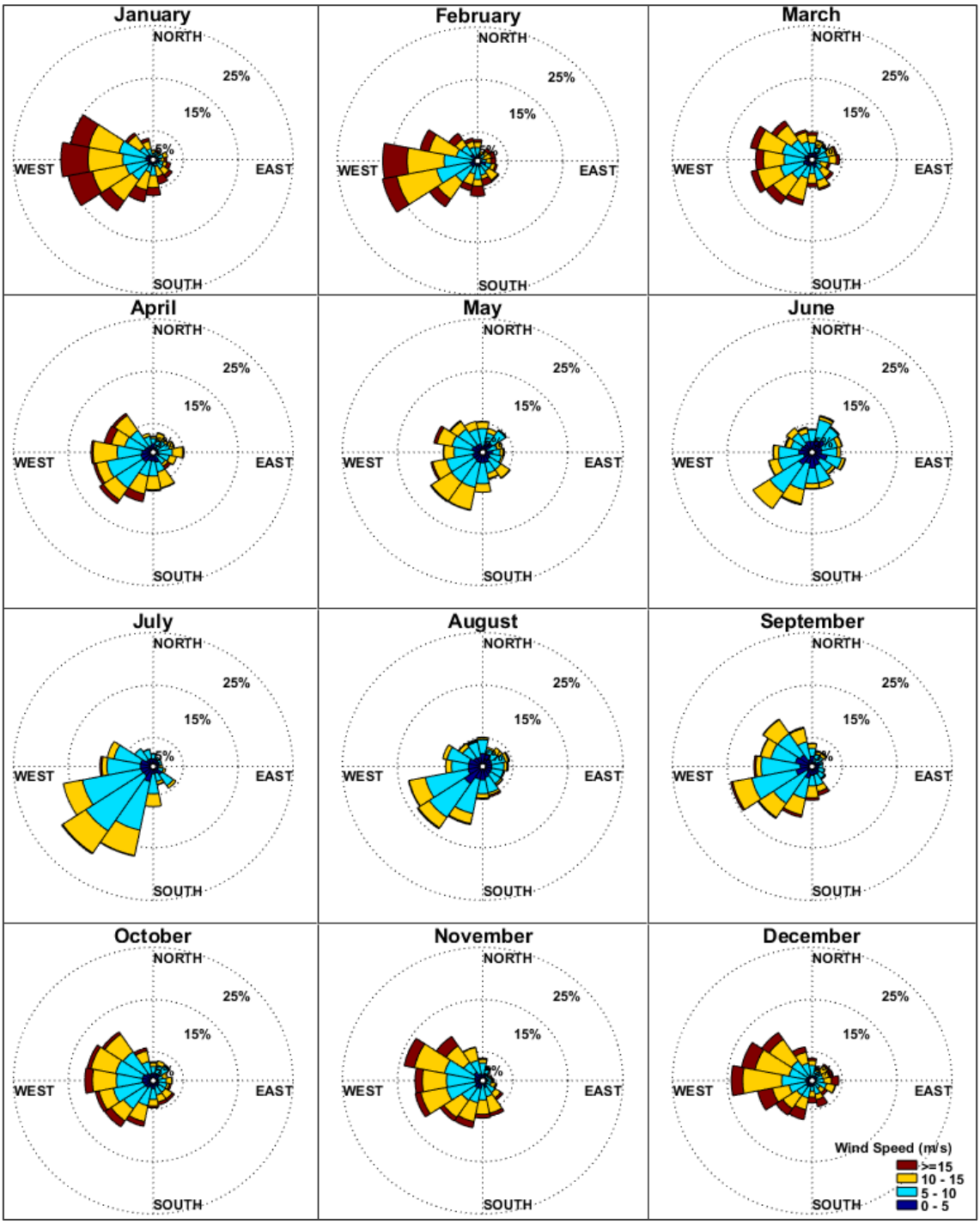

Figure 3-5. Monthly CFS wind roses near the West Flemish 1 Site. Wind speeds in m/s, using meteorological convention (i.e., direction wind is coming from).

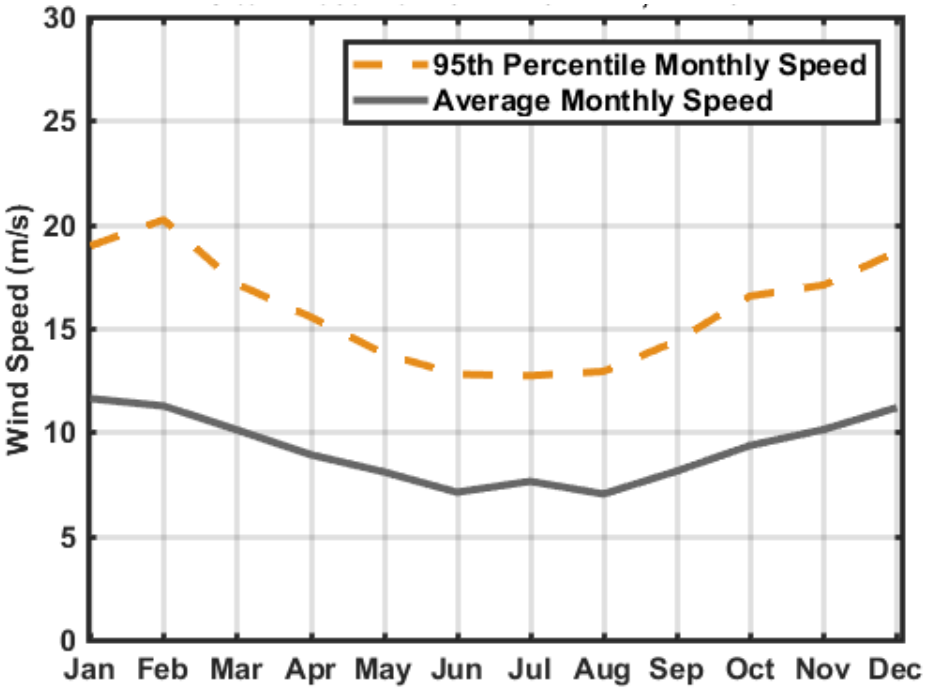

Figure 3-6. Average and 95th percentile monthly wind speeds near the West Flemish 1 site.

3.5 Currents

In addition to winds, the second main forcing factor on oil drift is currents. The Labrador Current dominates the large-scale ocean circulation in the Newfoundland region, originating in the Arctic Ocean and flowing south along the coasts of Labrador and Newfoundland (Figure 3-7 through Figure 3-9). This southerly current intensifies as waters funnel through the offshore branch, which follows the Flemish Pass along the 1,000 m contour depth between the Grand Banks and Flemish Cap. To a lesser extent, a portion of the Labrador Current flows through an inshore branch, which follows the Avalon Channel between Newfoundland and the Grand Banks. Over parts of the Grand Banks, currents can be generally weak and flow south (Petrie and Isenor, 1985). Maximum current speeds in the upper 200 m of the water column range from 0.3-2.0 m/s (C-NLOPB, 2014). The strong southerly current dominates the yearly average flow, and winds may only account for approximately 10% of current variability in this region (Petrie and Isenor, 1985). South of the Flemish Pass, the Labrador Current mixes with the North Atlantic Current. The region where these two currents converge is one of the most dynamic oceanographic areas in the world, where extremely energetic and variable frontal systems and eddies are produced on smaller scales on the order of kilometers (Volkov, 2005). Due to these eddies, local transport may advect parcels of water in nearly any direction. Satellite and drifter studies of current dynamics demonstrate this complexity. However, drifting parcels generally move to the south and east (Han and Tang, 1999; Petrie and Anderson, 1983; Richardson, 1983) where they intersect with the North Atlantic Current.

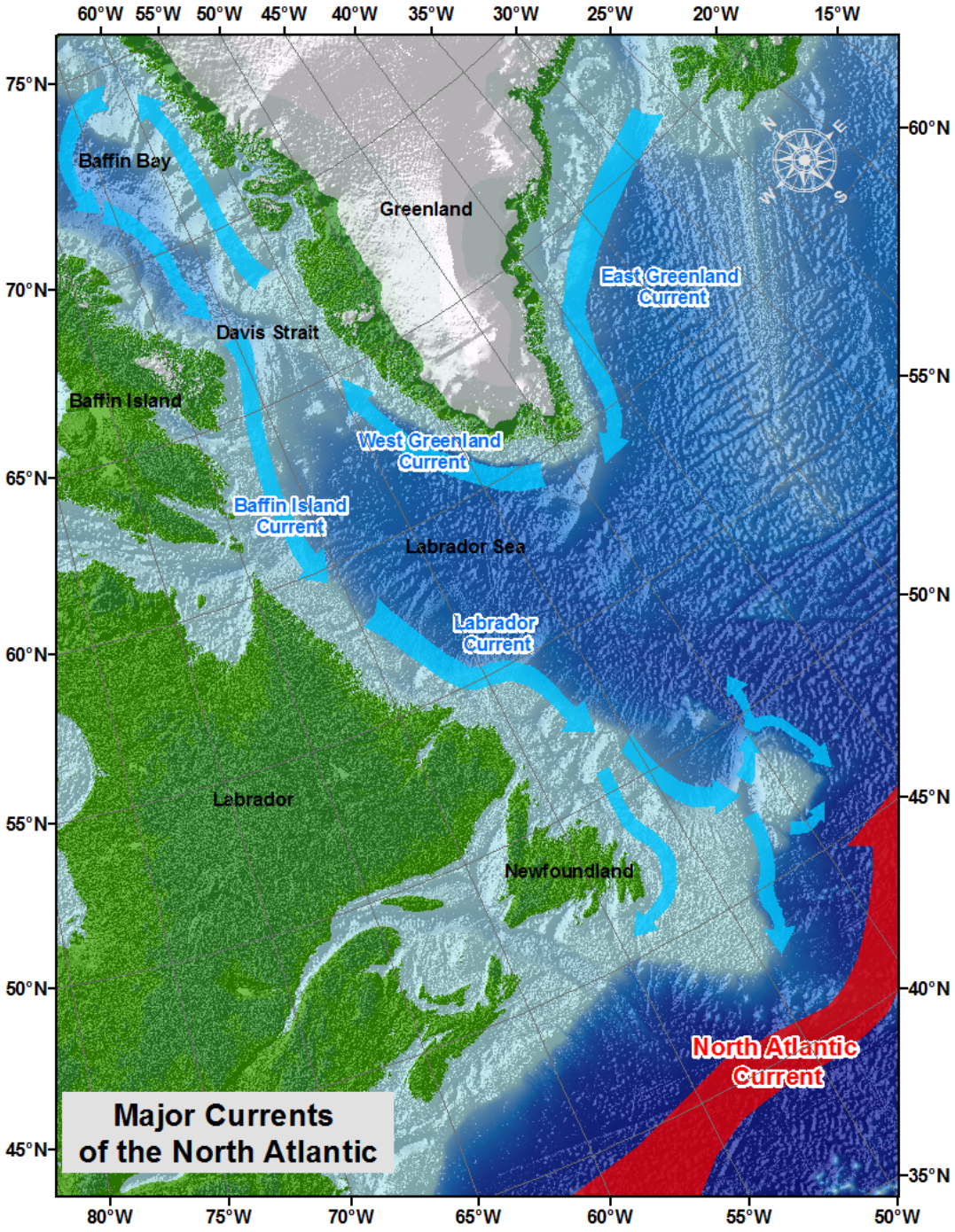

Figure 3-7. Large scale ocean currents in the Newfoundland region (USCG 2009).

Currents for the North Atlantic region were acquired from the HYCOM (HYbrid Coordinate Ocean Model) circulation model. HYCOM is a primitive-equation ocean general circulation model that evolved from the Miami Isopycnic-Coordinate Ocean Model (MICOM) (Halliwell, 2002; Halliwell et al., 1998; Bleck, 2002). MICOM is one of the premier ocean circulation models, following several validation studies (Chassignet et al., 1996; Roberts et al., 1996; Marsh et al., 1996). MICOM is used in numerous ocean climate studies (New and Bleck, 1995; New et al., 1995; Hu, 1996; Halliwell, 1997, 1998; Bleck, 1998). HYCOM uses Mercator projections between 78°S and 47°N and a bipolar patch for regions north of 47°N, to avoid computational problems associated with the convergence of the meridians at the pole. The 1/12° equatorial resolution provides gridded ocean data with an average spacing of ~7 km between each point. Several studies demonstrated that at least 1/10° horizontal resolution is required to resolve boundary currents and mesoscale variability in a realistic manner (Hurlburt and Hogan, 2000; Smith and Maltrud, 2000; Chassignet and Garaffo, 2001).

For the energetic eddies at the frontal systems that are of a smaller scale than ~7 km, the HYCOM model would not directly capture these features due to its low resolution (Volkov, 2005). However, from a broader-scale oil trajectory perspective, it is not required to capture these smaller scale features. The movement of water within an eddy is circular by nature, meaning that oil in the eddy would tend to be trapped, circulating within the grid cell. Therefore, while the rate of circulation (i.e., velocity of rotating water body) may be greater than the forward current speed of the eddy, it is irrelevant to the broader scale modelled transport processes. The general ocean circulation (i.e., forward movement of the eddy itself) would be resolved by the average current within the single grid cell, which captures the forward speed of the core of the eddies. In addition, the randomized advection and dispersion account for the variability in currents below the spatial and temporal resolution of each dataset. Because HYCOM does not resolve the trapping of oil in these small-scale features, results of the modelled simulations would tend to include a higher degree of dispersion and would therefore cover larger areas and may be considered more conservative. For eddies that are larger than approximately 14 km in diameter, the HYCOM gridding could capture the circular nature of the circulation in the multiple grid points.

In general, the resolution of underlying forcing data has the potential to influence the results of trajectory and fate simulations. If extremely coarse resolution forcing is used, intricate flow paths may be straightened, and velocities would tend to be closer to the mean. If extremely fine resolution gridding is used, smaller-scale features will be resolved. However, there is a balance and a “law of diminishing returns” when modelling these processes. When higher spatial and temporal resolutions are used, larger amounts of data are required, and the number of modelled time steps must increase. Shorter time steps are required with higher spatial resolution data to account for the distance traveled within each time step, to ensure the spatial scale is resolved (i.e. particles to not jump or skip adjacent grid cells). As the number of cells covering the same domain with higher resolution increases, the amount of time required to model will increase as will the amount of data storage for model outputs.

The HYCOM model leverages data assimilation techniques used in the Navy Coupled Ocean Data Assimilation (NCODA) system (Cummings, 2005). The NCODA system employs a Multi-Variate Optimal Interpolation scheme. This scheme uses model forecasts as a first guess, and then refines estimates from available satellite and in-situ temperature and salinity data that are applied through the water column using a downward projection of surface information (Cooper and Haines, 1996). Its bathymetry is derived from the General Bathymetric Chart of the Oceans (GEBCO; Supporting Volume to the GEBCO Digital Atlas, 1994). Surface forcing is derived

from the Navy Operational Global Atmospheric Prediction System (NOGAPS), which includes wind stress, wind speed, heat flux (using bulk formula), and precipitation.

For this study, daily HYCOM current data were obtained for the period of January 2006 through December 2012, for the North Atlantic region (HYCOM, 2016). The data spanned seven years, which encompasses the variability in winds and currents in daily, weekly, seasonal, and inter-annual scales, including calm periods, seasonal variations, and the full range of environmental forcing over the entire period. Because of the bi-weekly randomized sampling within the seven-year modelled period and the 160-day duration of the oil spill models themselves, the range of calm to more energetic periods would be captured in each stochastic analysis. While this subset of hydrodynamic data is not the most recent seven years of data, currents and winds in the study area would be representative of environmental conditions that are likely to be present. Similarly, while there may be questions regarding general circulation during specific time periods, it is important to note that oil spill trajectories are influenced by day to day currents, as opposed to seasonal or annual averages. Average surface current speeds (Figure 3-8 and Figure 3-9) and direction offshore Newfoundland (Figure 3-9) for 2006-2012 in the model domain depict large scale features such as the Labrador Current and the North Atlantic Current as well as bathymetric steering of currents around the Grand Banks and Flemish Cap. While these figures present an average current speed and direction for visual purposes, oil transport was defined by the daily currents throughout each modelled simulation.

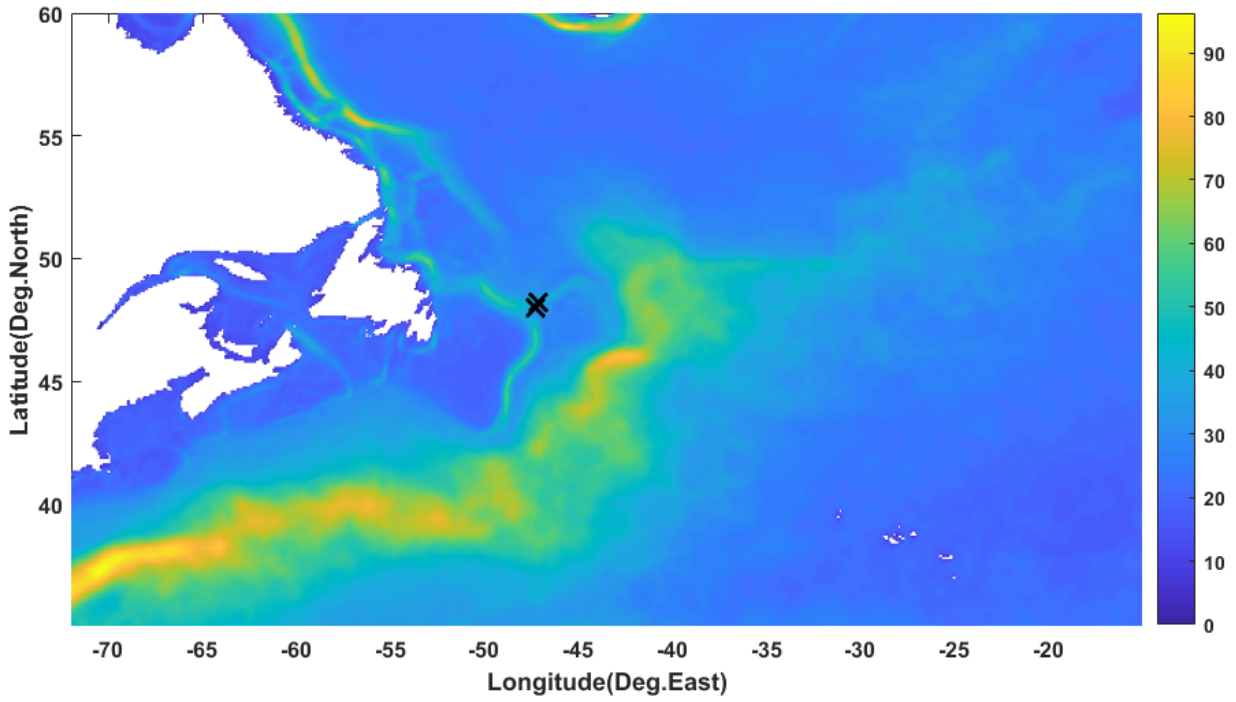

Figure 3-8. Average HYCOM surface current speeds (cm/s) off the coast of Newfoundland from 2006 – 2012. Black crosses represent the well locations.

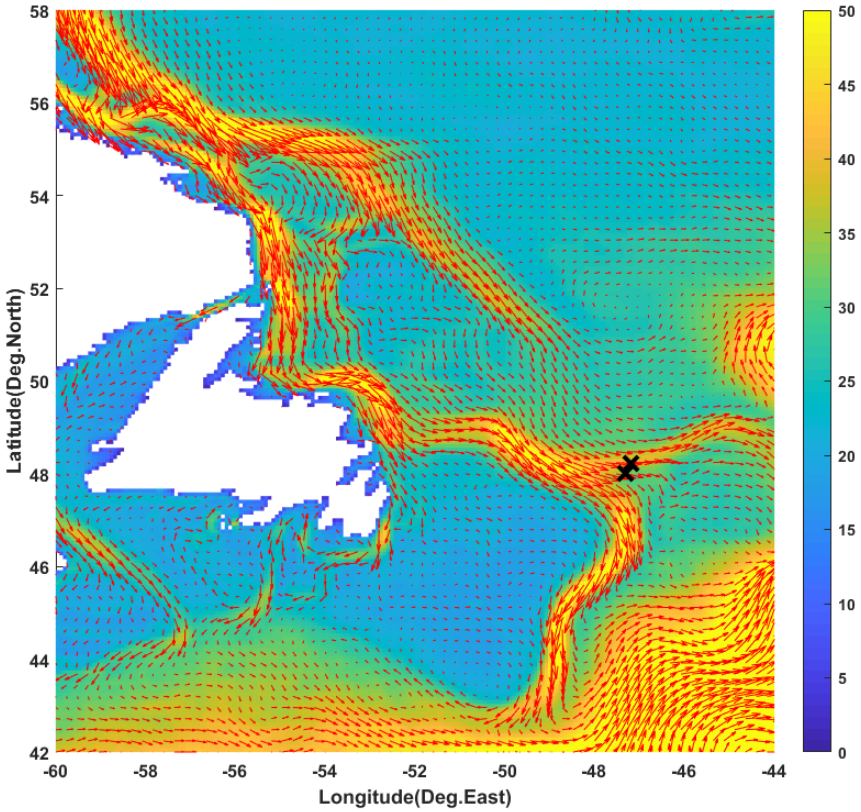

Figure 3-9. Averaged HYCOM surface current speed (cm/s) in color and arrow size, and direction presented as red vectors around the Newfoundland coast, including portions of Labrador (2006-2012). Black crosses represent the well locations.

3.6 Water Temperature & Salinity

Temperature and salinity values throughout the water column influence several oil transport and fate calculations including (but not limited to) density/buoyancy, viscosity, and evaporation (French McCay et al. 2018a). Temperature and salinity data were obtained from the World Ocean Atlas (WOA) 2013 high-resolution dataset, Version 2, which is compiled and maintained by the U.S. National Oceanographic Data Center (Levitus et al., 2014). The WOA originated from the Climatological Atlas of the World Ocean (Levitus, 1982) and was updated with new data records in 1994, 1998, 2001 (Conkright et al., 2001), and 2013. These data records consist of observations obtained from various global data management projects. The dataset includes up to 57 depth bins from the sea surface to the seabed and include averaged yearly, seasonally, and monthly data over a global grid with a 1/4° horizontal resolution. At both sites, the temperature sharply decreases with increasing depth, reaching the lowest value at approximately 75 m. Below this depth, the temperature rises again down to 400 m water depth. Below 400 m depth, temperature gradually decreases at West Flemish 1 and stays relatively stable at West Flemish 2. On the other hand, the salinity and density (represented by sigma-T plots) of the seawater increase with depth, with the top 250 m having the largest degree of variability (Figure 3-10).

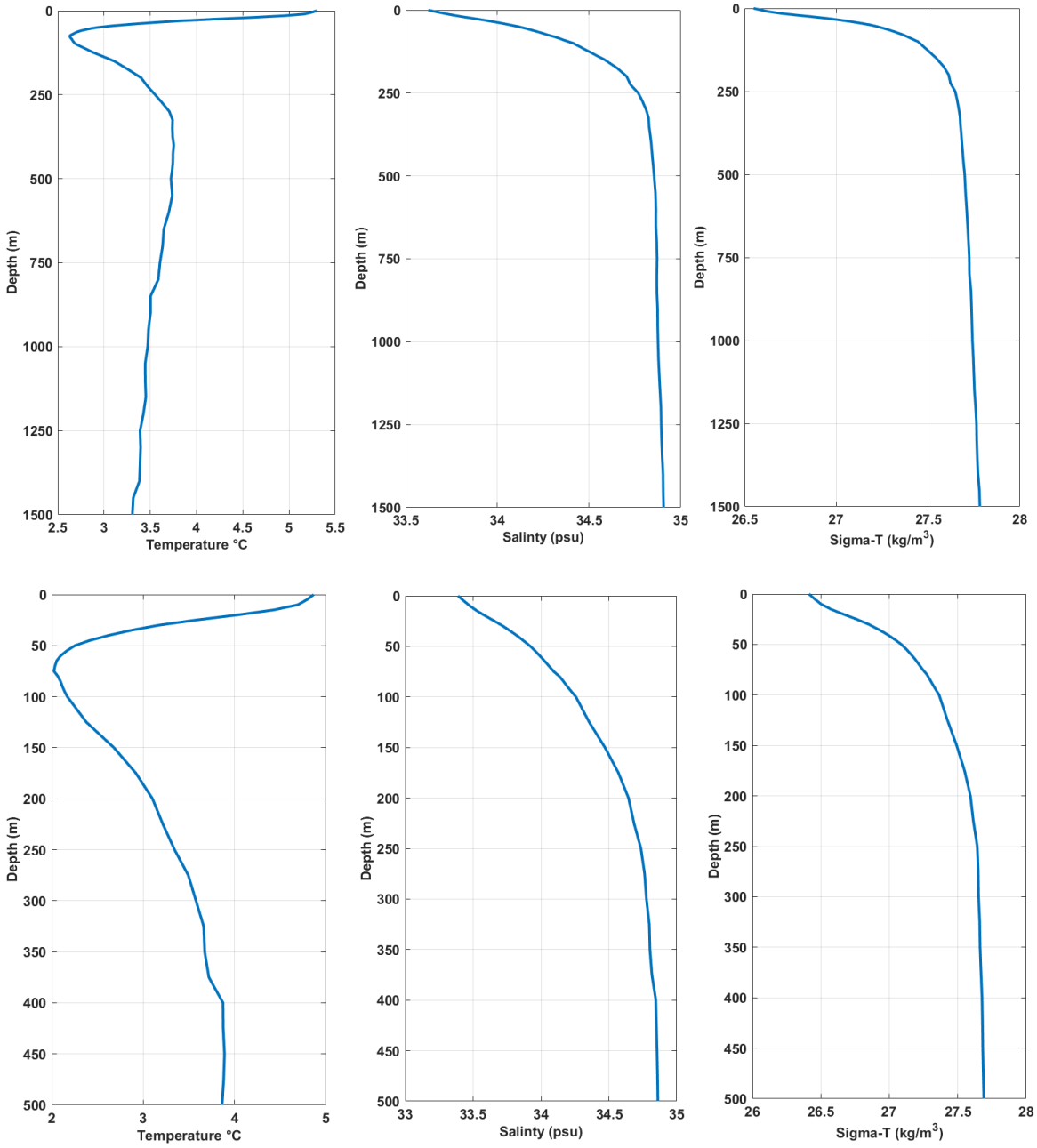

Figure 3-10. Profiles of annual water column temperature (left) and salinity (middle) from WOA13, and the corresponding calculated density (right) represented as sigma-t in the vicinity of the release site West Flemish 1 (top) and West Flemish 2 (bottom). The density profile was generated based on the temperature and salinity data using equations of state as published by UNESCO, 1981 (EOS – 80).

3.7 Blowout Model Scenario and Results

The nearfield model OILMAPDeep was used to predict the initial droplet size distribution associated with subsurface blowouts of WFPLO crude oil at two different release locations. Four subsurface blowouts of WFPLO were evaluated at West Flemish 1 and 2 as part of this study, capturing short (27 and 30 day) and long (123 and 135 day) releases (Table 2-1). Oil and gas were introduced to the water column near the seafloor to simulate an uncontrolled release from the wellhead frequently referred to as a blowout. The orifice diameter was assumed to be 21.6 cm (8.5 inches) at the seafloor (Table 2-4).

The droplet size model was used to predict the distribution of oil volume (mass) within different size ranges (measured by diameter) in response to the turbulence of the release, the gas content, the water depth, and the properties of the oil. The droplet model predicted the initial droplet size distributions for each scenario as well as the depth or “trap height” in the water column where the droplets would be released to the water column and rise according to their individual buoyancies. These values were then used to generate input files defining the size, mass, and depth of oil droplets entering the water column for use within the SIMAP far-field model.

Initial droplet sizes are primarily a function of the energy of the release, the chemical and physical parameters of the released oil, the gas to oil ratio (GOR), dispersant application, and several other factors. As an example, if the energy of a release or the amount of dispersant added were to increase, or if the viscosity of the released oil were lower, the resulting droplet sizes would be smaller. In the unmitigated scenarios simulated for this study, the oil was assumed to be untreated (i.e. no dispersant used). The energy of the release is a function of the volumetric flow rate and discharge orifice size, with higher energy releases occurring as greater volumes pass through smaller openings more quickly.

The predicted droplet size distribution was represented by seven discrete size bins for each modelled release scenario (Table 3-5). The non-uniform spacing between the droplet size bins is the result of the non-linear functionality of droplet size distribution. Each of the seven bins were determined such that an equal proportion of the released oil by mass (14.29%) was within each bin. Differences in release depth and blowout rate resulted in different droplet size distributions for each of the two modelled release rates.

Oil droplets rise through the water column at rates based on drag, calculated using their diameter (treated as a sphere) and the buoyancy (the density difference between the oil and the water), which varies with changing temperature and salinity by depth (Figure 3-10). Rise times for oil to reach the surface varied between hours to a few days, depending on droplet size and depth of release. Rise time estimates are approximated, based on the initial droplet size, initial droplet density, and bottom water density; neglecting dispersion, dissolution, and degradation (which were tracked within the oil spill model and modified the rise rates). The longest rise times were associated with the smallest droplets, with some rise times exceeding 5 days. At West Flemish 1, the smallest droplet size (148 µm) is predicted to take over 5 days to reach the water surface from the trap depth (795 m), while the largest droplet size (1,007 µm) would take approximately 0.32 day (7.8 hr) to rise to the water surface. At the shallower West Flemish 2, the smallest droplet size (65 µm) is predicted to take 3.58 days to reach the water surface from the trap depth (93 m), while the largest droplet size (2,486 µm) would take approximately 0.1 day (2.5 hr) to reach the water surface.

Table 3-5. Summary of droplet size distribution results for each of two modelled subsurface blowout release sites.

Median Droplet Size in Each of Seven Equal-Mass Bins, by Diameter (µm)	
West Flemish 1 WFPLO Oil (22,640 m^3/d)	**West Flemish 2 WFPLO Oil (20,190 m^3/d)**
148	65
339	149
422	185
508	223
613	269
767	336
1,007	442

4 MODEL RESULTS

4.1 Stochastic Analysis Results

Stochastic analyses characterize results from many tens to hundreds of individual modelled releases. This study included 171 individual subsurface releases modelled for 160 days for each stochastic scenario. Modelled start times were distributed over a period of seven years of environmental data at two release sites (West Flemish 1 and West Flemish 2) to capture the natural variability in the environment. In total, four stochastic analyses were completed, totaling 684 individual trajectories. Each stochastic analysis was defined by release site and release duration (long or short). The release durations were consistent at each site with short/long subsurface blowouts lasting 30/123 days at West Flemish 1 and 27/135 days at West Flemish 2. These scenarios represent the time required to mobilize and implement a capping stack to contain the release (short) or mobilize and a drilling platform and drill a relief well.

Because ice cover can affect the trajectory and fate of oil, individual model simulations within each stochastic scenario were broken into two groups based upon the specific modelled time period and associated presence or absence of ice cover. Statistics for all 171 releases within a stochastic scenario are referred to as “annual,” as they include all releases in any month over the course of the entire seven-year period. Sea-ice coverage in the region is present in specific regions from November through April, while May through October is mostly ice-free. Modelled releases with the majority of their simulated days (>80 of the 160-day modelled duration) experiencing mostly ice-free periods are referred to as “summer” simulations (89 modelled releases), while those releases with a majority of days experiencing periods with sea-ice coverage are referred to as “winter” simulations (82 modelled releases). Sea-ice coverage very rarely extended far enough offshore to reach within kilometers of the release locations, and when it did, <10% ice coverage was predicted. However, sea ice was present along most of the coastline in winter months, with February typically having the largest expanses of 90-100% sea-ice coverage (Figure 3-3).

The figures presented within this section illustrate the predicted spatial extent of surface floating oil, water column contamination, and shoreline contact above the specified socio-economic thresholds (Table 2-2). They include both the probabilities and associated minimum times to threshold exceedance for the four hypothetical release scenarios (Table 4-1 and Table 4-2). The probability maps define the area of potential exposure and the associated probability with which sea surface oil, water column contamination, or shoreline oil are expected to exceed the specified socio-economic thresholds at any point in time throughout each of the 171 simulations with 160-day modelled duration. The colored contours in the stochastic maps specify the probability boundaries for areas that may experience oil at or above the specified thresholds for each release scenario. Darker color contours denote areas that are more likely to exceed the specified threshold, but do *not* denote higher concentrations. Lighter color contours depict regions that are less likely to exceed the specified threshold. Note that the lightest mint-green line represents areas where oil may exceed the specified threshold in only 1% of modelled simulations. In other words, the likelihood that any oil exceeding the identified threshold would leave the area bounded by the mint-green line is <1% out of 171 individual simulations. The area between the 1% contour and the next (10%) has between a 1-10% probability of exceeding the threshold, based upon the environmental variability and given that the modelled release scenario has occurred.

The probabilities of oil exposure were calculated from a statistical analysis of the ensemble of individual trajectories modelled for each release scenario. The fundamental assumption for this modelling was that an unmitigated release occurred. Therefore, probability contours should be interpreted as “In the unlikely event of a release, the probability that any one specific area may experience contamination above the specified threshold is X%.” Stochastic figures do not imply that the entire contoured area would be covered with oil in the event of a single release, nor do they provide any information on the quantity of oil in a given area. Additionally, these figures do not provide the likelihood of a blowout occurring in any given year. Rather, these stochastic figures denote the probability that contamination may exceed identified socio-economic thresholds at any modelled time step (over 160 days), for each point within the modelled domain, assuming a release were to occur at some point in time.

The stochastic maps depicting water column contamination by dissolved hydrocarbon concentrations do not specify the depth at which the threshold exceedance occurs. The maps depict the vertical maximum at any time during or after the release. Thus, images do not imply that the entire water column (i.e., from surface to bottom) will experience a concentration above the threshold, but rather a threshold may be exceeded at a specific depth (typically within a few meters from the surface) in the mapped location.

The minimum time footprints correspond with the associated probability of oil exposure maps. Each figure illustrates the shortest amount of time required (from the initial release) for each point within the footprint to exceed the defined threshold. The time reported is the minimum value for each point considering the entire ensemble of trajectories. Together, probability and minimum time figures can be interpreted to read: “There is X% probability that oil is predicted to exceed the identified threshold at a specific location, and this exceedance could occur in as little as Y days.”

The Exclusive Economic Zones (EEZ) in the North Atlantic, as well as the international border, are depicted on each map to provide context for the spatial extent and potentially affected territorial waters from any potential release (VLIZ, 2014).

All figures depict data where the probability of a region exceeding the threshold is >1%. When comparing annual to seasonal results, the predicted percent exceedance depends on the total number of releases investigated in each subset of releases. Therefore, while only one scenario might be required to exceed the 1% threshold for visualization in seasonal results (82 or 89 modelled simulations), two scenarios would be required to exceed the same threshold in the annual analysis due to a greater number (171 modelled simulations) of modelled releases in the annual set of simulations being analyzed. Figures depicting stochastic results are provided for surface oil thickness >0.04 µm, dissolved hydrocarbon contamination >1 µg/L, and shoreline contact >1g/m^2 for annual, summer, and winter scenarios for the two release sites (Figure 4-2 to Figure 4-34).

4.1.1 West Flemish 1 Results

4.1.1.1 30-day Subsurface Release

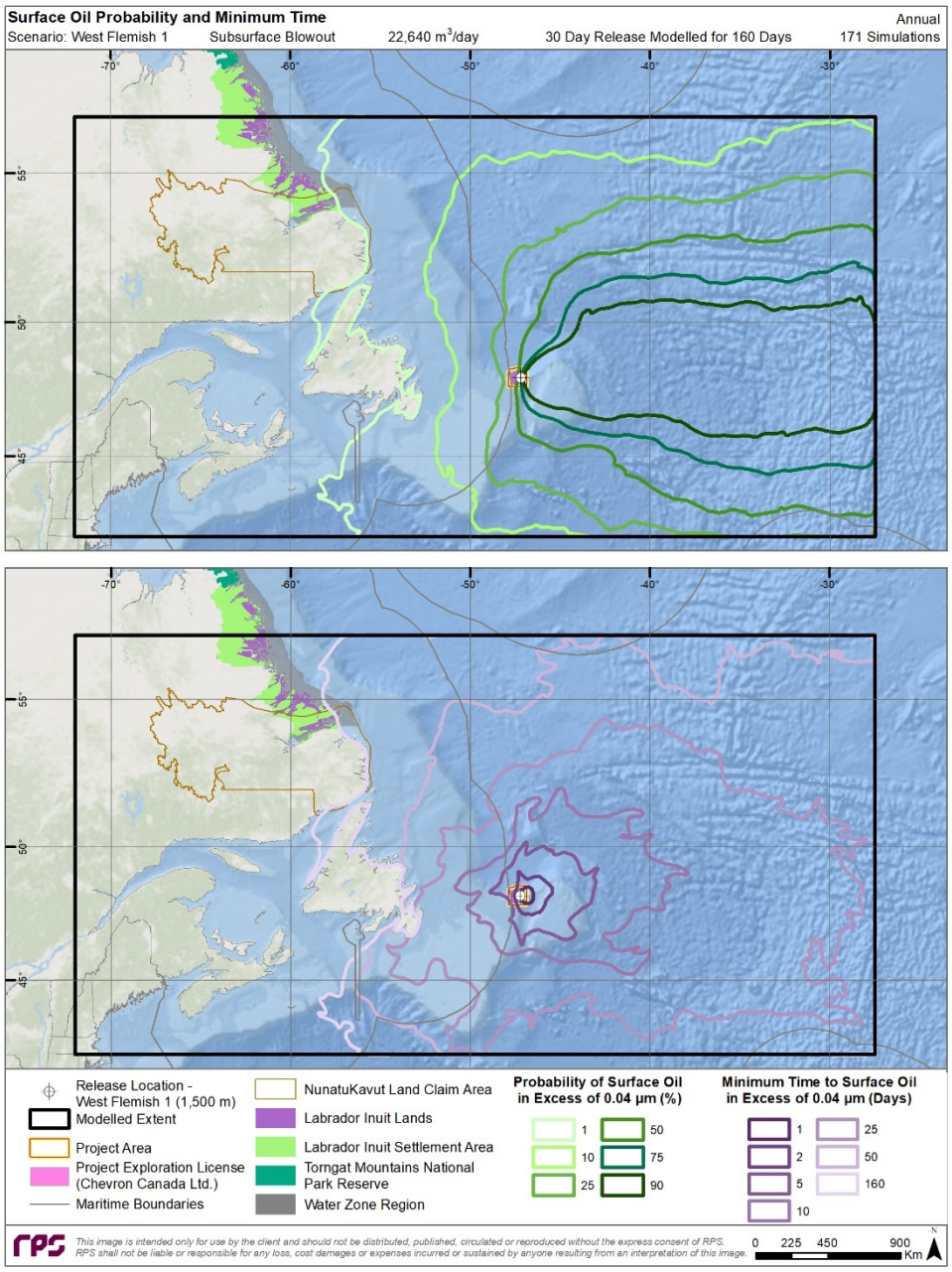

Figure 4-1. Annual probability of surface oil thickness >0.04 µm (top) and minimum time to threshold exceedance (bottom) predictions resulting from a 30-day subsurface blowout at West Flemish 1.

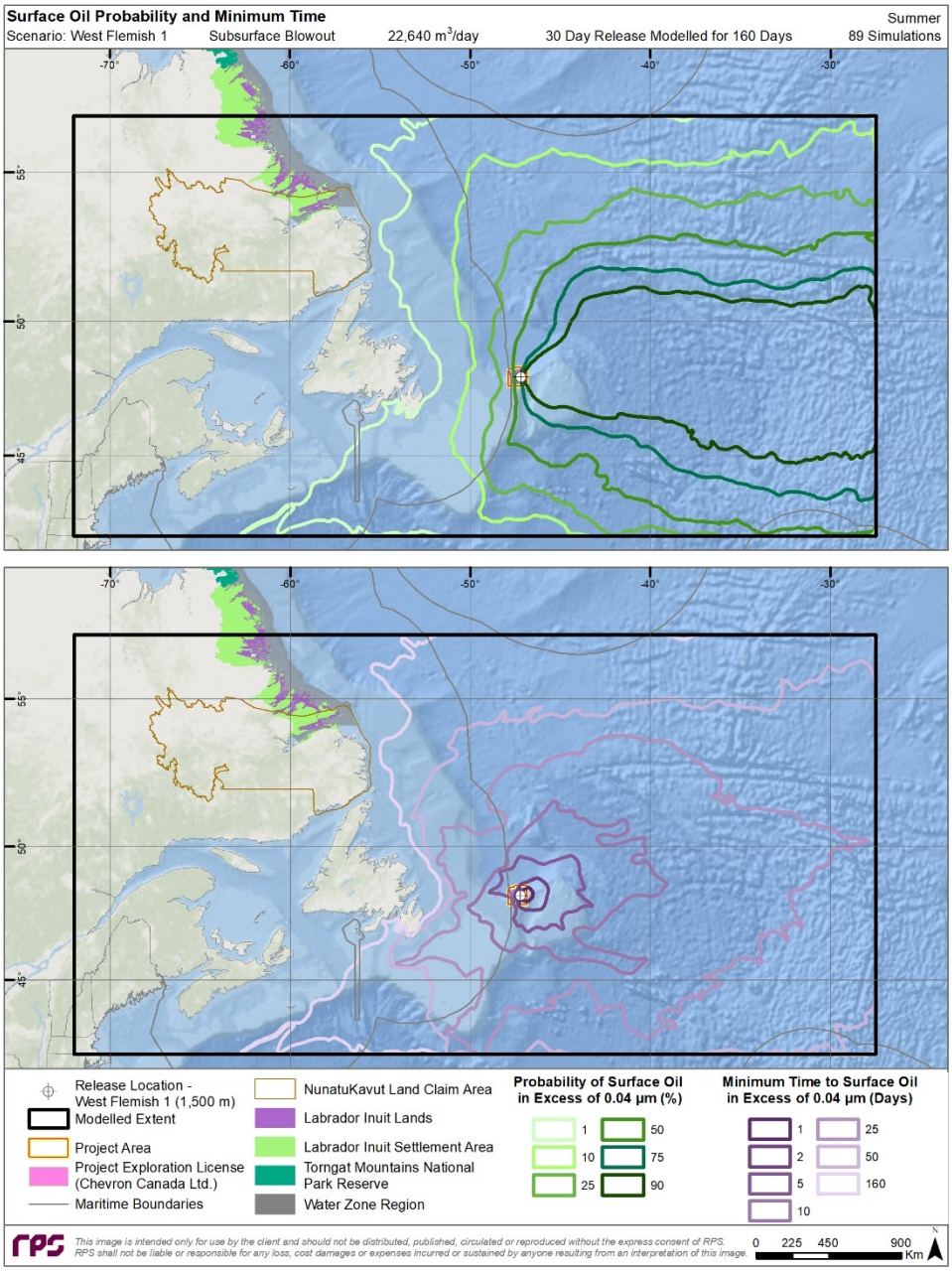

Figure 4-2. Summer probability of surface oil thickness >0.04 µm (top) and minimum time to threshold exceedance (bottom) predictions resulting from a 30-day subsurface blowout at West Flemish 1.

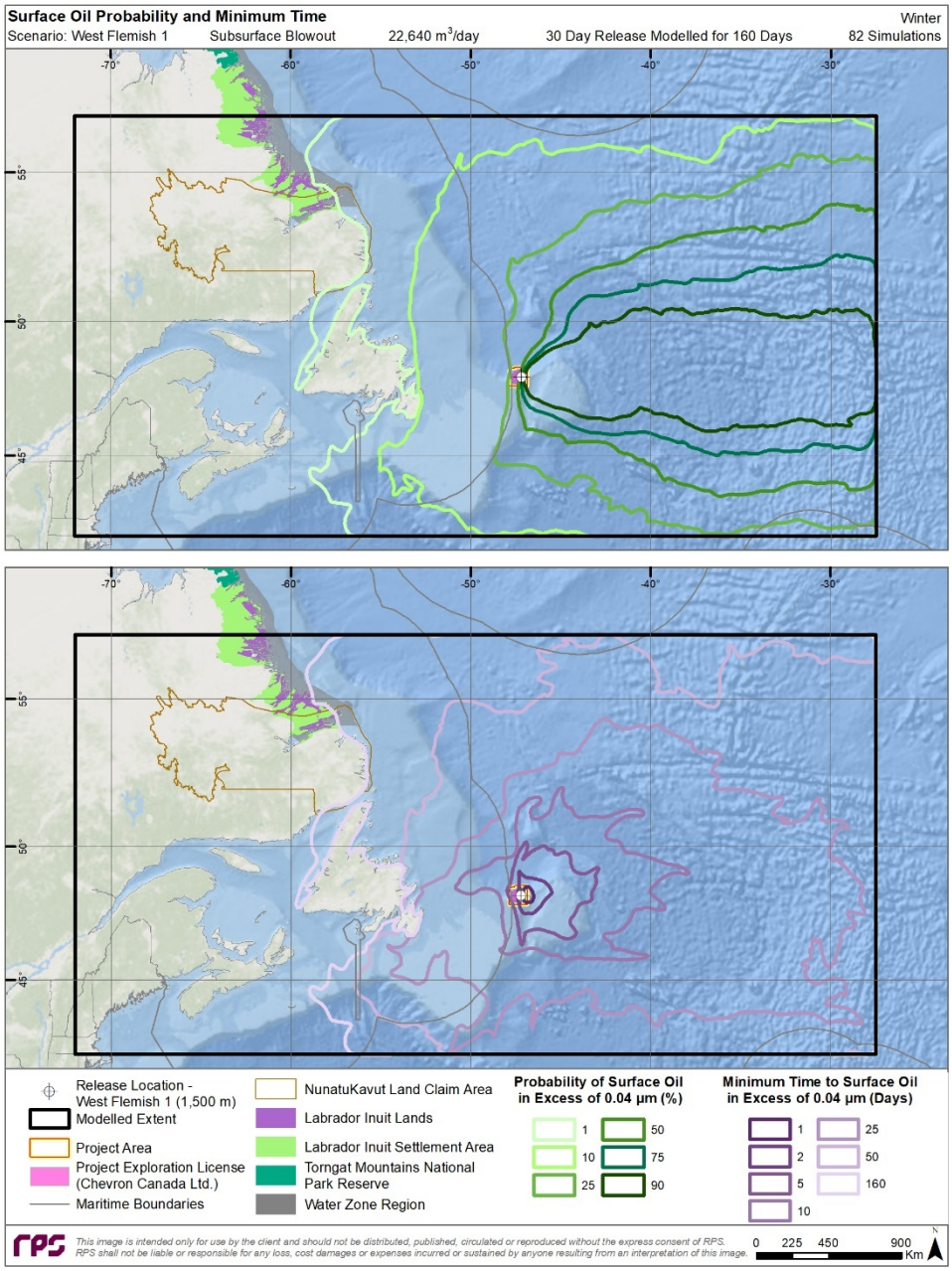

Figure 4-3. Winter probability of surface oil thickness >0.04 µm (top) and minimum time to threshold exceedance (bottom) predictions resulting from a 30-day subsurface blowout at West Flemish 1.

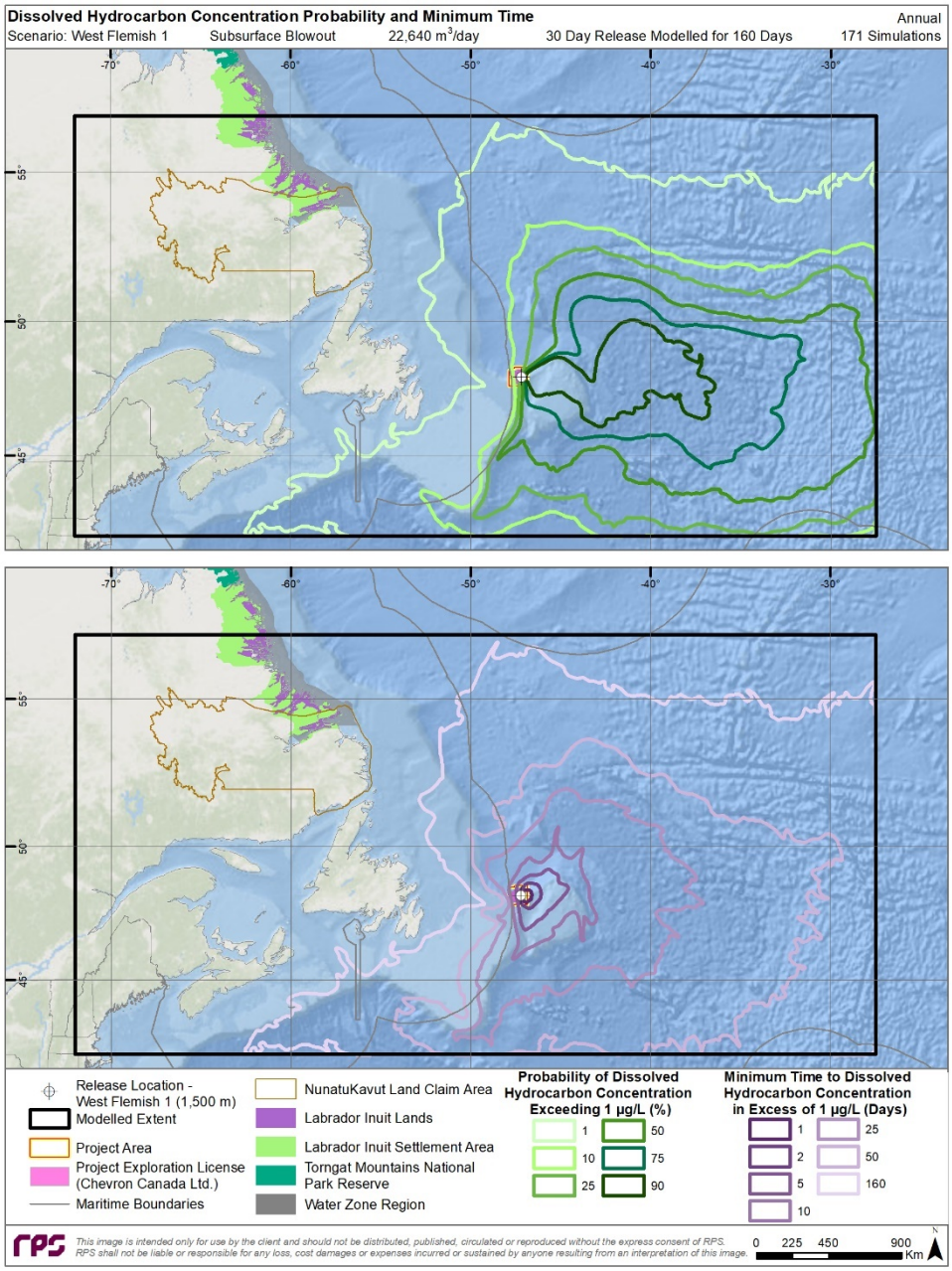

Figure 4-4. Annual probability of dissolved hydrocarbon concentrations >1 µg/L at some depth in the water column (top) and minimum time to threshold exceedance (bottom) predictions resulting from a 30-day subsurface blowout at West Flemish 1.

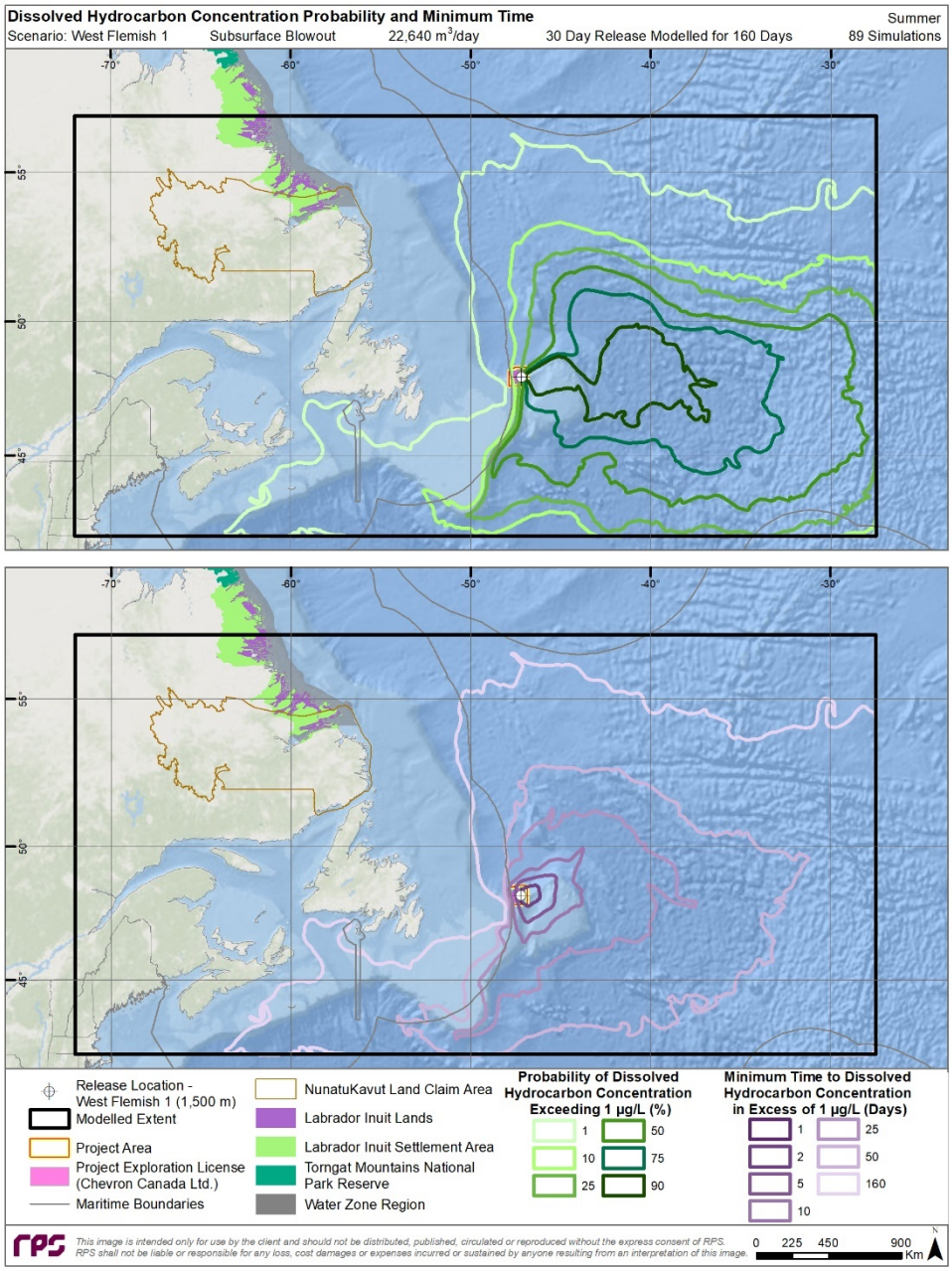

Figure 4-5. Summer probability of dissolved hydrocarbon concentrations >1 µg/L at some depth in the water column (top) and minimum time to threshold exceedance (bottom) predictions resulting from a 30-day subsurface blowout at West Flemish 1.

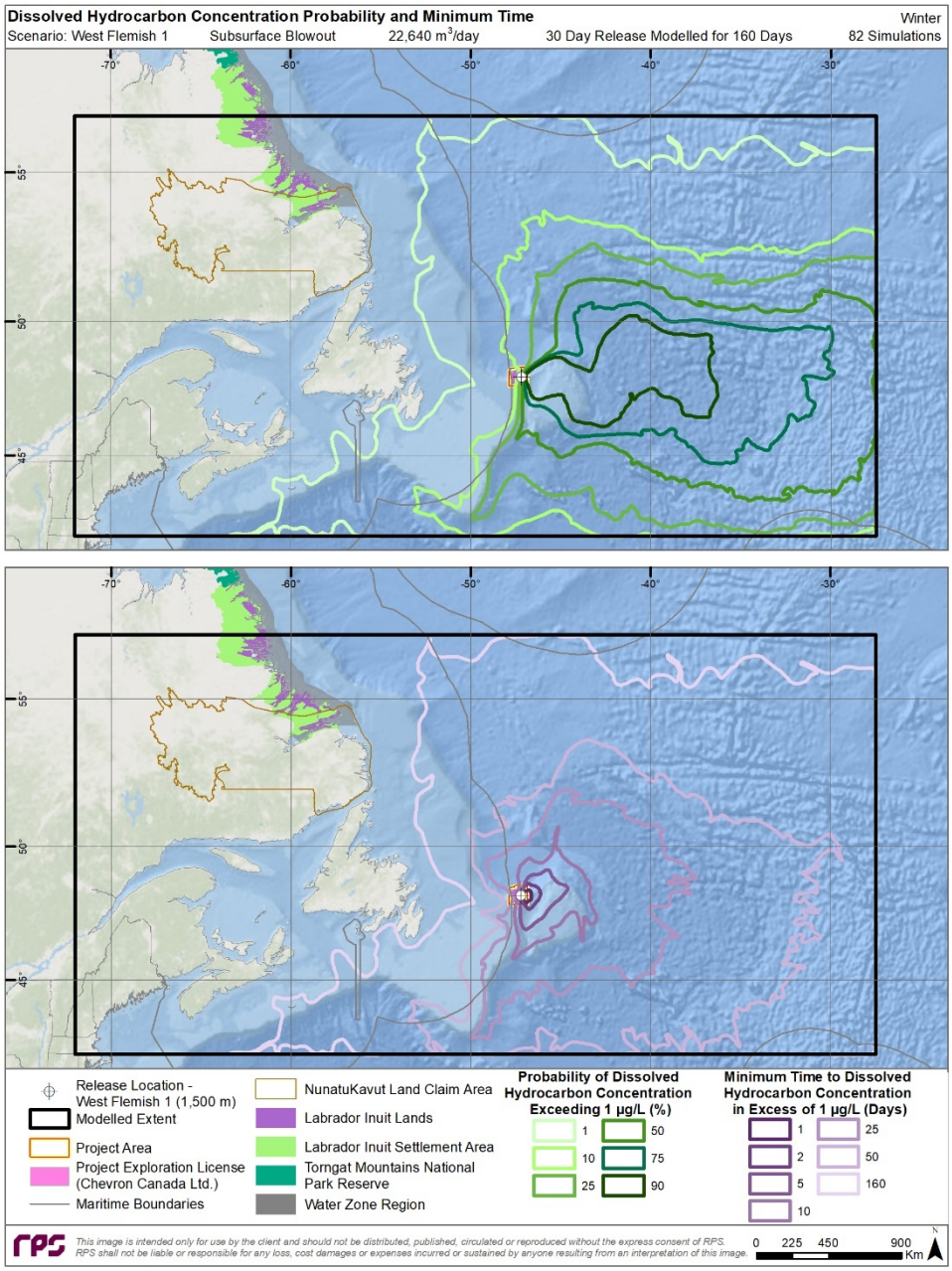

Figure 4-6. Winter probability of dissolved hydrocarbon concentrations >1 µg/L at some depth in the water column (top) and minimum time to threshold exceedance (bottom) predictions resulting from a 30-day subsurface blowout at West Flemish 1.

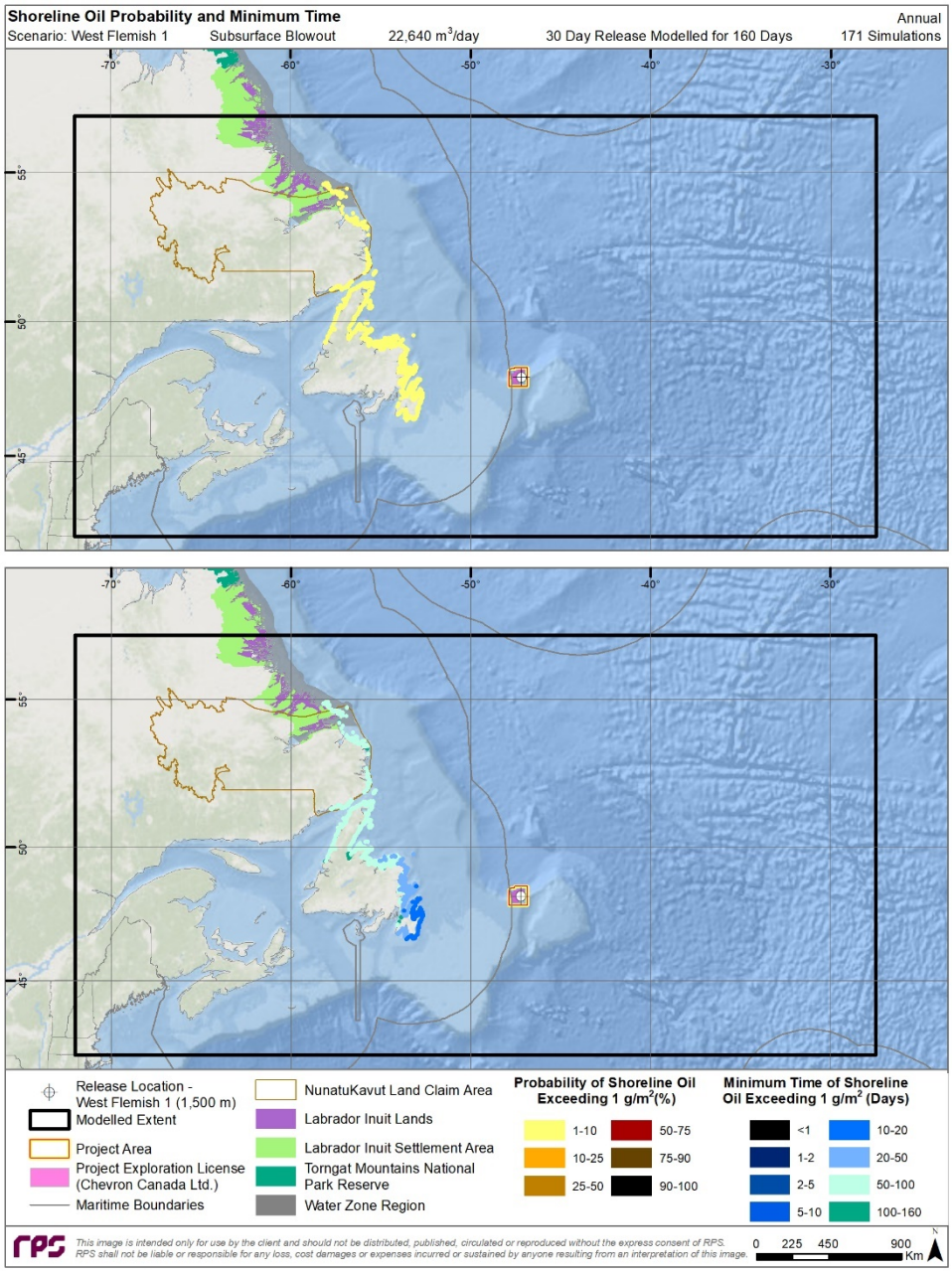

Figure 4-7. Annual probability of shoreline contact >1 g/m^2 (top) and minimum time to threshold exceedance (bottom) predictions resulting from a 30-day subsurface blowout at West Flemish 1.

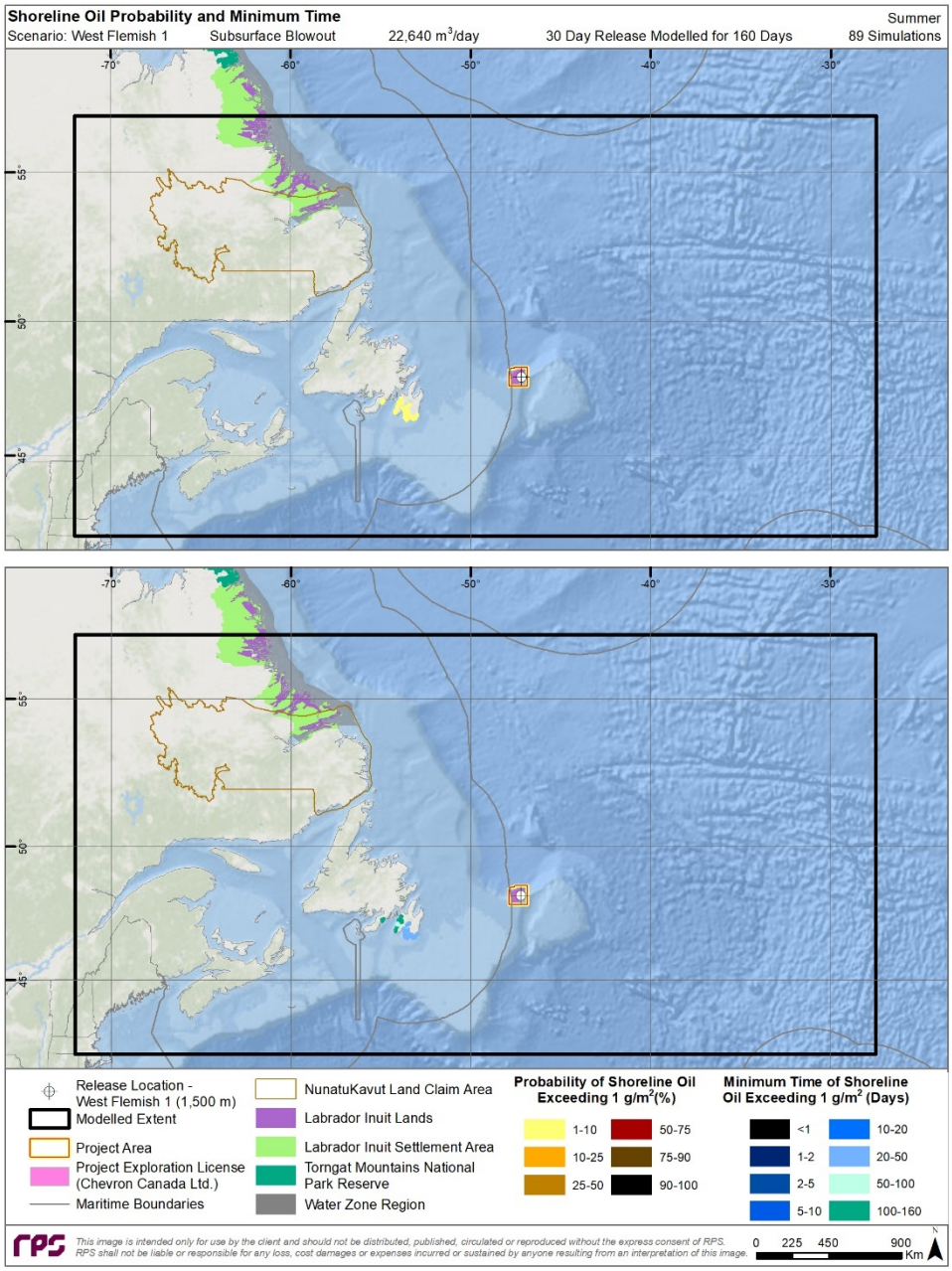

Figure 4-8. Summer probability of shoreline contact >1 g/m^2 (top) and minimum time to threshold exceedance (bottom) predictions resulting from a 30-day subsurface blowout at West Flemish 1.

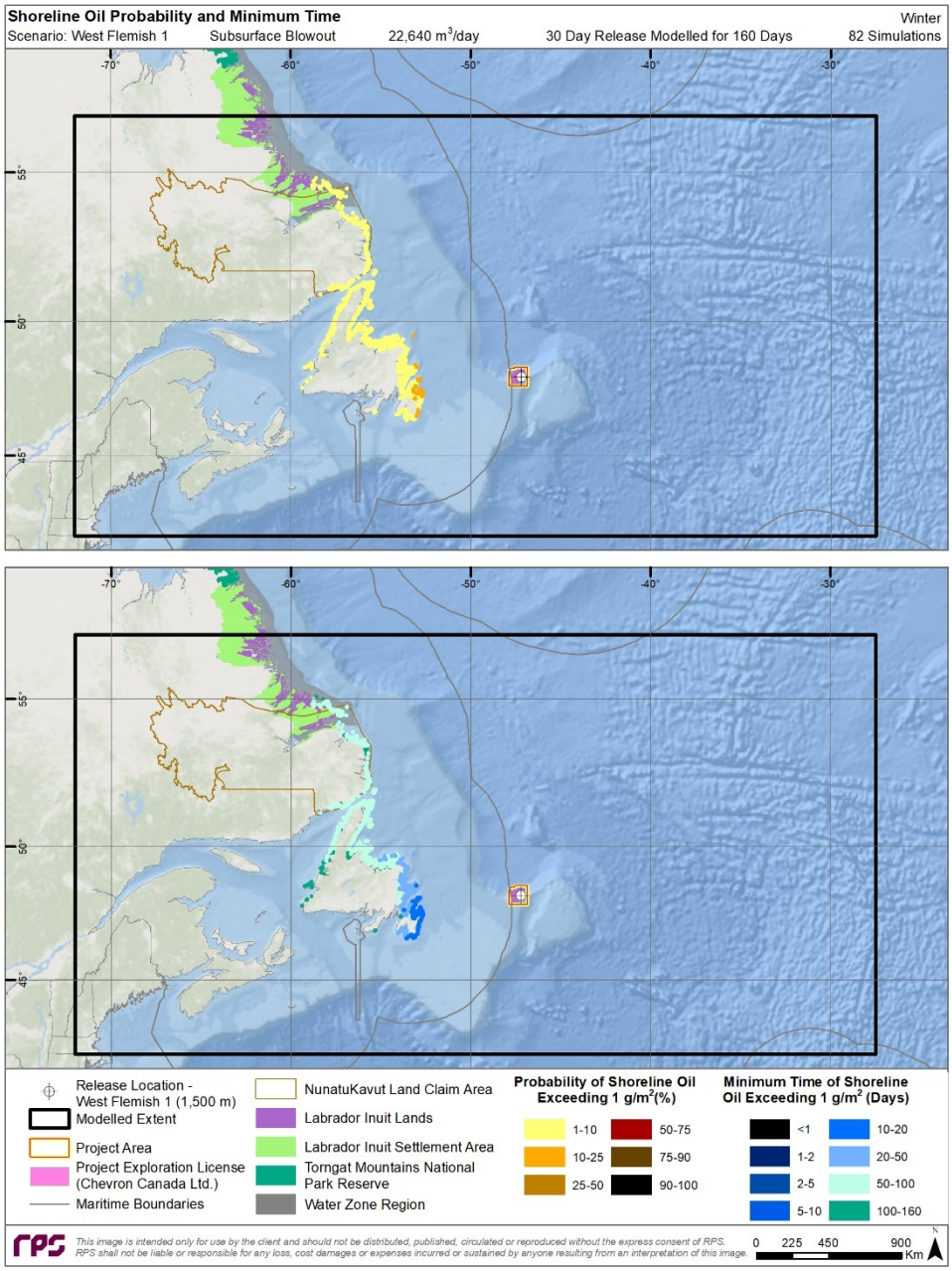

Figure 4-9. Winter probability of shoreline contact >1 g/m^2 (top) and minimum time to threshold exceedance (bottom) predictions resulting from a 30-day subsurface blowout at West Flemish 1.

4.1.1.2 123-day Subsurface Release

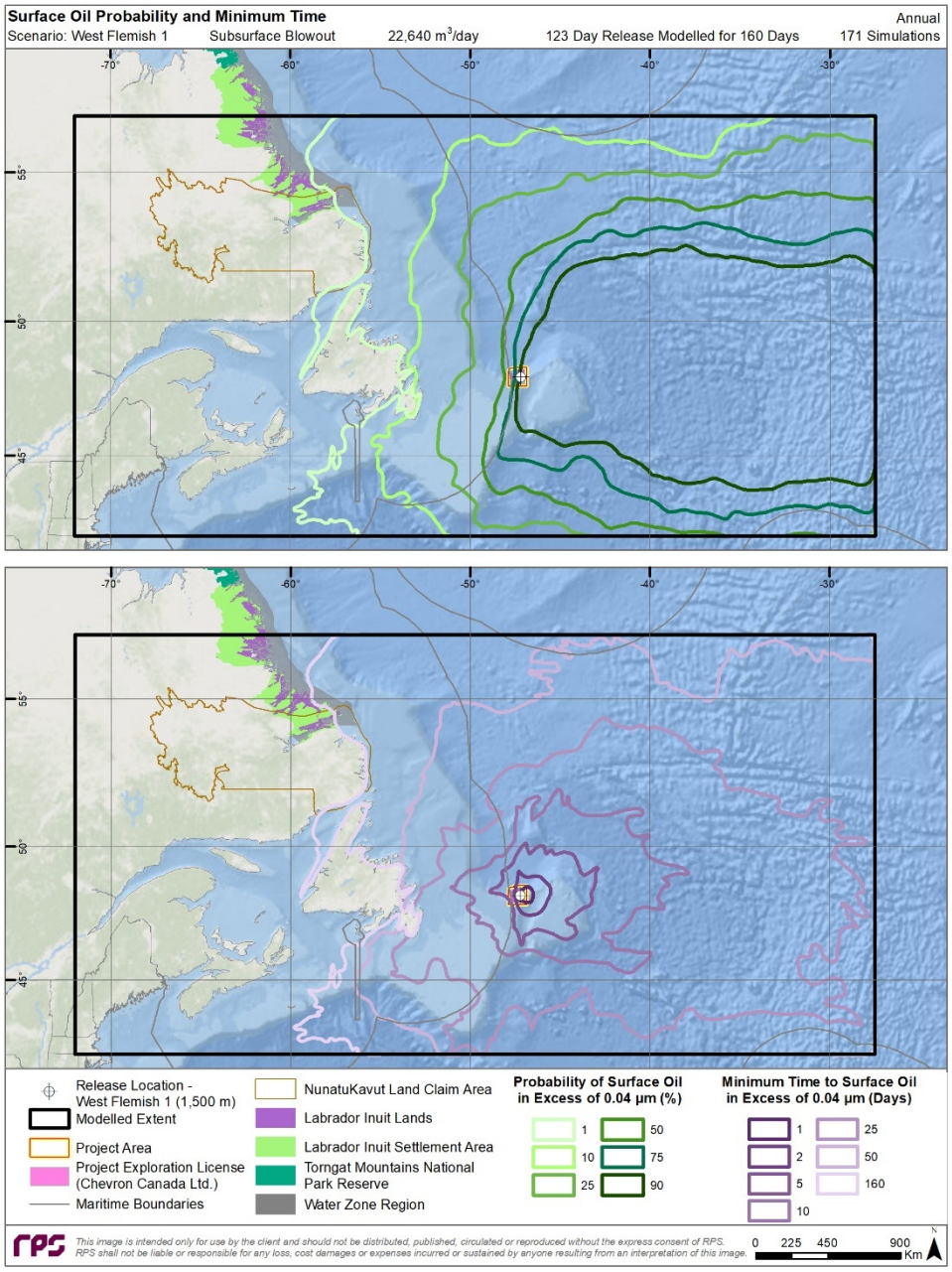

Figure 4-10. Annual probability of surface oil thickness >0.04 µm (top) and minimum time to threshold exceedance (bottom) predictions resulting from a 123-day subsurface blowout at West Flemish 1.

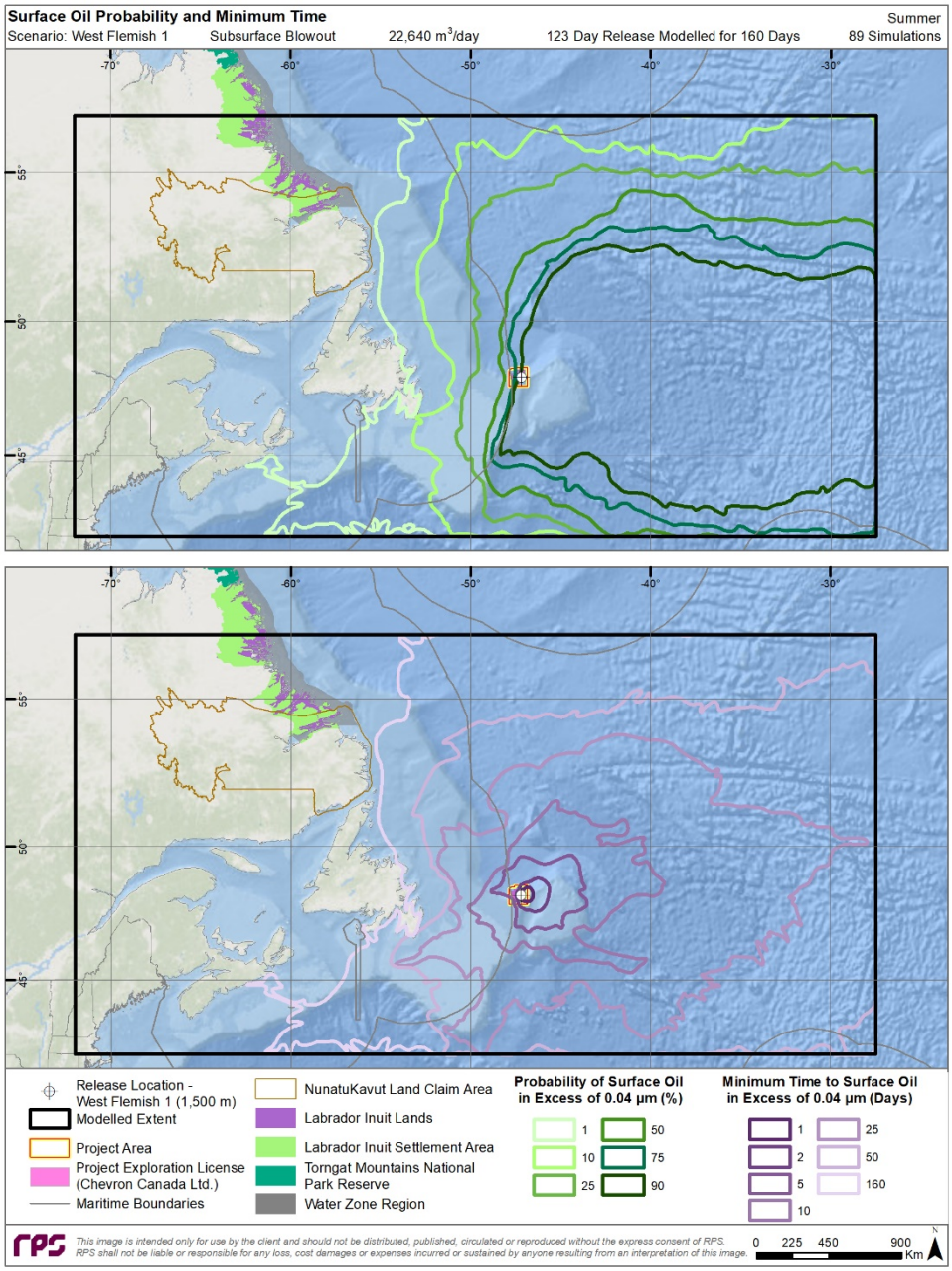

Figure 4-11. Summer probability of surface oil thickness >0.04 µm (top) and minimum time to threshold exceedance (bottom) predictions resulting from a 123-day subsurface blowout at West Flemish 1.

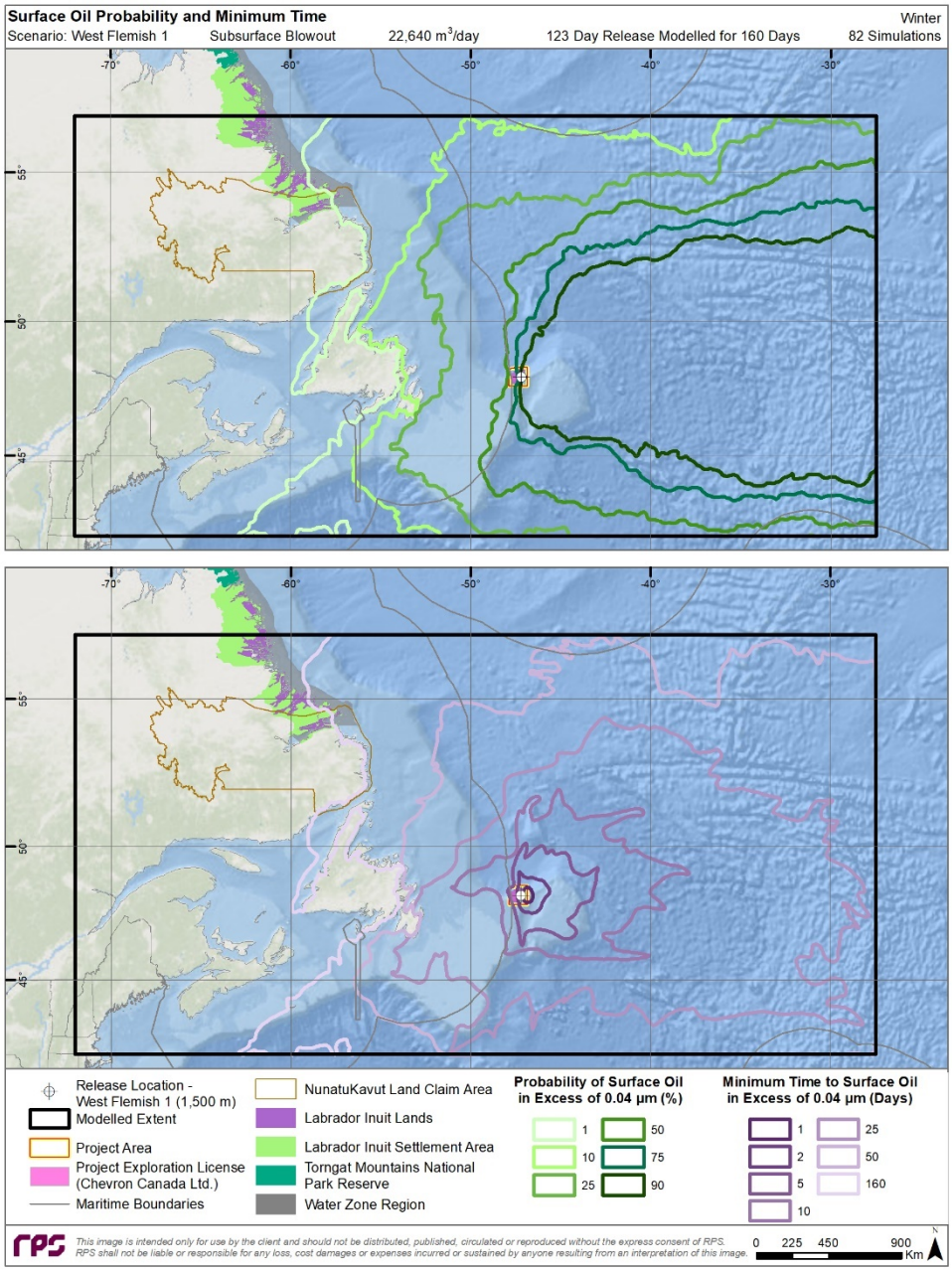

Figure 4-12. Winter probability of surface oil thickness >0.04 µm (top) and minimum time to threshold exceedance (bottom) predictions resulting from a 123-day subsurface blowout at West Flemish 1.

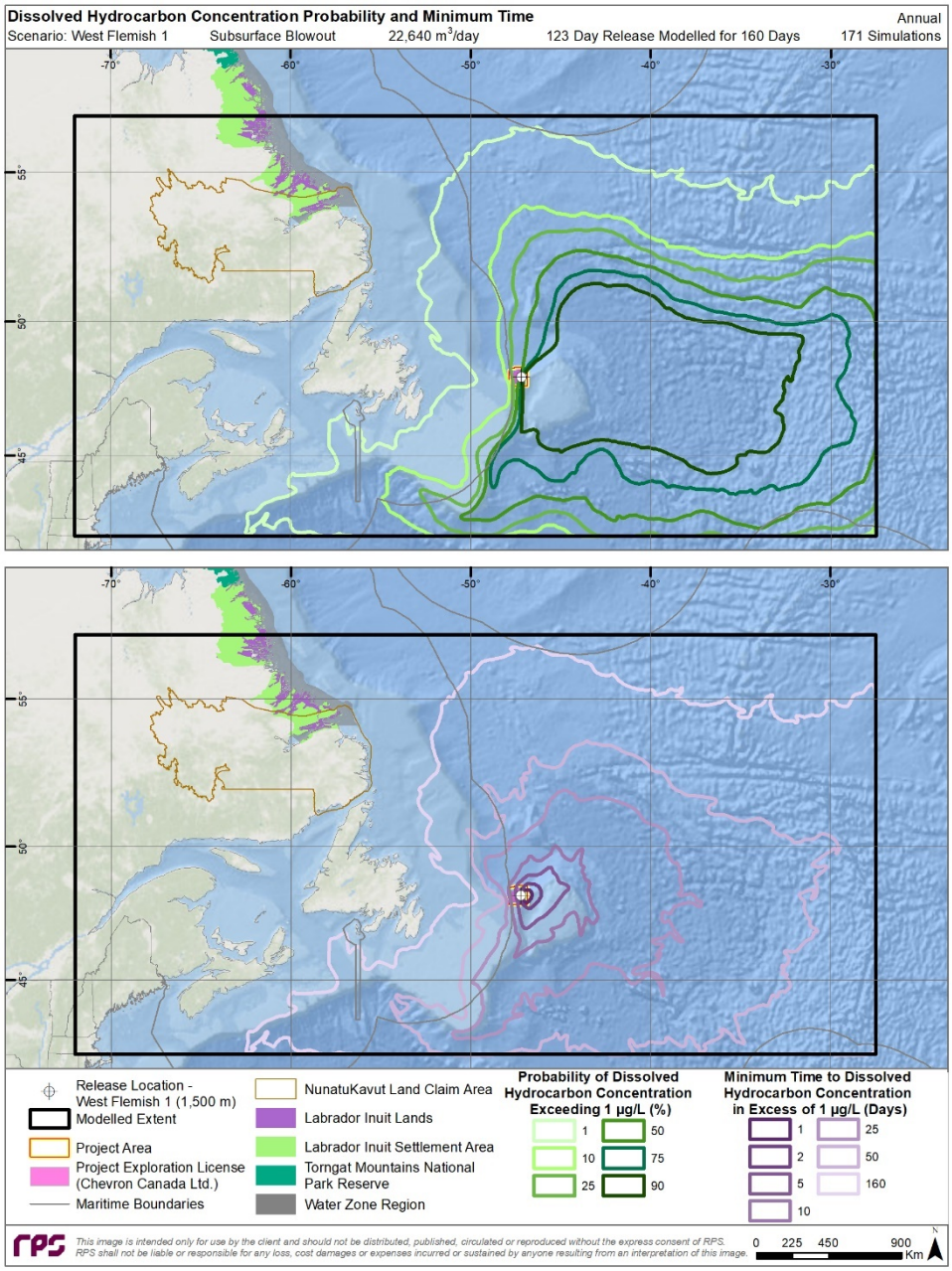

Figure 4-13. Annual probability of dissolved hydrocarbon concentrations >1 µg/L at some depth in the water column (top) and minimum time to threshold exceedance (bottom) predictions resulting from a 123-day subsurface blowout at West Flemish 1.

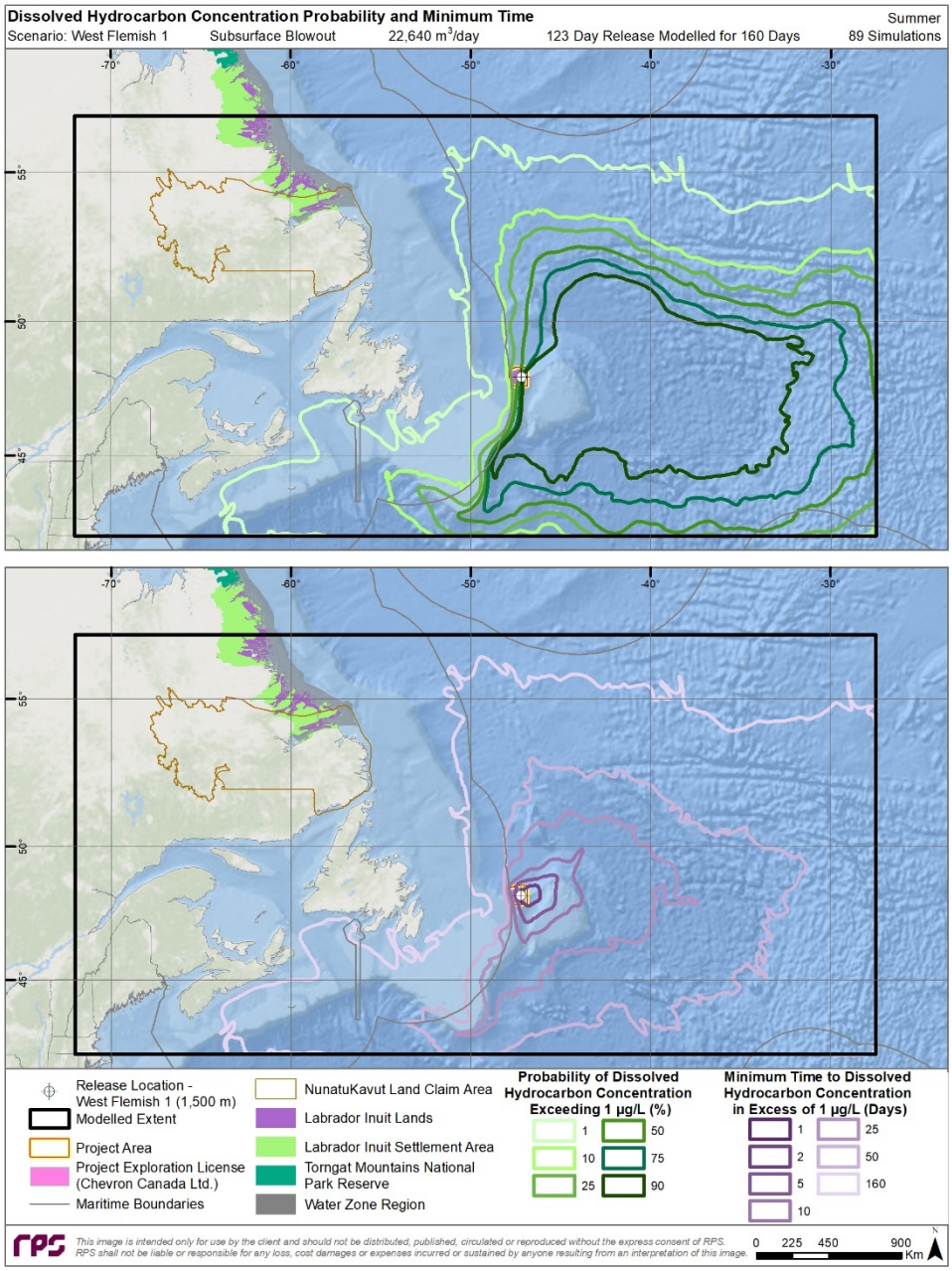

Figure 4-14. Summer probability of dissolved hydrocarbon concentrations >1 µg/L at some depth in the water column (top) and minimum time to threshold exceedance (bottom) predictions resulting from a 123-day subsurface blowout at West Flemish 1.

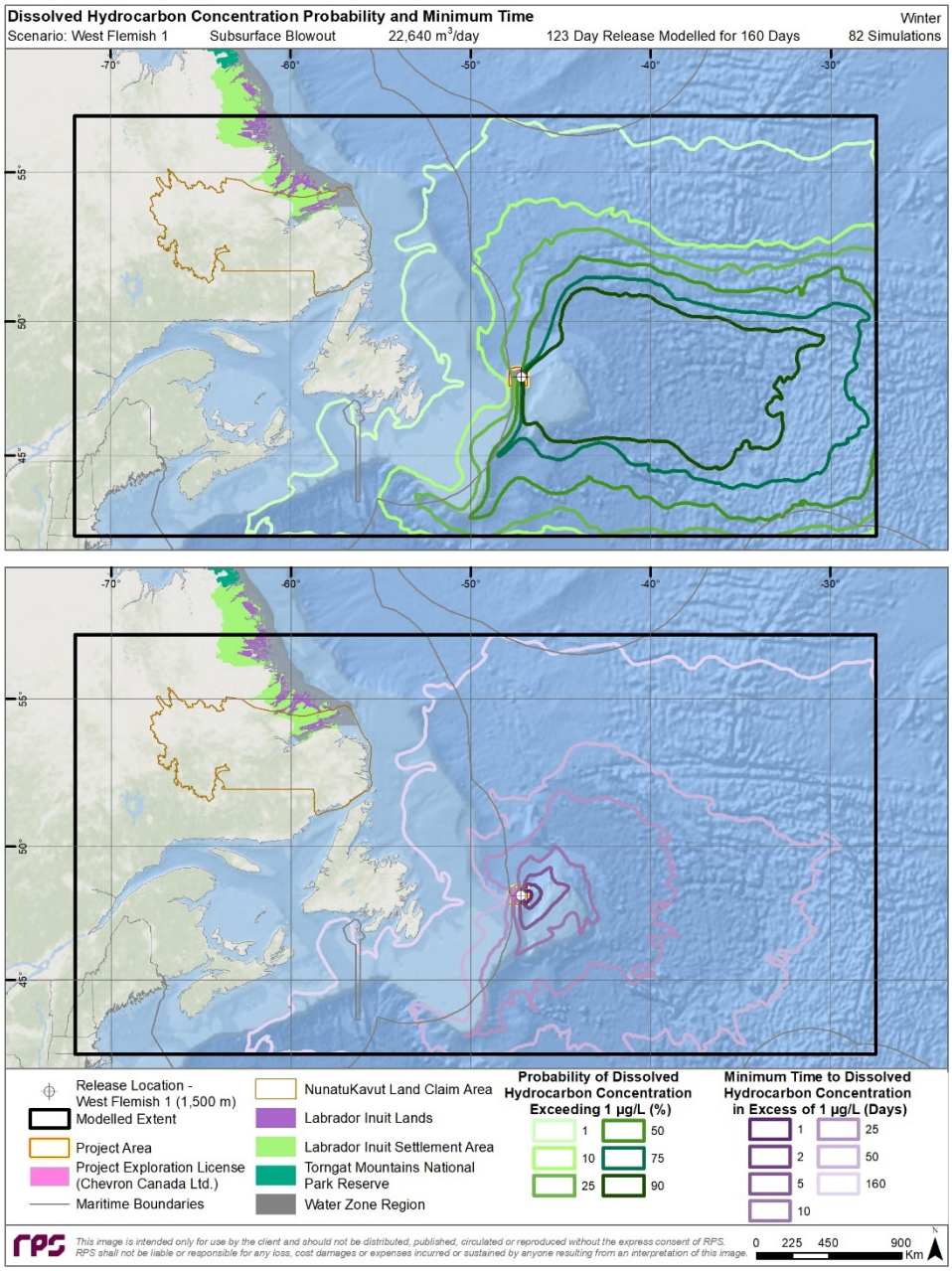

Figure 4-15. Winter probability of dissolved hydrocarbon concentrations >1 µg/L at some depth in the water column (top) and minimum time to threshold exceedance (bottom) predictions resulting from a 123-day subsurface blowout at West Flemish 1.

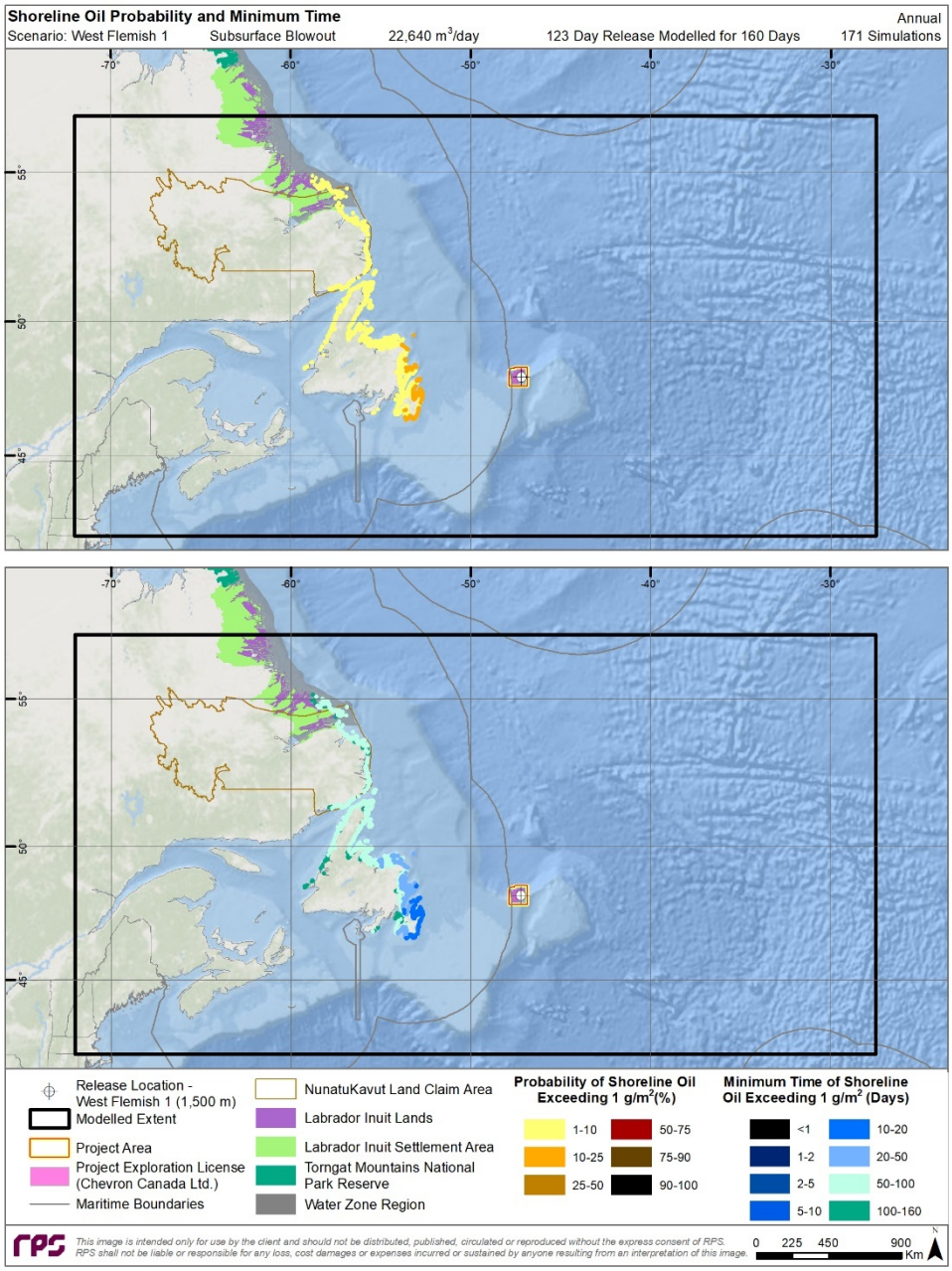

Figure 4-16. Annual probability of shoreline contact >1 g/m^2 (top) and minimum time to threshold exceedance (bottom) predictions resulting from a 123-day subsurface blowout at West Flemish 1.

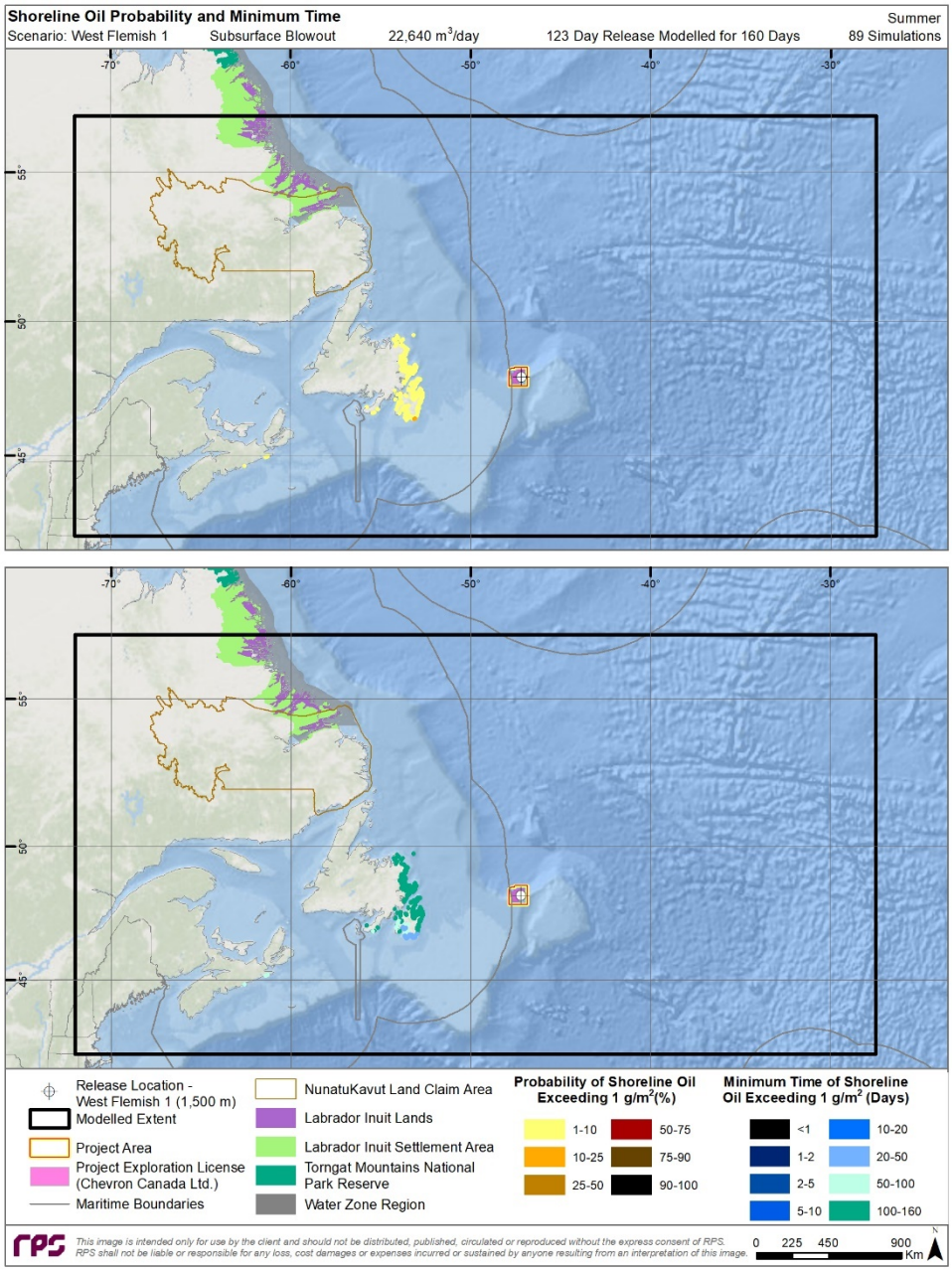

Figure 4-17. Summer probability of shoreline contact >1 g/m^2 (top) and minimum time to threshold exceedance (bottom) predictions resulting from a 123-day subsurface blowout at West Flemish 1.

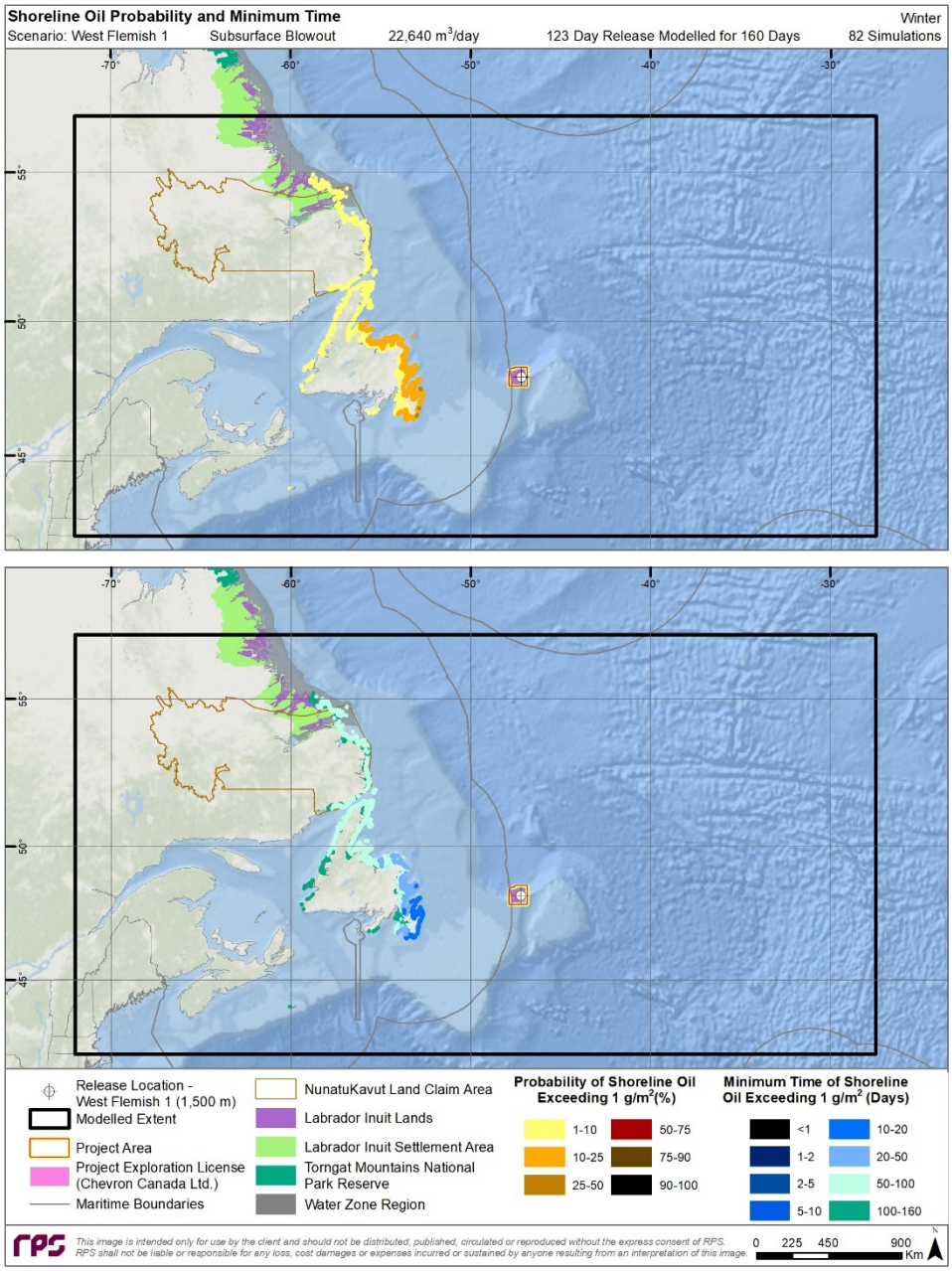

Figure 4-18. Winter probability of shoreline contact >1 g/m² (top) and minimum time to threshold exceedance (bottom) predictions resulting from a 123-day subsurface blowout at West Flemish 1.

4.1.2 West Flemish 2 Results

4.1.2.1 27-day Subsurface Release

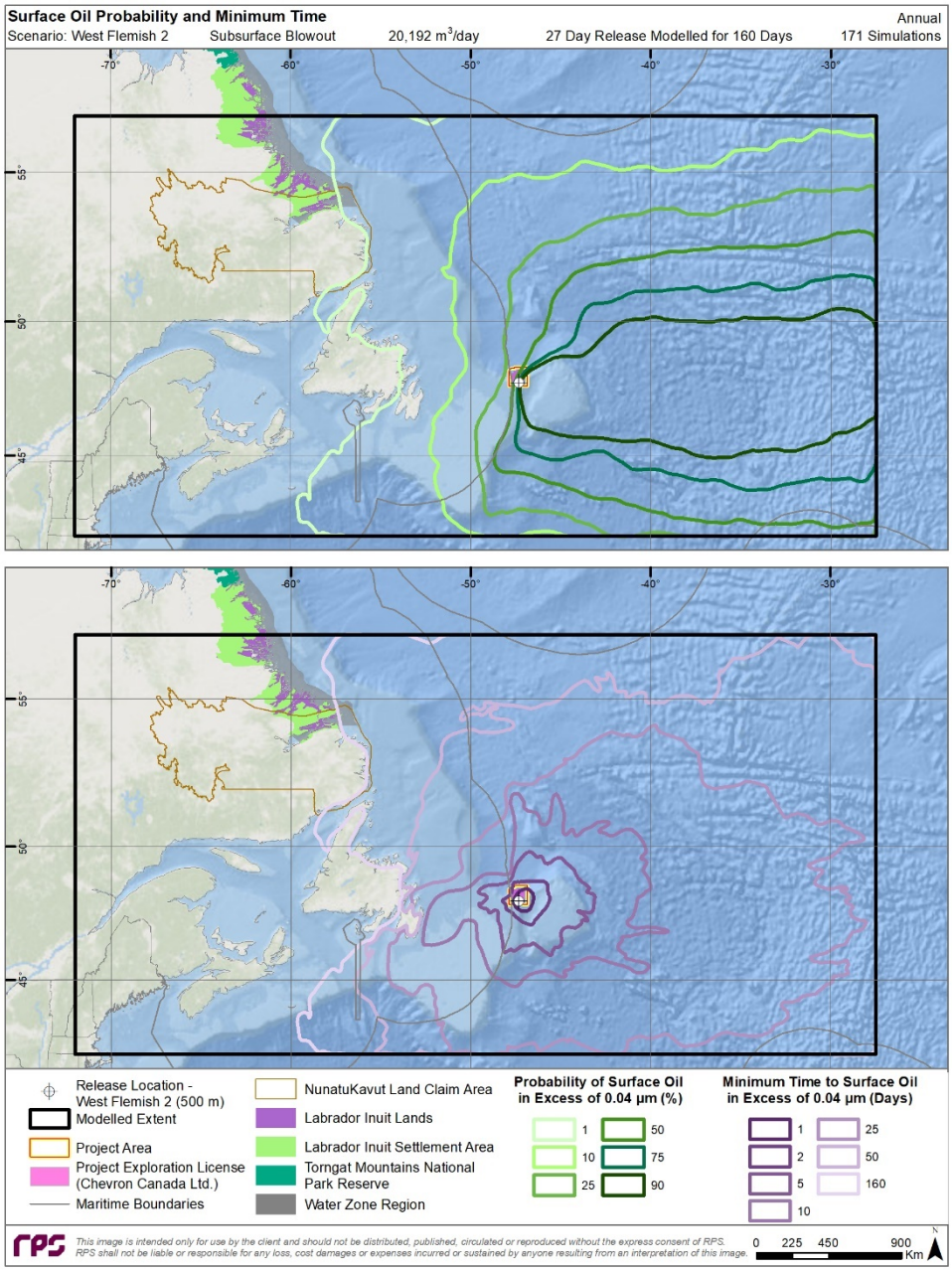

Figure 4-19. Annual probability of surface oil thickness >0.04 µm (top) and minimum time to threshold exceedance (bottom) predictions resulting from a 27-day subsurface blowout at West Flemish 2.

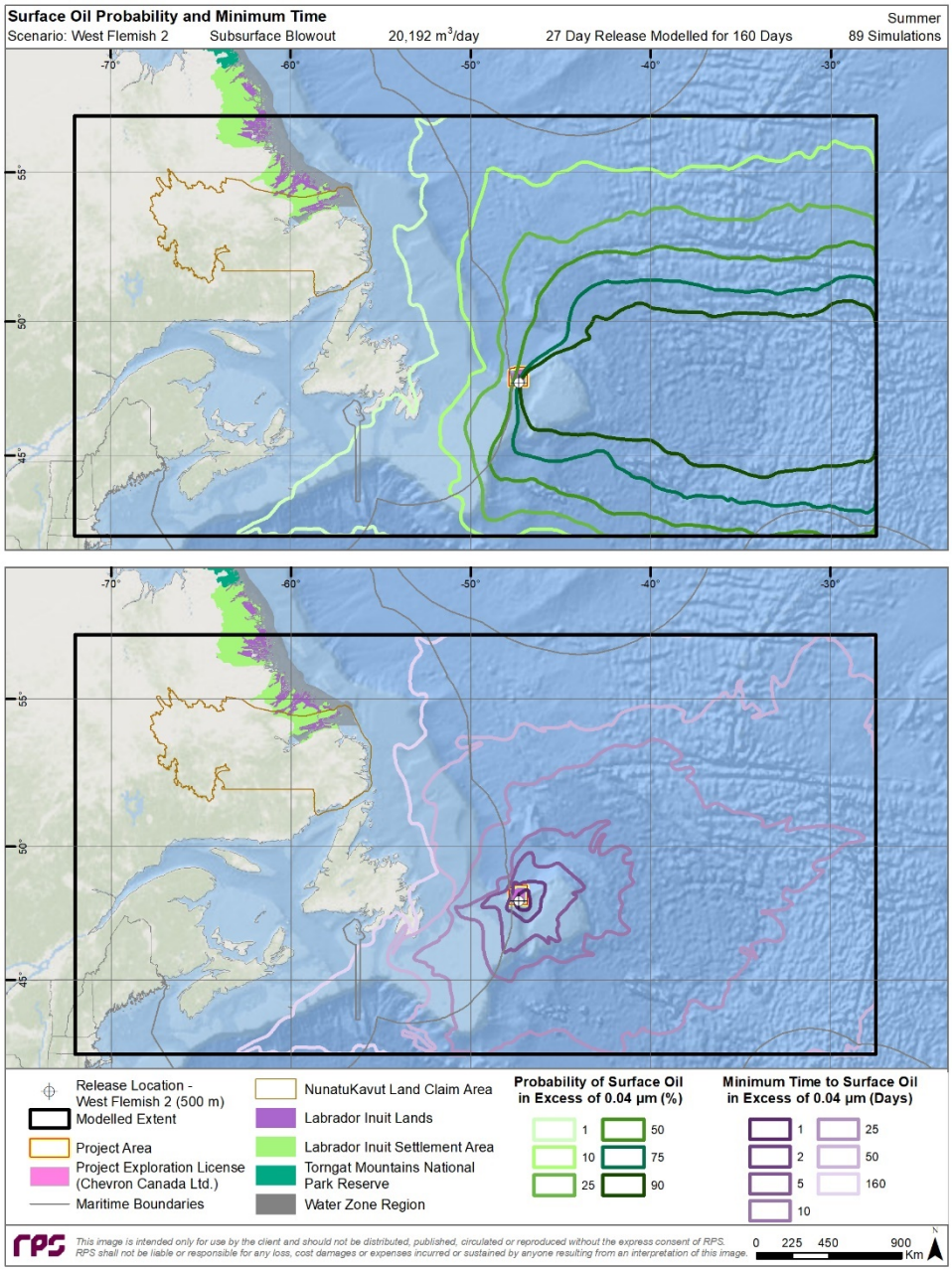

Figure 4-20. Summer probability of surface oil thickness >0.04 µm (top) and minimum time to threshold exceedance (bottom) predictions resulting from a 27-day subsurface blowout at West Flemish 2.

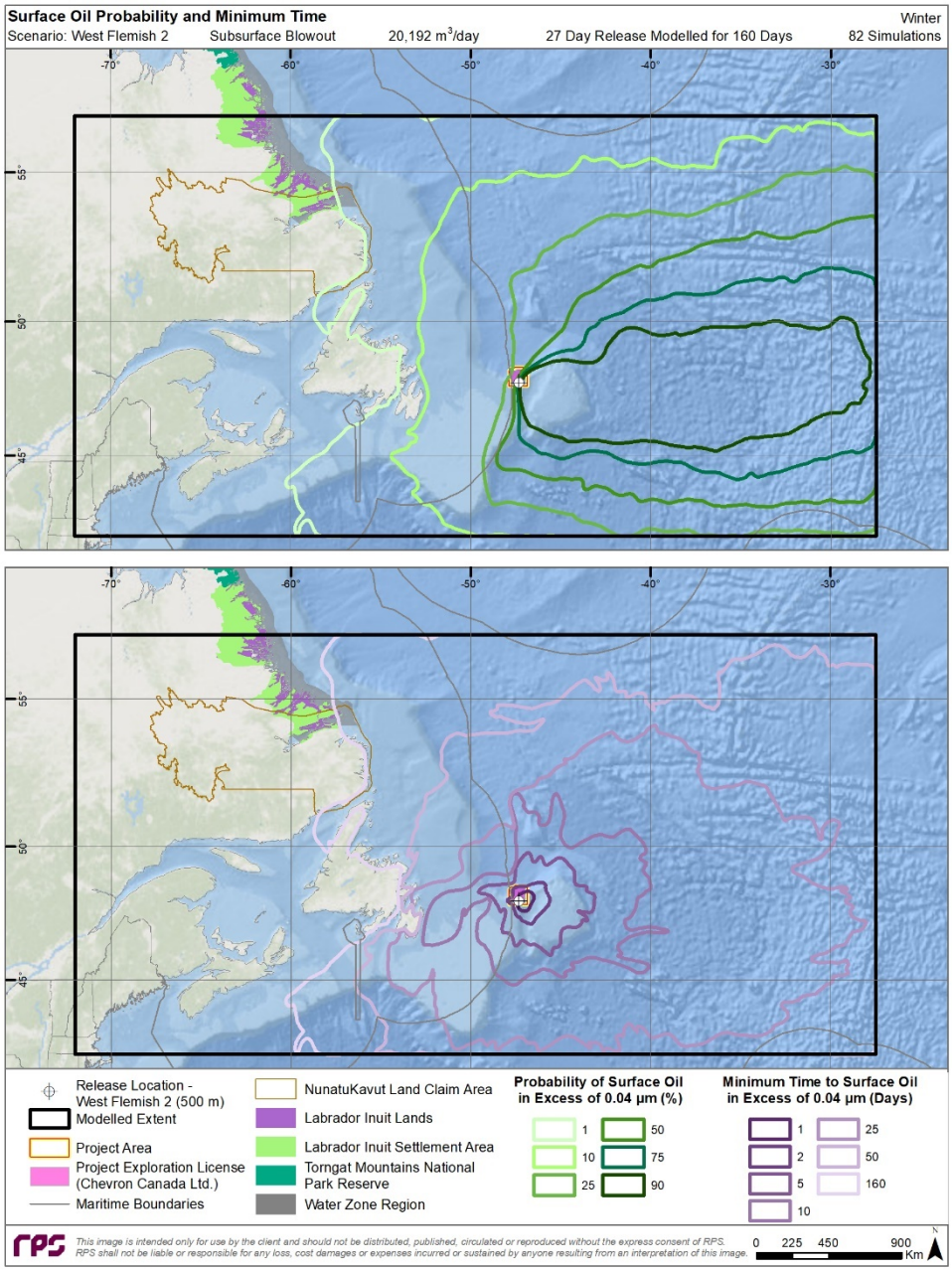

Figure 4-21. Winter probability of surface oil thickness >0.04 µm (top) and minimum time to threshold exceedance (bottom) predictions resulting from a 27-day subsurface blowout at West Flemish 2.

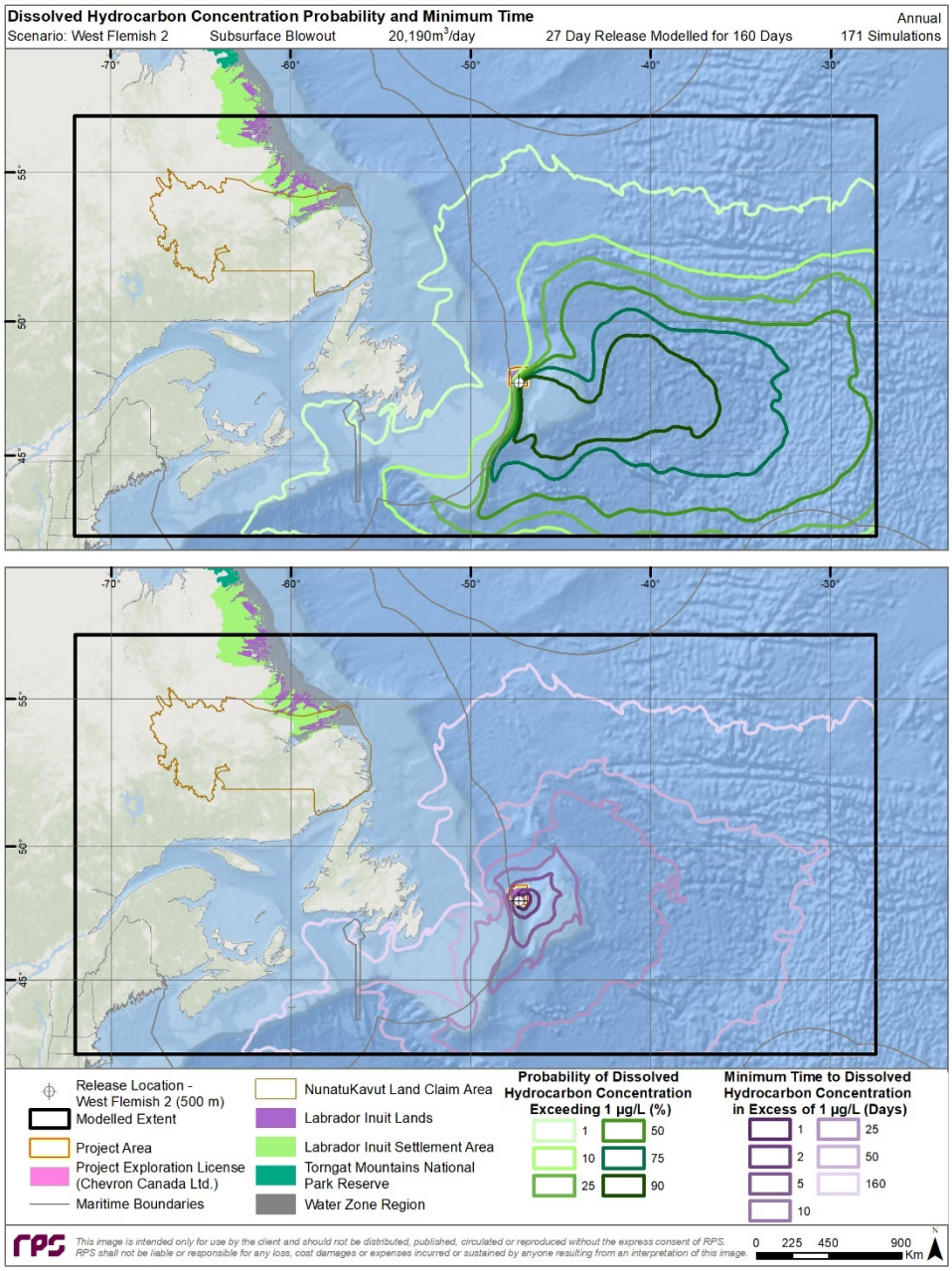

Figure 4-22. Annual probability of dissolved hydrocarbon concentrations >1 µg/L at some depth in the water column (top) and minimum time to threshold exceedance (bottom) predictions resulting from a 27-day subsurface blowout at West Flemish 2.

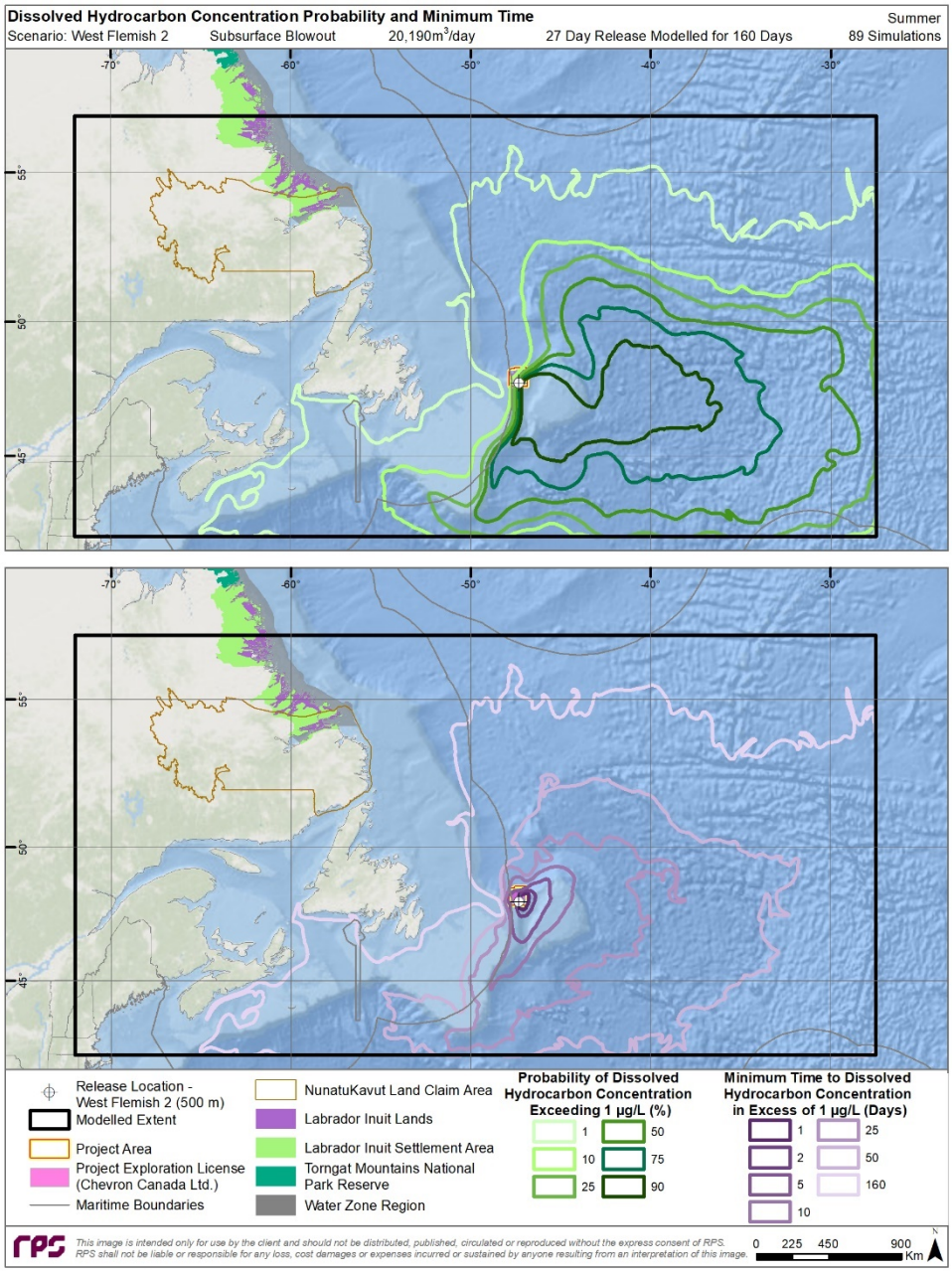

Figure 4-23. Summer probability of dissolved hydrocarbon concentrations >1 µg/L at some depth in the water column (top) and minimum time to threshold exceedance (bottom) predictions resulting from a 27-day subsurface blowout at West Flemish 2.

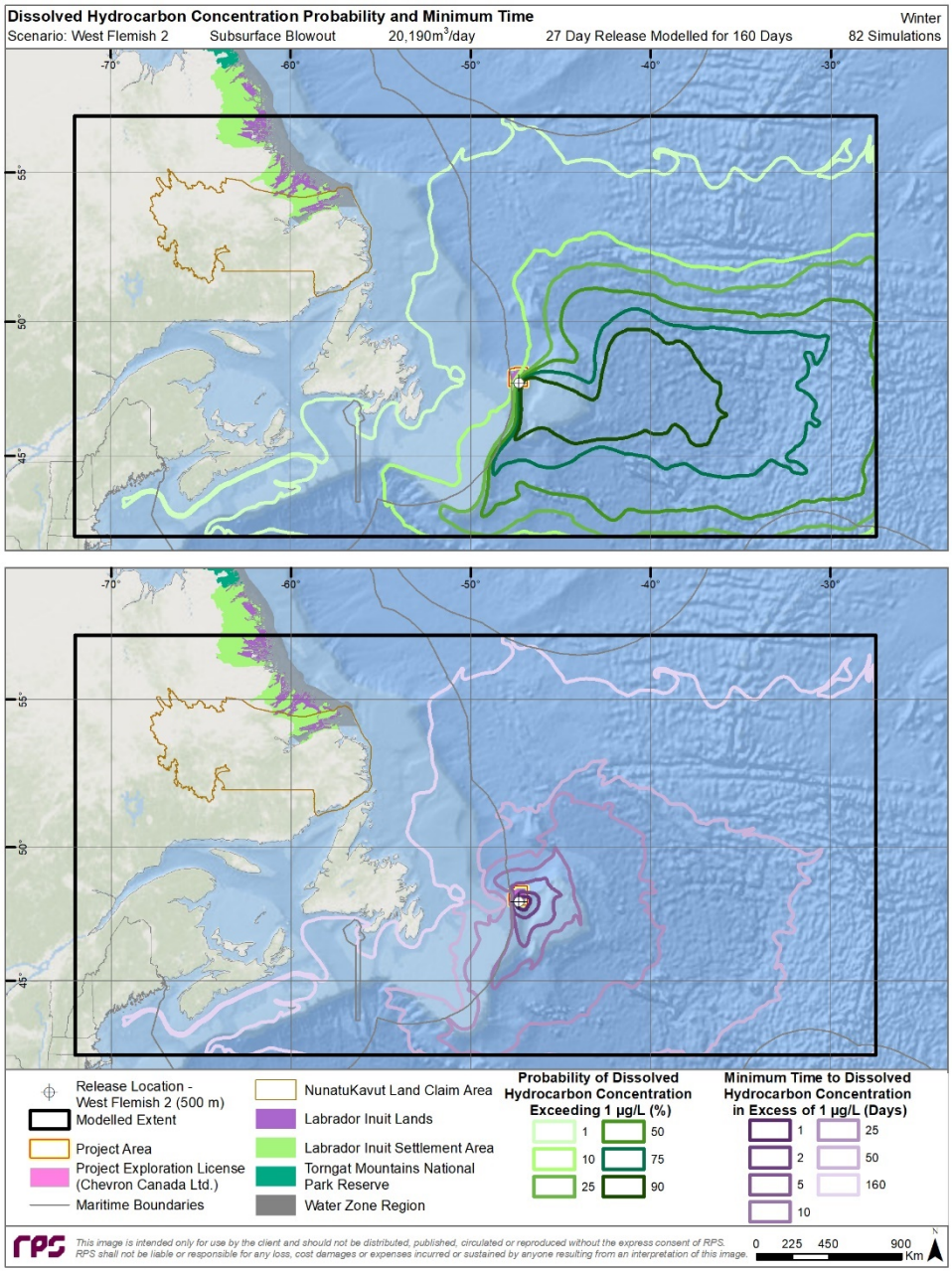

Figure 4-24. Winter probability of dissolved hydrocarbon concentrations >1 µg/L at some depth in the water column (top) and minimum time to threshold exceedance (bottom) predictions resulting from a 27-day subsurface blowout at West Flemish 2.

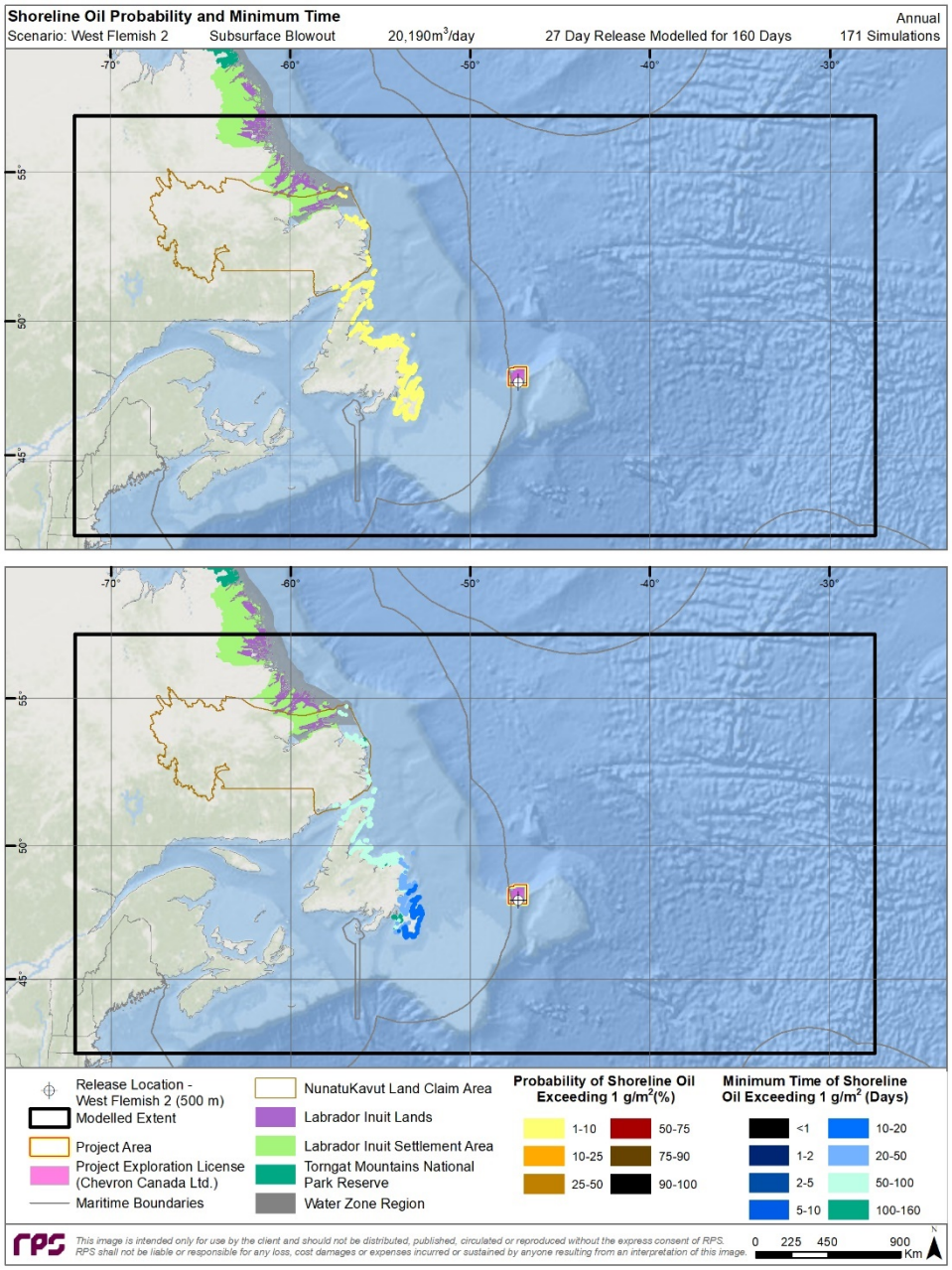

Figure 4-25. Annual probability of shoreline contact >1 g/m^2 (top) and minimum time to threshold exceedance (bottom) predictions resulting from a 27-day subsurface blowout at West Flemish 2.

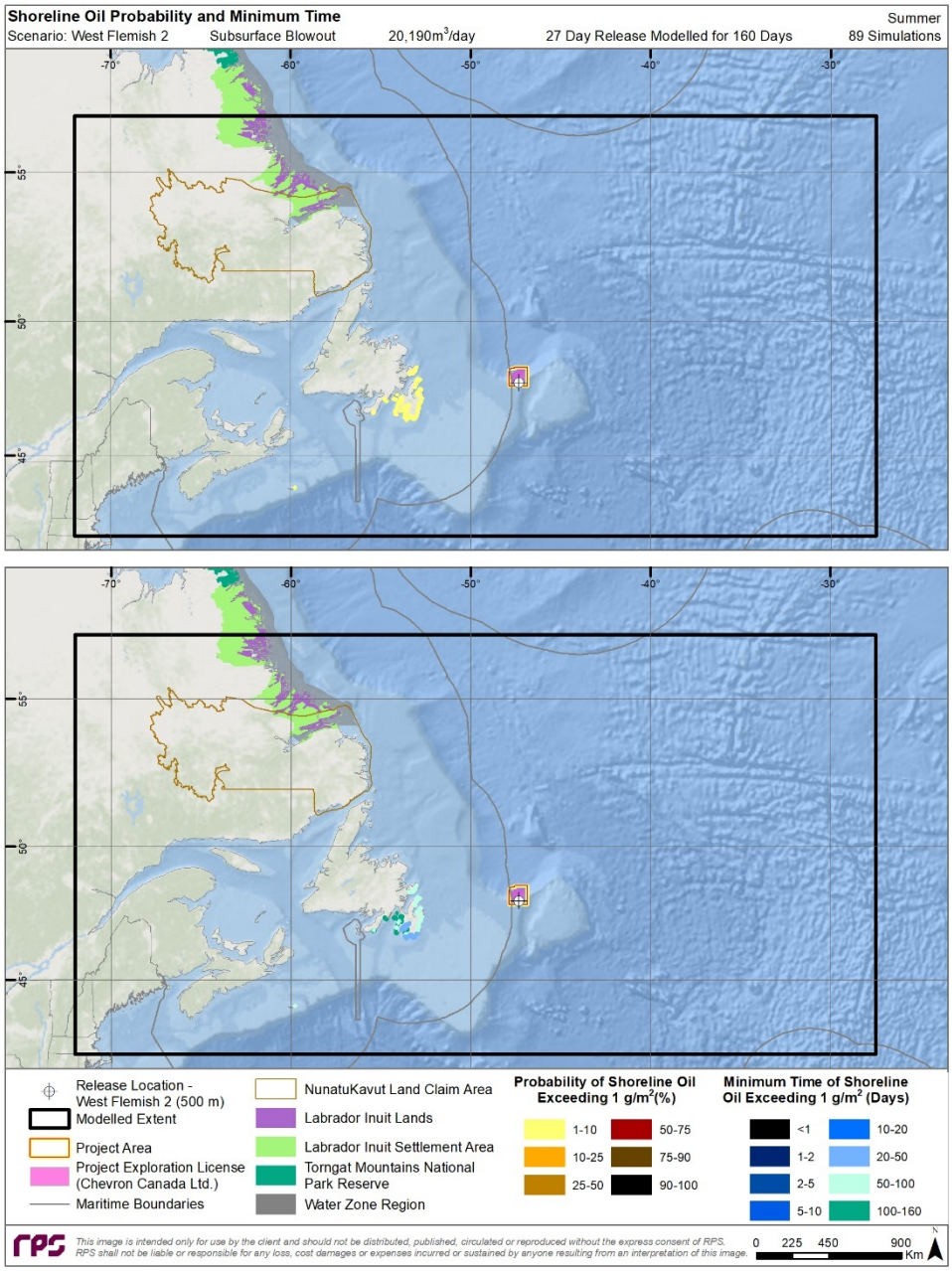

Figure 4-26. Summer probability of shoreline contact >1 g/m^2 (top) and minimum time to threshold exceedance (bottom) predictions resulting from a 27-day subsurface blowout at West Flemish 2.

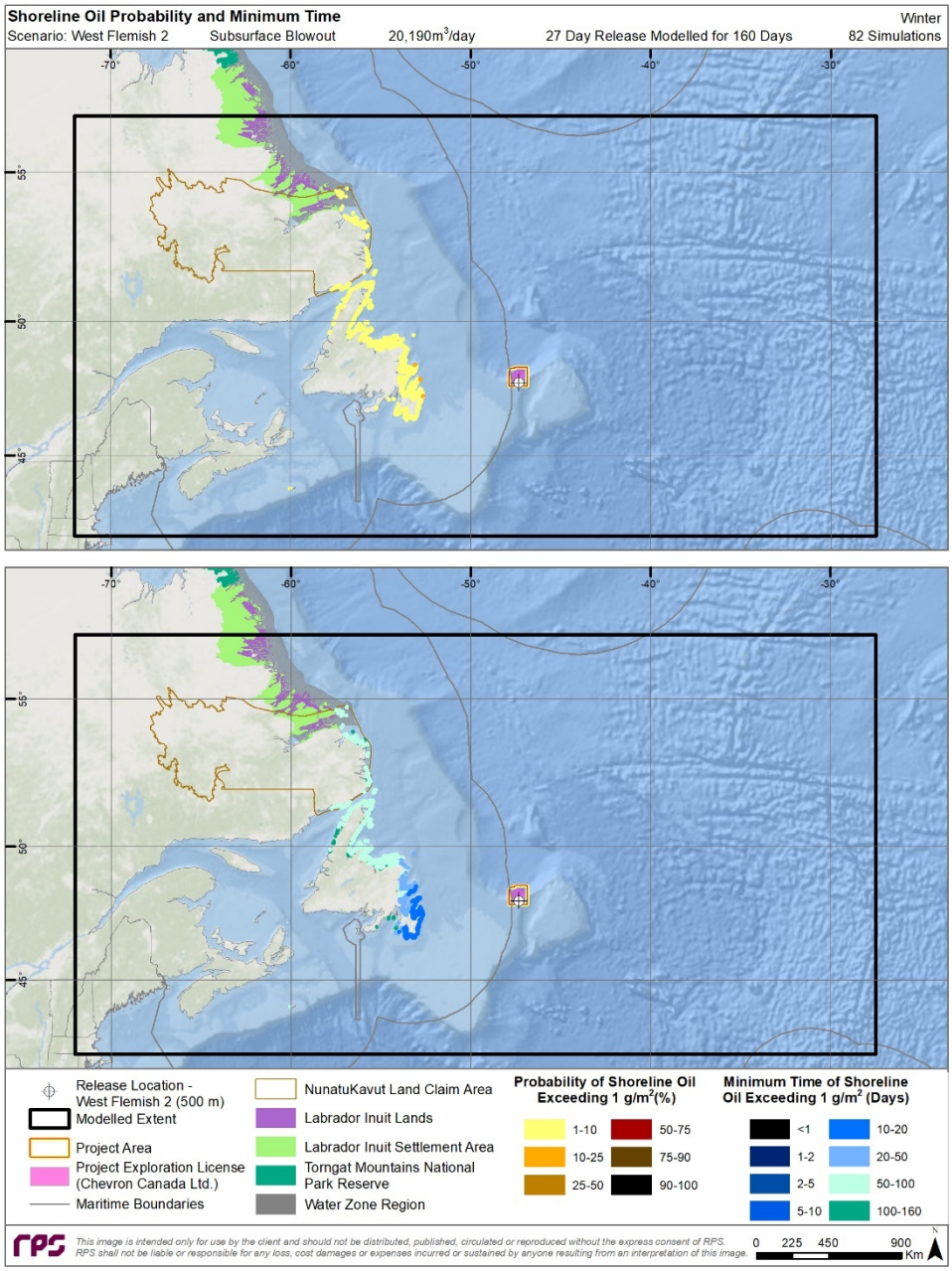

Figure 4-27. Winter probability of shoreline contact >1 g/m² (top) and minimum time to threshold exceedance (bottom) predictions resulting from a 27-day subsurface blowout at West Flemish 2.

4.1.2.2 135-day Subsurface Release

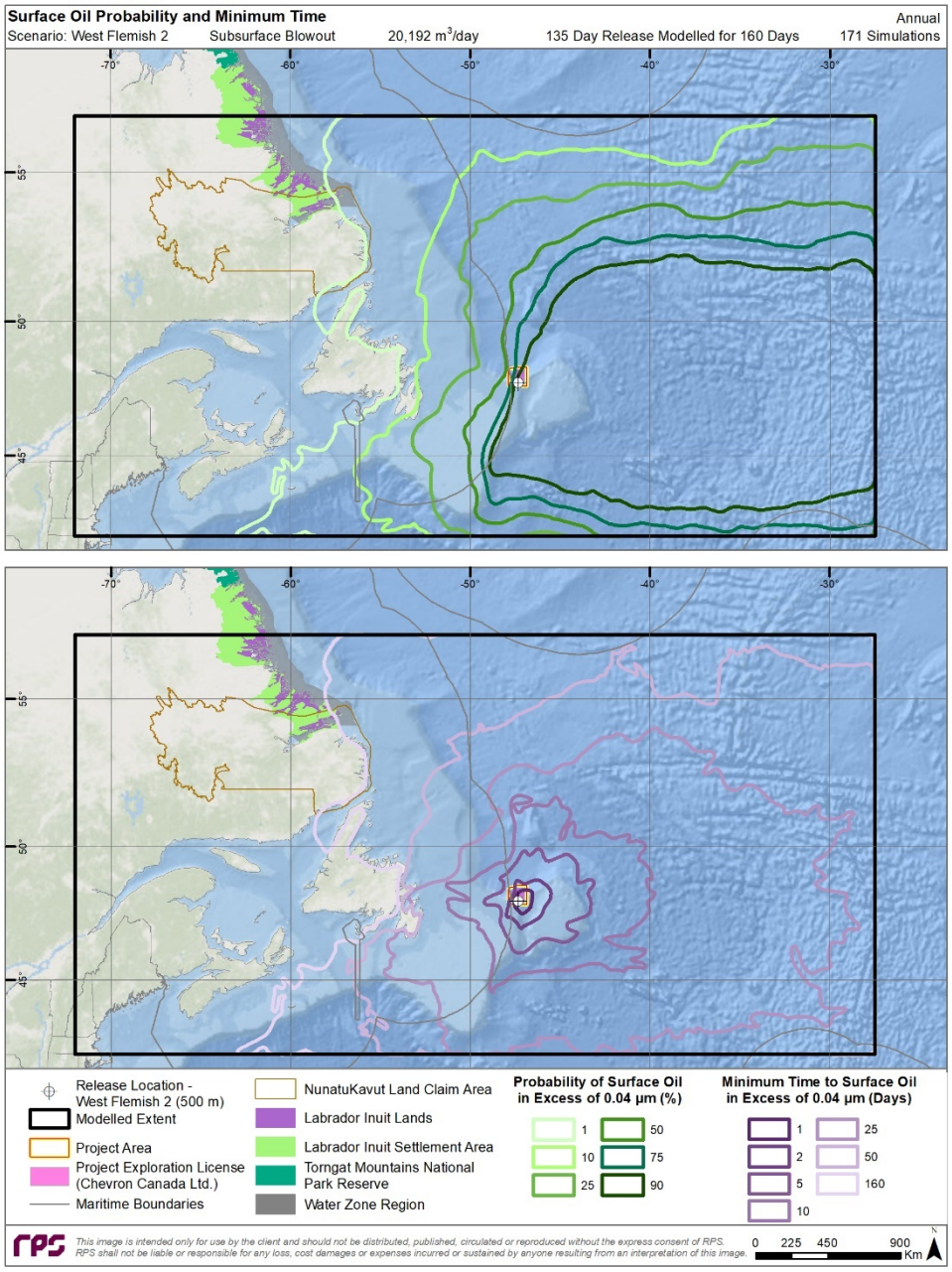

Figure 4-28. Annual probability of surface oil thickness >0.04 µm (top) and minimum time to threshold exceedance (bottom) predictions resulting from a 135-day subsurface blowout at West Flemish 2.

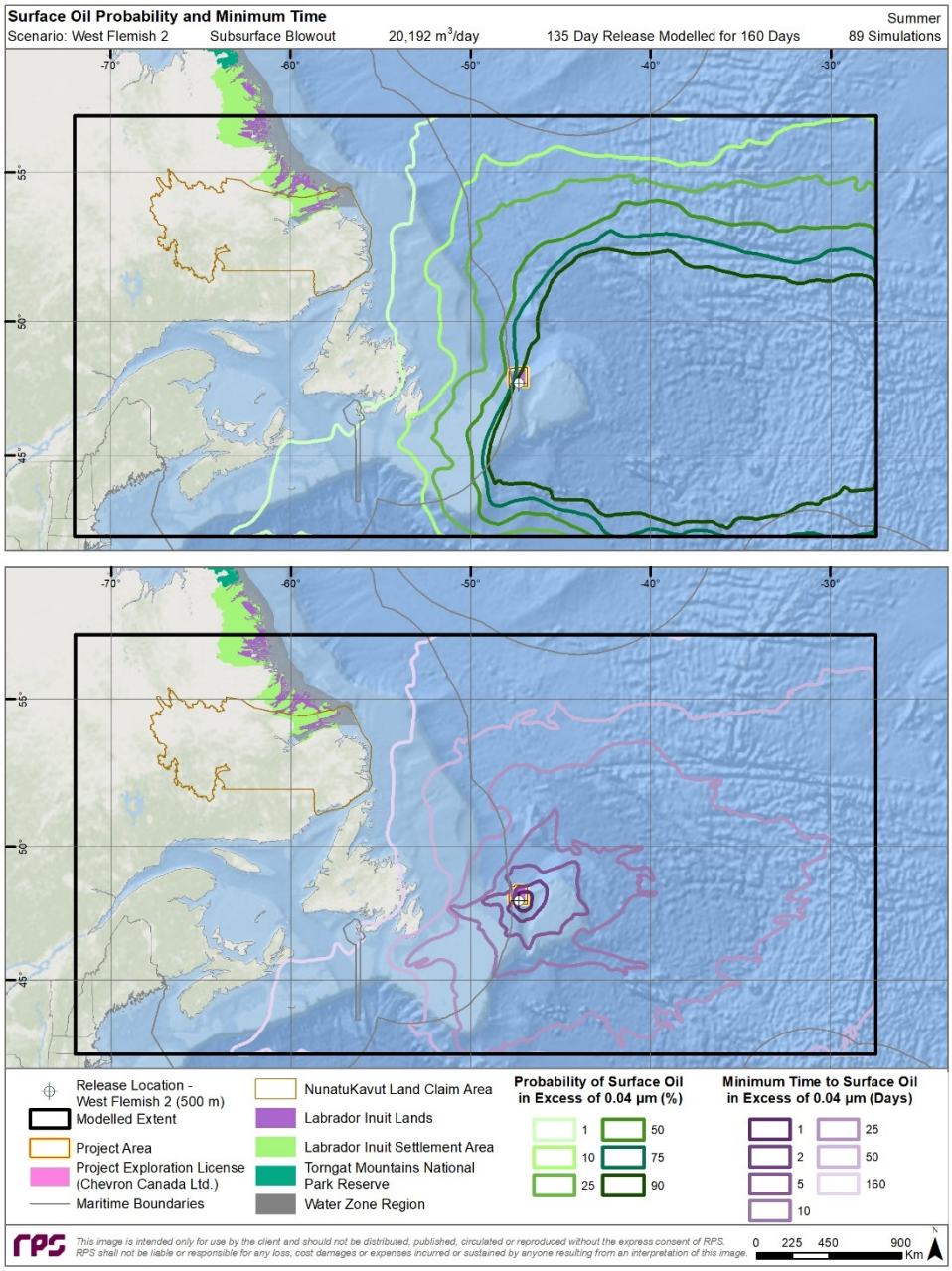

Figure 4-29. Summer probability of surface oil thickness >0.04 µm (top) and minimum time to threshold exceedance (bottom) predictions resulting from a 135-day subsurface blowout at West Flemish 2.

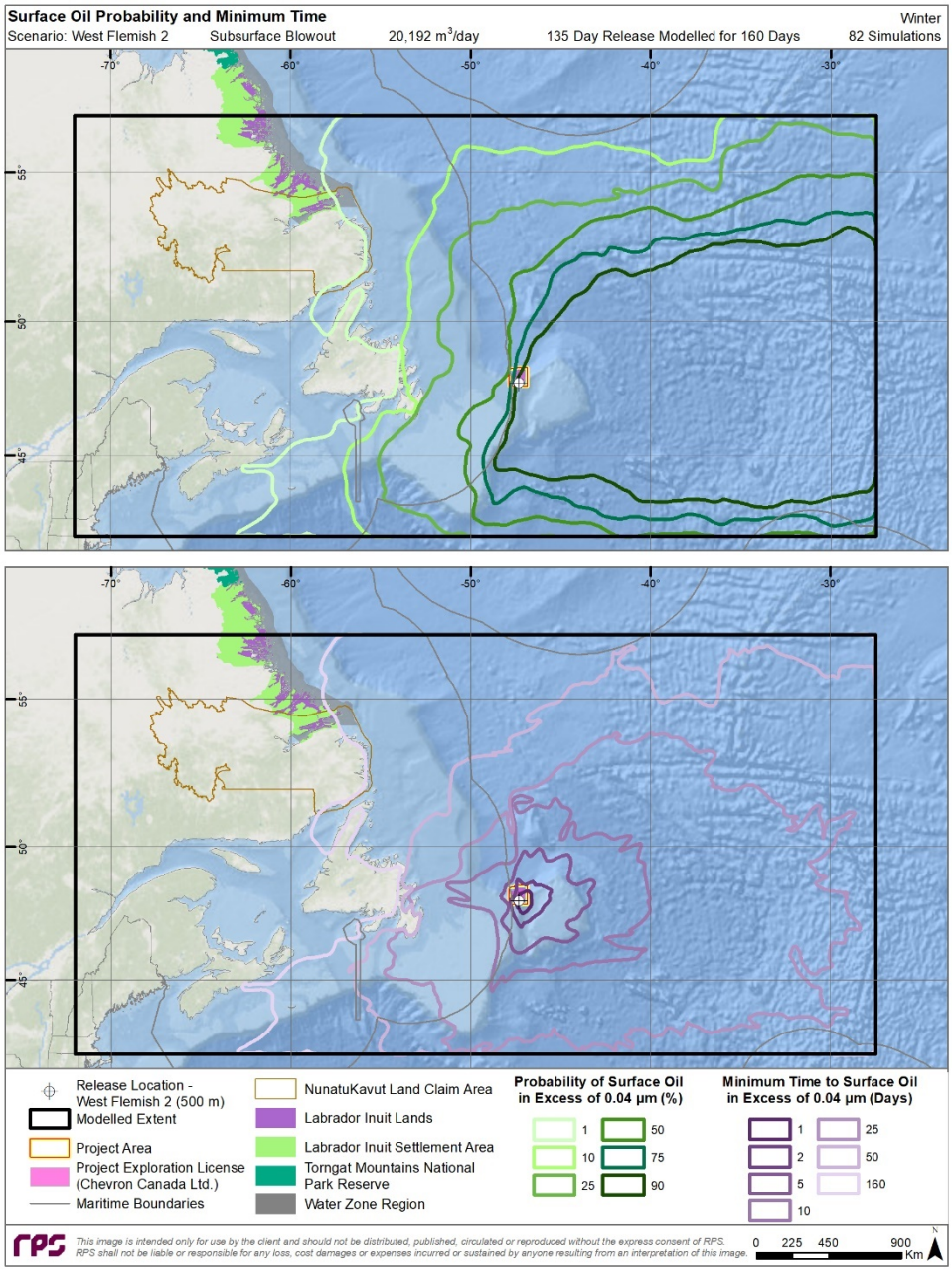

Figure 4-30. Winter probability of surface oil thickness >0.04 µm (top) and minimum time to threshold exceedance (bottom) predictions resulting from a 135-day subsurface blowout at West Flemish 2.

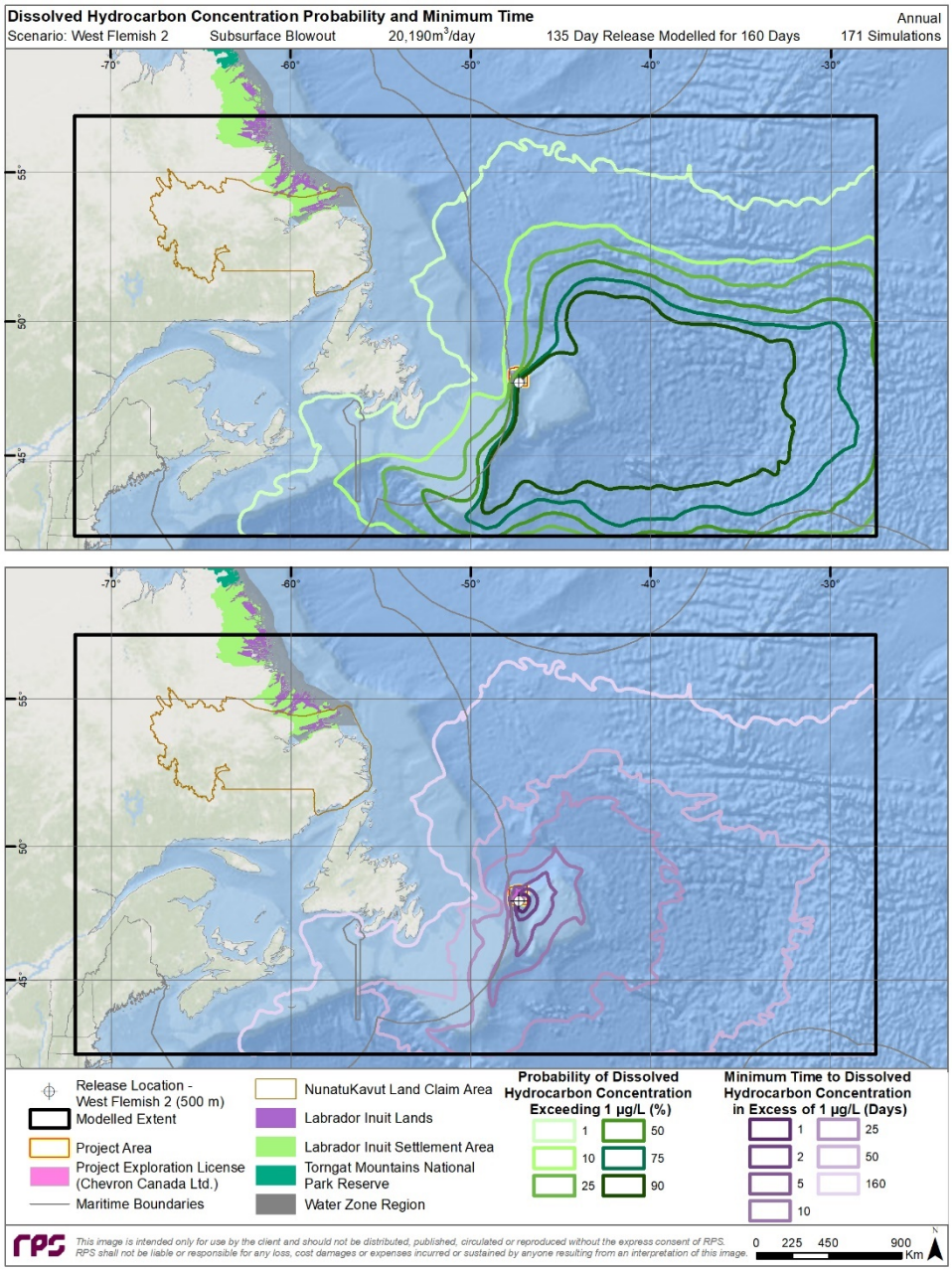

Figure 4-31. Annual probability of dissolved hydrocarbon concentrations >1 µg/L at some depth in the water column (top) and minimum time to threshold exceedance (bottom) predictions resulting from a 135-day subsurface blowout at West Flemish 2.

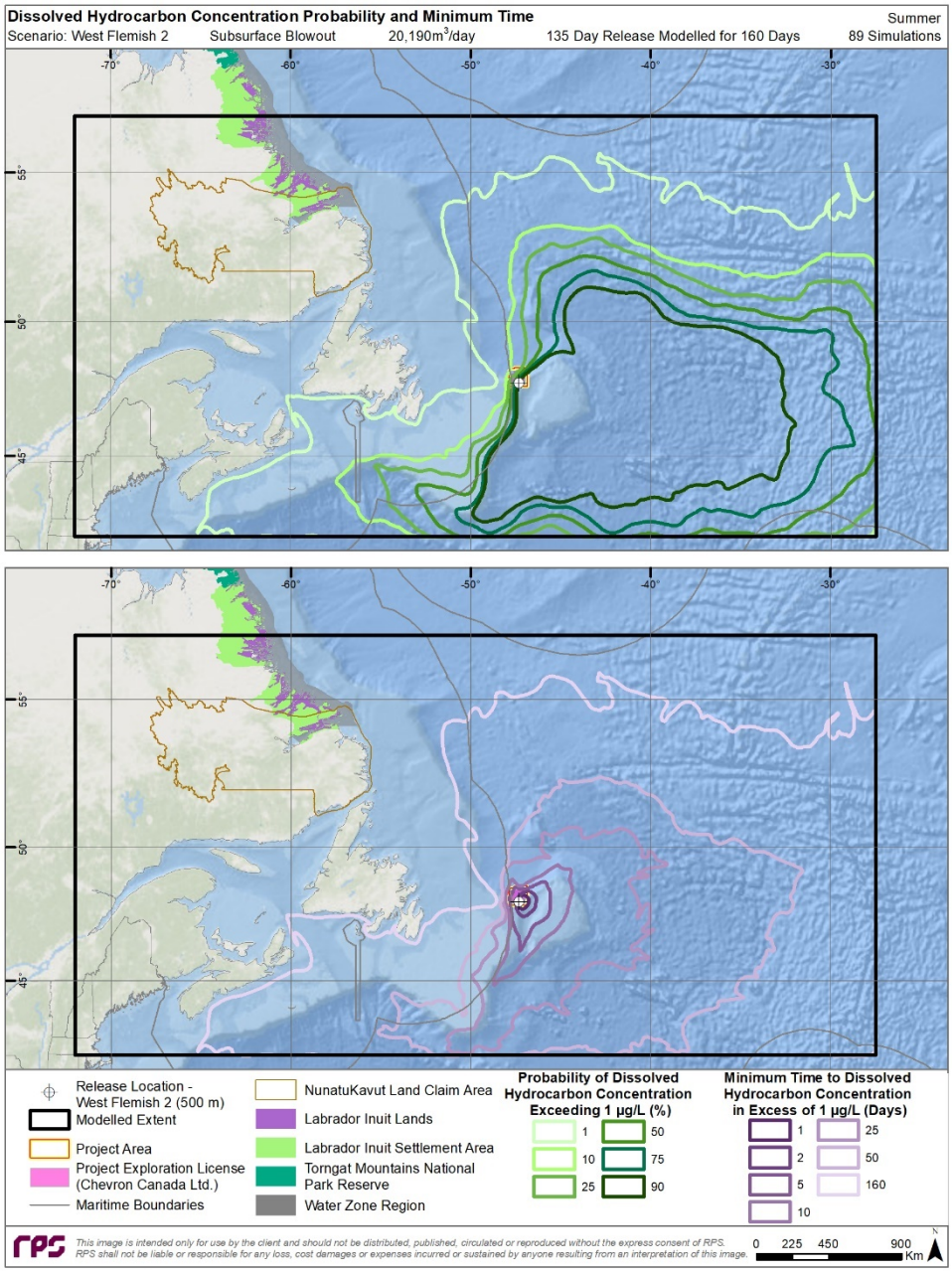

Figure 4-32. Summer probability of dissolved hydrocarbon concentrations >1 µg/L at some depth in the water column (top) and minimum time to threshold exceedance (bottom) predictions resulting from a 135-day subsurface blowout at West Flemish 2.

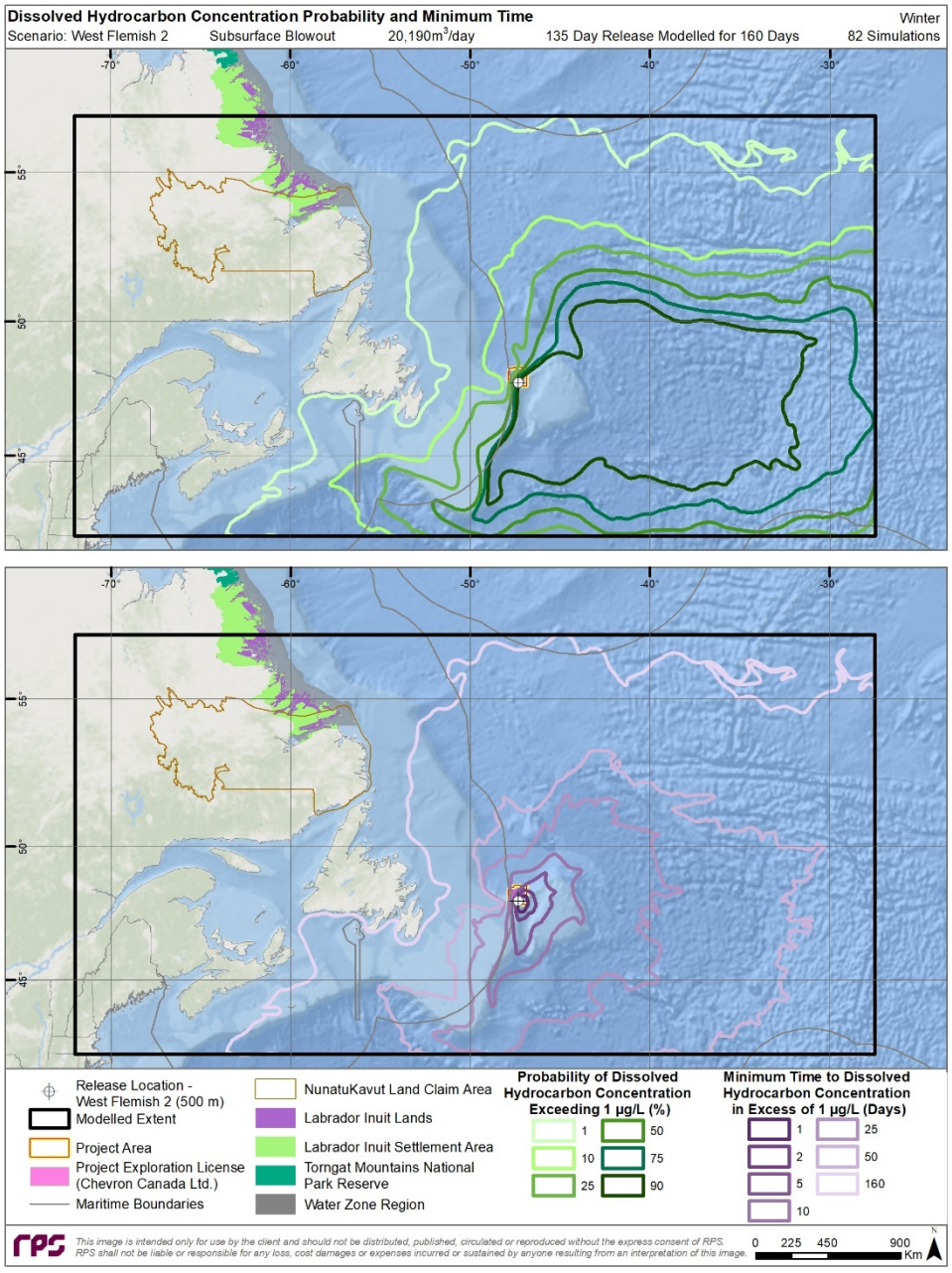

Figure 4-33. Winter probability of dissolved hydrocarbon concentrations >1 µg/L at some depth in the water column (top) and minimum time to threshold exceedance (bottom) predictions resulting from a 135-day subsurface blowout at West Flemish 2.

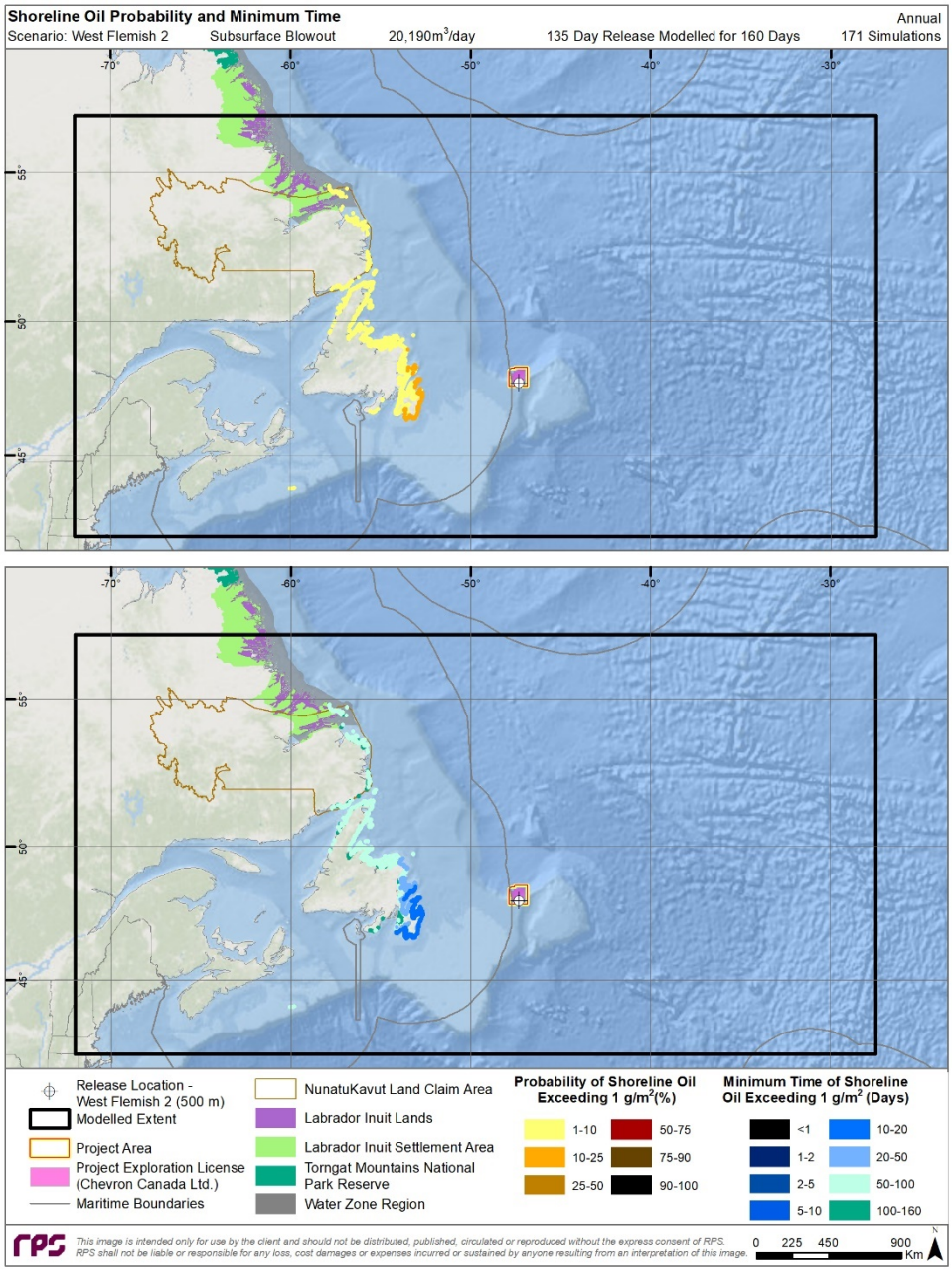

Figure 4-34. Annual probability of shoreline contact >1 g/m^2 (top) and minimum time to threshold exceedance (bottom) predictions resulting from a 135-day subsurface blowout at West Flemish 2.

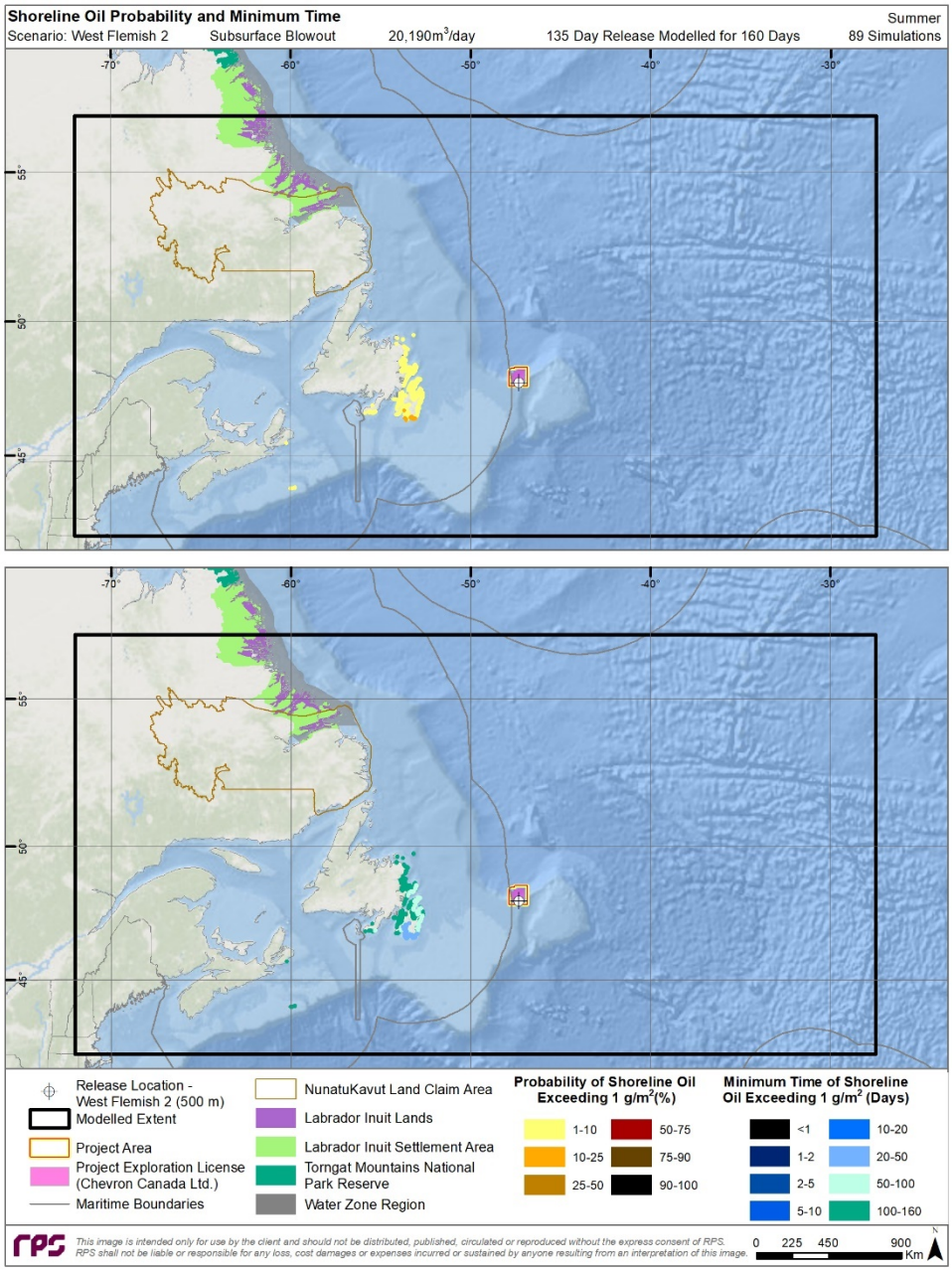

Figure 4-35. Summer probability of shoreline contact >1 g/m^2 (top) and minimum time to threshold exceedance (bottom) predictions resulting from a 135-day subsurface blowout at West Flemish 2.

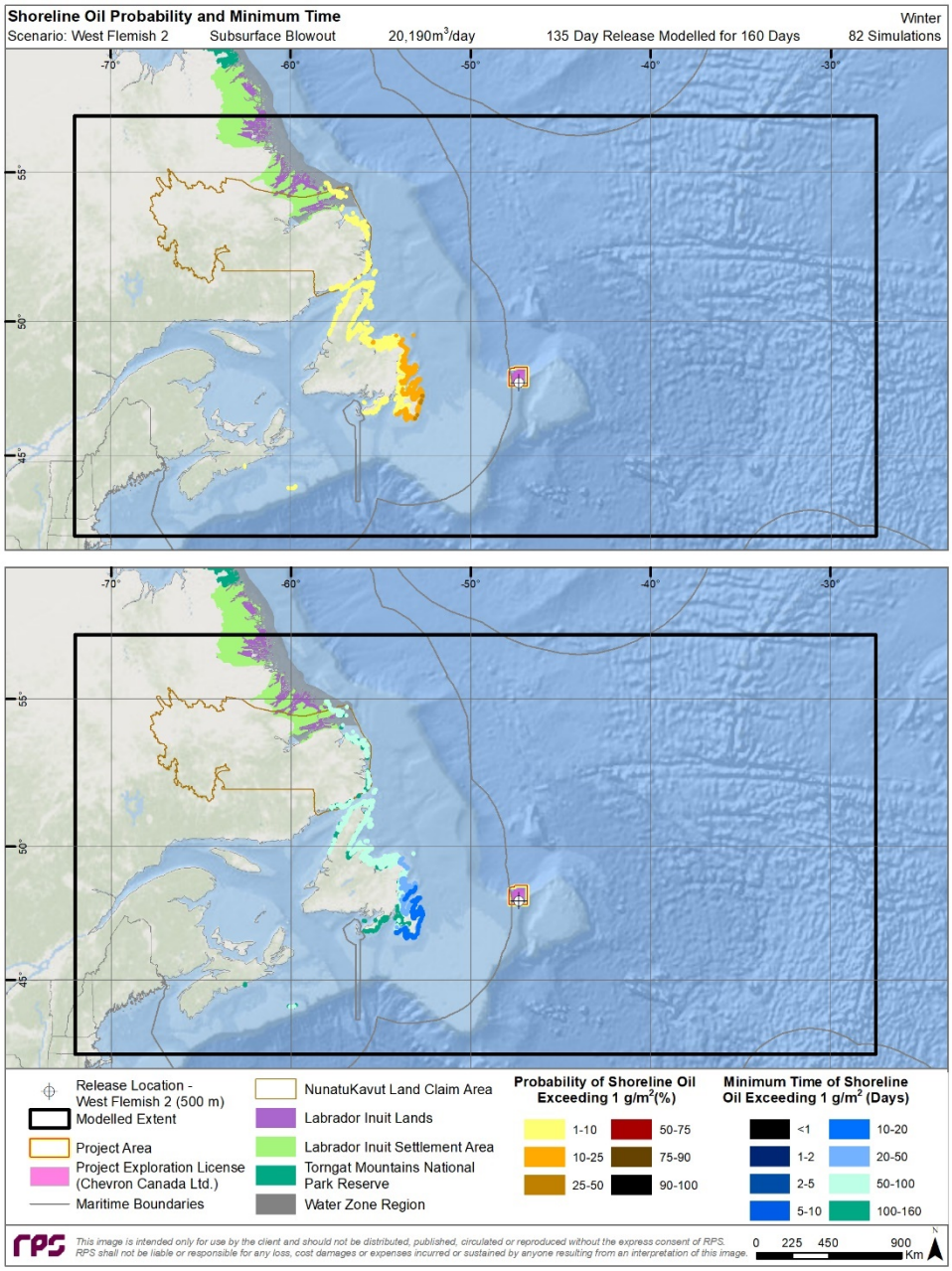

Figure 4-36. Winter probability of shoreline contact >1 g/m² (top) and minimum time to threshold exceedance (bottom) predictions resulting from a 135-day subsurface blowout at West Flemish 2.

4.1.3 Summary of Stochastic Results

A total of 171 unique model simulations were conducted for each stochastic analysis at the West Flemish 1 (1,500 m) and West Flemish 2 (500 m) hypothetical release sites, representing subsurface blowouts in waters offshore of Newfoundland. Four blowout release scenarios (two at each site) were modelled for 160-day periods to simulate short (30- and 27-day) and long (123- and 135-day) duration blowouts. The short duration releases were modelled to represent cap-and-stack response scenarios, while the long duration releases were modelled to represent the amount of time required to mobilize a drilling platform and drill a relief well. The total model duration of 160 days was used to track the trajectory and fate of spilled product as it continued to weather after the release had stopped.

For both release sites, summaries of the stochastic analyses of potential surface oil and water column exposure by dissolved hydrocarbons depict areas to the east of the release sites as having the highest potential likelihood (>90%) to exceed conservative socio-economic thresholds. The >90% likelihood area typically extended over 1,500 km to the east to the edge of the model domain for the surface oil, but typically fell short of the boundary for the water column contamination with the 50% line making contact with the easternmost extent. This is the result of the WFPLO being persistent, resulting in emulsified oil on the surface. The soluble and volatile fraction making up the water column contamination was more likely to evaporate and degrade over the amount of time required for oil to be transported to the easternmost boundary. Predicted water column probability footprints were smaller than surface oil footprints, with the probability of threshold exceedance predicted to decrease more rapidly for water column results as distance from the release site increased (Table 4-1). In nearly all stochastic scenarios, lower probabilities of threshold exceedance are predicted for surface and/or water column oil contamination to the north and south, while generally <25% of releases have the potential to exceed socio-economic thresholds >100 km to the west of the Project Area (Figure 4-1 through Figure 4-6; Figure 4-10 through Figure 4-15; Figure 4-19 through Figure 4-24; Figure 4-28 through Figure 4-33).

Due to the primarily eastward transport of oil from wind and currents, and the distance of the Project Area to the shoreline of Newfoundland, the maximum average probability of Canadian shoreline exposure above the threshold for the four stochastic scenarios was approximately 8.7% (Table 4-2). As the Labrador current flowed southward along the continental shelf, it was predicted to transport subsurface oil to the south, parallel to the coast (Figure 4-4 through Figure 4-6; Figure 4-13 through Figure 4-15; Figure 4-22 through Figure 4-24; Figure 4-31 through Figure 4-33). However, this trend is generally absent in the surface oil projections as wind forcing was more likely to transport oil to the east (Figure 4-1 through Figure 4-3; Figure 4-10 through Figure 4-12; Figure 4-19 through Figure 4-21; Figure 4-28 through Figure 4-30). Oil that was predicted to make its way to the shoreline of Canada would be patchy and discontinuous due to the considerable amount of weathering and natural dispersion that would take place over the weeks or months that were required for oil to reach shore. The minimum time to shorelines for threshold exceedance was 10.9-32 days along the Avalon peninsula and southeastern Newfoundland and 50-100 days along the shores of the northern shores of Newfoundland, eastern Gulf of St. Lawrence, and southwestern Labrador (Table 4-2, Figure 4-7 through Figure 4-9; Figure 4-16 through Figure 4-18; Figure 4-25 through Figure 4-27; Figure 4-34 through Figure 4-36). While oil was predicted to enter the EEZ for the United States in one of the 684 simulations over four stochastic scenarios that were modelled for 160 days (Figure 4-24), no oil was predicted to strand on U.S. shorelines in any of the simulations. Of note, the thin 1% contour line extending along the southern shore of Nova Scotia (summer and winter) and entering the Gulf of Maine (winter) represents a single subsurface Lagrangian particle of

hydrocarbons within the water column in a single simulation (Figure 4-23 and Figure 4-24). This oil did not result in any predicted shoreline oiling and was not at a level that would be expected to result in biological effects.

Although minimal, there was some level of seasonal variability in spill behavior. Regardless of release site and duration, the average stochastic probability of shoreline oiling was consistently about two times higher for winter releases (3.4-8.7%) than for summer releases (1.8-3.7%) (Table 4-2). Similarly, the minimum time to shoreline threshold exceedance was about 2-3 times longer in the summer (26-32 days) than the winter (10.9-11.4 days) (Table 4-2). The lower probability (i.e., 1% and 10%) footprints for surface oil contamination were larger in the winter compared to summer footprints, while the 90% footprints were larger in the summer (Table 4-1). This is due to the potential for greater westward transport of surface oil in the winter, associated with dynamic transitional periods, low pressure systems, and tropical and extra-tropical storms, when compared to the summer. As mentioned previously, as surface oil was transported to the east, it was predicted to reach the model domain boundaries in each modelled scenario due to the prevailing westerly winds and Gulf Stream current (Sections 3.4 and 3.5). However, the minimum time for oil to leave the boundary was always >25 days and typically >50 days, implying that the oil that left the domain was highly weathered, patchy, and discontinuous.

Due to the similarities in release location, rate, and duration of the scenarios modelled at West Flemish 1 and West Flemish 2, the stochastic analysis results were not very different between sites. Both sites had comparable footprints predicted for 90% probability surface oil threshold exceedances (Table 4-1). The 2,784,720 m^3 123-day release at West Flemish 1 resulted in a predicted annual 90% surface oil probability contour with an area of 1,214,000 km^2, while the 2,725,650 m^3 135-day release at West Flemish 2 resulted in a predicted annual 90% surface oil probability contour with an area of 1,423,000 km^2 (Table 4-1). Similarities were predicted for footprints of predicted threshold exceedance for water column contamination (Table 4-1). The likelihood of shoreline oiling was very similar between release locations, with a higher potential for shoreline oiling during winter periods, when compared to summer periods (Table 4-2).

Intuitively, the longer release durations led to larger spill volumes. The shorter duration (30- and 27-day) spill simulations released 679,200 m^3 and 545,130 m^3 while longer duration (123- and 135-day) simulations released 2,784,720 m^3 and 2,725,650 m^3 respectively (Table 2-1). Despite the larger spill volumes for the long duration spills (over four times higher), the size of the predicted stochastic footprints did not increase proportionally. This is due to the same underlying forcing (i.e. winds and currents) transporting different volumes of oil with the same speed and direction. While the overall footprint (down to the 1% contour) does not change to a large extent, the higher probability contours (e.g. 90%) were much larger for the larger volume releases (Table 4-1). At West Flemish 1, annual stochastic 90% probability footprints of surface and water column oil increased by 185% and 353%, respectively, from the short duration to the long duration release. Similarly, at West Flemish 2, annual stochastic 90% probability footprints of surface and water column oil increased by 204% and 365%, respectively. At both sites, nearly all expansion of footprints for long releases occurred to the east, northeast, and southeast of the release locations with very little expansion of lower probability footprints to the west. In other words, the longer spill duration mainly expanded probability footprints meridionally within the high probability areas east of the release sites. Increased release duration also resulted in more predicted potential for shoreline oiling above the 1% probability of threshold exceedance at West Flemish 1 (2,539 km

short vs. 3,498 km long) and West Flemish 2 (1,783 km short vs. 2,847 km long). In addition, there were predicted increases in the overall probability of shoreline oiling for longer duration releases (Table 4-2).

As stated previously, stochastic figures do not imply that the entire contoured area would be covered with oil in the event of a single release, nor do they provide any information on the quantity of oil in each area. Furthermore, the largest-area threshold exceedance footprints from the annual results are not the expected exposure from any single release of oil, but rather areas where there is >1% probability that exposure above the highly conservative socio-economic threshold could occur, based on the combination of either 171 (annual), 89 (summer), or 82 (winter) individual releases analyzed together.

Table 4-1. Summary of threshold exceedance information predicted at West Flemish 1 and West Flemish 2 for surface, water column, and shoreline oil exposure within the modelled domain are provided by season (annual, winter, summer). Predicted areas (km^2) exceeding surface and water column thresholds are provided for the >1%, 10%, or 90% likelihood of exposure to oil contours. The predicted length (km) of shoreline susceptible to exposure by oil is provided at 1-5%, 5-15%, and 15-30% contoured intervals.

Stochastic Scenario Parameters				Areas Exceeding Threshold (km^2)		
Component and Threshold	**Spill Location**	**Scenario**	**Probability Contour or Bin***	**Annual Results**	**Winter (ice cover)**	**Summer (ice-free)**
Surface Oil >0.04 µm, on average	West Flemish 1	30-day release	1%	3,447,000	3,477,000	3,270,000
			10%	2,676,000	2,892,000	2,521,000
			90%	655,300	580,600	772,100
		123-day release	1%	3,574,000	3,613,000	3,343,000
			10%	2,958,000	3,091,000	2,809,000
			90%	1,214,000	1,189,000	1,358,000
	West Flemish 2	27-day release	1%	3,474,000	3,518,000	3,276,000
			10%	2,610,000	2,778,000	2,510,000
			90%	696,800	579,600	819,000
		135-day release	1%	3,579,000	3,625,000	3,382,000
			10%	2,935,000	3,036,000	2,745,000
			90%	1,423,000	1,408,000	1,492,000
Water Column Dissolved Hydrocarbons >1 µg/L at some depth within the water column	West Flemish 1	30-day release	1%	2,811,000	3,040,000	2,709,000
			10%	1,877,000	1,955,000	1,830,000
			90%	174,800	203,900	155,200
		123-day release	1%	2,855,000	3,094,000	2,798,000
			10%	2,093,000	2,178,000	2,024,000
			90%	617,100	582,700	724,300
	West Flemish 2	27-day release	1%	2,743,000	3,006,000	2,715,000
			10%	1,922,000	1,971,000	1,868,000
			90%	219,300	254,600	192,600
		135-day release	1%	2,846,000	3,060,000	2,809,000
			10%	2,116,000	2,180,000	2,049,000
			90%	800,300	752,100	851,000

Stochastic Scenario Parameters				Areas Exceeding Threshold (km^2)		
Lengths Exceeding Threshold (km)						
Shoreline Oil >1 g/m^2, on average	West Flemish 1	30-day release	1 - 5%	2,481	2,048	147
			5 - 15%	58	942	-
			15 - 30%	-	-	-
			All Probabilities	2,539	2,990	147
		123-day release	1 - 5%	2,189	1,343	523
			5 - 15%	1,303	1,879	81
			15 - 30%	6	624	-
			All Probabilities	3,498	3,846	604
	West Flemish 2	27-day release	1 - 5%	1,747	1,779	325
			5 - 15%	36	365	15
			15 - 30%	-	-	-
			All Probabilities	1,783	2,144	330
		135-day release	1 - 5%	1,971	1,345	598
			5 - 15%	848	1,454	222
			15 - 30%	28	337	-
			All Probabilities	2,847	3,136	820

*Bins are based on stochastic probabilities; for example, 655,300 km^2 of the ocean surface is predicted to exceed the 0.04 µm surface oil threshold in 90% of the 171 modelled simulations from the 27-day release at West Flemish 1 over the entire 160-day modelled duration.

Table 4-2. Shoreline contamination probabilities and minimum time for oil exposure exceeding 1 g/m^2 for all shorelines.

All Shorelines						
Spill Location	**Scenario**	**Scenario Timeframe**	**Average Probability of Shoreline Oil Contamination (%)**	**Maximum Probability of Shoreline Oil Contamination (%)**	**Minimum Time to Shore (days)**	**Maximum Time to Shore (days)**
West Flemish 1	30-day release	Annual	2.6	7.0	26.4	140.5
		Winter	4.4	15.0	11.4	153.3
		Summer	1.9	4.0	11.4	128.5
	123-day release	Annual	5.1	18.0	11.2	155.4
		Winter	8.7	28.0	11.2	161.2
		Summer	2.4	12.0	26.1	159.6
West Flemish 2	27-day release	Annual	2.2	6.0	11.2	135.3
		Winter	3.4	12.0	11.2	155.8
		Summer	1.8	7.0	32.1	142.7
	135-day release	Annual	4.9	19.0	10.9	155.7
		Winter	7.5	28.0	10.9	159.9
		Summer	3.7	15.0	27.5	159.7

4.2 Deterministic Analysis Results

Individual trajectories of interest were selected from the stochastic ensemble of results for the deterministic analysis. The deterministic trajectory and fate simulations provided an estimate of the transport of oil through the environment as well as its physical and chemical behavior for the specific set of modelled environmental conditions. Representative 95th percentile credible "worst-case" trajectories for surface oil exposure, water column contamination, and contact with shoreline were identified from the stochastic scenarios for each site modelled (West Flemish 1 or 2) and release duration (i.e., 30 vs 123 days or 27 vs. 135 days). These highly conservative individual cases were selected based upon the size of the surface oil footprint, volume of oil in the water column, and the length of shoreline contacted with oil. This resulted in twelve individual trajectories associated with subsurface blowouts of WFPLO (Table 2-5). One additional batch spill of marine diesel (1,000 L) was modelled at the West Flemish 1 location.

The following sections (Sections 4.2.1 through 4.2.4) contain figures corresponding to each identified representative case and tables summarizing the areas exceeding specified thresholds. During modelling, components of oil were tracked as floating surface oil, entrained droplets of whole oil, dissolved hydrocarbon constituents, stranded oil on shorelines and sediments, evaporated, degraded, and left the model domain. The figures provided depict the cumulative footprint of all oil predicted to be within a region over the entire modelled duration. Therefore, the depicted footprints are much larger than the amount of oil that would be present in a region at any given time following the release of oil. This concept is illustrated in Figure 4-37 which portrays predicted surface oil thickness at five specific time steps or "snapshots" in time (days 2, 10, 50, 100, and 160) for the 95th percentile surface oil thickness case for the 123-day release at West Flemish 1. Note the patchy and discontinuous nature of the predicted footprint as the released oil dispersed and thinned over time. Figure 4-38 portrays the cumulative footprint for the exact same simulation. The area covered is much larger, depicting the maximum surface oil thickness that was predicted to occur at each location over the entire modelled time period. The remaining figures in this report will depict cumulative footprints as opposed to "snapshots" at given time steps to provide conservative estimates of potentially affected areas.

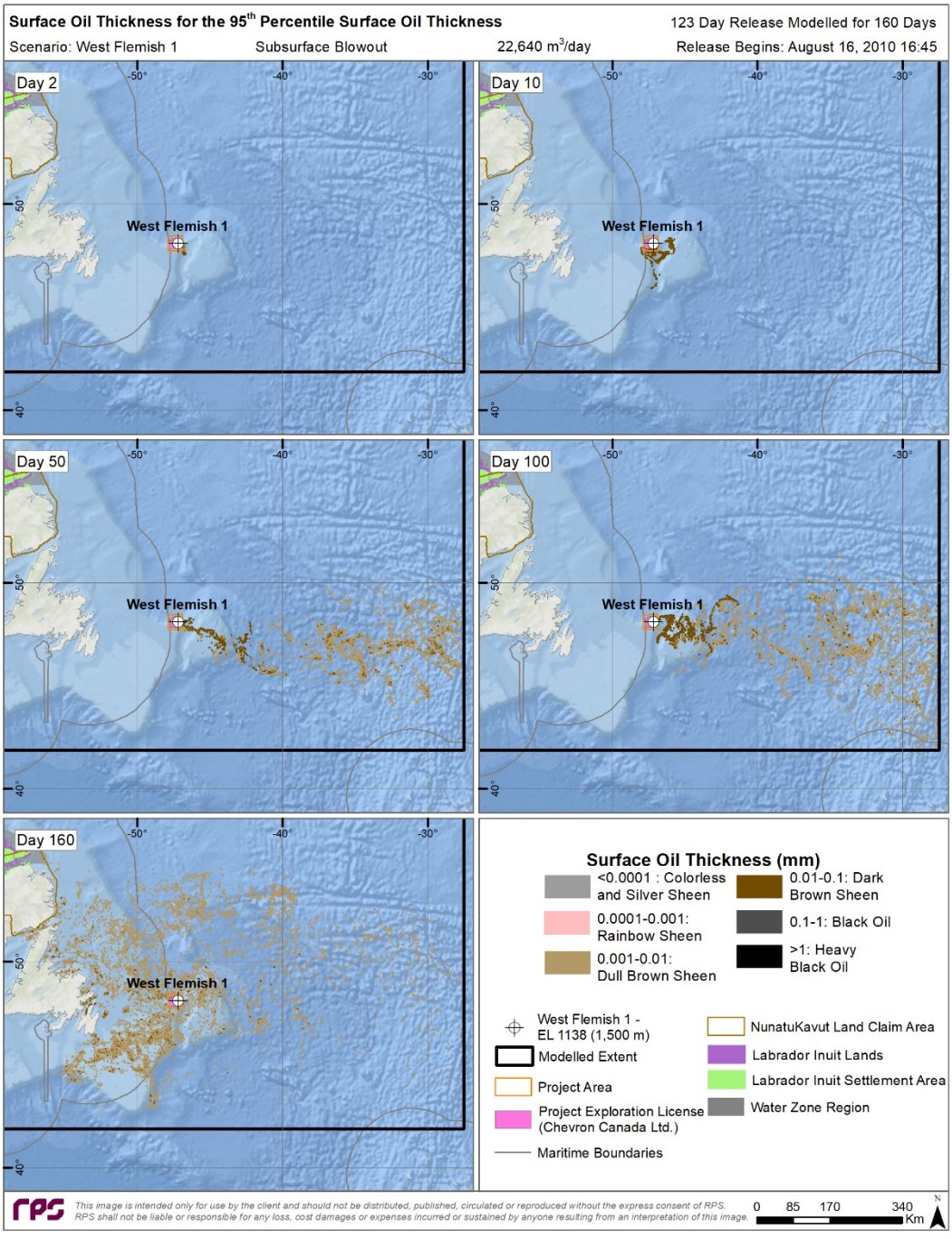

Figure 4-37. Predicted surface oil thickness for the 95th percentile surface oil exposure case for the 123-day release at West Flemish 1 at days 2, 10, 50, 100, and 160 to illustrate the variation in size of the surface oil footprint over the course of the model duration.

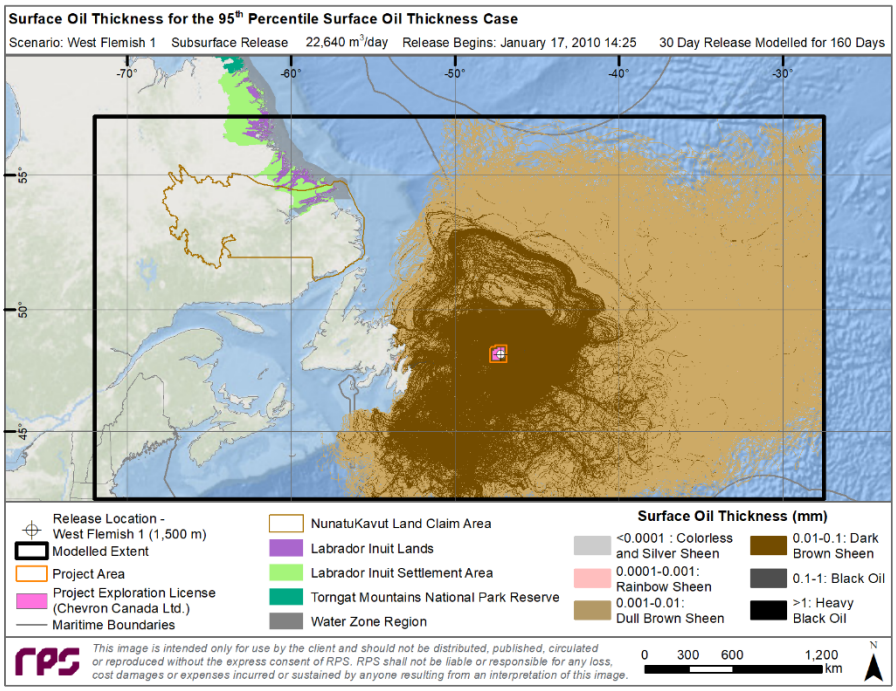

Figure 4-38. Maximum cumulative surface oil thickness for the 95th percentile surface oil exposure case for the 123-day release at West Flemish 1 to illustrate the much larger size of the cumulative surface oil footprint over the entire model duration, compared to the size of the surface oil footprint on any one day or time step.

The types of figures that were used to summarize modelling results are provided, along with brief descriptions of the information that they portray. Note that the thicknesses and concentrations for the modelled blowouts were calculated on a grid with a resolution (i.e., grid cell size) of 1,800 m by 2,500 m, which is equivalent to 0.02 degrees by 0.02 degrees. For concentration grids, vertical binning included 50 m increments over the entire water column.

1. **Mass Balance Plots**: Illustrate the predicted weathering and fate of oil for a specific run over the entire model duration as a fraction of the oil released up to that point. Components of the oil tracked over time include the amount of oil on the sea surface, the total entrained hydrocarbons in the water column, the amount of oil in contact with the shore or sediments, the amount of oil evaporated into the atmosphere, and the amount of oil degraded (accounts for both photo-oxidation and biodegradation).
2. **Surface Oil Thickness Maps:** Depict the predicted footprint of maximum floating surface oil and the associated oil thicknesses (mm) over all modelled time steps for an individual release simulation. The minimum thickness of surface oil > 0.04 µm is displayed (cumulative over all

modelled time steps). Note that floating oil mass is calculated as an average over grid cells, thus in reality, the oil would be patchy and discontinuous and could be thinner or thicker within particular areas of a single grid cell.

3. **Water Column Dissolved Hydrocarbon Concentration (DHC) Maps**: Depict the predicted footprint of the vertical maximum water column concentration of dissolved hydrocarbons over all modelled time steps for an individual release simulation. Dissolved hydrocarbons are the constituents of the oil with the greatest potential to affect water column biota. Only concentrations above 1 µg/L for the representative cases are displayed (Table 2-2).
4. **Water Column Total Hydrocarbon Concentration (THC) Maps:** Depict the predicted footprint of the vertical maximum water column concentration of total hydrocarbons over all modelled time steps for an individual release simulation. Only concentrations above 1 µg/L for the representative cases are displayed (Table 2-2).
5. **Shoreline and Sediment Total Hydrocarbon Concentration (THC) Maps:** Depict the predicted total mass of oil (per unit area as g/m^2) deposited onto the shoreline and on sediments.

4.2.1 Surface Oil Exposure Cases

Results for the identified 95th percentile (i.e., credible "worst-case") surface oil exposure cases for the short and long-duration releases at West Flemish 1 and 2 are provided. Note that the modelled release dates for the representative scenarios at each site differed (Table 2-5). Each of the trajectories in the stochastic analysis represented a different start date and associated environmental conditions (e.g., wind and current speed and direction), which resulted in different predicted outcomes. For example, both the short- and long-duration cases (30- and 123-day) at West Flemish 1 were representative of winter cases (i.e., start dates in January and August), while the West Flemish 2 cases were representative of both summer (27-day) and winter (135-day).

Overall predicted surface area exposed to oil greater than 0.001 mm (dull brown sheens to heavy black oil) was generally similar between sites and release durations for the selected deterministic cases, however the thicker values within the cumulative footprints of oil were predicted to extend further east for releases at West Flemish 2, when compared to West Flemish 1 (Figure 4-39 and Figure 4-44; Table 4-3).

The long-duration (i.e., 123- and 135-day releases) release scenarios were predicted to result in much larger areas (1,900,000 and 1,800,000 km^2) that had the potential to be affected by dark brown sheens (0.01-0.1 mm) at some point over the 160 day modelled simulation, than the short-duration releases (900,000 and 700,000 km^2) (Table 4-3). Specifically, the long-duration release cases at West Flemish 1 had the largest areas of potential exposure to dark brown sheens, relative to dull brown sheens, due to the larger release volume and the calm wind conditions that reduced the entrainment of surface oils into the water column, relative to higher wind conditions. Heavy black oil (> 1 mm) was not predicted in any of the selected deterministic cases due to the natural dispersion as oil rose from the relatively deep release locations as well as the nature of the WFPLO, which was a light oil with low density and low viscosity that spread rapidly. It is important to note that these scenarios were identified as some of the largest predicted cumulative surface oil footprints (95th percentile) out of all (171) of the 160-day simulations.

Water column concentrations (THC and DHC) were predicted to be of a similar magnitude between sites, with the exception of the direction of predicted contamination being more northward for dissolved hydrocarbons at West Flemish 1 (i.e., less southern transport through the Flemish Pass). Most of the waters with potential elevation in dissolved hydrocarbon concentrations (> 500 µg/L) were within 61-336 km of the release sites at West Flemish 1 and West Flemish 2, respectively. This was due to the soluble hydrocarbons entering the water column during the initial ascent of the oil to the surface, the rapid dispersion and degradation within the water column, and the rapid rate of evaporation of the soluble fraction (which is also volatile) at the surface, when compared to the slower rate of dissolution. Elevated concentrations in subsurface hydrocarbon contamination at depth were not predicted to cross into shallower waters over the shelf, as subsurface currents follow pressure surfaces (isopycnals), which circulated around the Flemish Cap and southwest along the shelf break (Figure 4-40 and Figure 4-45). Highest concentrations of total hydrocarbons (>15,000 µg/L) were predicted to occur at the release locations with highest levels of contamination to the east (West Flemish 1) and south (West Flemish 2) depending on the wind and currents at the time of release (Figure 4-41 and Figure 4-46).

At West Flemish 1, the 95th percentile surface oil exposure case was predicted to result in shoreline oiling of 100-500 g/m^2 along approximately 935 km of eastern Newfoundland for the short-duration release scenario (30-day release) and additional oiling into the Gulf of St. Lawrence and along the Labrador coast for the long-duration release scenario (123-day release), which totaled nearly 3,800 km (Table 4-3). Shoreline oiling above 100g/m^2 is expected to exceed the socio-economic threshold and enter into the potential for ecological impacts (Table 2-2). A very small area approximately 600 km to the southwest of the release location was predicted to experience sediment contamination <0.1 g/m^2 for the long-duration release scenario at West Flemish 1 (Figure 4-42). Unlike the results at West Flemish 1, the selected West Flemish 2 short-duration release scenario (27-day) was not predicted to result in shoreline oil contamination, however did result in low level sediment contamination (<0.1 g/m^2) approximately 1,000 km to the south of the release along the continental break (Figure 4-47). The long-duration release (135-day) was predicted to result in minimal shoreline oiling (21 km exceeding the socio-economic threshold and 4 km for ecological) along the Avalon Peninsula and a small extent of <0.1 g/m^2 sediment contamination immediately east of the release location and approximately 1,000 km to the south (Figure 4-47).

At the end of the 160-day simulations of the 95th percentile surface oil exposure for short- and long-duration releases at the West Flemish 1 site, large percentages of the oil evaporated (~47%) and degraded (32-38%), accounting for >79% of each modelled release. The amount of oil predicted to remain on the water surface was about 11% with <2% within the water column (Table 4-4). Up to 10% of oil (predominantly persistent surface oil) was predicted to be transported outside of the modelled domain. Shoreline contact made up a very small proportion of releases (<1%) and oil transported to the sediment was not a major fate pathway with <0.1% predicted to settle on sediments (Table 4-4).

At the West Flemish 2 site, predictions showed that approximately 48% of oil evaporated and 31-32% degraded. Less than 11% was predicted to remain floating on the water surface, 9.3-18% was transported outside the modelled domain, about 1% remained within the water column, and <0.1% settled on sediment. No oil made contact with the shoreline for either release duration (Table 4-4).

Frequent cycling of wind and calm events were evident in all surface oil exposure cases, as indicated by “see-sawing” between oil on the surface and entrained oil in the water column (Figure 4-43 and Figure 4-48). During calmer more quiescent periods, oil was predicted to rise to the surface forming slicks, while during periods with

wind, surface breaking waves were formed, which resulted in surface oil becoming entrained into the water column.

4.2.1.1 West Flemish 1

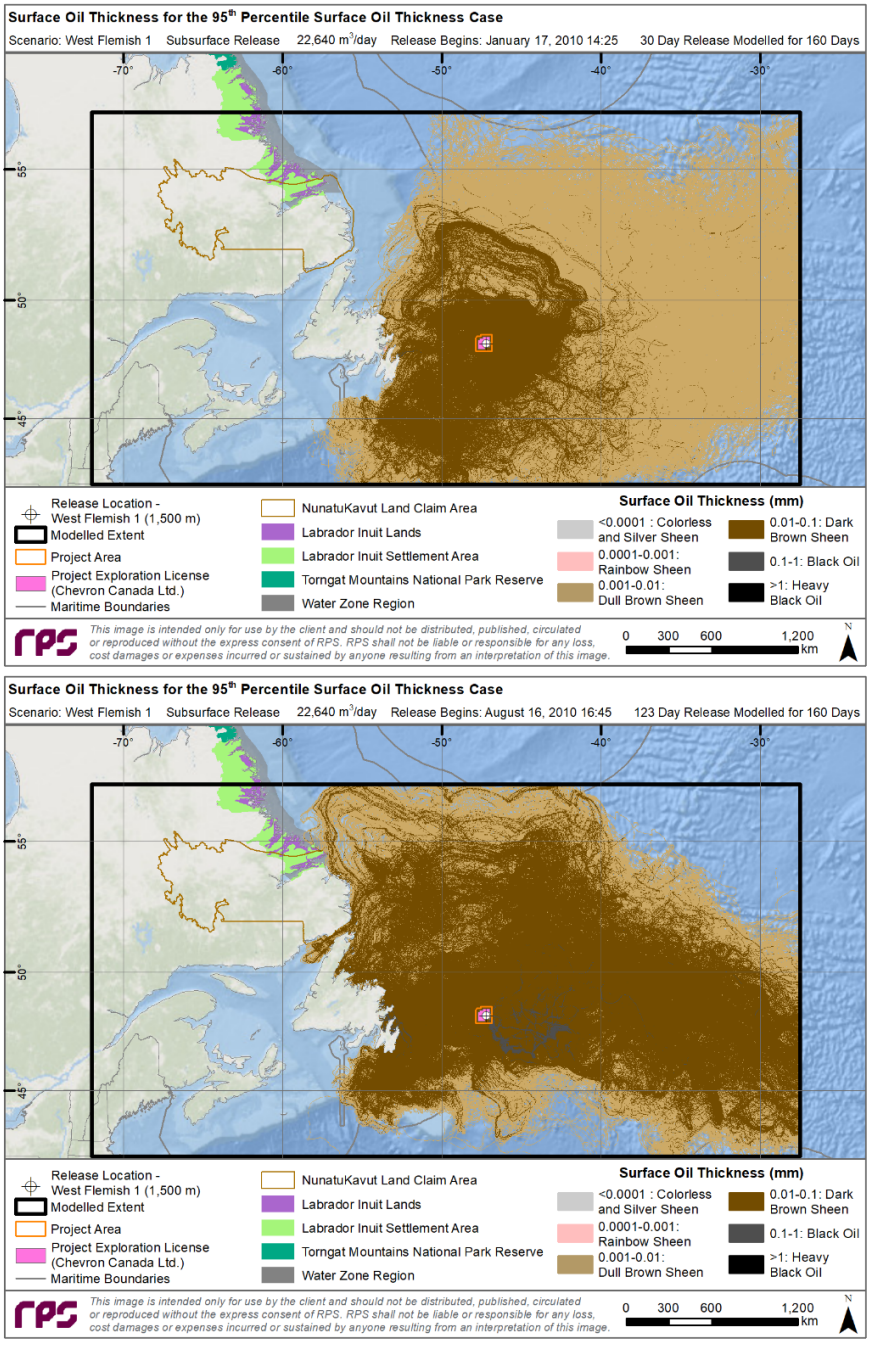

Figure 4-39. Surface oil thickness for the 95th percentile average surface oil thickness cases resulting from 30- (top) and 123-day (bottom) blowouts at West Flemish 1.

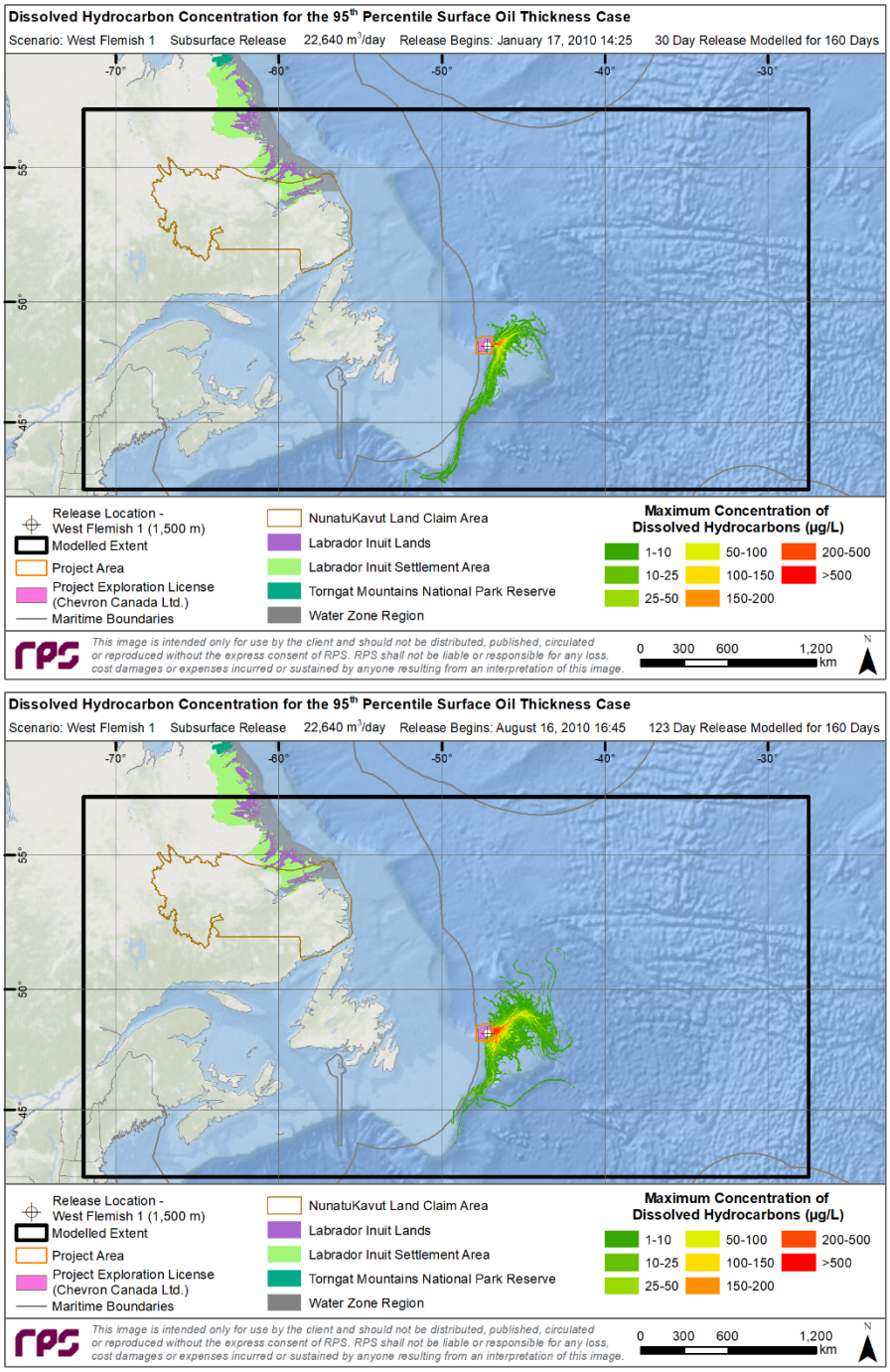

Figure 4-40. Maximum DHC at any depth in the water column for the 95th percentile average surface oil thickness cases resulting from 30- (top) and 123-day (bottom) blowouts at West Flemish 1.

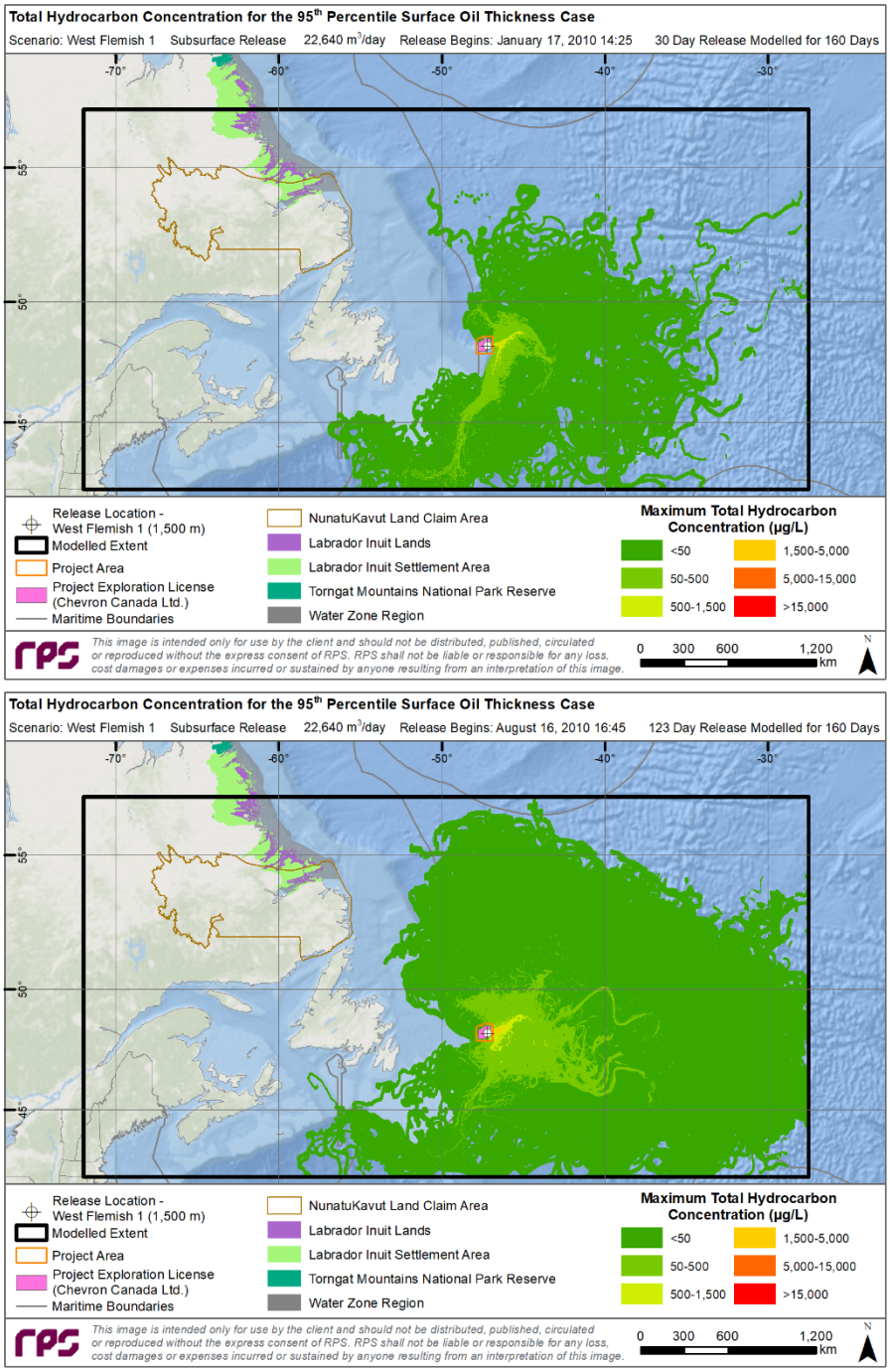

Figure 4-41. Maximum THC at any depth in the water column for the 95th percentile average surface oil thickness cases resulting from 30- (top) and 123-day (bottom) blowouts at West Flemish 1.

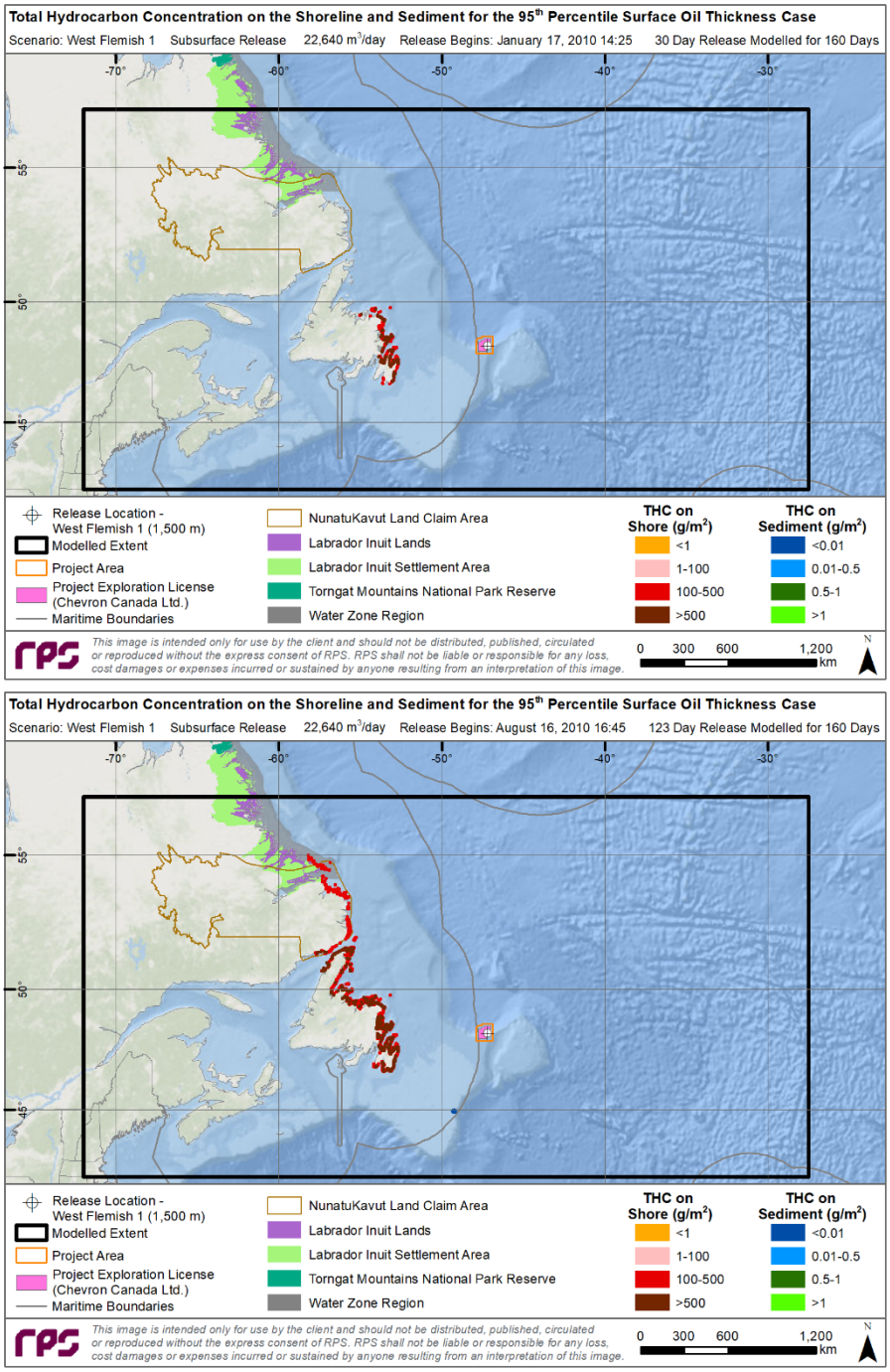

Figure 4-42. Total hydrocarbon concentration (THC) on the shore and sediment for the 95th percentile average surface oil thickness cases resulting from 30- (top) and 123-day (bottom) blowouts at West Flemish 1.

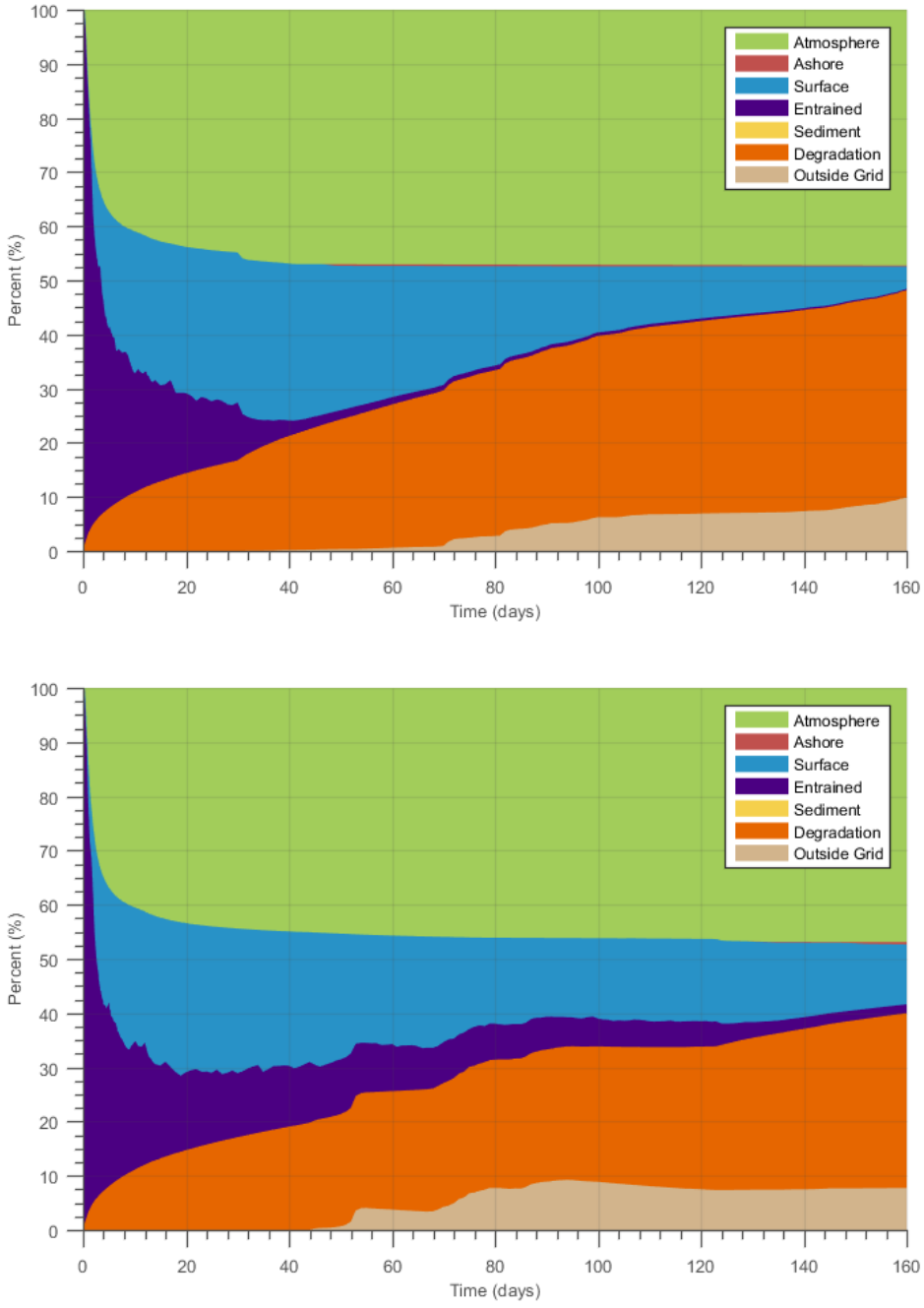

Figure 4-43. Mass balance plots of the 95th percentile surface oil thickness cases resulting from 30- (top) and 123-day (bottom) blowouts at West Flemish 1.

4.2.1.2 West Flemish 2

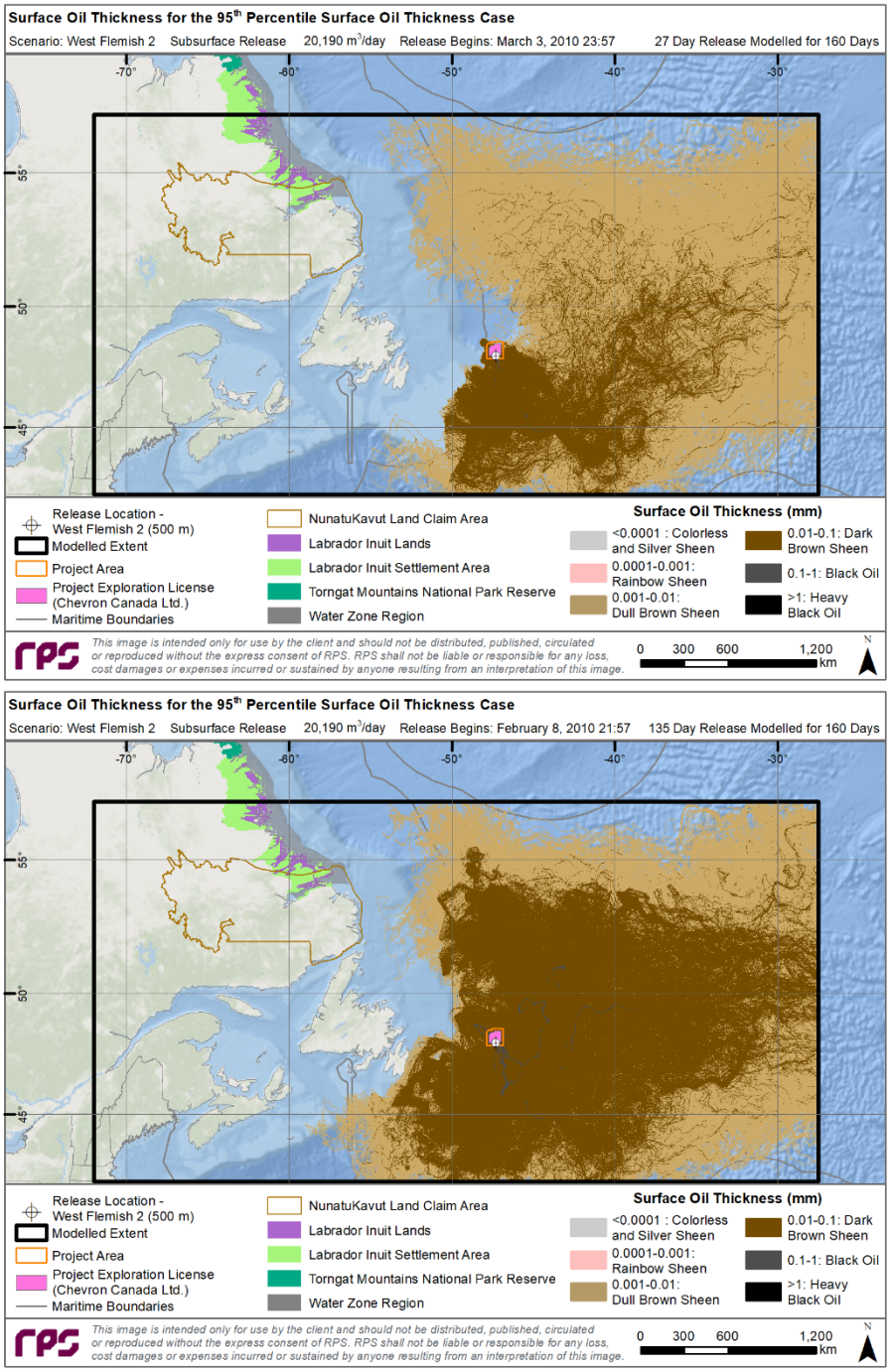

Figure 4-44. Surface oil thickness for the 95th percentile average surface oil thickness cases resulting from 27- (top) and 135-day (bottom) blowouts at the West Flemish 2.

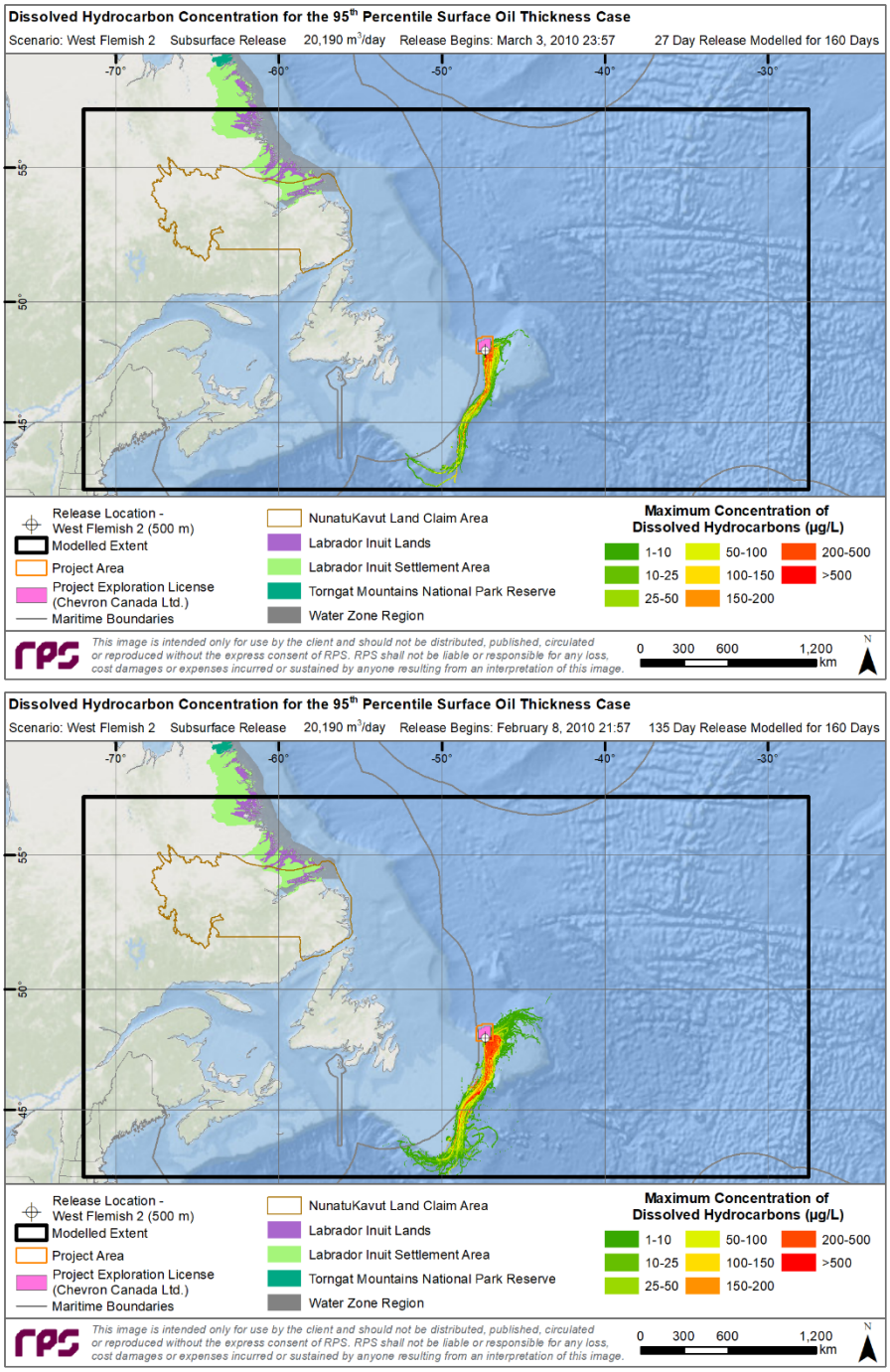

Figure 4-45. Maximum DHC at any depth in the water column for the 95th percentile average surface oil thickness cases resulting from 27- (top) and 135-day (bottom) blowouts at West Flemish 2.

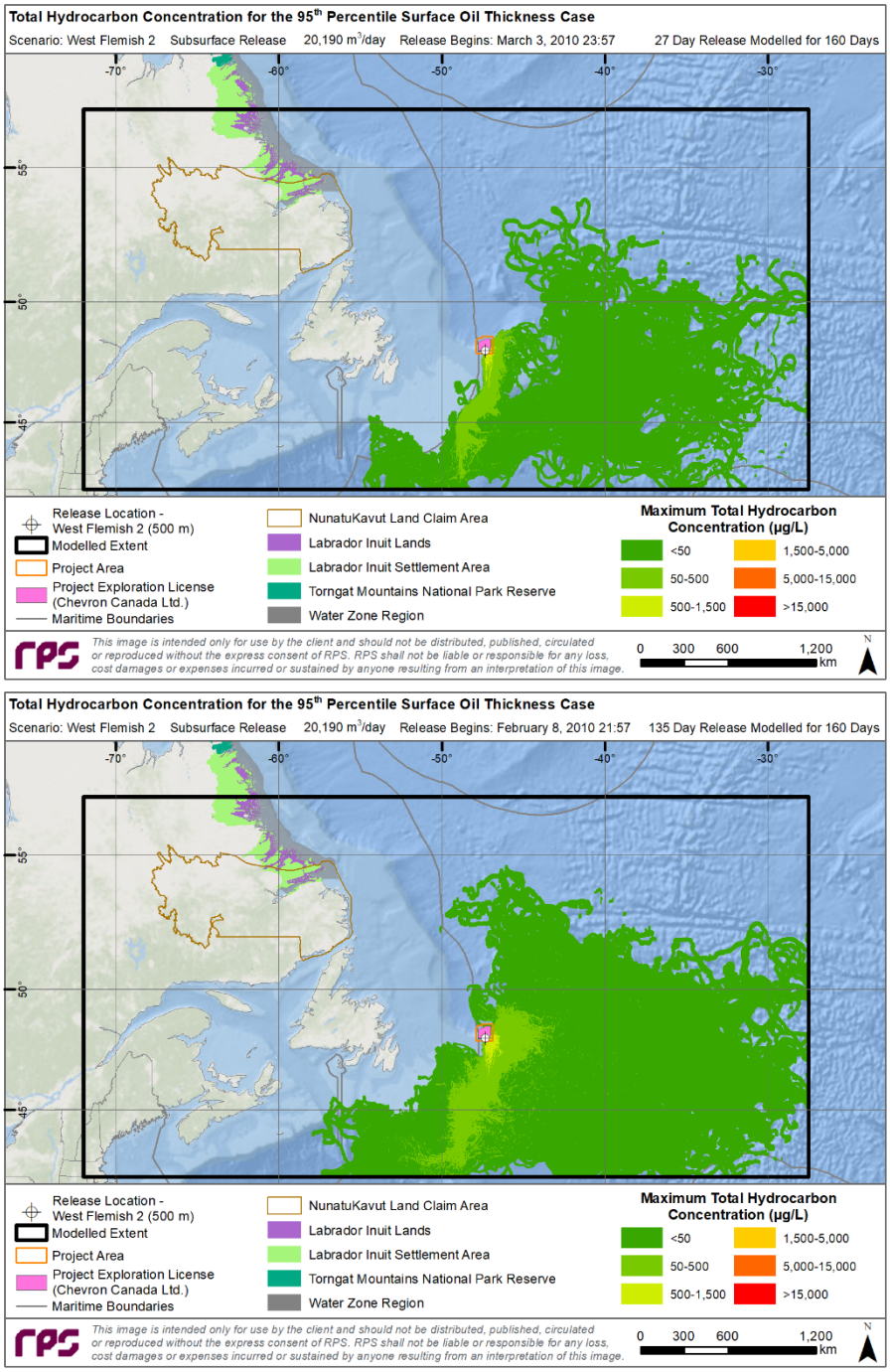

Figure 4-46. Maximum THC at any depth in the water column for the 95th percentile average surface oil thickness cases resulting from 27- (top) and 135-day (bottom) blowouts at West Flemish 2.

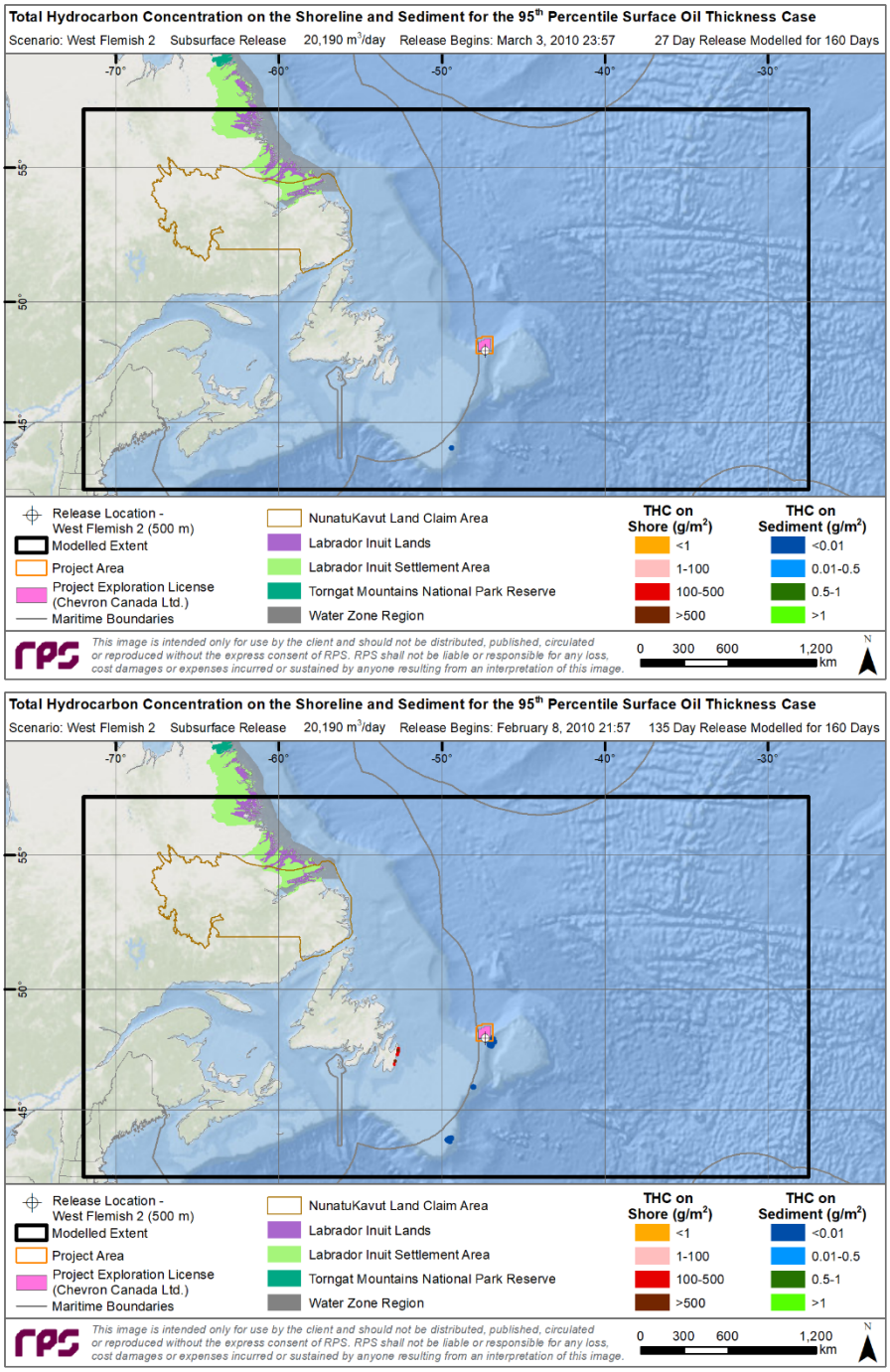

Figure 4-47. THC on the shore and sediment for the 95th percentile average surface oil thickness cases resulting from 27- (top) and 135-day (bottom) blowouts at West Flemish 2.

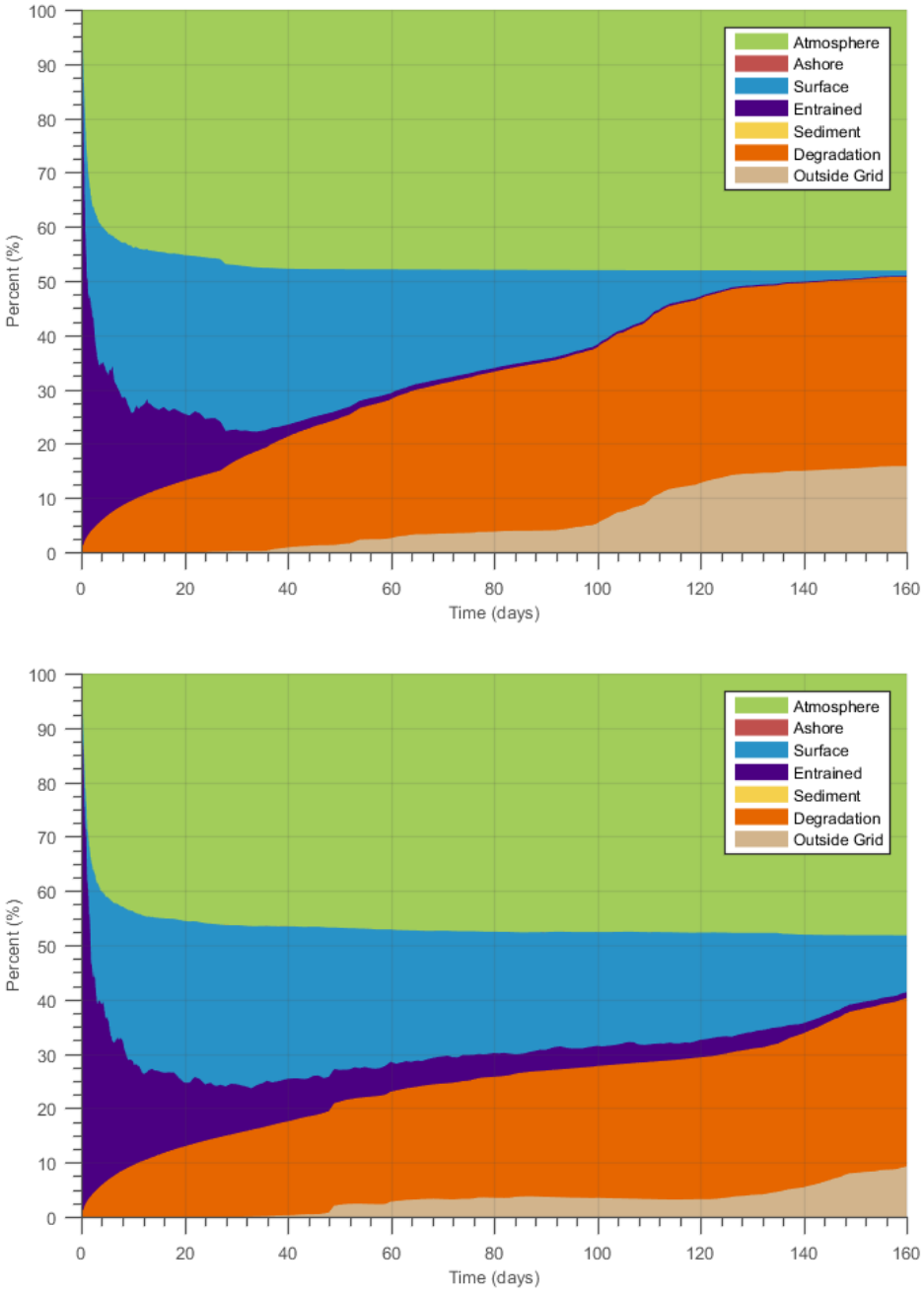

Figure 4-48. Mass balance plots of the 95th percentile surface oil thickness cases resulting from 27- (top) and 135-day (bottom) blowouts at West Flemish 2.

4.2.2 Water Column Exposure Cases

The results for the identified 95th percentile (i.e., credible "worst-case") water column exposure cases for the short- and long-duration releases at West Flemish 1 and 2 are provided in the figures below. Note that the modelled release dates for the representative scenarios at each site differed (Table 2-5). The cases at West Flemish 1 were representative of both winter (30-day) and summer (123-day) with corresponding start dates in September and June. At West Flemish 2, the cases were also representative of summer and winter with modelled start dates in June (27-day) and January (135-day).

The predicted total surface area and the cumulative footprints of surface area exposed to oil >0.001 mm (dull brown sheens) were generally similar between sites and release durations for the selected deterministic cases, with the exception of the long-duration release (135-day) at West Flemish 2 (Figure 4-49 and Figure 4-54; Table 4-3). While the other three cases were predicted to result in predominantly eastward transport, with limited transport to the north or south (Figure 4-49), the long-duration release at West Flemish 2 was predicted to result in a more radial distribution (Figure 4-54). Due to the larger volume of oil being released, the long-duration (123- and 135-day) releases were also predicted to result in much larger areas affected by dark brown sheens (0.01-0.1 mm), when compared to the short-duration (30- and 27-day) releases. Although heavy black oil (>1 mm) was not predicted in any of the selected deterministic scenarios, the potential for socio-economic and ecological impacts would be expected within the oiled region based on oil thickness (Table 4-3).

The high potential for surface oil entering into the water column in these four scenarios is the result of high wind speeds in the region, which result in surface breaking winds that entrain surface oil into the water column. The formation of persistent emulsions then increases the likelihood that oil will be see-sawing between the surface mixed layer and the surface of the water. Similar to the results from the representative surface oil exposure cases, water column concentrations of THC and DHC were very similar between sites, except for more extensive transport of dissolved hydrocarbons at West Flemish 2 to the south through the Flemish Pass (Figure 4-50 and Figure 4-55). Total hydrocarbon concentrations were predicted to be more uniform (low level contamination) than dissolved concentrations, particularly for the long-duration releases. This was due to the rapid dispersion, degradation, and volatilization of soluble constituents, and the rapid transport of surface oil by winds and persistence of the whole oil after it formed emulsions The highest predicted concentrations of total hydrocarbons (>15,000 µg/L) extended to the east over the Flemish Cap for West Flemish 1 and to the south for West Flemish 2 (Figure 4-51 and Figure 4-56).

At West Flemish 1, the deterministic cases were not predicted to result in any shoreline oil contamination (Figure 4-52). However, a small amount of sediment oil contamination (<0.1 g/m^2) was predicted for the long-duration release (123-day) to the east of the release location (Figure 4-52). At West Flemish 2, only the long-duration release (135-day) was predicted to result in shoreline oil contamination, which occurred at levels above both the socio-economic and ecological thresholds along the eastern Avalon Peninsula up to Fogo Island (Figure 4-57 and Table 4-3). The long-duration release at West Flemish 2 was also predicted to result in limited potential for sediment contamination (<0.1 g/m^2) to the east of the release site and along the shelf break approximately 1,000 km to the south (Figure 4-57).

At the end of the 160-day simulations of the 95th percentile water column exposure for short- and long-duration releases at the West Flemish 1 site, large percentages of the oil evaporated (~47%) and degraded (~31%), accounting for ~78% of each modelled release. Up to 16-21% of oil (predominantly persistent surface oil) was

predicted to be transported outside of the modelled domain. The amount of oil predicted to remain on the water surface was 5% and 0%, with <2% within the water column. Oil transported to the sediment was not a major fate pathway with <0.1% predicted to settle on sediments and no shoreline contact was predicted in either release duration.

At the West Flemish 2 site, predictions showed that approximately 48% of oil evaporated and about 31% degraded, accounting for ~79% of each modelled release. The amount of oil predicted to remain on the water surface was 1% and 12%, <1% remained in the water column, and <0.1% settled on sediment. Shoreline contact was not a major fates pathway with 0 and <0.1% of oil contacting the shoreline. Although <2% of the oil is remaining in the water column at the end of the identified scenarios, these cases still experienced the highest amount of water column exposure throughout the length of the simulation, and thus were chosen to be the 95th percentile worst-case scenarios (Table 4-4). Frequent cycling of wind and calm events were evident in all water column oil exposure cases, as indicated by “see-sawing” between oil on the surface and entrained oil in the water column (Figure 4-53 and Figure 4-58).

4.2.2.1 West Flemish 1

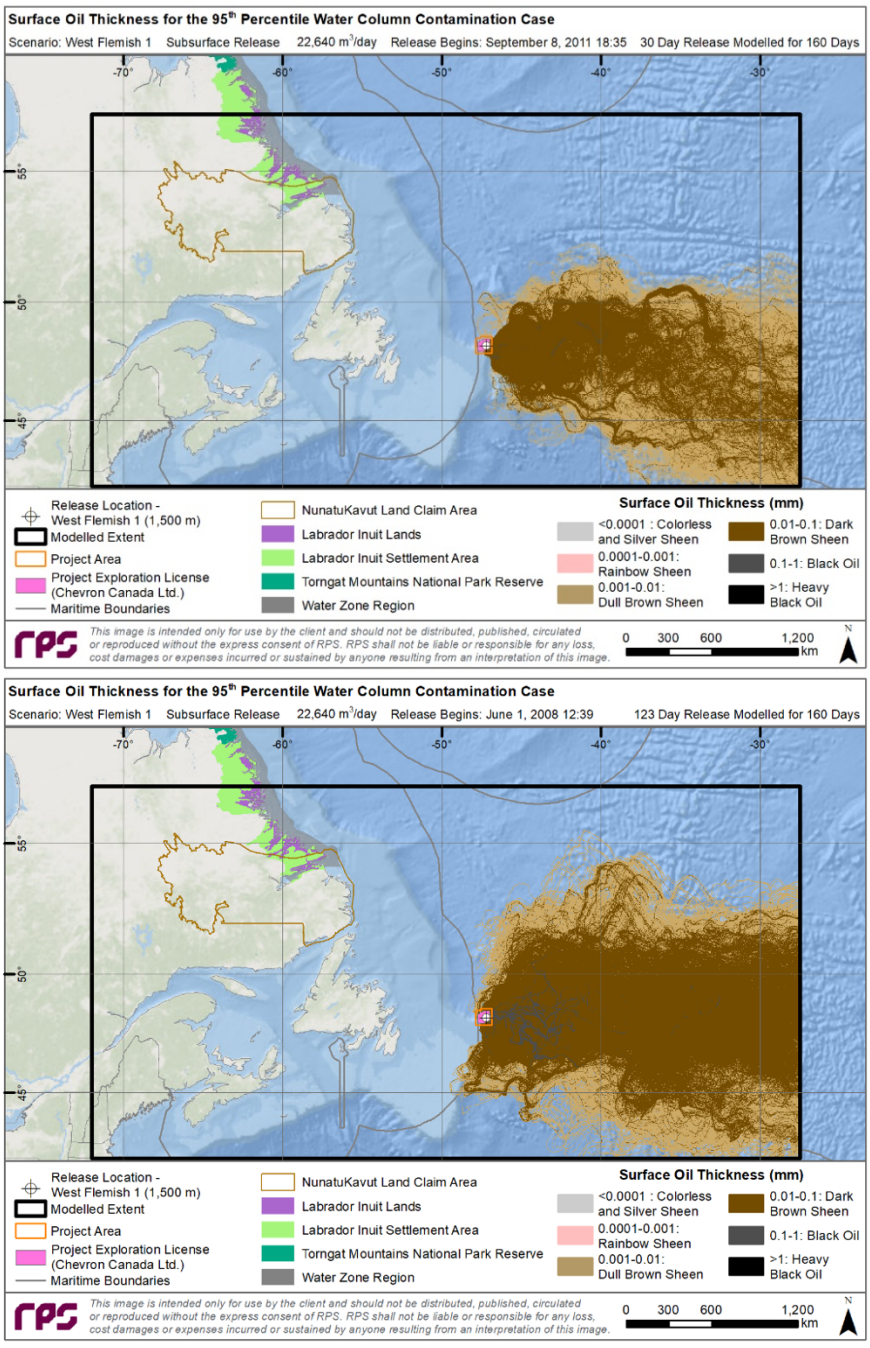

Figure 4-49. Surface oil thickness for the 95th percentile water column cases resulting from 30- (top) and 123-day (bottom) blowouts at West Flemish 1.

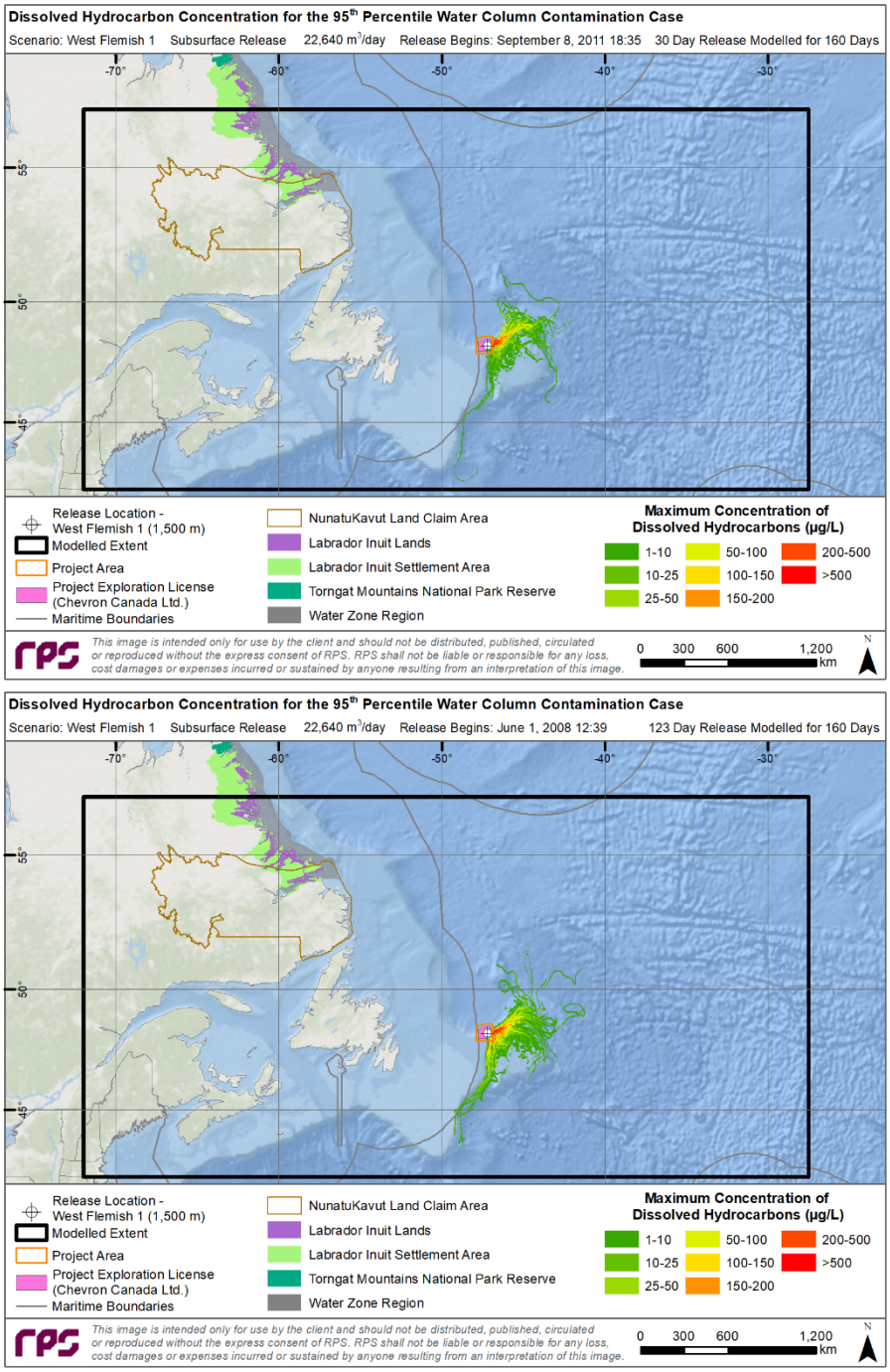

Figure 4-50. Maximum DHC at any depth in the water column for the 95th percentile water column cases resulting from 30- (top) and 123-day (bottom) blowouts at West Flemish 1.

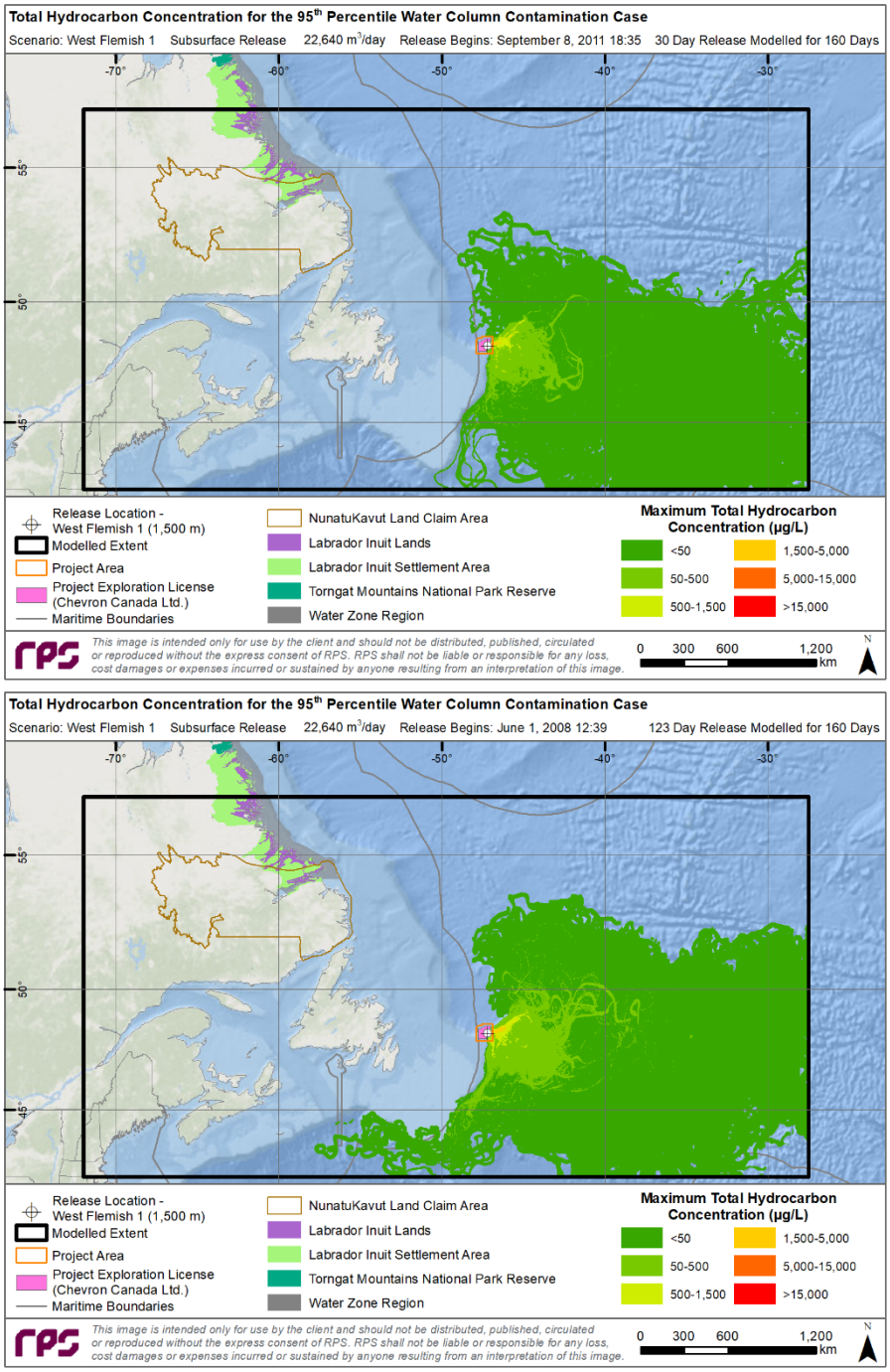

Figure 4-51. Maximum THC at any depth in the water column for the 95th percentile water column cases resulting from 30- (top) and 123-day (bottom) blowouts at West Flemish 1.

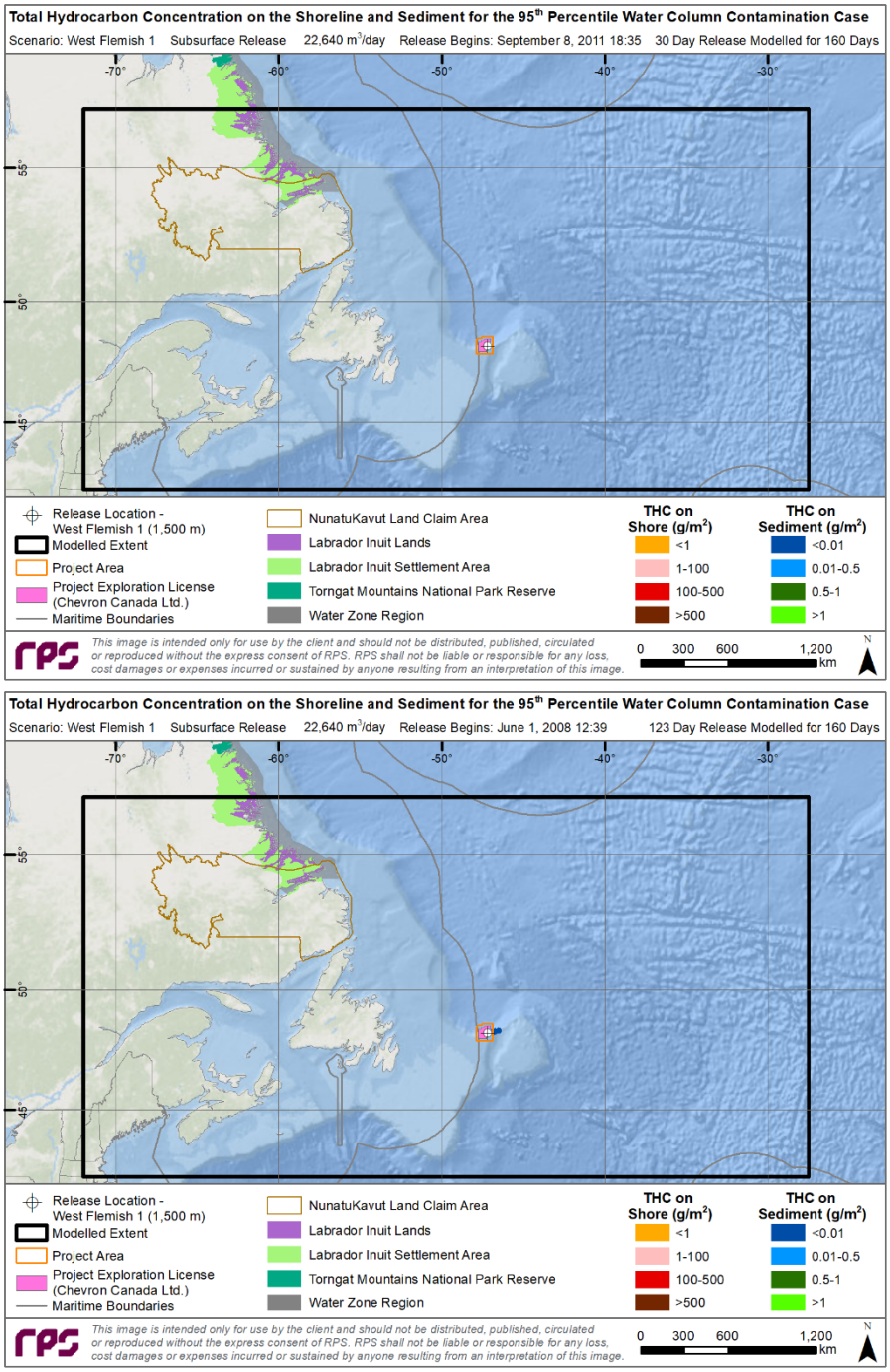

Figure 4-52. THC on the shore and sediment for the 95th percentile water column cases resulting from 30- (top) and 123-day (bottom) blowouts at West Flemish 1.

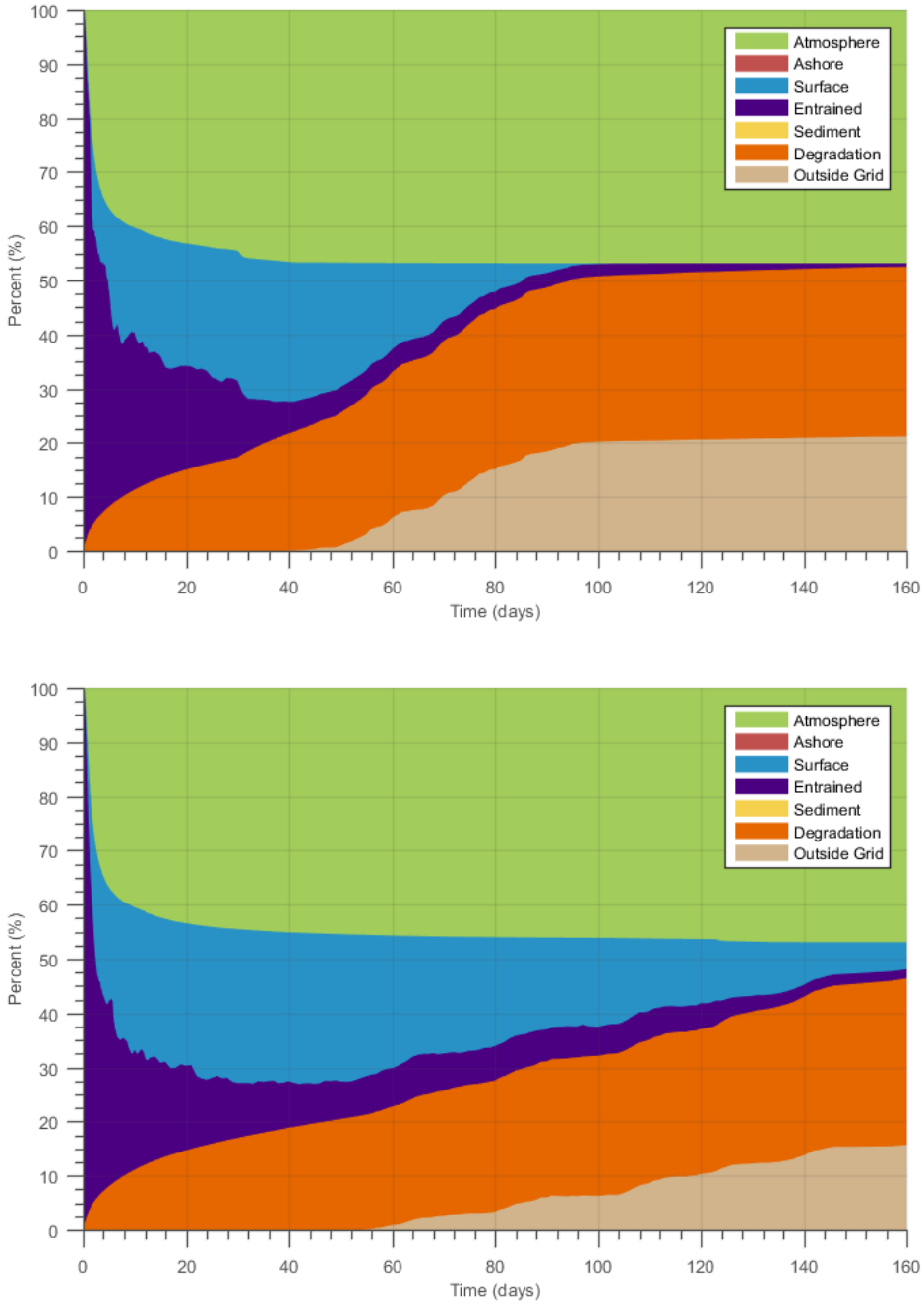

Figure 4-53. Mass balance plots of the 95th percentile water column cases resulting from 30- (top) and 123-day (bottom) blowouts at West Flemish 1.

4.2.2.2 West Flemish 2

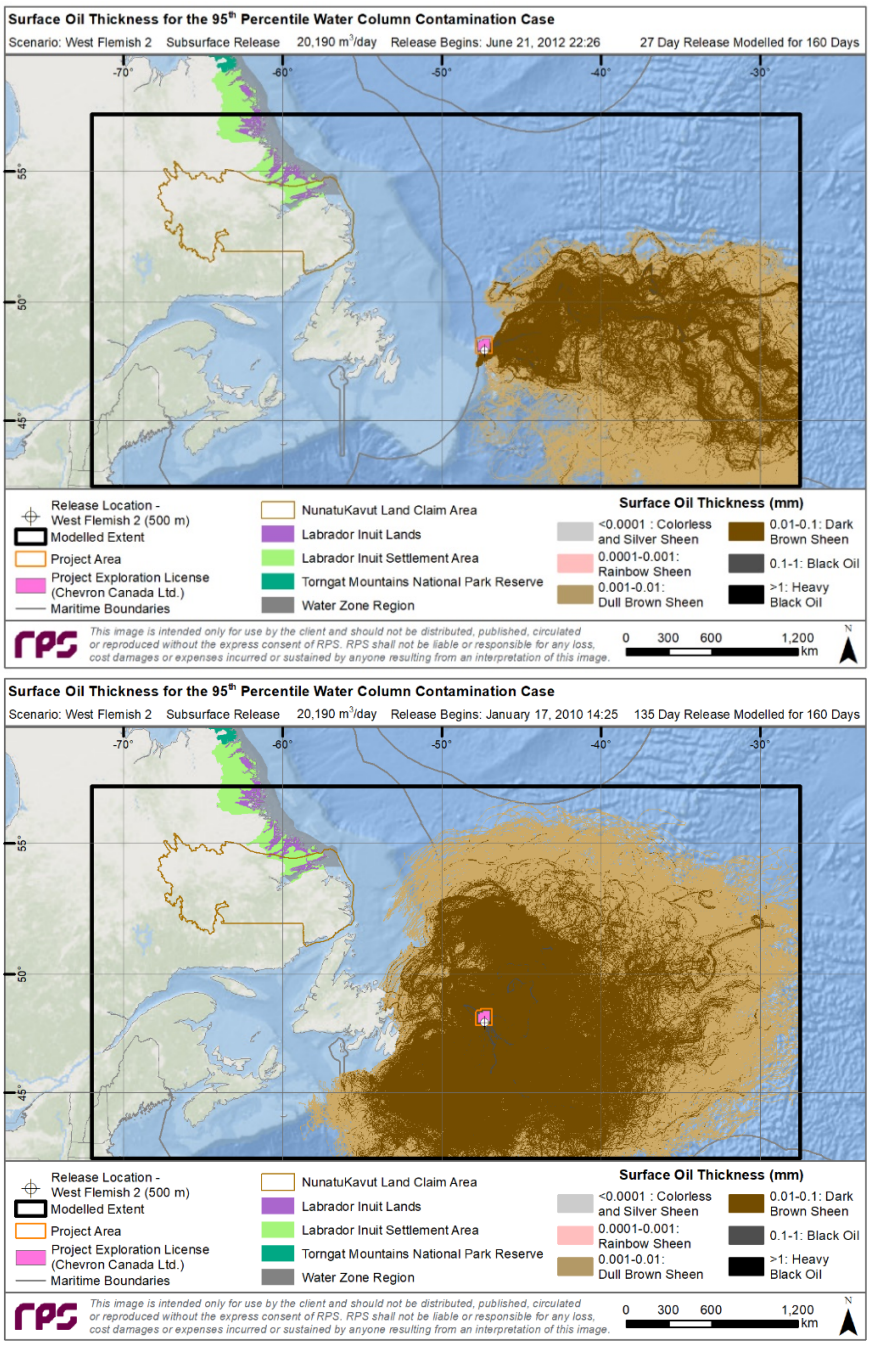

Figure 4-54. Surface oil thickness for the 95th percentile water column cases resulting from 27- (top) and 135-day (bottom) blowouts at West Flemish 2.

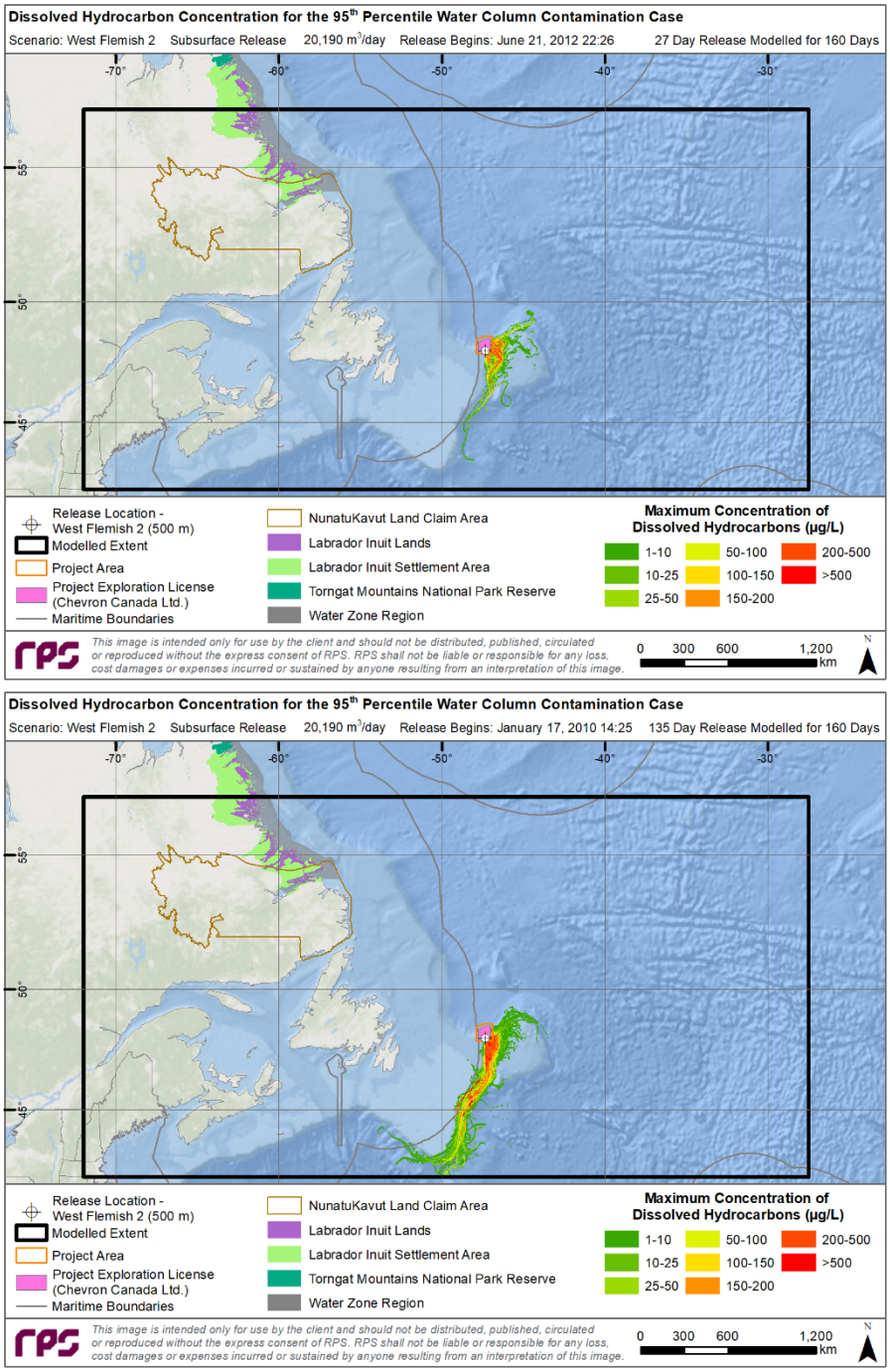

Figure 4-55. Maximum DHC at any depth in the water column for the 95th percentile water column cases resulting from 27- (top) and 135-day (bottom) blowouts at West Flemish 2.

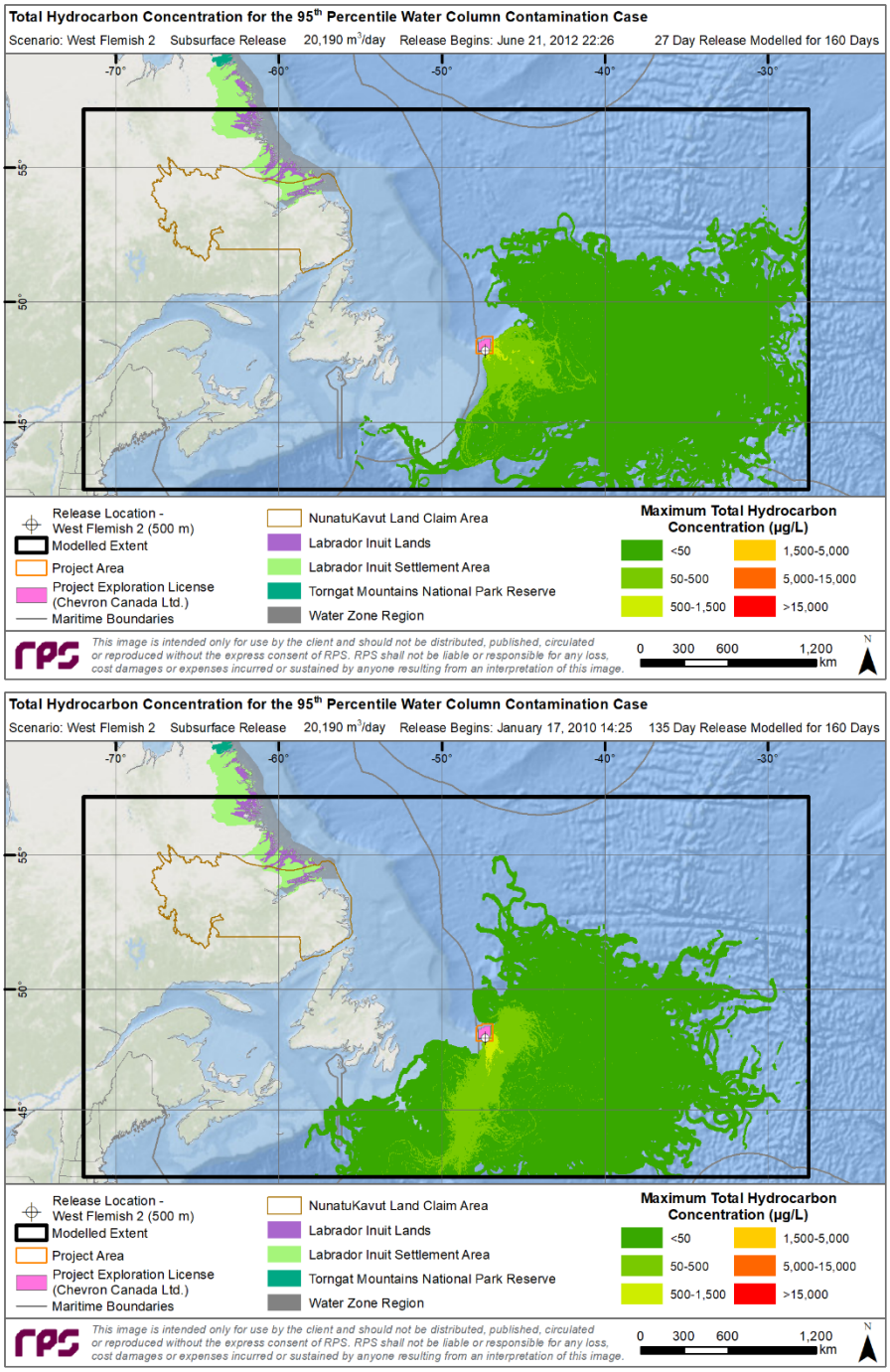

Figure 4-56. Maximum THC at any depth in the water column for the 95th percentile water column cases resulting from 27- (top) and 135-day (bottom) blowouts at West Flemish 2.

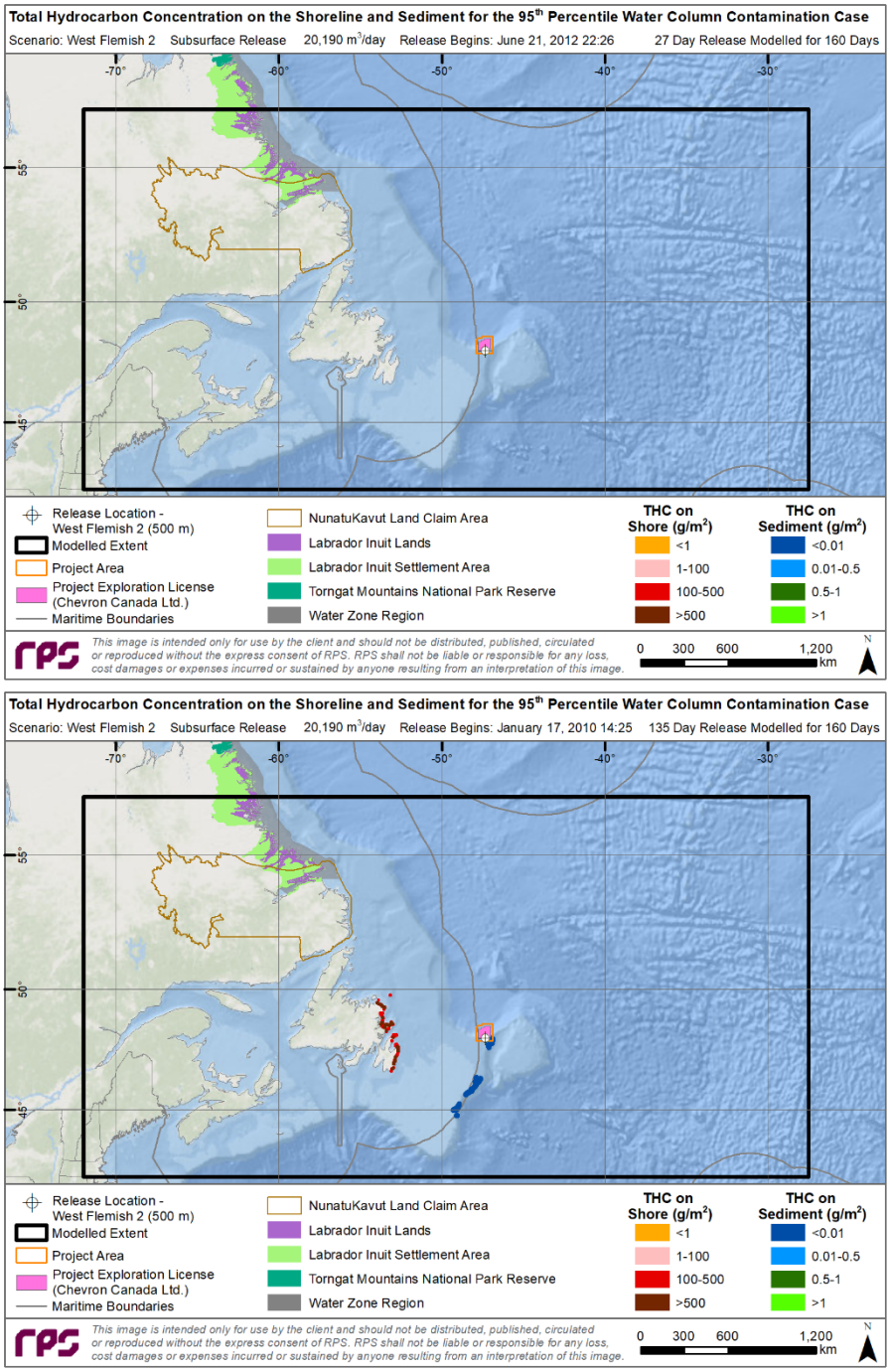

Figure 4-57. THC on the shore and sediment for the 95th percentile water column cases resulting from 27- (top) and 135-day (bottom) blowouts at West Flemish 2.

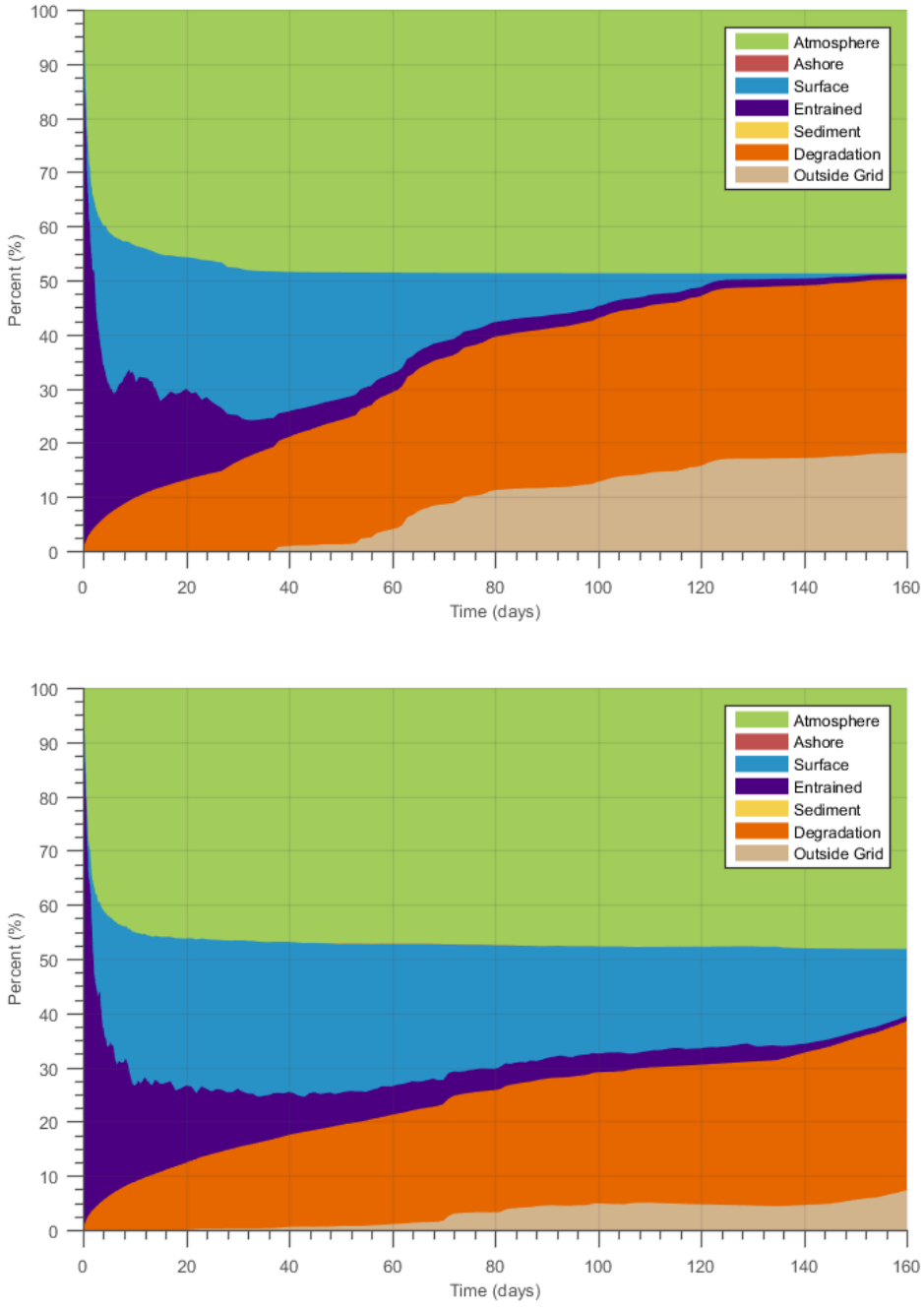

Figure 4-58. Mass balance plots of the 95th percentile water column cases resulting from 27- (top) and 135-day (bottom) blowouts at West Flemish 2.

4.2.3 Shoreline Exposure Cases

The results of the identified 95th percentile (i.e., credible worst-case) cases for shoreline exposure for the short- and long-duration releases at West Flemish 1 and 2 are provided below. Note that the modelled release dates for the representative scenarios at each site differed (Table 2-5). For example, both the short- and long-duration release cases (30- and 123-day) at West Flemish 1 were representative of winter cases (i.e., start dates in December and January), while the cases at West Flemish 2 were representative of both winter (27-day) and summer (135-day).

The predicted total surface area and the cumulative footprints of surface area exposed to oil >0.001 mm (dull brown sheens) were generally similar between sites and release durations for the selected deterministic cases (Figure 4-59 and Figure 4-64; Table 4-3). Each of the cases were predicted to result in cumulative surface oil footprints that extended radially around the release location with varying degrees of symmetry. However, the predicted surface oil exposure resulting from the short-duration release at West Flemish 2 was predicted to be more zonally elongated and centered east of the release site. The long-duration releases (123- and 135-day) were predicted to result in much larger areas affected by dark brown sheens (0.01-0.1 mm) than the short-duration releases. The short-duration release at West Flemish 2 also stood out due to its larger area of dull brown sheen, relative to dark brown sheen (Figure 4-64). Although, heavy black oil (> 1 mm) was not noticeably present in any of the selected deterministic scenarios, the potential for socio-economic impacts would be expected within the cumulative oiled region based on oil thickness (Table 4-3).

Generally, the representative cases modelled at West Flemish were not dispersed as widely as West Flemish 1 and consequently larger areas with DHC concentrations >200 µg/L (Figure 4-60 and Figure 4-65). Predicted cumulative THC footprints were larger than DHC, particularly for the long-duration release as the dissolved portion was predicted to disperse, degrade, and volatilize/evaporate. Highest concentrations of total hydrocarbons (>500 µg/mL) were predicted to occur in the general area encompassing and southwest of the Flemish Cap, with cumulative THC footprints centered to the sound and east of the release sites (Figure 4-61 and Figure 4-66).

The identified representative shoreline exposure cases were predicted to result in 98-1,061 km of shoreline oiling. The long-duration releases (123- and 135-day) at both sites resulted in similar lengths of shoreline with the potential for contamination along the east coast of Newfoundland, mostly in excess of 500 g/m^2. However, the scenario modelled at West Flemish 1 was predicted to be patchier and more discontinuous, resulting in lighter oiling from the southern tip of the Avalon Peninsula north to Fleur-de-lys, while West Flemish 2 resulted in heavier predicted oiling from the southern Avalon Peninsula north to Fogo Island. The short-duration (30-day) release at West Flemish 1 resulted in a predicted shoreline oil contamination footprint similar to the long-duration releases, while the short-duration (27-day) release at West Flemish 2 resulted in predicted shoreline oil contamination primarily 100-500 g/m^2 extending northward as far as portions of the Labrador coast (Figure 4-62 and Figure 4-67). The long-duration release (135-day) at West Flemish 2 was also predicted to result in shoreline contamination on Sable Island. In general, the oil that was predicted to reach shorelines was expected to be highly weathered, patchy, and discontinuous, as it would have weathered for well over a week (or more) before contacting shore. Limited sediment contamination of <0.1 g/m^2 was predicted to the east of the release site for both releases at West Flemish 2 and only for the long-duration release at West Flemish 1 (Figure 4-62 and Figure 4-67).

At the end of the 160-day simulations of the 95th percentile shoreline exposure for short- and long-duration releases at the West Flemish 1 site, large percentages of the oil evaporated (~47%) and degraded (34-40%), accounting for >81% of each modelled release. The amount of oil predicted to remain on the water surface was 8% and 13%, with ~0.5% within the water column. Up to 5% of oil (predominantly persistent surface oil) was predicted to be transported outside of the modelled domain. Oil transported to the sediment and shoreline were not major fate pathways with <0.1% predicted to settle on sediments and 0.1% was predicted to remain on the shoreline.

At the West Flemish 2 site, approximately 49% of oil was predicted to evaporate and 29-34% degraded, accounting for >78% of each modelled release. The amount of oil predicted to remain on the water surface was 2-11%, 10-14% was transported outside the modelled domain, <2% remained in the water column, and <0.1% settled on sediment. Shoreline contact was not a major fates pathway with ≤0.1% of oil making contact with the shoreline (Table 4-4). Frequent cycling of wind and calm events were evident in all shoreline oil exposure cases, as indicated by “see-sawing” between oil on the surface and entrained oil in the water column (Figure 4-63 and Figure 4-68).

4.2.3.1 West Flemish 1

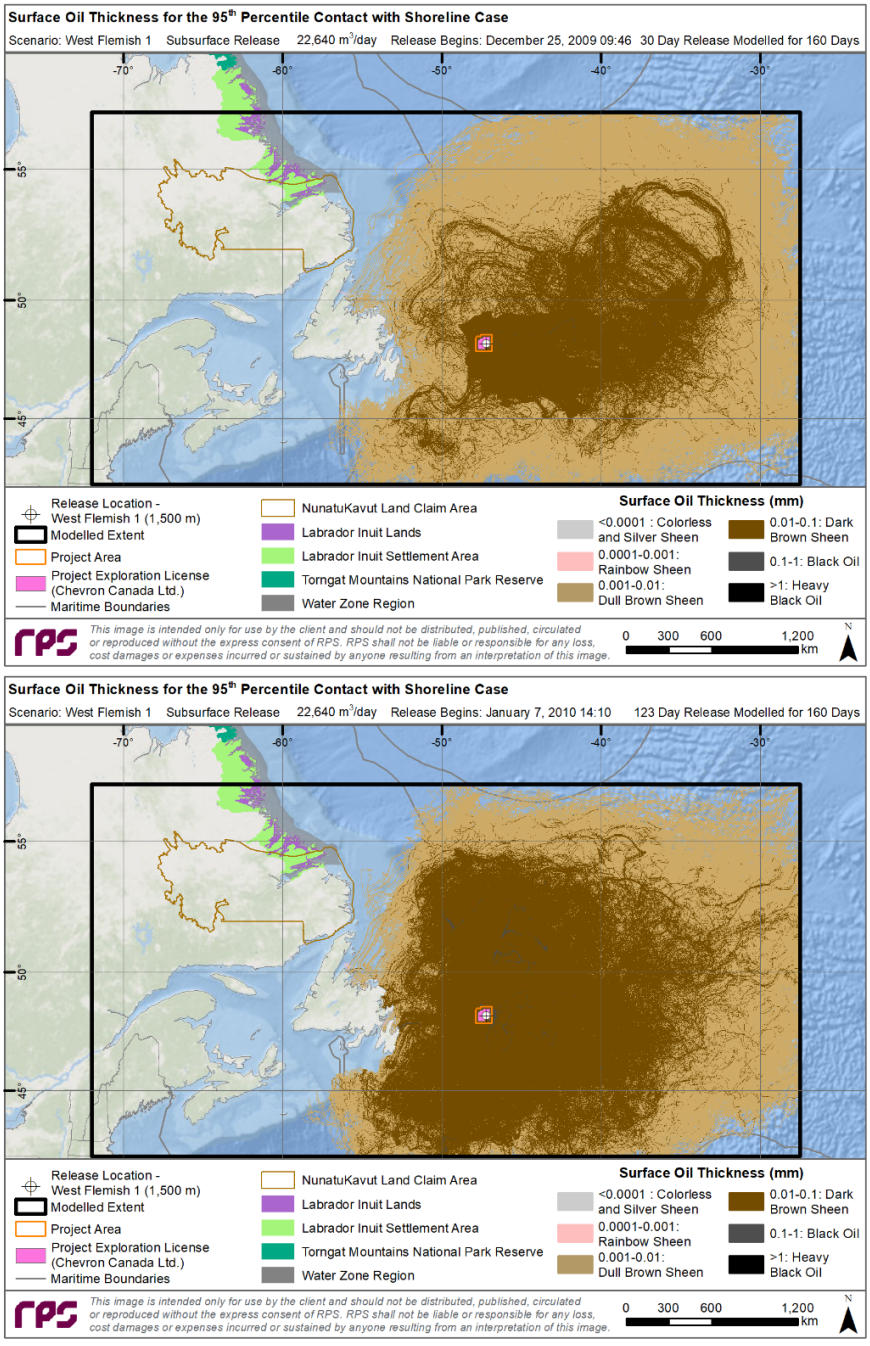

Figure 4-59. Surface oil thickness for the 95th percentile shoreline cases resulting from 30- (top) and 123-day (bottom) blowouts at West Flemish 1.

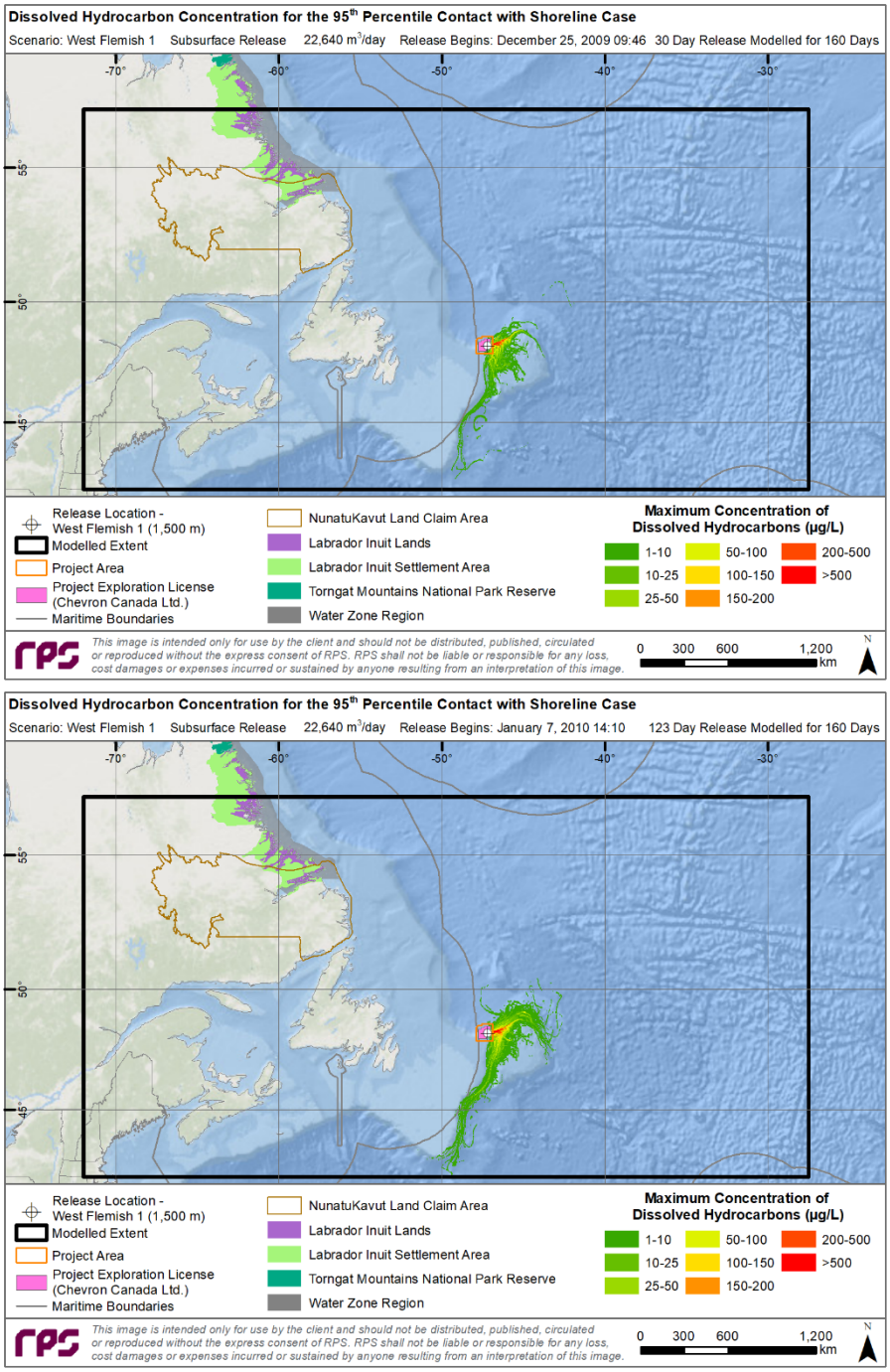

Figure 4-60. Maximum DHC at any depth in the water column for the 95th percentile shoreline cases resulting from 30- (top) and 123-day (bottom) blowouts at West Flemish 1.

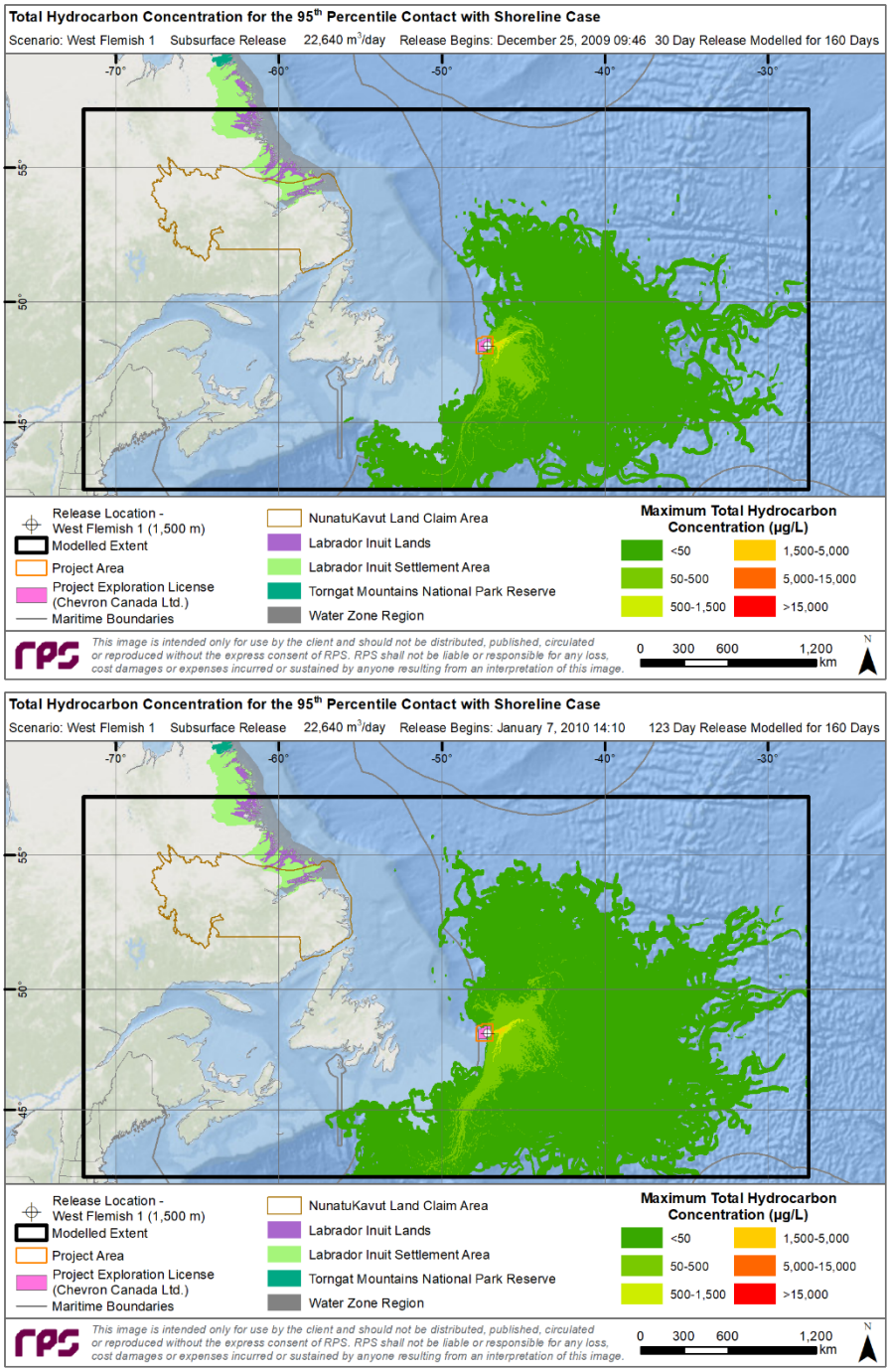

Figure 4-61. Maximum THC at any depth in the water column for the 95th percentile shoreline cases resulting from 30- (top) and 123-day (bottom) blowouts at West Flemish 1.

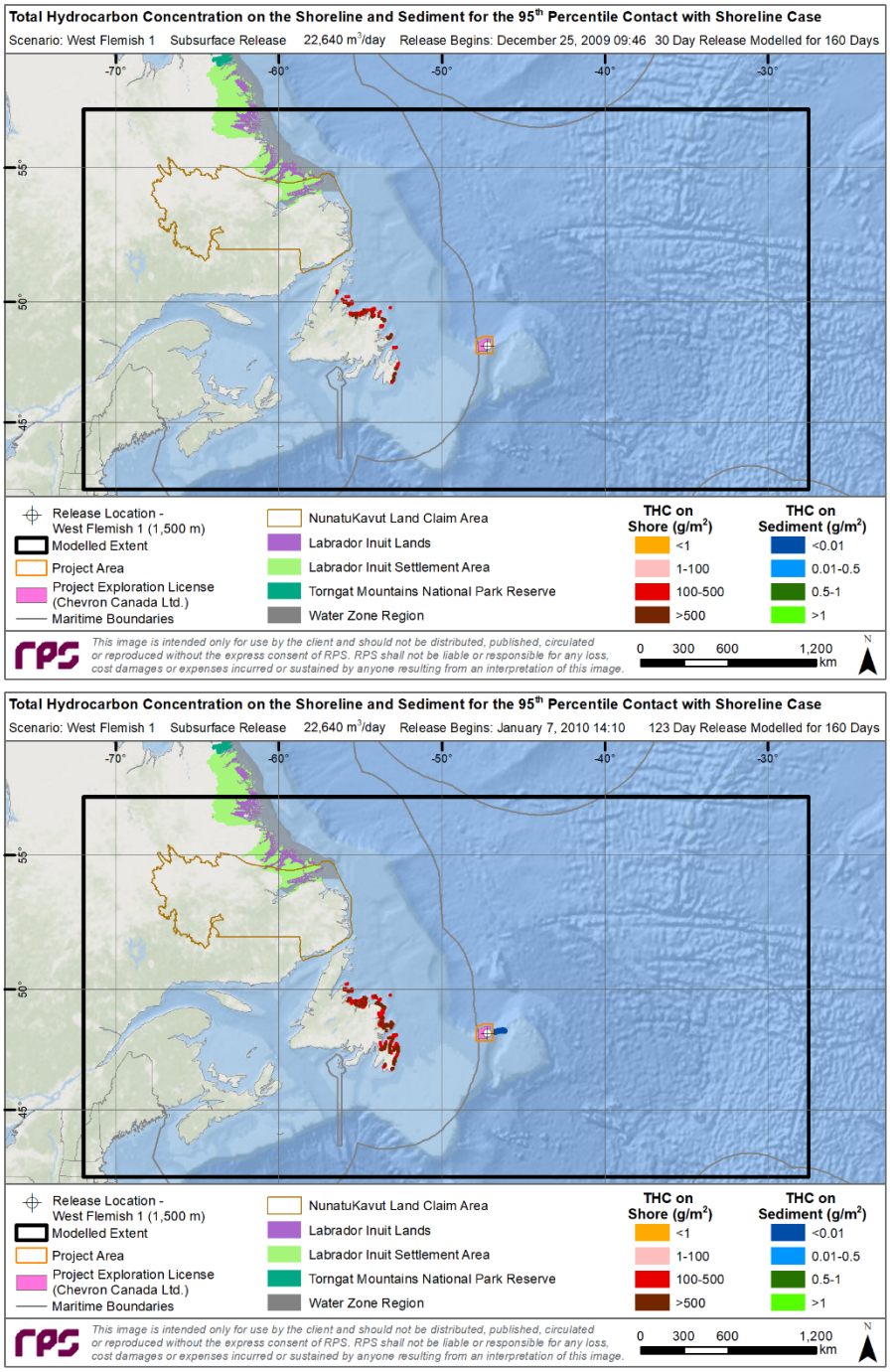

Figure 4-62. THC on the shore and sediment for the 95th percentile shoreline cases resulting from 30- (top) and 123-day (bottom) blowouts at West Flemish 1.

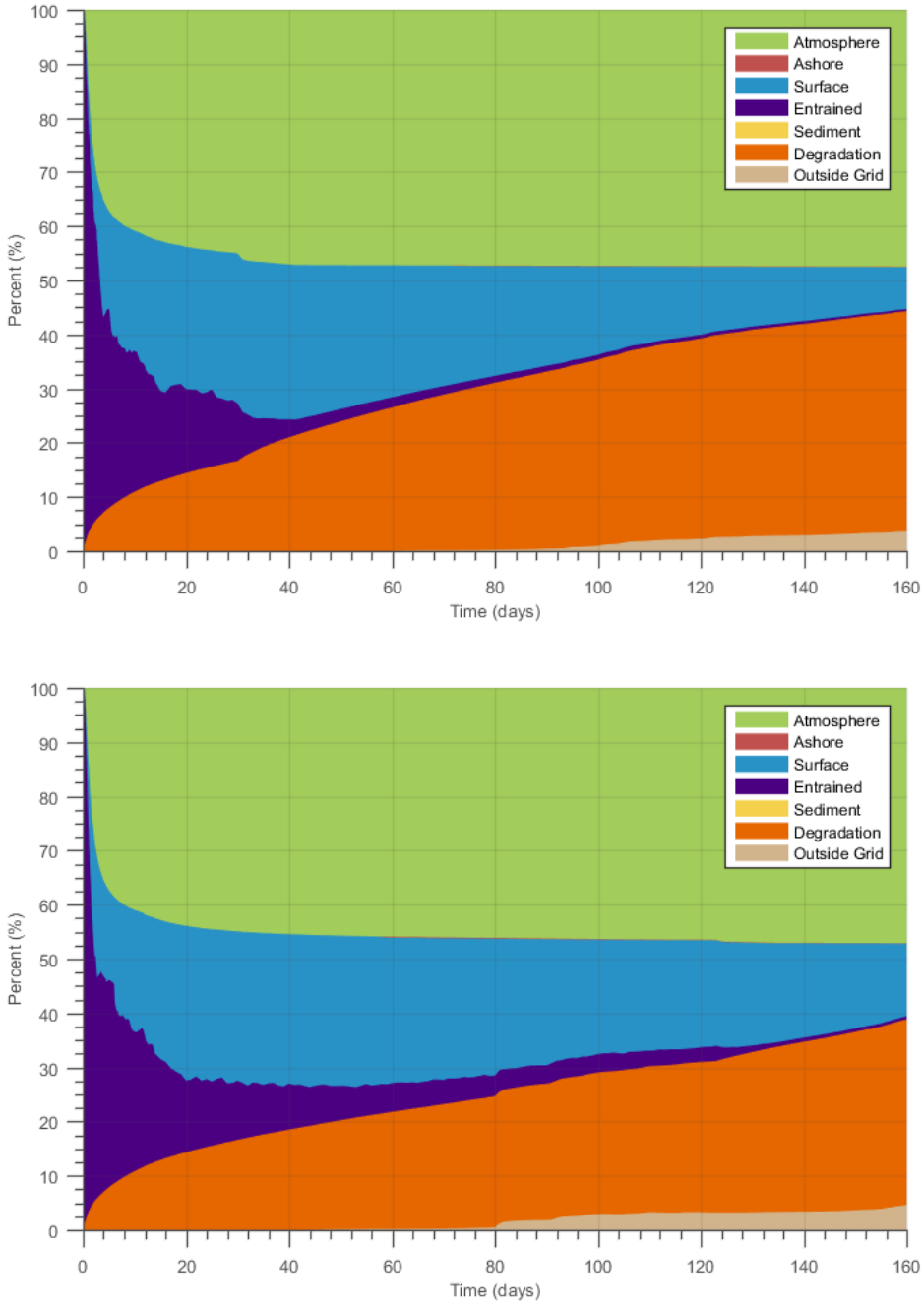

Figure 4-63. Mass balance plots of the 95th percentile shoreline cases resulting from 30- (top) and 123-day (bottom) blowouts at West Flemish 1.

4.2.3.2 West Flemish 2

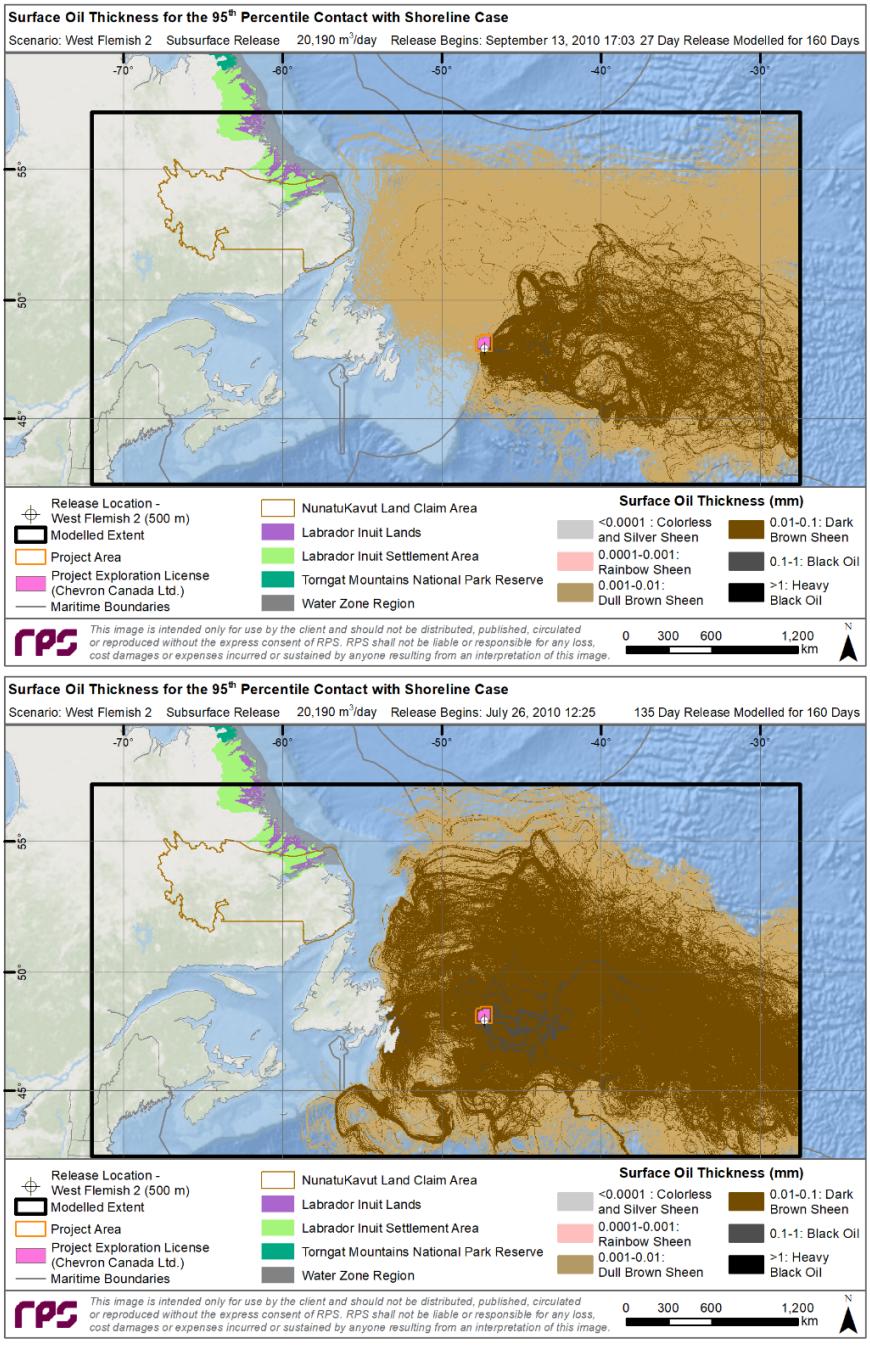

Figure 4-64. Surface oil thickness for the 95th percentile shoreline cases resulting from 27- (top) and 135-day (bottom) blowouts at West Flemish 2.

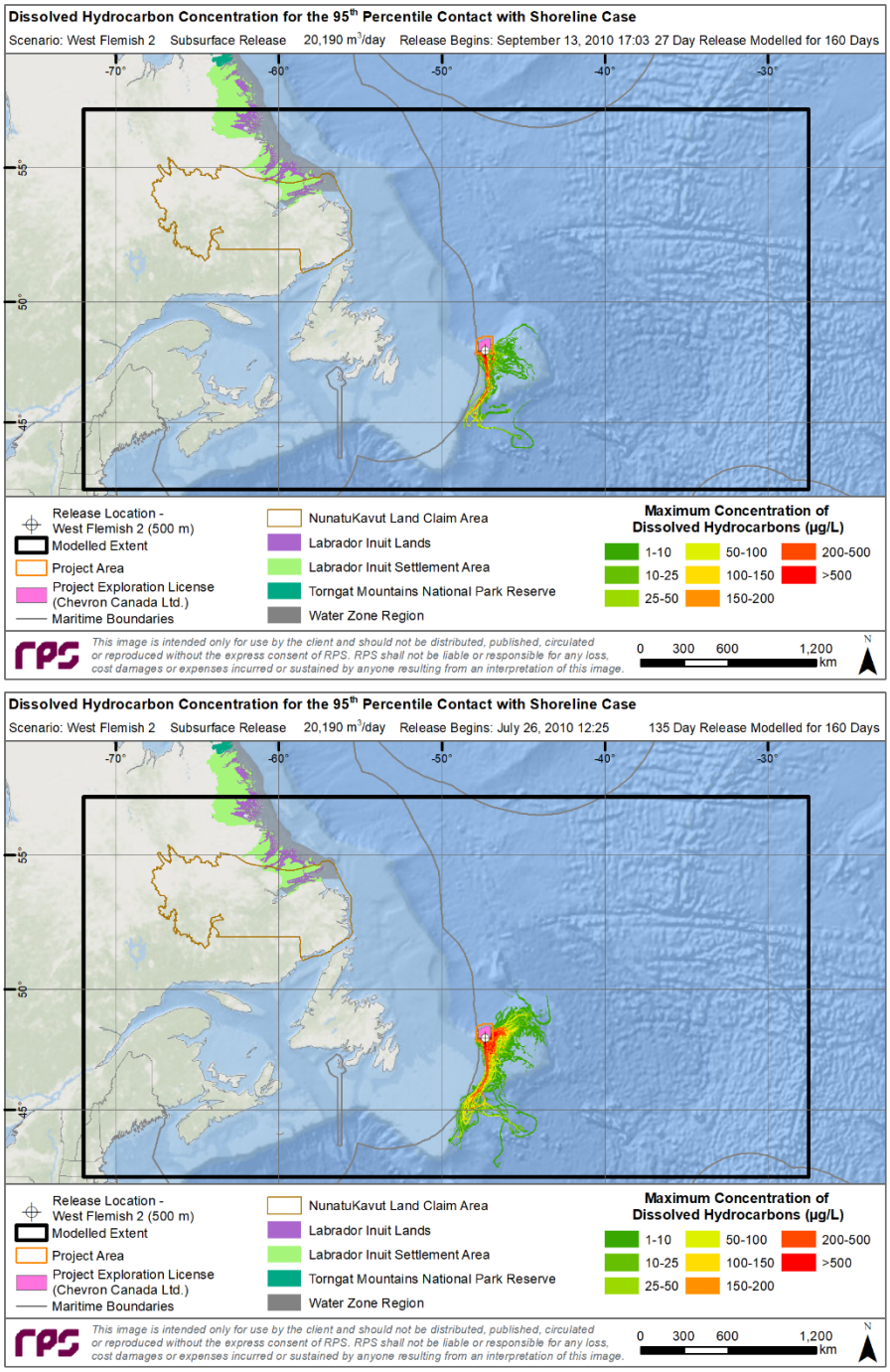

Figure 4-65. Maximum DHC at any depth in the water column for the 95th percentile shoreline cases resulting from 27-day (top) and 135-day (bottom) blowouts at West Flemish 2.

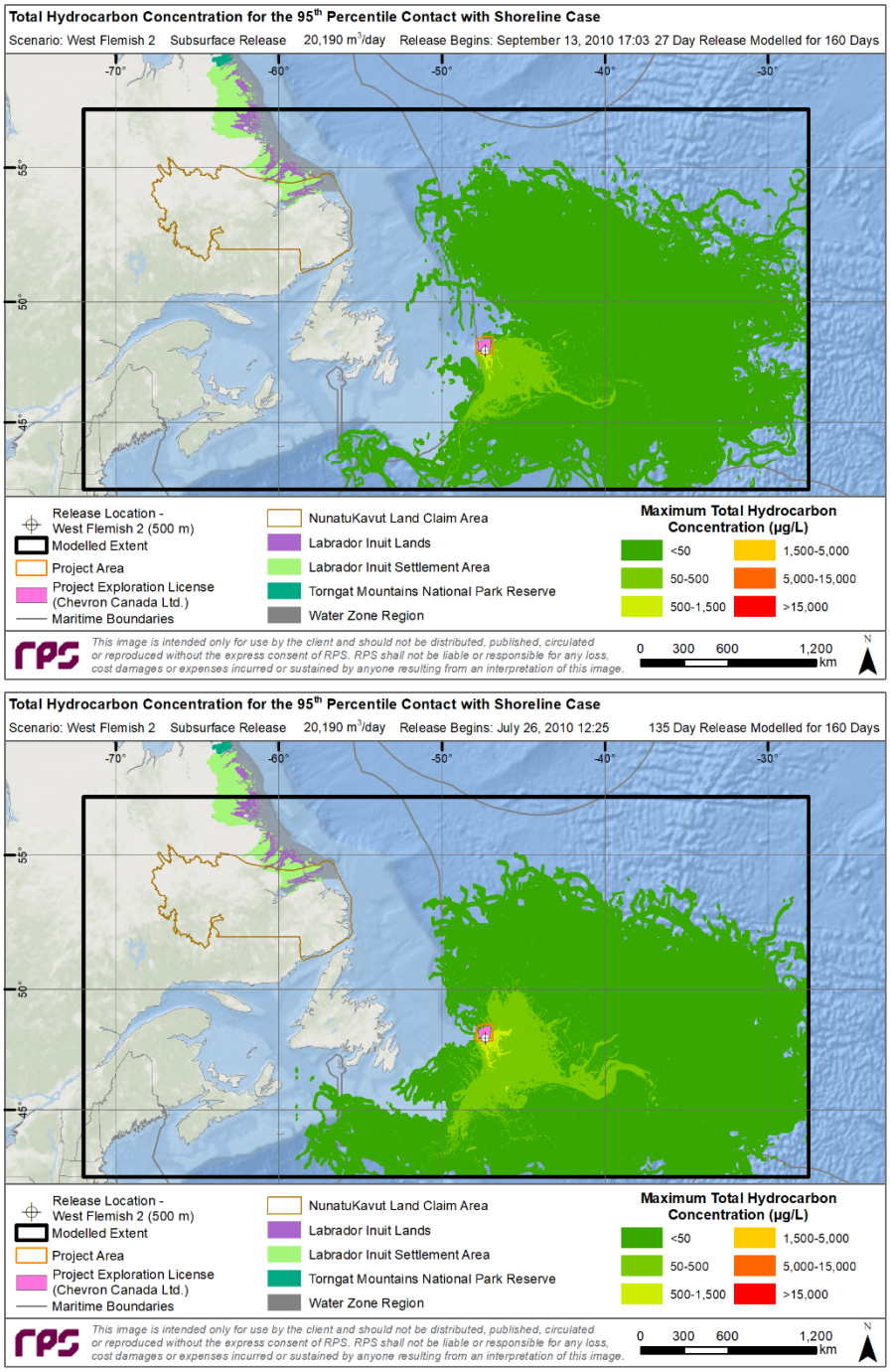

Figure 4-66. Maximum THC at any depth in the water column for the 95th percentile shoreline cases resulting from 27-day (top) and 135-day (bottom) blowouts at West Flemish 2.

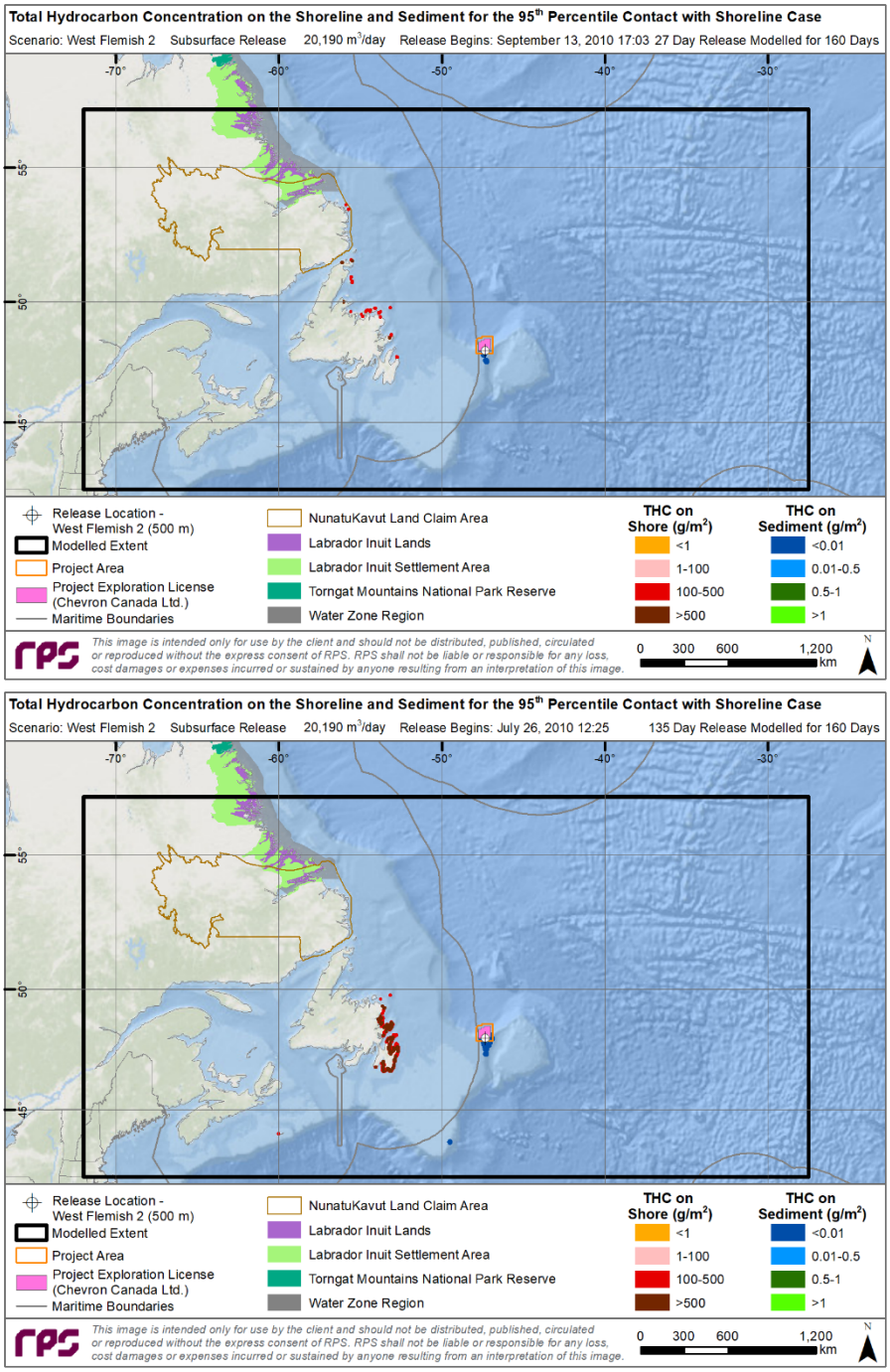

Figure 4-67. THC on the shore and sediment for the 95th percentile shoreline cases resulting from 27-day (top) and 135-day (bottom) blowouts at West Flemish 2.

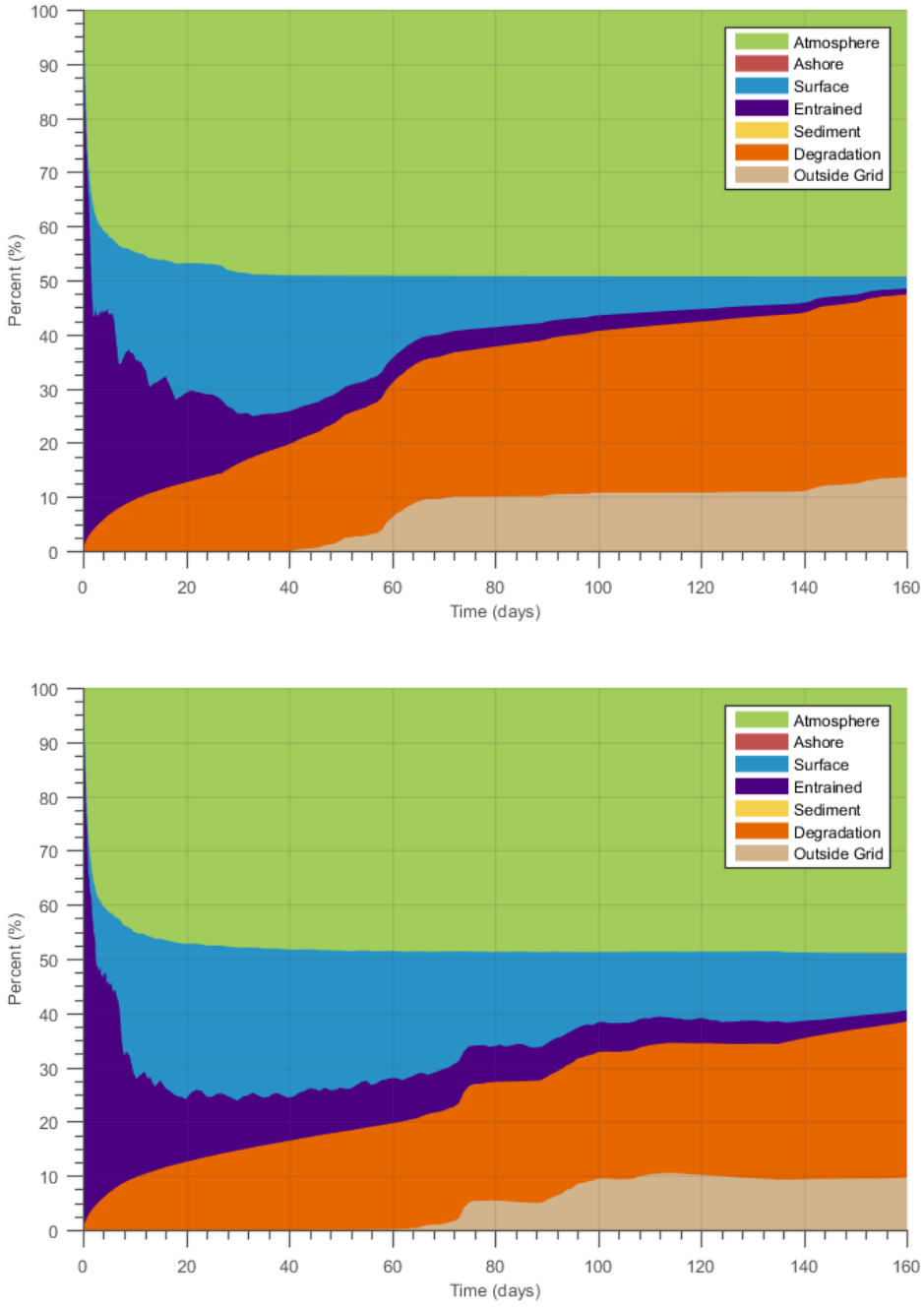

Figure 4-68. Mass balance plots of the 95th percentile shoreline cases resulting from 27- (top) and 135-day (bottom) blowouts at West Flemish 2.

4.2.4 Batch Spill Results

Results for the hypothetical batch spill resulting from bunkering operations are provided in the mass balance and cumulative figures below. The simulation was comprised of a nearly instantaneous release of 1,000 L of marine diesel at the surface, which was then modelled for 30 days. The scenario was assumed to occur during the calmest wind-speed period during the summer/ice-free conditions, as they would result in the largest amount of oil on the surface. The release was simulated from West Flemish 1 on June 4, 2009.

The cumulative footprint of surface oil (marine diesel) was predicted to be transported to the east, clockwise around the perimeter of the Flemish Cap for approximately 1,500 km at thicknesses that were representative of colorless or silver sheens (<0.0001 mm) (Figure 4-69). Due to the small release volume, low amount of entrainment (due to low winds), and size of the concentration gridding (150 m by 150 m), predicted concentrations of dissolved or total hydrocarbons in the water column did not register above a recordable threshold (Figure 4-70 and Figure 4-71). In addition, the batch spill was not predicted to make contact with any shorelines or result in oil settling on sediments (Figure 4-72).

At the end of the 30-day marine diesel batch spill simulation, 64% was predicted to evaporated into the atmosphere, 25% degraded, 11% remained entrained in the water column, while 0.1% of the released volume was predicted to remain floating on the water surface, and 0% contacted shorelines or settled on sediments (Figure 4-73 and Table 4-4).

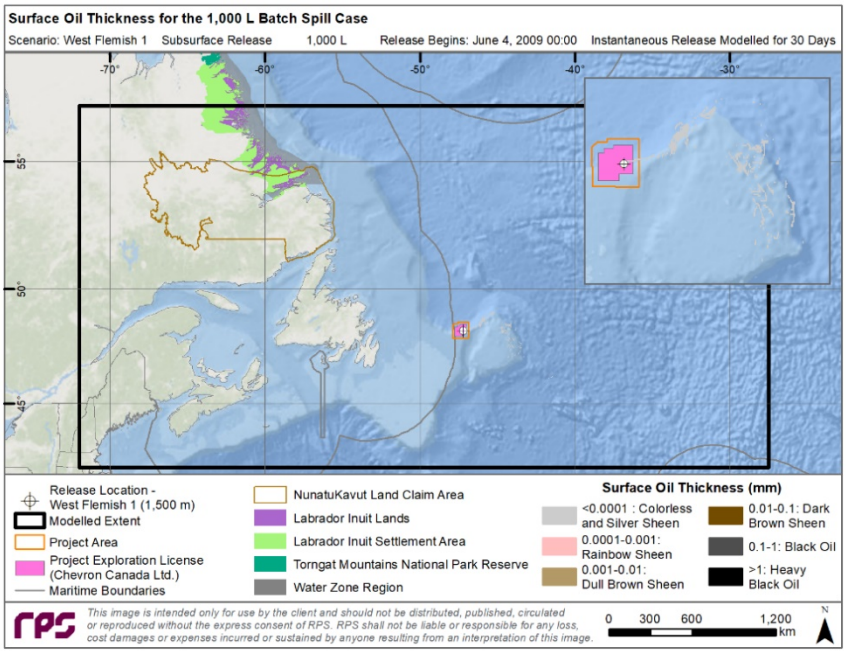

Figure 4-69. Surface oil thickness for the Marine Diesel batch spill of 1,000 L at West Flemish 1.

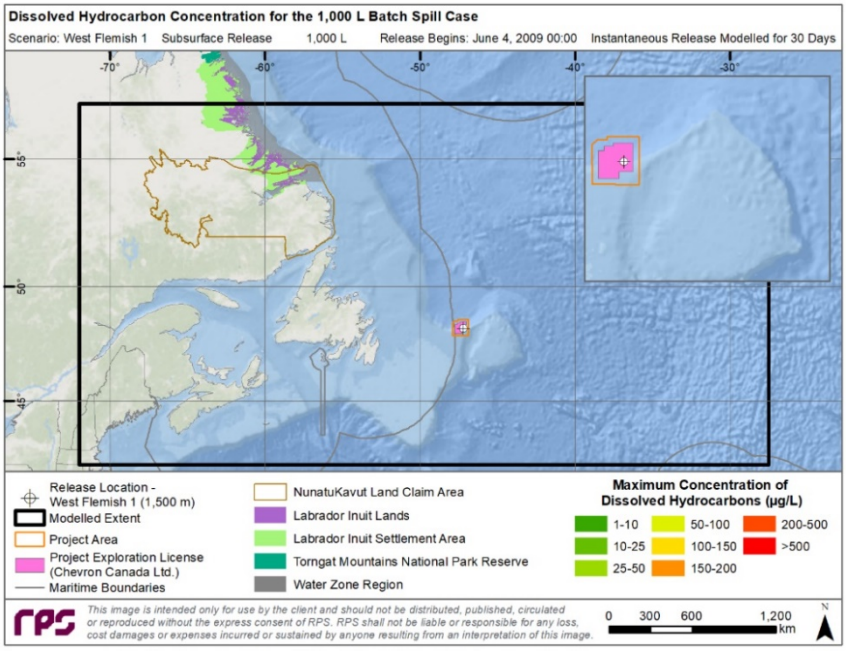

Figure 4-70. Maximum DHC at any depth in the water column for the Marine Diesel batch spill of 1,000 L at West Flemish 1.

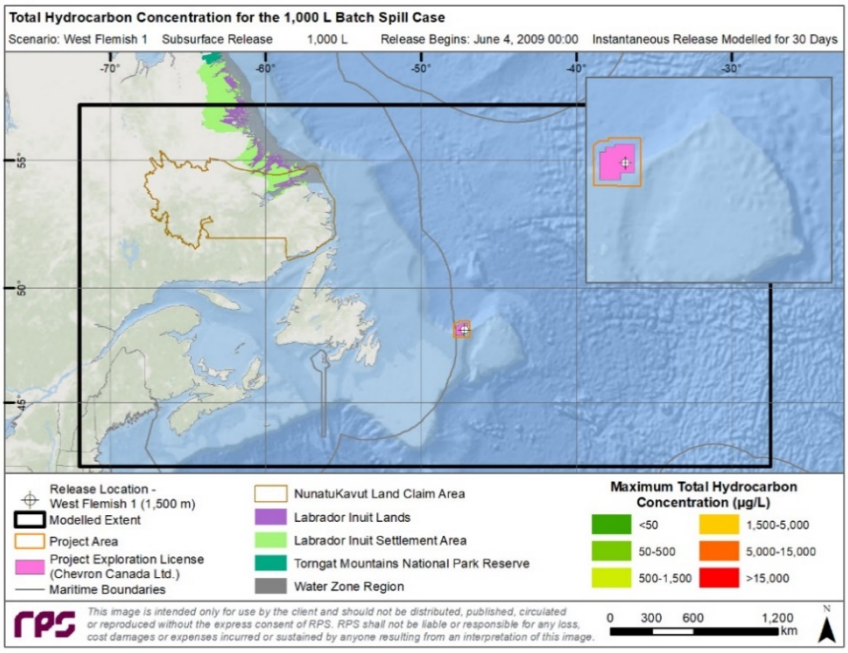

Figure 4-71. Maximum THC at any depth in the water column for the Marine Diesel batch spill of 1,000 L at West Flemish 1.

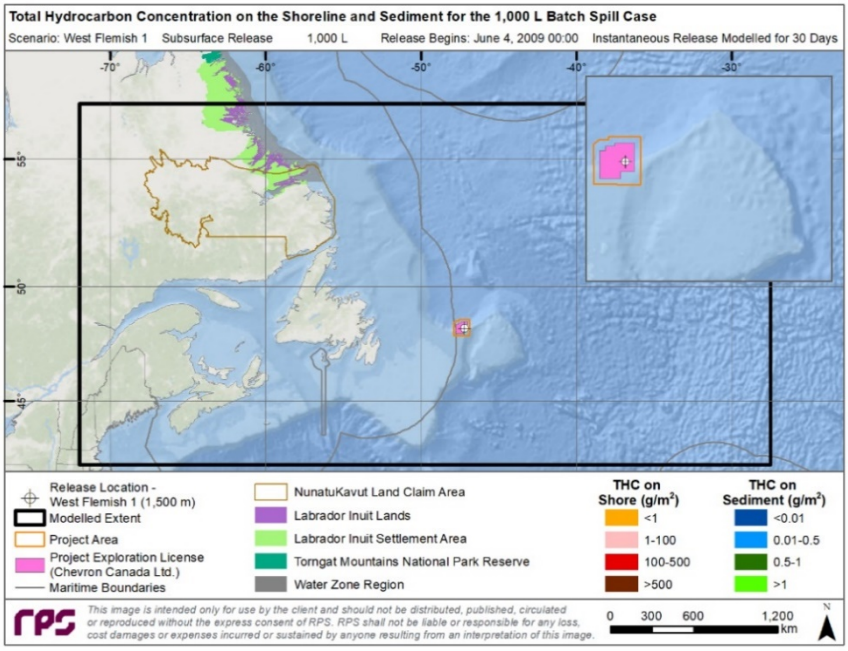

Figure 4-72. THC on the shore and sediment for the Marine Diesel batch spill of 1,000 L at West Flemish 1.

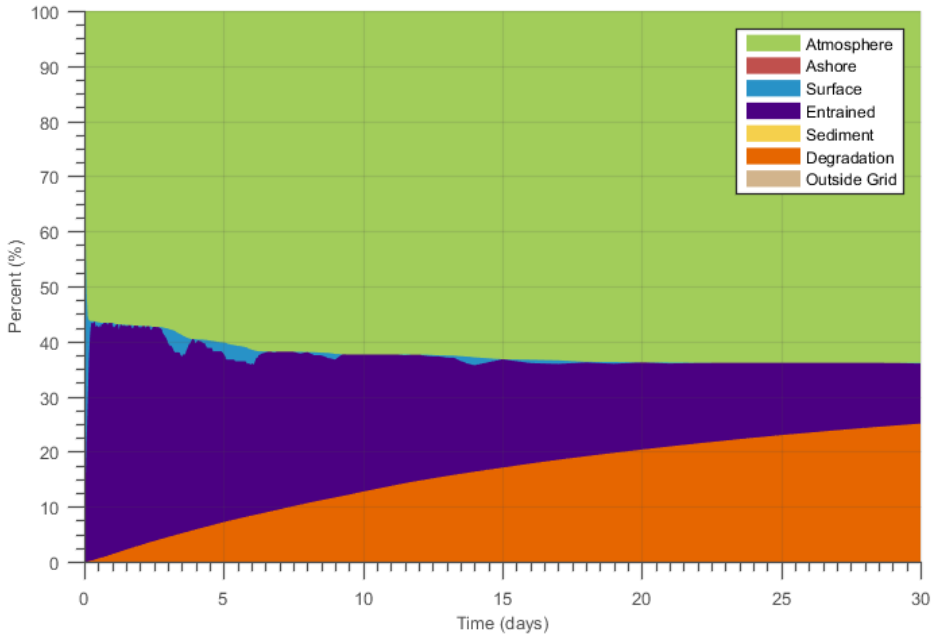

Figure 4-73. Mass balance plot of the Marine Diesel batch spill of 1,000 L at West Flemish 1.

4.2.5 Summary of Deterministic Results

4.2.5.1 Representative Cases: Surface, Water Column, and Shoreline Oil

For the representative credible "worst-case" deterministic scenarios at West Flemish 1 and West Flemish 2, subsurface oil was predicted to rise through the water column where it surfaced and predominantly was transported to the east and south. In several simulations, oil was predicted to strand on the Newfoundland shoreline, as well as to a lesser extent the southern shores of Labrador and even Sable Island, over the unmitigated releases modelled for 160 days. In each scenario, nearly half of the oil was predicted to evaporate, while a third was predicted to degrade by natural processes (Table 4-4). Of the remaining roughly 15-20% of the released oil, 1-15% was predicted to remain on the surface, <2% remain in the water column, <0.1% to 0.4% stranded on shorelines, and <0.1% settled onto sediments over 160 days. Because the simulations were so long, between 3.6 to 21.2% of the oil (predominantly surface oil as heavily weathered emulsifications and tarballs) was predicted to leave the model domain to the east. Note that all scenarios assume a completely unmitigated release, which is an unlikely situation because various emergency response tactics would typically be employed immediately in the event of a spill.

The predicted cumulative surface oil footprints of most of the identified representative cases were centered to the east of the release sites, due to surface oil transport mainly towards the east, with natural dispersion to the north and south. Cumulative maximum surface oil in all cases was predicted to have an average thickness within the range of 0.001–0.1 mm (1 –100 µm), which would appear as discontinuous, patchy brown sheens to dark brown sheens, with thinner features predicted further from the release site (Figure 4-39 and Figure 4-44). In some cases, patchy black oil (0.1-1 mm) was predicted to occur near the release site as it was transported, primarily to the east, up to a few hundred kilometers away. The predicted areas of surface oil exposure for the short (27- and 30-day) and long (123- and 135-day) 95th percentile cases were similar between sites, with short releases have the potential to affect a total of 1,221,000-2,910,000 km^2 above the socio-economic threshold over 160 days and long releases having the potential to affect a total of 1,701,000-2,991,000 km^2 over 160 days (Table 4-3).

The maximum subsurface water volumes exposed to THC concentrations for the 95th percentile water column cases were predicted to range between 77,020 km^3 and 89,310 km^3 (Table 4-3). Areas of relatively high THC concentration (500-5,000 µg/L) occurred in the Flemish Pass and Flemish Cap region in most scenarios (Figure 4-51 and Figure 4-56). Regions of >500 µg/L dissolved hydrocarbons were predicted to be transported primarily northeast and southwest of the release site in the 95th percentile cases at West Flemish 1 and primarily southwest at West Flemish 2. These differences in dissolved hydrocarbon transport were due to the rising oil droplets from the release and the site locations relative to the strong subsurface currents (e.g. Labrador current) moving within the Flemish Pass and along the shelf break. Entrained oil concentrations in surface waters were predicted to vary considerably from day to day as expected from variable wind and wave conditions that control entrainment, mixing, and resurfacing rates.

For the shoreline oil exposure cases, shoreline oil contamination was predicted to range from approximately 100-1,060 km for socioeconomic effects and 98-946 km for ecological effects (Table 4-3). In general, most oiling in these scenarios was predicted along the eastern and southern shores of Newfoundland, although stochastic results did result in the potential for shoreline oiling from southern Newfoundland up through Labrador. The oil that was predicted to strand along shorelines was generally in the 100 to > 500g/m^2 range,

but would be patchy, discontinuous, and generally highly weathered by the time it reached shore. Offshore sediment contamination was much less prevalent and occurred at very low levels (<0.01 g/m^2) at locations near the release sites and to the south along the continental shelf break. The extents of shoreline exposures were predicted to be less for West Flemish 2, especially for the short-duration release (Figure 4-62 and Figure 4-67).

The contrasting results demonstrate the importance of stochastic probability footprints outlining the range of spill outcomes from environmental variability rather than differences in site characteristics. In general, stochastic results provided an understanding of the locations that were susceptible to potential effects, while representative deterministic results provide more context with the anticipated magnitude of effects for 95th percentile “worst-case” scenarios.

4.2.5.2 Batch Spill

A smaller scale near-instantaneous batch spill of marine diesel was modelled as an accidental release. One 1,000 L release was modelled at West Flemish 1 and was simulated for thirty days (Table 2-5). The marine diesel used in this scenario was a standard diesel that had a low viscosity and a high aromatic content that was expected to evaporate quickly during the summertime releases. The marine diesel release was predicted to result in a patchy distribution of colorless or silver sheen of oil <0.0001 mm (0.1 µm), where the total area of that was exposed to oil >0.04 µm over 30 days was 8 km^2 (Figure 4-69). Due to the small release volume, low entrainment, and size of the concentration gridding (150 m by 150 m), predicted concentrations of dissolved or total hydrocarbons in the water column did not register above the threshold (Figure 4-70 and Figure 4-71).Oil was not predicted to reach any shorelines from the modelled batch spill.

Table 4-3. Representative deterministic cases and associated areas, lengths, and volumes exceeding specified thresholds for 95th percentile surface, water column, and shoreline contact trajectories at the West Flemish 1 and 2 sites and batch spill.

95th Percentile Scenario	Site	Released Volume	Approximate Surface Area exceeding thickness thresholds (km²)		Approximate Shore Length exceeding mass per unit area thresholds (km)		Approximate Subsurface Volume exceeding THC threshold (km³)
			Socio-economic (0.04 µm)	Ecologic (10 µm)	Socio-economic (1 g/m²)	Ecologic (100 g/m²)	Socio-economic* (1 µg/L)
Subsurface Blowout Releases							
Surface oil exposure case- 30 d	West Flemish 1	679,200 m³ (22,640 m³/d)	2,800,000	888,200	935	425	66,720
Water column case- 30 d			1,221,000	673,200	-	-	77,410
Shoreline contact case- 30 d			2,910,000	1,039,000	425	314	65,880
Surface oil exposure case- 123 d		2,784,720 m³ (22,640 m³/d)	2,759,000	1,917,000	3779	3694	125,500
Water column case- 123 d			1,701,000	1,137,000	-	-	89,310
Shoreline contact case- 123 d			2,991,000	1,741,000	1061	790	84,940
Surface oil exposure case- 23 d	West Flemish 2	545,130 m³ (20,190 m³/d)	2,412,000	710,900	-	-	67,010
Water column case- 23 d			1,499,000	676,700	-	-	77,530
Shoreline contact case- 23 d			2,332,000	712,400	100	98	98,410
Surface oil exposure case- 135 d		2,725,650 m³ (20,190 m³/d)	2,843,000	1,756,000	21	4	95,790
Water column case- 135 d			2,602,000	1,437,000	350	145	77,020
Shoreline contact case- 135 d			2,730,000	1,804,000	993	946	111,000
Batch Spill							
Surface Batch Spill of 1,000 L	West Flemish 1	1,000 L	8	-	-	-	-

*There is only 1 category threshold (socio-economic) for THC –calculated by multiplying the area times the depth of the grid cell.

Table 4-4. Summary of the mass balance information for all representative scenarios. All values represent a percentage (%) of the total amount of released oil at the end of the representative (95th percentile) deterministic or batch spill scenarios.

95th Percentile Scenario	Site	Percent of Total Released Oil (%)						
		Surface	Evaporated	Water Column	Sediment	Ashore	Degraded	Outside Grid
Subsurface Blowout Releases								
Surface oil exposure case- 30 d	West Flemish 1	4.2	47.2	0.2	<0.1	0.2	38.3	9.9
Water column case- 30 d		0.0	46.8	0.6	<0.1	0.0	31.4	21.2
Shoreline contact case- 30 d		7.8	47.5	0.4	<0.1	0.1	40.7	3.6
Surface oil exposure case- 123 d		11.0	46.9	1.6	<0.1	0.4	32.3	7.7
Water column case- 123 d		5.0	46.9	1.7	<0.1	0.0	30.7	15.7
Shoreline contact case- 123 d		13.4	47.1	0.6	<0.1	0.1	34.3	4.6
Surface oil exposure case- 23 d	West Flemish 2	0.2	48.7	0.8	<0.1	0.0	32.2	18.1
Water column case- 23 d		1.0	48.1	0.1	<0.1	0.0	34.9	15.9
Shoreline contact case- 23 d		2.2	49.3	1.1	<0.1	<0.1	33.8	13.7
Surface oil exposure case- 135 d		10.4	48.2	1.1	<0.1	0.0	31.0	9.3
Water column case- 135 d		12.4	48.2	0.9	<0.1	<0.1	31.2	7.3
Shoreline contact case- 135 d		10.5	48.9	2.0	<0.1	0.1	28.8	9.7
Batch Spill								
Surface Batch Spill of 1,000 L	West Flemish 1	0.1	63.9	10.9	<0.1	0.0	25.1	0.0

5 DISCUSSION AND CONCLUSIONS

Most surface oil from both release locations was predicted to move eastward because of prevailing westerly winds and the North Atlantic current. The Labrador and North Atlantic currents have steady velocities in the region throughout the year resulting in fairly consistent subsurface oil exposure patterns, but wind speeds increase during the winter months leading to an increase in the probability of shoreline oiling. Based on the results of the stochastic analysis of hundreds of model scenarios, the average probability of shoreline oiling ranged from 1.9-3.4% in the summer and 3.4-8.7% in the winter. Individual points along shore did have maximum probability of shoreline oil contamination ranging from 4-28%, depending on the scenario. Depending on the time of year and environmental conditions, areas susceptible to shoreline oiling included the entire east coast and much of the west coast of Newfoundland, the Avalon Peninsula, the southern shores of Labrador reaching into the Gulf of St. Lawrence, and Sable Island. Oil that reached shore was expected to be patchy, discontinuous, and weathered, as it would have taken a minimum of 10 days (and frequently much longer) to reach shore.

Surface exposures above the ecological impact threshold were between 673,200 and 1,917,000 km^2 for selected deterministic simulations. Subsurface volumes exceeding the THC socio-economic threshold ranged from 65,880 to 125,500 km^3. Shoreline length exceeding mass per unit area thresholds ranged from a mode of 0 up to 3,779 km with most cases having less than 100 km. In general, most simulated cases led to predicted surface oil thickness and water column concentrations at or above socio-economic and ecological thresholds for potential impacts in the immediate vicinity and to the east of the release sites, with often little or no predicted shoreline contact after 160 days.

The releases modelled in this study may be considered representative of other potential releases in the Project Area. The depth of release of West Flemish 1 and 2 (1,500 and 500 m, respectively) are within the range of water depths present within the Project Area (300 m to 2,500 m).

The hypothetical releases modelled in this study are not intended to predict a specific future event, but rather are intended to be used as a tool in environmental assessments and spill contingency planning. The results presented in this document demonstrate that there are a range of potential trajectories and fates that could result if a release of crude oil or a batch spill of marine diesel were to occur at any point throughout the year. The specific trajectories and fates vary greatly for each release based upon the environmental conditions occurring at the time of the release. While each oil release is unique, and uncertainties exist, the results of this modelling study suggest that, if oil were to be released in the Project Area, it has a high likelihood of moving away from shore to the east with less likelihood of shoreline oil exposure. Furthermore, this modelling assumes completely unmitigated releases, which is an unlikely situation because emergency response measures would typically be employed in the event of a spill.

6 REFERENCES

Atlas, R. and Bragg, J. 2009. Bioremediation of marine oil spills: when and when not – the Exxon Valdez experience. Microbial Biotechnology 2(2):213-221.

Bleck, R., 1998: Ocean modeling in isopycnic coordinates. Chapter 18 in Ocean Modeling and Parameterization, E. P. Chassignet and J. Verron, Eds., NATO Science Series C: Mathematical and Physical Sciences, Vol. 516, Kluwer Academic Publishers, 4223-448.

Bleck, R. 2002. An oceanic general circulation model framed in hybrid isopycnic-cartesian coordinates. Ocean Modeling, 4, 55-88.

Bonn Agreement. 2009. Bonn Agreement Aerial Operations Handbook, 2009. London, UK. Available: http://www.bonnagreement.org/site/assets/files/1081/ba-aoh revision 2 april 2012-1.pdf, Accessed 4 June 2015.

Bonn Agreement, 2011. Bonn Agreement Oil Appearance Code Photo Atlas. Available: http://www.bonnagreement.org/site/assets/files/1081/photo_atlas_version_20112306-1.pdf. Accessed: April 2017.

Canada-Newfoundland and Labrador Offshore Petroleum Board (C-NLOPB). 2014. Eastern Newfoundland Strategic Environmental Assessment. Final Report. Prepared by AMEC Environment & Infrastructure, AMEC TF 1382502. Available: http://www.cnlopb.ca/pdfs/enlsea/ch1-3.pdf?lbisphpreq=1. Accessed: March 2017.

Chassignet, E. P., L. T. Smith, R. Bleck, and F. O. Bryan, 1996: A model comparison: numerical simulations of the North and Equatorial Atlantic oceanic circulation in depth and isopycnic coordinates. J. Phys. Oceanogr., 26, 1849-1867.

Chassignet, E.P., Z.D. Garraffo, 2001. Viscosity parameteriation and gulf stream separation. In: Hawaii U., Muller P., Henderson, D. (Eds.). String to Mixing in Stratified Ocean, Proceedings of Aha Huliko'a Hawaiian Winter Workshop, pp. 27-41.

Clark, R.B., 1984. Impact of Oil Pollution on Seabirds. Environmental Pollution (Series A) 33: 1-22.

Conkright, M.E., J.I. Antonov, O. Baranova, T.P. Boyer, H.E. Garcia, R. Gelfeld, D. Johnson, R.A. Locarnini, P.P. Murphy, T.D. O'Brien, I. Smolyar, and C. Stephens. 2002. World Ocean Database 2001, Volume 1: Introduction. Sydney Levitus (ed.). NOAA Atlas NESDIS 42, U.S. Government Printing Office, Washington, D.C., 167 pp.

Cooper, M. and K.A. Haines, 1996.Altimetric assimilation with water property conservation. Journal of Geophysical Research, vol. 24, pp. 1059-1077.

Cummings, J.A. 2005. Operational multivariate ocean data assimilation. Quarterly Journal of the Royal Meteorological Society. Part C, 133(613), 3583-3604.

DF Dickins Associates LTD. 2004. Advancing Oil Spill Response In Ice-Covered Waters. Available: http://www.pws-osri.org/publications/OilIce_final.pdf. Accessed: March 2017.

Engelhardt, F.R., 1983. Petroleum Effects on Marine Mammals. Aquatic Toxicology 4: 199-217.

Environment and Climate Change Canada (ECCC). 2001. Oil Properties. Available: http://www.etc-cte.ec.gc.ca/databases/OilProperties/. Accessed: March 2019.

Environment and Climate Change Canada (ECCC). 2017. Canadian Ice Service. Available: https://www.ec.gc.ca/glaces-ice/. Accessed: March 2017.

French, D., M. Reed, K. Jayko, S. Feng, H. Rines, S. Pavignano, T. Isaji, S. Puckett, A. Keller, F.W. French III, D. Gifford, J. McCue, G. Brown, E. MacDonald, J. Quirk, S. Natzke, R. Bishop, M. Welsh, M. Phillips, and B.S. Ingram, 1996. Final Report, The CERCLA Type A Natural Resource Damage Assessment Model for Coastal and Marine Environments (NRDAM/CME), Technical Documentation, Vol. I - V., Office of Environmental Policy and Compliance, U.S. Department of the Interior, Washington, DC, Contract No. 14-0001-91-C-11.

French McCay, D.P., 2002. Development and Application of an Oil Toxicity and Exposure Model, OilToxEx. Environmental Toxicology and Chemistry 21(10): 2080-2094.

French McCay, D.P., 2004. Oil release impact modelling: Development and validation. Environmental Toxicology and Chemistry 23(10): 2441-2456.

French McCay, D.P, 2009. State-of-the-Art and Research Needs for Oil Release Impact Assessment Modelling. In Proceedings of the 32nd AMOP Technical Seminar on Environmental Contamination and Response, Emergencies Science Division, Environment Canada, Ottawa, ON, Canada, pp. 601-653.

French McCay, D. 2016. Potential Effects Thresholds for Oil Spill Risk Assessments. In: Proceedings of the 39th AMOP Technical Seminar on Environmental Contamination and Response, Emergencies Science Division, Environment Canada, Ottawa, ON, Canada. p. 285-303.

French McCay, D.P. and J.J. Rowe. 2004. Evaluation of Bird Impacts in Historical Oil Release Cases Using the SIMAP Oil Release Model. Proceedings of the Twenty-seventh Arctic and Marine Oil Spill Program (AMOP) Technical Seminar. Emergencies Science Division, Environment Canada, Ottawa, ON, Canada. pp. 421-452.

French McCay, D., Reich, D., Rowe, J., Schroeder, M., and E. Graham. 2011. Oil Spill Modeling Input to the Offshore Environmental Cost Model (OECM) for US-BOEMRE's Spill Risk and Cost Evaluations. In Proceedings of the 34th AMOP Technical Seminar on Environmental Contamination and Response, Emergencies Science Division, Environment Canada, Ottawa, ON, Canada.

French McCay, D., Reich, D., Michel, J., Etkin, D., Symons, L., Helton, D., and J. Wagner. 2012. Oil Spill Consequence Analyses of Potentially-Polluting Shipwrecks. In Proceedings of the 34th AMOP

Technical Seminar on Environmental Contamination and Response, Emergencies Science Division, Environment Canada, Ottawa, ON, Canada.

French McCay, D., M.S. Gearon, Y.H. Kim, K. Jayko and T. Isaji, 2014. Modeling Oil Transport and Fate in the Beaufort Sea. In Proceedings of the 37th AMOP Technical Seminar on Environmental Contamination and Response, Emergencies Science Division, Environment Canada, Ottawa, ON, Canada.

French McCay D.P., Jayko K, Li Z, Horn M, Kim Y. 2015. Technical Reports for Deepwater Horizon Water Column Injury Assessment–WC_TR14: Modeling Oil Fate and Exposure Concentrations in the Deepwater Plume and Cone of Rising Oil Resulting from the DWHOS. DWH NRDA Water Column Technical Working Group Report. Prepared for National Oceanic and Atmospheric Administration by RPS ASA, South Kingstown, RI. Administrative Record no. DWH-AR0285776.pdf. Available online: https://www.doi.gov/deepwaterhorizon/adminrecord

French McCay, D., Balouskus, D.R., Ducharme J., Schroeder Gearon, M., Kim, Y., Zamorski, S., Li, Z., and Rowe, J., 2016. Simulation of oil spill trajectories during the broken ice period in the Chukchi and Beaufort Seas, Prepared for U.S. Fish and Wildlife Service, Marine Mammals Management, Anchorage, Alaska, pp. 189.

French McCay, D., Balouskus D.R., Ducharme, J., Schroeder Gearon, M., Kim, Y., Zamorski, S., Li, Z., and Rowe, J., 2017a. Potential Oil Trajectories and Surface Oil Exposure from Hypothetical Discharges in the Chukchi and Beaufort Seas. Proceedings of the 40th AMOP Technical Seminar on Environmental Contamination and Response, Emergencies Science Division, Environment Canada, Ottawa, ON, Canada. pp. 660-693.

French McCay, D., Tajalli Bakhsh, T., and Spaulding, M.L., 2017b. Evaluation of Oil Spill Modeling in Ice Against In Situ Drifter Data from the Beaufort Sea In: Proceedings, International Oil Spill Conference, May 2017, Paper 2017-356, American Petroleum Institute, Washington, DC.

French McCay, D., Jayko, K., Li, Z., Horn, M, Isaji, T., Spaulding, M. 2018a. Volume II: Appendix II - Oil Transport and Fates Model Technical Manual. p.60-277 in: Galagan, C.W., French-McCay, D., Rowe, J., and McStay L., editors. Simulation Modeling of Ocean Circulation and Oil Spills in the Gulf of Mexico. Prepared by RPS ASA for the US Department of the Interior, Bureau of Ocean Energy Management, Gulf of Mexico OCS Region, New Orleans, LA. OCS Study BOEM 2018-040.

French-McCay, D., D. Crowley, J. Rowe, M. Bock, H. Robinson, R. Wenning, A. H. Walker, J. Joeckel, and T. Parkerton. 2018b. Comparative Risk Assessment of Spill Response Options for a Deepwater Oil Well Blowout: Part I. Oil Spill Modeling. Mar. Pollut. Bull. https://doi.org/10.1016/j.marpolbul.2018.05.042.

French-McCay, D.P., Tajalli-Bakhsh, T., Jayko, K., Spaulding, M. L., and Li, Z., 2018c. Validation of oil spill transport and fate modeling in Arctic ice. Arctic Science Vol. 4, pp. 71–97. dx.doi.org/10.1139/as-2017-0027.

General Bathymetric Chart of the Oceans (GEBCO). 2003. Centenary Edition of the GEBCO Digital Atlas, published on behalf of the Intergovernmental Oceanographic Commission (IOC) and the International Hydrographic Organization (IHO) as part of the General Bathymetric Chart of the Oceans; British Oceanographic Data Centre (BODC), Liverpool.

Geraci, J.R. and D.J. St. Aubin, 1988. Synthesis of Effects of Oil on Marine Mammals, Report to U.S. Department of the Interior, Minerals Management Service, Atlantic OCS Region, OCS Study, MMS 88 0049, Battelle Memorial Institute, Ventura, CA, 292 p.

Halliwell, G. R., Jr., 1997.Simulation of decadal/interdecadal variability the North Atlantic driven by the anomalous wind field. Proceedings, Seventh Conference on Climate Variations, Long Beach, CA, 97-102.

Halliwell, G. R., Jr., 1998. Simulation of North Atlantic decadal/multi-decadal winter SST anomalies driven by basin-scale atmospheric circulation anomalies. Journal of Physical Oceanography, 28, 5-21.

Halliwell, G.R. 2002.HYCOM Overview. http://www.hycom.org. June 27, 2011.

Halliwell, G. R., Jr., R. Bleck, and E. Chassignet, 1998. Atlantic Ocean simulations performed using a new hybrid-coordinate ocean model. EOS, Fall 1998 AGU Meeting.

Halliwell, G .R, R. Bleck, E. P. Chassignet, and L.T. Smith, 2000: mixed layer model validation in Atlantic Ocean simulations using the Hybrid Coordinate Ocean Model (HYCOM). EOS, 80, OS304.

Han, G. and C.L. Tang, 1999. Velocity and transport of the Labrador Current determined from altimetric, hydrographic, and wind data. Journal of Geophysical Research: Oceans Banner. Volume 4, Issue C8, 15 August 1999. pp. 18047-18057.

Hu, D., 1996: On the Sensitivity of Thermocline Depth and Meridional Heat Transport to Vertical Diffusivity in OGCMs. J. Physical Oceanography, 26, 1480-1494.

Hurlburt, H.E., Hogan, P.J., 2000. Impact of 1/8 to 1/64 resolution on Gulf stream model-data comparisons in basin-scale Atlantic Ocean models. Dynamics of Atmospheres and Oceans, No. 32, pp. 283-329.

Jenssen, B.M., 1994. Review article: effects of oil pollution, chemically treated oil, and cleaning on thermal balance of birds. Environmental Pollution. 86(2):207-215.

Jones, R.K., 1997. A Simplified Pseudo-Component of Oil Evaporation Model. In Proceedings of the 20th Arctic and Marine Oil Spill Program (AMOP) Technical Seminar, Environment Canada, pp. 43-61.

Lehr, W.J., D. Wesley, D. Simecek-Beatty, R. Jones, G. Kachook, and J. Lankford, 2000. Algorithm and interface modifications of the NOAA oil spill behavior model. In Proceedings of the 23rd Arctic and Marine Oil Spill Program (AMOP) Technical Seminar, Vancouver, BC, Environmental Protection Service, Environment Canada, pp. 525-539.

Levitus, S. 1982. Climatological Atlas of the World Ocean, NOAA/ERL GFDL Professional Paper 13, Princeton, N.J., 173 pp. (NTISPB83-184093).

Levitus, S., T.P., Boyer, H.E. Garcia, R.A. Locarnini, M.M. Zweng, A.V. Mishonov, J.R. Reagan, J.I. Antonov, O.K. Baranova, M. Biddle, M. Hamilton, D.R. Johnson, C.R. Paver, and D. Seidov. 2014. World Ocean Atlas 2013 (NODC accession 0114815). National Oceanographic Data Center, NOAA.

Lewis, A. 2007. Current Status of the BAOAC; Bonn Agreement Oil Appearance Code. A report to the Netherlands North Sea Agency Directie Noordzee. Alan Lewis Oil Release Consultant, submitted January, 2007.

Maine Department of Environmental Protection (MDEP). 2016. Releases and Site Cleanup: Maine Environmental Vulnerability Index Maps. Available: http://www.maine.gov/dep/releases/emergreleaseresp/evi/. Accessed: March 2017.

Marsh, R., M. J. Roberts, R. A. Wood, and A. L. New, 1996: An intercomparison of a Bryan-Cox-type ocean model and an isopycnic ocean model, part II: the subtropical gyre and meridional heat transport. J. Phys. Oceanogr., 26, 1528-1551.

National Oceanic and Atmospheric Administration (NOAA), 2014. Can the ocean freeze? Available: http://oceanservice.noaa.gov/facts/oceanfreeze.html. Accessed: April 2017.

National Oceanic and Atmospheric Administration (NOAA), 2016a. Environmental Sensitivity Index (ESI) Maps. Available: http://response.restoration.noaa.gov/maps-and-spatial-data/environmental-sensitivity-index-esi-maps.html. Accessed: 2011 - 2012.

National Oceanic and Atmospheric Administration (NOAA). 2016b. Open water oil identification job aid for aerial observation. U.S. Department of Commerce, Office of Response and Restoration [http://response.restoration.noaa.gov/oil-and-chemical-releases/oil-releases/resources/open-water-oil-identification-job-aid.html]

National Research Council (NRC), 1985. Oil in the Sea: Inputs, Fates and Effects. National Academy Press, Washington, D.C. 601p.

New, A. and R. Bleck, 1995: An isopycnic model of the North Atlantic, Part II: interdecadal variability of the subtropical gyre. J. Phys. Oceanogr., 25, 2700-2714.

New, A., R. Bleck, Y. Jia, R. Marsh, M. Huddleston, and S. Barnard, 1995: An isopycnic model of the North Atlantic, Part I: model experiments. J. Phys. Oceanogr., 25, 2667-2699.

New Brunswick Department of Natural Resources (NBDNR). 2013. New Brunswick Canada: Regulated Wetlands. Available: http://www.snb.ca/geonb1/e/DC/RW.asp. Accessed: March 2019.

Nova Scotia Department of Natural Resources (NSDNR). 2013. Nova Scotia Canada: DNR Ecosystems and Habitats Program Overview. Available: https://novascotia.ca/natr/wildlife/habitats/wetlands.asp. Accessed: March 2019.

Payne, J.R., B.E. Kirstein, G.D. McNabb, Jr., J.L. Lambach, R. Redding R.E. Jordan, W. Hom, C. deOliveria, G.S. Smith, D.M. Baxter, and R. Gaegel, 1984. Multivariate analysis of petroleum weathering in the

marine environment – sub Arctic. Environmental Assessment of the Alaskan Continental Shelf, OCEAP, Final Report of Principal Investigators, Vol. 21 and 22, Feb. 1984, 690p.

Payne, J.R., B.E. Kirstein, J.R. Clayton, Jr., C. Clary, R. Redding, G.D. McNabb, Jr., and G. Farmer, 1987. Integration of suspended particulate matter and oil transportation study. Final Report. Minerals Management Service, Environmental Studies Branch, Anchorage, AK. Contract No. 14-12-0001-30146, 216 p.

Petrie, B. and Anderson, C., 1983. Circulation on the Newfoundland continental shelf. Atmosphere-Ocean, 21(2), pp.207-226.

Petrie, B. A. Isenor, 1985. The Near-Surface Circulation and Exchange in the Newfoundland Grand Banks Region. Atmosphere-Ocean, vol. 23, no. 3, pp. 209-227.

Richardson, P.L., 1983. Eddy Kinetic Energy in the North Atlantic From Surface Drifters. Journal of Geophysical Research, vol. 88, no. C7, pp. 4355-4367.

Roberts, M. J., R. Marsh, A. L. New, and R. A. Wood, 1996: An intercomparison of a Bryan-Cox-type ocean model and an isopycnic ocean model, part I: the subpolar gyre and high latitude processes. J. Phys. Oceanogr., 26, 1495-1527.

Saha, S., et al. 2010. NCEP Climate Forecast System Reanalysis (CFSR) 6-hourly Products, January 1979 to December 2010. Research Data Archive at the National Center for Atmospheric Research, Computational and Information Systems Laboratory. http://dx.doi.org/10.5065/D69K487J.

Saha, S., S. Moorthi, X. Wu, J. Wang, and Coauthors, 2014. The NCEP Climate Forecast System Version 2. Journal of Climate, vol. 27, pp. 2185–2208.

Smith, R.D. Maltrud, M.E., 2000. Numerical simulations of the North Atlantic Ocean at 1/10. Journal of physical Oceanography, no. 30, pp.1532-1561.

Socolofsky, S. A., Adams, E. E. , and Sherwood, C. R. 2011. Formation dynamics of subsurface hydrocarbon intrusions following the Deepwater Horizon blowout. Geophys. Res. Let., vol. 38 no. 9, pp. L09602.

Socolofsky, S. A., Adams, E. E., Boufadel, M. C., Aman, Z. M., Johansen, Ø., Konkel, W. J., Lindo, D., Madsen, M. N., North, E. W., Paris, C. B., Rasmussen, D., Reed, M., Rønningen, P., Sim, L. H., Uhrenholdt, T., Anderson, K. G., Cooper, C. and Nedwed, T. J.. 2015. Intercomparison of oil spill prediction models for accidental blowout scenarios with and without subsea chemical dispersant injection. Marine Pollution Bulletin, Vol. 96, pp. 110-126.

Therrien, A., 2017. Shoreline Segmentation (SCAT Classification). Environment and Climate Change Canada.

Trudel, B.K., R.C. Belore, B.J. Jessiman and S.L. Ross., 1989. A micro-computer based release impact assessment system for untreated and chemically dispersed oil releases in the U.S. Gulf of Mexico. 1989 International Oil Release Conference.

UNESCO, 1981. Background papers and supporting data on the international equation of State of Sea Water, 1980. UNESCO Technical Papers in Marine Science. No. 38, 192 pp.

United States Coast Guard (USCG). 2009. How do the Labrador and Gulf Stream Currents Affect Icebergs. Labrador and Gulf Stream currents affect icebergs in the North Atlantic Ocean. USCG Navigation Center. U.S. Department of Homeland Security. Available: https://navcen.uscg.gov/?pageName=iipHowDoTheLabradorAndGulfStreamCurrentsAffectIcebergsInTheNorthAtlanticOcean. Accessed: March 2017.

VLIZ (2014). Maritime Boundaries Geodatabase, version 8. Available online at http://www.marineregions.org/. Consulted on 2014-04-14.

Volkov, D.L., 2005. Interannual Variability of the Altimetry-Derived Eddy Field and Surface Circulation in the Extratropical North Atlantic Ocean in 1993-2001. Journal of Physical Oceanography, Vol. 35, pp. 405-426.

Wilson, Ryan R., Craig Perham, Deborah P. French-McCay, Richard Balouskus, 2018. Potential impacts of offshore oil spills on polar bears in the Chukchi Sea, Environmental Pollution, Volume 235, April 2018, Pages 652-659, ISSN 0269-7491, https://doi.org/10.1016/j.envpol.2017.12.057.

Zahed, M. A., Aziz, H.A., Isa, M.H., Mohajeri, L., Mohajeri, S. and Kutty, S.R.M. 2011. Kinetic modeling and half-life study on bioremediation of crude oil dispersed by Corexit 9500. Journal of Hazardous Materials 185(2-3):1027-1031.

CHEVRON CANADA LIMITED WEST FLEMISH PASS EXPLORATION DRILLING PROJECT 2021-2030 19-P-202035

Oil Spill Trajectory and Fate Assessment
Appendix A: SIMAP and OILMAPDeep Model Descriptions

Oil Spill Risk Assessment
Chevron Canada Limited
West Flemish Pass
Exploration Drilling Project
2021-2030
19-P-202035
Final
June 25, 2019

rpsgroup.com

Document status

Version	Purpose of document	Authored by	Reviewed by	Approved by	Review date
Final	Appendix to Oil Spill Trajectory and Fate Assessment: Technical Report	LM, ST, JZ, DT, MM, TT, MF, JD, MH	MH	MH	**June 25, 2019**

Approval for issue

<Original signed by>

Matt Horn 2019-06-25

This report was prepared by RPS Group, Inc. ('RPS') within the terms of its engagement and in direct response to a scope of services. This report is strictly limited to the purpose and the facts and matters stated in it and does not apply directly or indirectly and must not be used for any other application, purpose, use or matter. In preparing the report, RPS may have relied upon information provided to it at the time by other parties. RPS accepts no responsibility as to the accuracy or completeness of information provided by those parties at the time of preparing the report. The report does not take into account any changes in information that may have occurred since the publication of the report. If the information relied upon is subsequently determined to be false, inaccurate or incomplete then it is possible that the observations and conclusions expressed in the report may have changed. RPS does not warrant the contents of this report and shall not assume any responsibility or liability for loss whatsoever to any third party caused by, related to or arising out of any use or reliance on the report howsoever. No part of this report, its attachments or appendices may be reproduced by any process without the written consent of RPS. All enquiries should be directed to RPS.

Prepared by:

RPS Group, Inc.

Lisa McStay, Steven Tadros, Joseph Zottoli, Daniel Torre, Mahmud Monim, Tayebeh Tajalli Bakhsh, Matthew Frediani, Jenna Ducharme

Project Lead & Senior Scientist:
Matt Horn, PhD
Director
55 Village Square Drive
South Kingstown, RI 02879

T 401-789-6224
E matt.horn@rpsgroup.com

Prepared for:

Stantec

Ellen Tracy
Senior Associate, Environmental Management

141 Kelsey Drive
St. John's NL A1B 0L2

T **709 576-1458**
E **Ellen.Tracy@stantec.com**

Contents

Figures

Tables

1 SIMAP MODEL DESCRIPTION

The analysis was performed using the model system developed by RPS called SIMAP (Spill Impact Model Analysis Package). SIMAP originated from the oil fates and biological effects submodels in the Natural Resource Damage Assessment Models for Coastal and Marine Environments (NRDAM/CME) and Great Lakes Environments (NRDAM/GLE), which ASA developed in the early 1990s for the U.S. Department of the Interior for use in "type A" Natural Resource Damage Assessment (NRDA) regulations under the Comprehensive Environmental Response, Compensation and Liability Act of 1980 (CERCLA). The most recent version of the type A models, the NRDAM/CME (Version 2.4, April 1996) was published as part of the CERCLA type A NRDA Final Rule (Federal Register, May 7, 1996, Vol. 61, No. 89, p. 20559-20614). The technical documentation for the NRDAM/CME is in French et al. (1996 a-c). This technical development involved several in-depth peer reviews, as described in the Final Rule.

While the NRDAM/CME and NRDAM/GLE were developed for simplified natural resource damage assessments of small spills in the United States, SIMAP is designed to evaluate fates and effects of both real and hypothetical spills in marine, estuarine and freshwater environments worldwide. Additions and modifications to prepare SIMAP were made to increase model resolution, allow modification and site-specificity of input data, allow incorporation of temporally varying current data, evaluate subsurface releases and movements of subsurface oil, track multiple chemical components of the oil, enable stochastic modelling, and facilitate analysis of results.

Below are brief descriptions of the fates and effects models presented in SIMAP. Detailed descriptions of the algorithms and assumptions in the model are in published papers (French McCay, 2002; 2003; 2004; 2009). The model has been validated with more than 20 case histories, including the *Exxon Valdez* and other large spills (French and Rines, 1997; French McCay, 2003; 2004; French McCay and Rowe, 2004) as well as test spills designed to verify the model (French et al., 1997).

1.1 Physical Fates Model

The three-dimensional physical fates model estimates distribution (as mass and concentrations) of whole oil and oil components on the water surface, on shorelines, in the water column, and in sediments. Oil fate processes included are oil spreading (gravitational and by shearing), evaporation, transport, randomized dispersion, emulsification, entrainment (natural and facilitated by dispersant), dissolution, volatilization of dissolved hydrocarbons from the surface water, adherence of oil droplets to suspended sediments, adsorption of soluble and sparingly-soluble aromatics to suspended sediments, sedimentation, and degradation.

Oil is a mixture of hydrocarbons of varying physical, chemical, and toxicological characteristics. In the model, oil is represented by component categories, and the fate of each component is tracked separately. The "pseudo-component" approach (Payne et al., 1984; 1987; French et al., 1996a; Jones, 1997; Lehr et al., 2000) is used, where chemicals in the oil mixture are grouped by physical-chemical properties, and the resulting component category behaves as if it were a single chemical with characteristics typical of the chemical group.

The most toxic components of oil to aquatic organisms are low molecular weight aromatic compounds (monoaromatic and polycyclic aromatic hydrocarbons, MAHs and PAHs), which are both volatile and soluble in water. Their acute toxic effects are caused by non-polar narcosis, where toxicity is related to the octanol-water partition coefficient (K_{ow}), a measure of hydrophobicity. The more hydrophobic the compound, the more toxic it is likely to be. However, as K_{ow} increases, the compound also becomes less soluble in water, and so there is less exposure to aquatic organisms. The toxicity of compounds having log(K_{ow}) values greater than about 5.6 is limited by their very low solubility in water, and consequent low bioavailability to aquatic biota (French McCay, 2002, Di Toro et al., 2000). Thus, the potential for acute effects is the result of a balance between bioavailability (exposure),

toxicity once exposed, and duration of exposure. French McCay (2002) contains a full description of the oil toxicity model in SIMAP, and French McCay (2002) describes the implementation of the toxicity model in SIMAP.

Because of these considerations, the SIMAP fates model focuses on tracking the lower molecular weight aromatic components divided into chemical groups based on volatility, solubility, and hydrophobicity. In the model, the oil is treated as comprising eight components (defined in **Error! Reference source not found.**). Six of the components (i.e., all but the two non-volatile residual components representing non-volatile aromatics and aliphatics) evaporate at rates specific to the pseudo-component. Solubility is strongly correlated with volatility, and the solubility of aromatics is higher than aliphatics of the same volatility. The MAHs are the most soluble, the 2-ring PAHs are less soluble, and the 3-ring PAHs slightly soluble (Mackay et al., 1992). Both the solubility and toxicity of the non-aromatic hydrocarbons are much less than for the aromatics, and dissolution (and water concentrations) of non-aromatics is safely ignored. Thus, dissolved concentrations are calculated only for each of the three soluble aromatic pseudo-components.

Table 1. Definition of four distillation cuts and the eight pseudo-components in the model (Monoaromatic Hydrocarbons, MAHs; Benzene + Toluene + Ethylbenzene + Xylene, BTEX; Polycyclic Aromatic Hydrocarbons, PAHs).

Characteristic	Volatile and Highly Soluble	Semi-volatile and Soluble	Low Volatility and Slightly Soluble	Residual (non-volatile and very low solubility)
Distillation cut	1	2	3	4
Boiling Point (°C)	< 180	180 - 265	265 - 380	>380
Molecular Weight	50 - 125	125 - 168	152 - 215	> 215
Log(K_{ow})	2.1-3.7	3.7-4.4	3.9-5.6	>5.6
Aliphatic pseudo-components: Number of Carbons	volatile aliphatics: C4 – C10	semi-volatile aliphatics: C10 – C15	low-volatility aliphatics: C15 – C20	non-volatile aliphatics: > C20
Aromatic pseudo-component name: included compounds	MAHs: BTEX, MAHs to C3-benzenes	2 ring PAHs: C4-benzenes, naphthalene, C1-, C2-naphthalenes	3 ring PAHs: C3-, C4-naphthalenes, 3-4 ring PAHs with log(K_{ow}) < 5.6	≥4 ring aromatics: PAHs with log(K_{ow}) > 5.6 (very low solubility)

This number of components provides sufficient accuracy for the evaporation and dissolution calculations, particularly given the time frame (minutes) over which dissolution occurs from small droplets and the rapid resurfacing of large droplets (see discussion above). The alternative of treating oil as a single compound with empirically-derived rates (e.g., Mackay et al., 1980; Stiver and Mackay, 1984) does not provide sufficient accuracy for environmental effects analyses because the effects to water column organisms are caused by MAHs and PAHs, which have specific properties that differ from the other volatile and soluble compounds. The model has been validated both in predicting dissolved concentrations and resulting toxic effects, supporting the adequacy of the use of this number of pseudo-components (French McCay, 2003).

The lower molecular weight aromatics dissolve from the whole oil and are partitioned in the water column and sediments according to equilibrium partitioning theory (French et al., 1996a; French McCay, 2004). The residual fractions in the model are composed of non-volatile and insoluble compounds that remain in the “whole oil” that spreads, is transported on the water surface, strands on shorelines, and disperses into the water column as oil droplets or remains on the surface as tar balls. This is the fraction that composes black oil, mousse, and sheen.

1.2 Oil Fate Model Processes

The schematic in Figure 1 depicts oil fates processes simulated in open water conditions, while the schematic in Figure 2 depicts oil fates processes that are simulated at and near the shoreline. Because oil contains many

chemicals with varying physical-chemical properties, and the environment is spatially and temporally variable, the oil rapidly separates into different phases or parts of the environment:

- Surface oil;
- Emulsified oil (mousse) and tar balls;
- Oil droplets suspended in the water column;
- Oil adhering to suspended particulate matter in the water;
- Dissolved lower molecular weight components (MAHs, PAHs, and other soluble components) in the water column;
- Oil on and in the sediments;
- Dissolved lower molecular weight components (MAHs, PAHs, and other soluble components) in the sediment pore water;
- Oil on and in the shoreline sediments and surfaces.

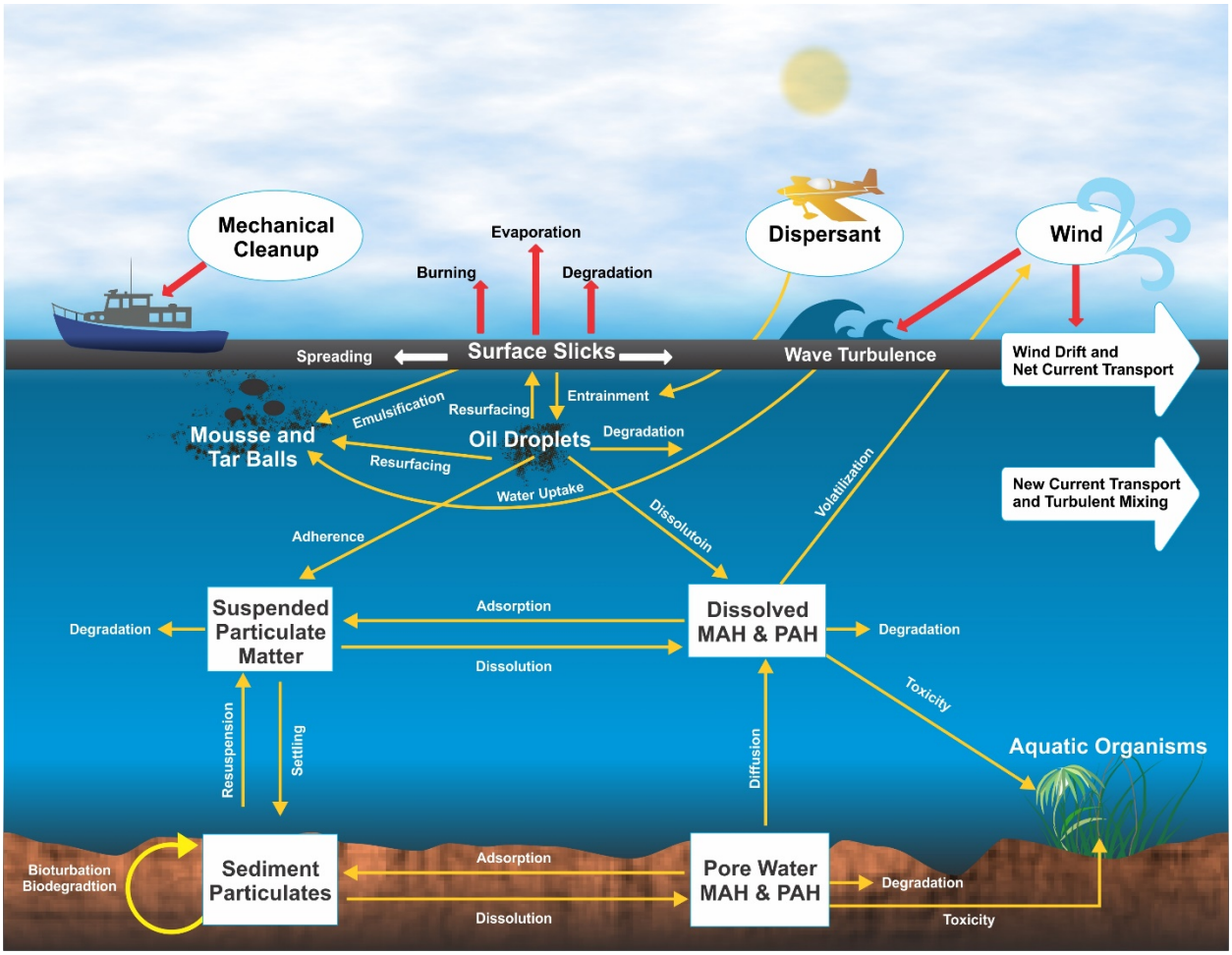

Figure 1. Simulated oil fates processes in open water in the SIMAP model.

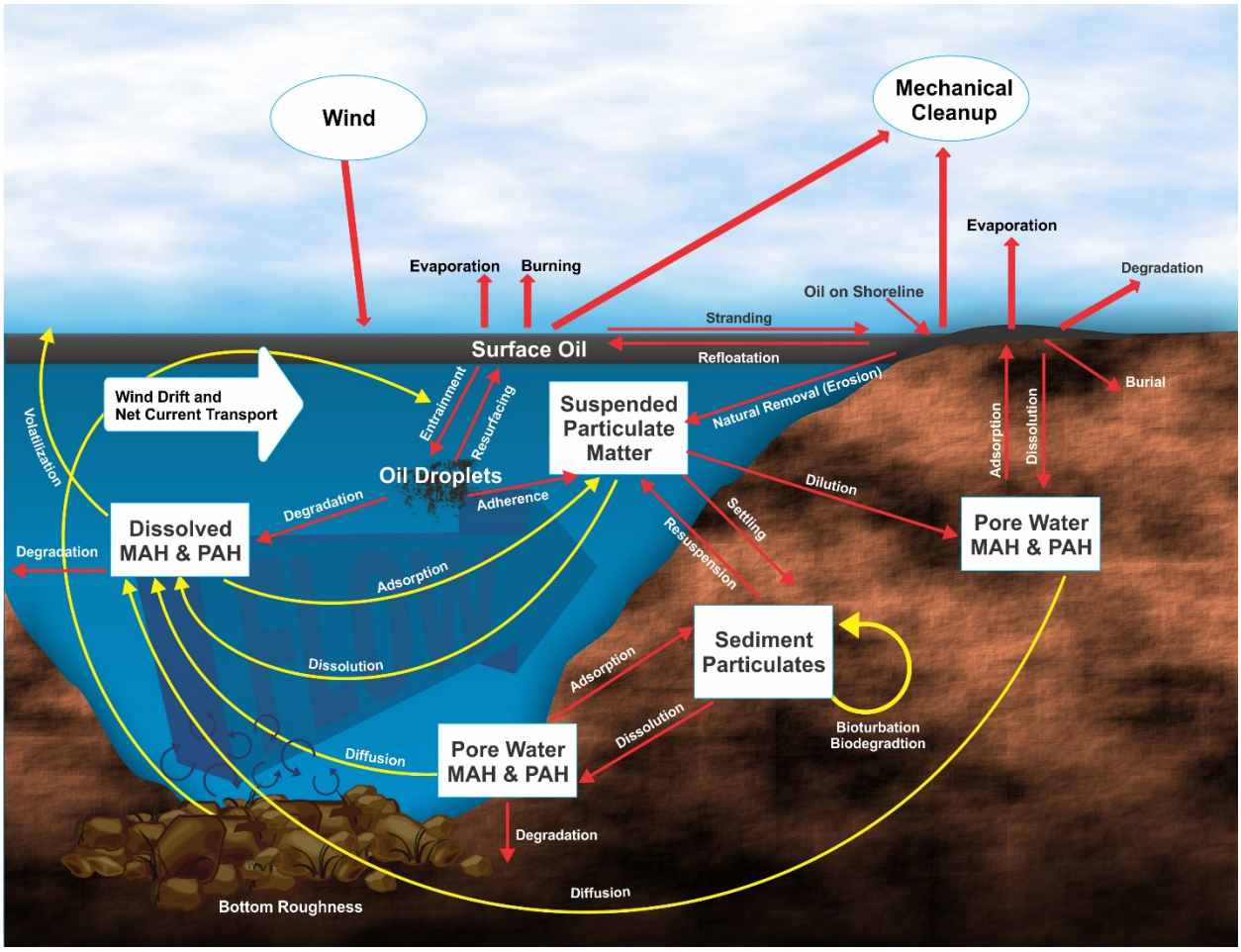

Figure 2. Simulated oil fates processes at the shoreline in the SIMAP model.

The schematics in Figure 1 and Figure 2 represent oil fates processes that are simulated in the model:

- Spreading is the thinning and broadening of surface slicks caused by gravitational forces and surface tension. This occurs rapidly after oil is spilled on the water surface. The rate of spreading is faster if oil viscosity is lower. Viscosity decreases as temperature increases. Viscosity increases as oil emulsifies.
- Transport is the process where oil is carried by currents.
- Turbulent dispersion: Typically there are also “sub-scale” currents (not included in the current data), better known as turbulence that move and mix oil in three dimensions. The process by which turbulence mixes and spreads oil components on the water surface and in the water is called turbulent dispersion.
- Evaporation is the process where volatile components of the oil diffuse from the oil and enter the gaseous phase (atmosphere). Evaporation from surface and shoreline oil increases as the oil surface area, temperature, and wind speed increase. As lighter components evaporate off, the remaining “weathered” oil becomes more viscous.
- Emulsification is the process where water is mixed into the oil, such that the oil makes a matrix with embedded water droplets. The resulting mixture is commonly called mousse. It is technically referred to as a water-in-oil emulsion. The rate of emulsification increases with increasing wind speed and turbulence on the surface of the water. Viscosity increases as oil emulsifies.

- Entrainment is the process where waves break over surface oil and carry it as droplets into the water column. At higher wind speeds, or where currents and bottom roughness induce turbulence, wave heights may reach a threshold where they break. In open waters, waves break beginning at about 12 knots of wind speed and wave breaking increases as wind speed becomes higher. Thus, entrainment becomes increasingly important (higher rate of mass transfer to the water) the higher the wind speed. As turbulence from whatever source increases, the oil droplet sizes become smaller. Application of chemical dispersant increases the entrainment rate of oil and decreases droplet size at a given level of turbulence. Entrainment rate is slower, and droplet size is larger, as oil viscosity increases (by emulsification and evaporation loss of lighter volatile components). The droplet size determines how fast and whether the oil resurfaces.
- Resurfacing of entrained oil rapidly occurs for larger oil droplets. Smaller droplets resurface when the wave turbulence decreases. The smallest droplets do not resurface, as typical turbulence levels in the water keep them in suspension indefinitely. Local winds at the water surface can also prevent oil from surfacing. Resurfaced oil typically forms sheens. In open water where currents are relatively slow, surface slicks are usually blown downwind faster than the underlying water, resurfacing droplets come up behind the leading edge of the oil, effectively spreading the slicks in the down-wind direction.
- Dissolution is the process where water-soluble components diffuse out of the oil into the water. Dissolution rate increases the higher the surface area of the oil relative to its volume. As the surface area to volume ratio is higher for smaller spherical droplets, the smaller the droplets the higher the dissolution rate. The higher the wave turbulence, the smaller the droplets of entrained oil. Dissolution from entrained small droplets is much faster than from surface slicks in the shape of flat plates. The soluble components are also volatile, and evaporation from surface slicks is faster than dissolution into the underlying water. Thus, the processes of evaporation and dissolution are competitive, with evaporation the dominant process for surface oil.
- Volatilization of dissolved components from the water to the atmosphere occurs as they are mixed and diffuse to the water surface boundary and enter the gas phase. Volatilization rate increase with increasing air and water temperature.
- Adsorption of dissolved components to particulate matter in the water occurs because the soluble components are only sparingly so. These compounds (MAHs and PAHs) preferentially adsorb to particulates when the latter are present. The higher the concentration of suspended particulates, the more adsorption. Also, the higher the molecular weight of the compound, the less soluble, and the more the compound adsorbs to particulate matter.
- Adherence is the process where oil droplets combine with particles in the water. If the particles are suspended sediments, the combined oil/suspended sediment agglomerate is heavier than the oil itself and than the water. If turbulence subsides sufficiently, the oil-sediment agglomerates will settle.
- Sedimentation (settling) is the process where oil-sediment agglomerates and particles with adsorbed sparingly-soluble components (MAHs and PAHs) settle to the bottom sediments. Adherence and sedimentation can be an important pathway of oil in near shore areas when waves are strong and subsequently subside. Generally, oil-sediment agglomerates transfer more PAH to the bottom than sediments with PAHs that were adsorbed from the dissolved phase in the water column.
- Resuspension of settled oil-sediment particles and particles with adsorbed sparingly-soluble components (MAHs and PAHs) may occur if current speeds and turbulence exceed threshold values where cohesive forces can be overcome.
- Diffusion is the process where dissolved compounds move from higher to lower concentration areas by the random motion of molecules and microscale turbulence. Dissolved components in bottom and shoreline sediments can diffuse out to the water where concentrations are relatively low. Bioturbation, groundwater discharge and hyporheic flow of water through stream-bed sediments can greatly increase the rate of diffusion from sediments (see below).

- Dilution occurs when water of lower concentration is mixed into water with higher concentration by turbulence, currents, or shoreline groundwater.
- Bioturbation is the process where animals in the sediments mix the surface sediment layer while burrowing, feeding, or passing water over their gills. In open-water soft-bottom environments, bioturbation effectively mixes the surface sediment layer about 10 cm thick (in non-polluted areas).
- Degradation is the process where oil components are changed either chemically or biologically (biodegradation) to another compound. It includes breakdown to simpler organic carbon compounds by bacteria and other organisms, photo-oxidation by solar energy, and other chemical reactions. Higher temperature and higher light intensity (particularly ultraviolet wavelengths) increase the rate of degradation.
- Floating oil may strand on shorelines and refloat as water levels rise, allowing the oil to move further down current (downstream).

For a spill on the water surface, the gravitational spreading occurs very rapidly (within hours) to a minimum thickness. Thus, the area exposed to evaporation is high relative to the oil volume. Evaporation proceeds faster than dissolution. Thus, most of the volatiles and semi-volatiles evaporate, with a smaller fraction dissolving into the water. Degradation (photo-oxidation and biodegradation) also occurs at a relatively slow rate compared to these processes.

Evaporation is more rapid as the wind speed increases. However, when wind speeds exceed approximately 12 knots (6 m/s) and in open water, white caps begin to form and the breaking waves entrain oil as droplets into the water column. Higher wind speeds (and turbulence) increase entrainment and results in smaller droplet sizes. From Stoke's Law, larger droplets resurface faster and form surface slicks. Thus, a dynamic balance evolves between entrainment and resurfacing. As high-wind events occur, the entrainment rate increases. When the winds subside to less than 12 knots, the larger oil droplets resurface and remain floating. Similar dynamics occur in turbulent streams.

The smallest oil droplets remain entrained in the water column for an indefinite period. Larger oil droplets rise to the surface at varying rates. While the droplets are under water, dissolution of the light and soluble components occurs. Dissolution rate is a function of the surface area available. Thus, most dissolution occurs from droplets, as opposed to from surface slicks, since droplets have a higher surface area to volume ratio, and they are not in contact with the atmosphere (and so the soluble components do not preferentially evaporate as they do from surface oil).

If oil is released or driven underwater, it forms droplets of varying sizes. More turbulent conditions result in smaller droplet sizes. From Stoke's Law, larger droplets rise faster, and surface if the water is shallow. Resurfaced oil behaves as surface oil after gravitational spreading has occurred. The surface oil may be re-entrained. The smallest droplets in most cases remain in the water permanently. As a result of the higher surface area per volume of small droplets, the dissolution rate is much higher from subsurface oil than from floating oil on the water surface.

Because of these interactions, the majority of dissolved constituents (which are of concern because of potential effects on aquatic organisms) are from droplets entrained in the water. For a given spill volume and oil type/composition, with increasing turbulence either at the water surface and/or at the stream bed: there is an increasing amount of oil entrained; the oil is increasingly broken up into smaller droplets; there is more likelihood of the oil remaining entrained rather than resurfacing; the dissolved concentrations will be higher. Entrainment and dissolved concentrations increase with (1) higher wind speed, (2) increased turbulence from other sources of turbulence (waves on a beach, rapids, and waterfalls in rivers, etc.), (3) subsurface releases (especially under higher pressure and turbulence), and (4) application of chemical dispersants. Chemical dispersants both increase the amount of oil entrained and decrease the oil droplet size. Thus, chemical dispersants increase the dissolution rate of soluble components.

These processes that increase the rate of supply of dissolved constituents are balanced by loss terms in the model: (1) transport (dilution), (2) volatilization from the dissolved phase to the atmosphere, (3) adsorption to suspended particulate material (SPM) and sedimentation, and (4) degradation (photo-oxidation or biologically mediated). Also, other processes slow the entrainment rate: (1) emulsification increases viscosity and slows or eliminates entrainment; (2) adsorption of oil droplets to SPM and settling removes oil from the water; (3) stranding on shorelines removes oil from the water; and (4) mechanical cleanup and burning removes mass from the water surface and shorelines. Thus, the model-predicted concentrations are the resulting balance of all these processes and the best estimates based on our quantitative understanding of the individual processes.

The algorithms used to model these processes are described in French McCay (2004). Lagrangian elements (spillets) are used to simulate the movements of oil components in three dimensions over time. Surface floating oil, subsurface droplets, and dissolved components are tracked in separate spillets. Transport is the sum of advective velocities by currents input to the model, surface wind drift, vertical movement according to buoyancy, and randomized turbulent diffusive velocities in three dimensions. The vertical diffusion coefficient is computed as a function of wind speed in the surface wave-mixed layer. The horizontal and deeper water vertical diffusion coefficients are model inputs.

The oil (whole and as pseudo-components) separates into different phases or parts of the environment, i.e., surface slicks; emulsified oil (mousse) and tar balls; oil droplets suspended in the water column; dissolved lower molecular weight components (MAHs and PAHs) in the water column; oil droplets adhered and hydrocarbons adsorbed to suspended particulate matter in the water; hydrocarbons on and in the sediments; dissolved MAHs and PAHs in the sediment pore water; and hydrocarbons on and in the shoreline sediments and surfaces.

1.3 Oil Fates Algorithms

1.3.1 Transport

Lagrangian particles (spillets) are moved in three dimensions over time. For each model time step, the new vector position of the spillet center is calculated from the old plus the vector sum of east-west, north-south, and vertical components of advective and diffusive velocities:

$$X_t = X_{t-1} + \Delta t \, (U_t + D_t + R_t + W_t)$$

where X_t is the vector position at time t, X_{t-1} is the vector position the previous time step, Δt is the time step, U_t is the sum of all the advective (current) velocity components in three dimensions at time t, D_t is the sum of the randomized diffusive velocities in three dimensions at time t, R_t is the rise or sinking velocity of whole oil droplets in the water column, and W_t is the surface wind transport (“wind drift”). The magnitudes of the components of D_t are scaled by horizontal and vertical diffusion coefficients (Okubo and Ozmidov, 1970; Okubo, 1971). The vertical diffusion coefficient is computed as a function of wind speed in the surface wave-mixed layer (which ranges from centimeter scales in rivers and near lee shorelines to potentially meters in large water bodies away from shore when wind speeds are high), based on Thorpe (1984). R_t is computed by Stokes law, where velocity is related to the difference in density between the particle and the water, and to the particle diameter. The algorithm developed by Youssef and Spaulding (1993) is used for wind transport in the surface wave-mixed layer (W_t, described below).

1.3.2 Shoreline Stranding

The fate of spilled oil that reaches the shoreline depends on characteristics of the oil, the type of shoreline, and the energy environment. The stranding algorithm is based on work by CSE/ASA/BAT (1986), Gundlach (1987), and Reed and Gundlach (1989) in developing the COZOIL model for the U.S. Minerals Management Service. In SIMAP, deposition occurs when an oil spillet intersects shore surface. Deposition ceases when the volume holding capacity for the shore surface is reached. Subsequent oil coming ashore is not allowed to remain on the shore

surface. It is refloated by rising water, and carried away by currents and wind drift. The remaining shoreline oil is then removed exponentially with time. Data for holding capacity and removal rate are taken from CSE/ABA/BAT (1986) and Gundlach (1987), and are a function of oil viscosity and shore type. The algorithm and data are in French et al. (1996a).

1.3.3 Spreading

Spreading determines the areal extent of the surface oil, which in turn influences its rates of evaporation, dissolution, dispersion (entrainment) and photo-oxidation, all of which are functions of surface area. Spreading results from the balance among the forces of gravity, inertia, viscosity, and surface tension (which increases the diameter of each spillet); turbulent diffusion (which spreads the spillets apart); and entrainment followed by resurfacing, which can spatially separate the leading edge of the oil from resurfaced oil transported in a different direction by subsurface currents.

For many years Fay's (1971) three-regime spreading theory was widely used in oil spill models (ASCE, 1996). Mackay et al. (1980; 1982) modified Fay's approach and described the oil as thin and thick slicks. Their approach used an empirical formulation based on Fay's (1971) terminal spreading behavior. They assumed the thick slick feeds the thin slick and that 80-90% of the total slick area is represented by the thin slick. In SIMAP, oil spillets on the water surface increase in diameter according to the spreading algorithm empirically-derived by Mackay et al. (1980; 1982). Sensitivity analyses of this algorithm led to the discovery that the solution was affected by the number of spillets used. Thus, a formulation was derived to normalize the solution under differing numbers of surface spillets (Kolluru et al., 1994). Spreading is stopped when an oil-specific terminal thickness is reached.

1.3.4 Evaporation

The rate of evaporation depends on surface area, thickness, vapor pressure and mass transport coefficient, which in turn are functions of the composition of the oil, wind speed and temperature (Fingas, 1996; 1997; 1998; 1999; Jones, 1997). As oil evaporates its composition changes, affecting its density and viscosity as well as subsequent evaporation. The most volatile hydrocarbons evaporate most rapidly, typically in less than a day and sometimes in under an hour (McAuliffe, 1989). As the oil continues to weather, and particularly if it forms a water-in-oil emulsion, evaporation will be significantly decreased.

The evaporation algorithm in SIMAP is based on accepted evaporation theory, which follows Raoult’s Law that each component will evaporate with a rate proportional to the saturation vapor pressure and mole fraction present for that component. The pseudo-component approach (Payne et al., 1984; French et al., 1996a; Jones, 1997; Lehr et al., 2000) is used, such that each component evaporates according to its mean vapor pressure, solubility, and molecular weight (Table 2-3). The mass transfer coefficient is calculated using the methodology of Mackay and Matsugu (1973), as described in French et al. (1996a).

1.3.5 Entrainment

As oil on the water surface is exposed to wind and waves, or if oil moves into a turbulent area of a stream or river, it is entrained (or dispersed) into the water column. Entrainment is a physical process where globules of oil are transported from the water surface into the water column due to breaking waves or other turbulence. It has been observed that entrained oil is broken into droplets of varying sizes. Smaller droplets spread and diffuse in the water column, while larger ones rise back to the surface.

Entrainment by Breaking Surface Wave Action

In open waters, breaking waves created by the action of wind and waves on the water surface are the primary sources of energy for entrainment. Entrainment is strongly dependant on turbulence and is greater in areas of high wave energy (Delvigne and Sweeney, 1988).

Delvigne and Sweeney (1988), using laboratory and flume experimental observations, developed a relationship for entrainment rate and oil droplet size distribution as a function of turbulent energy level and oil viscosity. Entrained droplets in the water column rise according to Stokes law, where velocity is related to the difference in density between the particle and the water, and to the particle diameter. The data and relationships in Delvigne and Sweeney (1988) are used in SIMAP to calculate mass and particle size distribution of droplets entrained. Particle size decreases with higher turbulent energy level and lower oil viscosity. The natural dispersion particle sizes observed by Delvigne and Sweeney (1988) are confirmed by field observations by Lunel (1993a,b).

Use of chemical dispersants (not modelled in the scenarios examined here) decrease the median particle size, increasing the number of droplets in the <70 µm range (Daling et al., 1990; Lunel, 1993a,b). Particle size distributions for dispersed oil are available for several oils from these studies. When dispersant is applied, the model entrains surface oil, creating subsurface droplets in the appropriate size distribution for dispersant use. The median particle size for permanently dispersed droplets is set at 20 microns, the median size observed by Lunel (1993a,b). The fraction of oil permanently dispersed is set by the assumed dispersant efficiency. The IKU/SINTEF studies provide data on the viscosity range where oils may be dispersed chemically. Typically, dispersants are effective up to about 10,000 cP (Aamo et al., 1993; Daling and Brandvik, 1988; 1991; Daling et al., 1997). In the model, oil is dispersed up to 10,000 cP.

Entrained oil is well mixed in (i.e., mixed uniformly throughout) the wave-mixed zone. Vertical mixing is simulated by random placement of particles within the wave-mixed layer each time step. Settling of particles does not occur in water depths where waves reach the bottom (taken as 1.5 times wave height). Wave height is calculated from wind speed, duration and fetch (distance upwind to land), using the algorithms in CERC (1984). Wave height is on the scale of centimetres in small rivers and streams, and near lee shorelines; whereas it may increase to metres in open waters under windy conditions.

1.3.6 Emulsification (Mousse Formation)

The formation of water-in-oil emulsions, or mousse, depends on oil composition and turbulence level. Emulsified oil can contain as much as 80% water in the form of micrometre-sized droplets dispersed within a continuous phase of oil (Daling and Brandvik, 1988; Fingas et al., 1997). Viscosities are typically much higher than that of the parent oil. The incorporation of water also dramatically increases the oil/water mixture volume.

The Mackay and Zagorski (1982) emulsification scheme is implemented in SIMAP for floating oil. Water content increases exponentially, with the rate related to the square of wind speed and previous water incorporation. Viscosity is a function of water content. The change in viscosity feeds back in the model to the entrainment rate.

1.3.7 Dissolution

Dissolution is the process by which soluble hydrocarbons enter the water from a surface slick or from entrained oil droplets. The lower molecular weight hydrocarbons tend to be both more volatile and more soluble than those of higher molecular weight. For surface slicks, since the partial pressures tend to exceed the solubilities of these lower molecular weight compounds, evaporation accounts for a larger portion of the mass than dissolution (McAuliffe, 1989), except perhaps under ice. Dissolution and evaporation are competitive processes. The dissolved component concentration of hydrocarbons in water under a surface slick shows an initial increase followed by a rapid decrease after some hours due to the evaporative loss of components. Most soluble components are also volatile and direct evaporation (volatilization) from the water column depletes their concentrations in the water. Dissolution is particularly important where evaporation is low (dispersed oil droplets and ice-covered surfaces). Dissolution can be significant from entrained droplets because of the lack of atmospheric exposure and because of the higher surface area per unit of volume.

The model developed by Mackay and Leinonen (1977) is used in SIMAP for dissolution from a surface slick. The slick (spillet) is treated as a flat plate, with a mass flux (Hines and Maddox, 1985) related to solubility and

temperature. It assumes a well-mixed layer with most of the resistance to mass transfer lying in a hypothetical stagnant region close to the oil. For subsurface oil, dissolution is treated as a mass flux across the surface area of a droplet (treated as a sphere) in a calculation analogous to the Mackay and Leinonen (1977) algorithm. The dissolution algorithm was developed in French et al. (1996a).

1.3.8 Volatilization from the Water column

The procedure outlined by Lyman et al. (1982), based on Henry's Law and mass flux (Hines and Maddox, 1985), is followed in the SIMAP fates model. The volatilization depth for dissolved substances is limited to the maximum of one half the wave height. Wave height is computed from the wind speed and fetch (CERC, 1984). The volatilization algorithm was developed in French et al. (1996a).

1.3.9 Adsorption and Sedimentation

Aromatics dissolved in the water column are carried to the sediments primarily by adsorption to suspended particulates, and subsequent settling. The ratio of adsorbed (C_a) to dissolved (C_{dis}) concentrations is computed from standard equilibrium partitioning theory as

$$C_a / C_{dis} = K_{oc} C_{ss}$$

K_{oc} is a dimensionless partition coefficient and C_{ss} is the concentration of suspended particulate matter (SPM) in the water column expressed as mass of particulate per volume of water. As a default, the model uses a mean value of total suspended solids of 10 mg/l (Kullenberg, 1982); alternatively, suspended sediment concentration is specified as model input.

Sedimentation of oil droplets occurs when the specific gravity of oil increases over that of the surrounding water. Several processes may act on entrained oil and surface slicks to increase density: weathering (evaporation, dissolution and emulsification), adhesion or sorption onto suspended particles or detrital material, and incorporation of sediment into oil during interaction with suspended particulates, bottom sediments, and shorelines. Rates of sedimentation depend on the concentration of suspended particulates and the rates of particulate flux into and out of an area. In areas with high suspended particulate concentrations, rapid dispersal and removal of oil is found due to sorption and adhesion (Payne and McNabb, 1984).

Kirstein et al. (1987) and Payne et al. (1987) used a reaction term to characterize the water column interactions of oil and suspended particulates. The reaction term represents the collision of oil droplets and suspended matter, and both oiled and unoiled particulates are accounted for. The model formulation developed by Kirstein et al. (1987) is used to calculate the volume of oil adhered to particles. In the case where the oil mass is larger than the adhered sediment (i.e., the sediment has been incorporated into the oil) the buoyancy of the oil droplet will control its settling or rise rate. The Stoke's law formulation is used to adjust vertical position of these particles. If the mass of adhered droplets is small relative to the mass of the sediment it has adhered to, the sediment settling velocity will control the fate of the combined particulate.

1.3.10 Degradation

Degradation may occur as the result of photolysis, which is a chemical process energized by ultraviolet light from the sun, and by biological (bacterial) breakdown, termed biodegradation. In the model, degradation occurs on the surface slick, deposited oil on the shore, the entrained oil and aromatics in the water column, and oil in the sediments. A first order decay algorithm is used, with a specified (total) degradation rate for each of surface oil, water column oil and sedimented oil (French et al., 1999).

1.4 Habitat Type

Ecological habitat types (**Error! Reference source not found.**) are broadly categorized into two zones within SIMAP: shoreline and submerged (or intertidal versus subtidal in estuarine and marine areas, where intertidal habitats are those above spring low water tide level, with subtidal being all water areas below that level). In modelled scenarios, the shoreline habitats may become oiled as surface oil makes contact with these cells. Submerged or subtidal cells are always underwater. Intertidal/shoreline areas may be extensive, such that they are wide enough to be represented by an entire grid cell at the resolution of the grid. These are typically either mud flats or wetlands, and are coded 20 (seaward mudflat), 21 (seaward wetland), 50 (landward mudflat), or 51 (landward wetland). All other intertidal/shoreline habitats are typically much narrower than the size of a grid cell. Thus, these fringing intertidal/shore types (indicated by F in **Error! Reference source not found.**) have typical (for the region, e.g., French et al., 1996a for estuarine and marine areas) widths associated with them in the model. Boundaries between land and water are fringing habitat types. On the waterside of fringing grid cells, there may be extensive intertidal/shoreline grid cells if the wetlands or mudflats are extensive. Otherwise, subtidal/submerged habitats border the fringing cells.

Table 2. Classification of habitats. seaward (Sw) and landward (Lw) system codes are listed. (fringing types indicated by (F) are only as wide as the intertidal zone or shoreline width where oiling might occur. Others (W = water) are a full grid cell.

Habitat Code (Sw,Lw)	Ecological Habitat	F or W
	Intertidal / Shore	
1,31	Rocky Shore	F
2,32	Gravel Shore	F
3,33	Sand Beach or Shore	F
4,34	Fringing Mud Flat	F
5,35	Fringing Wetland (Emergent or Forested)	F
6,36	Macroalgal Bed	F
7,37	Mollusk Reef	F
8,38	Coral Reef (marine only)	F
	Subtidal / Submerged	
9,39	Rock Bottom	W
10,40	Gravel Bottom	W
11,41	Sand Bottom	W
12,42	Silt-mud Bottom	W
13,43	Wetland (submerged areas)	W
14,44	Macroalgal Bed	W
15,45	Mollusk Reef	W
16,46	Coral Reef (marine only)	W
17,47	Submerged Aquatic Vegetation Bed	W
Intertidal / Shore		
18,48	Man-made, Artificial	F
19,49	Ice Edge	F
20,50	Extensive Mud Flat	W
21,51	Extensive Wetland (Emergent or Forested)	W

1.5 References

Aamo, O.M., M. Reed and P. Daling, 1993. A laboratory based weathering model: PC version for coupling to transport models. In Proceedings of the 16th Arctic and Marine Oil Spill Program (AMOP) Technical Seminar, Environmental Protection Service, Emergencies Science Division, Environment Canada, Ottawa, ON, Canada, pp. 617-626.

ASCE Task Committee on Modeling Oil Spills, 1996. State-of-the-art Review of Modeling Transport and Fate of Oil Spills, Water Resources Engineering Division, ASCE, Journal of Hydraulic Engineering 122(11): 594-609.

Coastal Engineering Research Center (CERC), 1984. Shore Protection Manual, Vol. I. Coastal Engineering Research Center, Department of the Army, Waterways Experiment Station, U.S. Army Corps of Engineers, Vicksburg, Mississippi, 1,105p. plus 134p. in appendices.

CSE/ASA/BAT, 1986. Development of a Coastal Oil Spill Smear Model. Phase 1: Analysis of Available and Proposed Models, Prepared for Minerals Management Service by Coastal Science & Engineering, Inc. (CSE) with Applied Science Associates, Inc. (ASA) and Battelle New England Research Laboratory (BAT), 121p.

Daling, P.S. and P.J. Brandvik, 1988. A Study of the Formation and Stability of Water-in-Oil Emulsions. In Proceedings of the 11th Arctic and Marine Oil Spill Program Technical Seminar. Emergencies Science Division, Environment Canada, Ottawa, ON, Canada, pp.153-170.

Daling, P.S., D. Mackay, N. Mackay, and P.J. Brandvik, 1990. Droplet size distributions in chemical dispersion of oil spills: Towards a mathematical model. Oil and Chemical Pollution 7: 173-198.

Daling, P.S. and P.J. Brandvik, 1991. Characterization and prediction of the weathering properties of oils at sea – A manual for the oils investigated in the DIWO project. IKU SINTEF Group report 91.037, DIWO report no. 16 02.0786.00/16/91, 29 May 1991, 140p.

Daling, P.S., O.M. Aamo, A. Lewis, and T. Strom-Kritiansen, 1997. SINTEF/IKU Oil-Weathering Model: Predicting Oil's Properties at Sea. In Proceedings 1997 Oil Spill Conference, Publication No. 4651, American Petroleum Institute, Washington, D.C., pp. 297-307.

Daling, P.S. A.Lewis, S. Ramstad. 1999. The use of colour as a guide to oil film thickness – Main report. SINTEF Report STF66 F99082. 48p., SINTEF, Trondheim, Norway.

Delvigne, G.A.L. and C.E. Sweeney, 1988. Natural Dispersion of Oil. Oil and Chemical Pollution 4: 281-310.

Di Toro, D.M., J.A. McGrath and D.J. Hansen, 2000. Technical basis for narcotic chemicals and polycyclic aromatic hydrocarbon criteria. I. Water and tissue. Environmental Toxicology and Chemistry 19(8): 1951-1970.

Fay, J.A., 1971. Physical processes in the spread of oil on a water surface. In Proceedings, Conference on Prevention and Control of Oil Spills, sponsored by API, EPA, and US Coast Guard, American Petroleum Institute, Washington, D.C., June 15-17, 1971, pp. 463-467.

Fingas, M., 1996. The Evaporation of Crude Oil and Petroleum Products. PhD Dissertation, McGill University, Montreal, Canada, 181p.

Fingas, M., B. Fieldhouse, and J.V. Mullin, 1997. Studies of Water-in-Oil Emulsions: Stability Studies. In Proceedings of 20th Arctic and Marine Oil Spill Program (AMOP) Technical Seminar, Emergencies Science Division, Environment Canada, Ottawa, ON, Canada, pp. 21-42.

Fingas, M., 1997. The Evaporation of Oil Spills: Prediction of Equations Using Distillation Data. In Proceedings of the 20th Arctic and Marine Oil Spill Program (AMOP) Technical Seminar, Emergencies Science Division, Environment Canada, Ottawa, ON, Canada, pp. 1-20.

Fingas, M.F., 1998. Studies on the Evaporation of Crude Oil and Petroleum Products: II. Boundary Layer Regulation. Journal of Hazardous Materials, Vol. 57, pp.41-58.

Fingas, M.F., 1999. The Evaporation of Oil Spills: Development and Implementation of New Prediction Methodology. In Proceedings of the 1999 International Oil Spill Conference, American Petroleum Institute, Washington, D.C., pp. 281-287.

Fingas, M., B. Fieldhouse, and J.V. Mullin, 1997. Studies of Water-in-Oil Emulsions: Stability Studies. In: Proceedings of 20th Arctic and Marine Oil Spill Program (AMOP) Technical Seminar, Emergencies Science Division, Environment Canada, Ottawa, ON, Canada, pp. 21-42.

French, D., M. Reed, K. Jayko, S. Feng, H. Rines, S. Pavignano, T. Isaji, S. Puckett, A. Keller, F. W. French III, D. Gifford, J. McCue, G. Brown, E. MacDonald, J. Quirk, S. Natzke, R. Bishop, M. Welsh, M. Phillips and B.S. Ingram, 1996a. The CERCLA type A natural resource damage assessment model for coastal and marine environments (NRDAM/CME), Technical Documentation, Vol. I - Model Description. Final Report, submitted to the Office of Environmental Policy and Compliance, U.S. Dept. of the Interior, Washington, DC, April, 1996, Contract No. 14-0001-91-C-11.

French, D., M. Reed, S. Feng and S. Pavignano, 1996b. The CERCLA type A natural resource damage assessment model for coastal and marine environments (NRDAM/CME), Technical Documentation, Vol. III - Chemical and Environmental Databases. Final Report, Submitted to the Office of Environmental Policy and Compliance, U.S. Dept. of the Interior, Washington, DC, April, 1996, Contract No. 14-01-0001-91-C-11.

French, D., S. Pavignano, H. Rines, A. Keller, F.W. French III and D. Gifford, 1996c. The CERCLA type A natural resource damage assessment model for coastal and marine environments (NRDAM/CME), Technical Documentation, Vol.IV - Biological Databases. Final Report, Submitted to the Office of Environmental Policy and Compliance, U.S. Dept. of the Interior, Washington, DC, April, 1996, Contract No. 14-01-0001-91-C-11.

French, D.P. and H. Rines, 1997. Validation and use of spill impact modeling for impact assessment. Proceedings, 1997 International Oil Spill Conference, Fort Lauderdale, Florida, American Petroleum Institute Publication No. 4651, Washington, DC, pp-829-834.

French, D.P., H. Rines and P. Masciangioli, 1997. Validation of an Orimulsion spill fates model using observations from field test spills. Proceedings, Twentieth Arctic and Marine Oil Spill Program Technical Seminar, Vancouver, Canada, June 10-13, 1997.

French, D., H. Schuttenberg, and T. Isaji, 1999. Probabilities of Oil Exceeding Thresholds of Concern: Examples from an Evaluation for Florida Power and Light. In Proceedings of the 22nd Arctic and Marine Oil Spill Program (AMOP) Technical Seminar, June 2-4, 1999, Calgary, Alberta, Environment Canada, pp.243-270.

French McCay, D. and J.R. Payne, 2001. Model of Oil Fate and Water concentrations with and without application of dispersants. In Proceedings of the 24th Arctic and Marine Oil Spill Program (AMOP) Technical Seminar, Emergencies Science Division, Environment Canada, Ottawa, ON, Canada, pp. 601-653.

French McCay, D.P., 2002. Development and Application of an Oil Toxicity and Exposure Model, OilToxEx. Environmental Toxicology and Chemistry 21(10): 2080-2094.

French McCay, D.P., 2003. Development and Application of Damage Assessment Modeling: Example Assessment for the North Cape Oil Spill. Marine Pollution Bulletin, Volume 47, Issues 9-12, September-December 2003, pp. 341-359.

French McCay, D.P., 2004. Oil spill impact modeling: Development and validation. Environmental Toxicology and Chemistry 23(10): 2441-2456.

French McCay, D.P., and J.J. Rowe, 2004. Evaluation of Bird Impacts in Historical Oil Spill Cases Using the SIMAP Oil Spill Model. In Proceedings of the 27th Arctic and Marine Oil Spill Program (AMOP) Technical Seminar, Emergencies Science Division, Environment Canada, Ottawa, ON, Canada, pp. 421-452.

Gundlach, E.R., 1987. Oil Holding Capacities and Removal Coefficients for Different Shoreline Types to Computer Simulate Spills in Coastal Waters. In Proceedings of the 1987 Oil Spill Conference, pp. 451-457.

Hines, A.L. and R.N. Maddox, 1985. Mass Transfer Fundamentals and Application. Prentice-Hall, Inc., Englewood Cliffs, New Jersey, 542p.

Jones, R.K., 1997. A Simplified Pseudo-Component of Oil Evaporation Model. In Proceedings of the 20th Arctic and Marine Oil Spill Program (AMOP) Technical Seminar, Environment Canada, pp. 43-61.

Kirstein, B.E., J.R. Clayton, C. Clary, J.R. Payne, D. McNabb, Jr., G. Fauna and R. Redding, 1987. Integration of Suspended Particulate Matter and Oil Transportation Study. Minerals Management Service, OCS Study MMS87-0083, Anchorage, Alaska, 216p.

Kolluru, V., M.L. Spaulding and E. Anderson, 1994. A three dimensional subsurface oil dispersion model using a particle based approach. In Proceedings of 17th Arctic and Marine Oil Spill Program (AMOP) Technical Seminar, Vancouver, British Columbia, June 8-10, 1994, Emergencies Science Division, Environment Canada, Ottawa, ON, Canada, pp. 867-893.

Kullenberg, G. (ed.), 1982. Pollutant transfer and transport in the sea. Volume I. CRC Press, Boca Raton, Florida. 227 p.

Lehr, W.J., D. Wesley, D. Simecek-Beatty, R. Jones, G. Kachook and J. Lankford, 2000. Algorithm and interface modifications of the NOAA oil spill behavior model. In Proceedings of the 23rd Arctic and Marine Oil Spill Program (AMOP) Technical Seminar, Vancouver, BC, Environmental Protection Service, Environment Canada, pp. 525-539.

Lunel, T., 1993a. Dispersion: Oil droplet size measurements at sea. In Proceedings of the 16th Arctic Marine Oilspill Program (AMOP) Technical Seminar, Environment Canada, Calgary, Alberta, June 7-9, 1993, pp. 1023-1056.

Lunel, T., 1993b. Dispersion: Oil droplet size measurements at sea. In Proceedings of the 1993 Oil Spill Conference, pp. 794-795.

Lyman, C.J., W.F. Reehl, and D.H. Rosenblatt, 1982. Handbook of Chemical Property Estimation Methods. McGraw-Hill Book Co., New York, 960p.

Mackay, D. and R.M. Matsugu, 1973. Evaporation rates of liquid hydrocarbon spills on land and water. Canadian Journal of Chemical Engineering 51: 434-439.

Mackay, D. and P.J. Leinonen, 1977. Mathematical model of the behavior of oil spills on water with natural and chemical dispersion. Prepared for Fisheries and Environment Canada. Economic and Technical Review Report EPS-3-EC-77-19, 39p.

Mackay, D., S. Paterson and K. Trudel, 1980. A mathematical model of oil spill behavior. Department of Chemical and Applied Chemistry, University of Toronto, Canada, 39p.

Mackay, D., and W. Zagorski, 1982. Water-In-Oil Emulsions. Environment Canada Manuscript Report EE-34, Ottawa, Ontario, Canada, 93p.

Mackay, D, W.Y. Shiu, K. Hossain, W. Stiver, D. McCurdy and S. Peterson, 1982. Development and calibration of an oil spill behavior model. Report No. CG-D-27-83, U.S. Coast Guard, Research and Development Center, Groton, Connecticut, 83p.

Mackay, D., W.Y. Shiu, and K.C. Ma, 1992. Illustrated Handbook of Physical-Chemical Properties and Environmental Fate for Organic Chemicals, Vol. I-IV. Lewis Publishers, Inc, Chelsea, Michigan.

McAuliffe, C.D., 1987. Organism exposure to volatile/soluble hydrocarbons from crude oil spills –a field and laboratory comparison. Proceedings of the 1987 Oil Spill Conference. Washington, D.C.: API. pp. 275-288.

McAuliffe, C.D., 1989. The Weathering of Volatile Hydrocarbons from Crude Oil Slicks on Water. In Proceedings of the 1989 Oil Spill Conference, San Antonio, Texas, American Petroleum Institute, Washington, D.C., pp. 357-364.

Okubo, A. and R.V. Ozmidov, 1970. Empirical dependence of the coefficient of horizontal turbulent diffusion in the ocean on the scale of the phenomenon in question. Atmospheric and Ocean Physics 6(5):534-536.

Okubo, A., 1971. Oceanic diffusion diagrams. Deep-Sea Research 8:789-802.

Payne, J.R. and G.D. McNabb Jr., 1984. Weathering of Petroleum in the Marine Environment. Marine Technology Society Journal 18(3):24-42.

Payne, J.R., B.E. Kirstein, G.D. McNabb, Jr., J.L. Lambach, R. Redding R.E. Jordan, W. Hom, C. deOliveria, G.S. Smith, D.M. Baxter, and R. Gaegel, 1984. Multivariate analysis of petroleum weathering in the marine environment – sub Arctic. Environmental Assessment of the Alaskan Continental Shelf, OCEAP, Final Report of Principal Investigators, Vol. 21 and 22, Feb. 1984, 690p.

Payne, J.R., B.E. Kirstein, J.R. Clayton, Jr., C. Clary, R. Redding, G.D. McNabb, Jr., and G. Farmer, 1987. Integration of suspended particulate matter and oil transportation study. Final Report. Minerals Management Service, Environmental Studies Branch, Anchorage, AK. Contract No. 14-12-0001-30146, 216 p.

Reed, M. and E. Gundlach, 1989. Hindcast of the *Amoco Cadiz* event with a coastal zone oil spill model. Oil and Chemical Pollution. Vol. 5. Iss. 6. Pp. 451-476.

Stiver, W. and D. Mackay, 1984. Evaporation rate of oil spills of hydrocarbons and petroleum mixtures. Environmental Science and Technology 18: 834-840.

Thorpe, S.A., 1984. On the Determination of K in the Near Surface Ocean from Acoustic Measurements of Bubbles. Journal of Physical Oceanography 14: 855-863.

Youssef, M. and M.L. Spaulding, 1993. Drift current under the action of wind waves, Proceedings of the 16th Arctic and Marine Oil Spill Program Technical Seminar, Calgary, Alberta, Canada, pp. 587-615.

1.6 References – SIMAP Example Applications and Validations

Copies of these papers can be provided by sending a request to matt.horn@rpsgroup.com and requesting one or more specific papers.

French, D.P., and H. Rines, 1997. Validation and use of spill impact modeling for impact assessment. In Proceedings, 1997 International Oil Spill Conference, Fort Lauderdale, Florida, American Petroleum Institute Publication No. 4651, Washington, DC, pp-829-834.

French, D. P., 1998a. Estimate of Injuries to Marine Communities Resulting from the North Cape Oil Spill Based on Modeling of Fates and Effects. Report to US Department of

14 Commerce, National Oceanic and Atmospheric Administration (NOAA), Damage Assessment Center, Silver Spring, MD, January 1998.

French, D. P., 1998b. Updated Estimate of Injuries to Marine Communities Resulting from the North Cape Oil Spill Based on Modeling of Fates and Effects. Report to US Department of Commerce, National Oceanic and Atmospheric Administration (NOAA), Damage Assessment Center, Silver Spring, MD, December 1998.

French, D.P., 1998c. Modeling the Impacts of the North Cape, p. 387-430.In Proceedings, 21st Arctic and Marine Oilspill Program (AMOP) Technical Seminar, June 10-12, 1998, West Edmonton Mall Hotel Edmonton, Alberta, Canada, Emergencies Science Division, Environment Canada, Ottawa, ON, Canada.

French McCay, D. and James R. Payne, 2001.Model of Oil Fate and Water concentrations with and with out application of dispersants. In Proceedings of the 2001 24th Arctic and Marine Oil spill Program (AMOP) Technical Seminar, June 12-14, 2001, Environment Canada, pp.611-645.

French, D. P., Jones, M. A., and Coakley, L., 2001. Use of Oil Spill Modeling for Contingency Planning and Impact Assessment: Application for Florida Power and Light. In Proceedings of the 2001 International Oil Spill Conference & Exposition, American Petroleum Institute, March 26-29, 2001, Tampa, Florida.

French, D.P. and H. Schuttenberg, 1999.Evaluation of net environmental benefit using fates and effects modeling. Paper ID #321. In Proceedings, 1999 International Oil Spill Conference, American Petroleum Institute.

French McCay, D. 2002. Modeling Evaluation of Water Concentrations and Impacts Resulting from Oil Spills With and Without the Application of Dispersants. International Marine Environmental Seminar 2001, Journal of Marine Systems, Special Issue 2002.

French McCay, D., N. Whittier, S. Sankaranarayanan, J. Jennings, and D. S. Etkin, 2002.Modeling Fates and Impacts for Bio-Economic Analysis of Hypothetical Oil Spill Scenarios in San Francisco Bay. In Proceedings of the Twenty Fifth Arctic and Marine Oil Spill Program (AMOP) Technical Seminar, Environment Canada, Calgary, AB, Canada, 2002, p. 1051-1074.

French McCay, D., N. Whittier, T. Isaji, and W.Saunders, 2003. Assessment of the Potential Impacts of Oil Spills in the James River, Virginia. In Proceedings of the 26th Arctic and Marine Oil Spill Program (AMOP) Technical Seminar, Emergencies Science Division, Environment Canada, Ottawa, ON, Canada, p. 857-878.

French McCay, D., N. Whittier, S. Sankaranarayanan, J. Jennings, and D. S. Etkin, 2003.Estimation of Potential Impacts and Natural Resource Damages of Oil. J. Hazardous Materials (in press).

French McCay, D. and N. Whittier, 2003.Modeling Assessment of Potential Fates and Exposure for Orimulsion and Heavy Fuel Oil Spills. In: Proceedings, International Oil Spill Conference, April 2003, Paper 157, American Petroleum Institute, Washington, DC.

French McCay, D.P., 2003. Development and Application of Damage Assessment Modeling: Example Assessment for the North Cape Oil Spill. Marine Pollution Bulletin, Volume 47, Issues 9-12, September-December 2003, pp. 341-359.

French McCay, D.P., and J.J. Rowe, 2004.Evaluation of Bird Impacts in Historical Oil Spill Cases Using the SIMAP Oil Spill Model. In Proceedings of the 27th Arctic and Marine Oil Spill Program (AMOP) Technical Seminar, Emergencies Science Division, Environment Canada, Ottawa, ON, Canada, pp. 421-452.

French-McCay, D.P., J.J. Rowe, N. Whittier, S. Sankaranarayanan, D. S. Etkin, and L. Pilkey- Jarvis, 2005. Evaluation of the Consequences of Various Response Options Using Modeling of Fate, Effects and NRDA Costs of Oil Spills into Washington Waters. In: Proceedings, International Oil Spill Conference, May 2005, Paper 395, American Petroleum Institute, Washington, DC.

French-McCay, D.P., N. Whittier, C. Dalton, J.J. Rowe, and S. Sankaranarayanan, 2005.Modeling fates and impacts of hypothetical oil spills in Delaware, Florida, Texas, California, and Alaska waters, varying response options including use of dispersants. In: Proceedings, International Oil Spill Conference, May 2005, Paper 399, American Petroleum Institute, Washington, DC.

French McCay, D., N. Whittier, J.J. Rowe, S. Sankaranarayanan and H.-S.Kim, 2005. Use of Probabilistic Trajectory and Impact Modeling to Assess Consequences of Oil Spills with Various Response Strategies. In Proceedings of the 28th Arctic and Marine Oil Spill Program (AMOP) Technical Seminar, Emergencies Science Division, Environment Canada, Ottawa, ON, Canada, pp. 253-271, 2005.

French-McCay, D.P., M. Horn, Z. Li, K. Jayko, M. Spaulding, D. Crowley, and D. Mendelsohn. 2017. Modeling Distribution, Fate, and Concentrations of Deepwater Horizon Oil in Subsurface Waters of the Gulf of Mexico. In: S.A. Stout and Z. Wang (eds.) Case Studies in Oil Spill Environmental Forensics. Elsevier.

2 OILMAP DEEP MODEL DESCRIPTION

OILMAP Deep was used to characterize the near field blowout conditions for use in the SIMAP model, which characterized the far field effects. OILMAP Deep contains two sub-models, a plume model and a droplet size model. The plume model predicts the evolution of plume position, geometry, centerline velocity, and oil and gas concentrations until the plume either surfaces or reaches a terminal height at which point the plume is trapped (Figure 3). The droplet model predicts the size and volume (mass) distribution of the oil droplets. Provided below is an overview of blowout theory and modelling implementation.

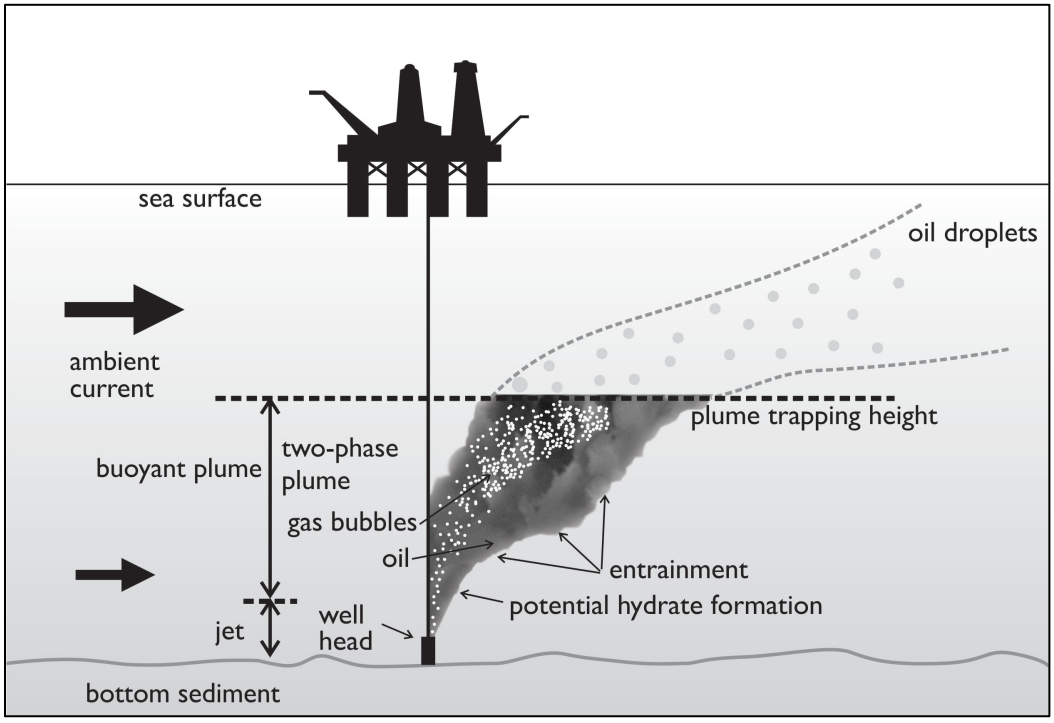

Figure 3. Modelled processes for a subsea blowout in OILMAP Deep.

2.1 Blowout Model Theory

RPS' oil blowout model is based on the work of McDougall (gas plume model, 1978), Fanneløp and Sjøen (1980a, plume/free surface interaction), Spaulding (1982, oil concentration model), Kolluru, (1994, World Oil Spill Model implementation), Spaulding et.al. (2000, hydrate formation) and Zheng et.al. (2002, 2003, gas dissolution). A simplified integral jet theory is employed for the vertical as well as for the horizontal motions of the gas-oil plume. The necessary model parameters defining the rates of entrainment and spreading of the jet are obtained from laboratory studies (Fanneløp and Sjøen 1980a). The gas plume analysis is described in McDougall (1978), Spaulding (1982), and Fanneløp and Sjøen (1980a). The hydrate formation and dissociation is formulated based on a unique equilibrium kinetics model developed by R. Bishnoi and colleagues at the University of Calgary. A brief description of the governing equations used in RPS ASA's blowout model and the solution methodology are described in Spaulding et al., 2000. The core components of this model are conservation of water mass, conservation of oil mass, conservation of momentum, and conservation of buoyancy.

Oil droplet size distribution calculations are based on the methodology presented by Yapa and Zheng (2001a&b) and Chen and Yapa (2007), which uses a maximum diameter calculation and the associated volumetric droplet size distribution. The maximum diameter can is determined using Hinze (1955) and coefficients consistent with Chen and Yapa (2007). The droplet size distribution is defined using a Rosin-Rammler (1933) function.

2.2 Blowout Model Implementation

The results of the near-field blowout model provide information to the far field fates model about the plume (the three-dimensional extent of the mixture of gas/oil/water) and characterization of the initial dispersion/mixing of the oil discharged during the blowout. Key factors in this analysis are the volume flux of oil and gas, gas to oil ratio (GOR), depth, exit flow velocity and environmental water column conditions (the profile of water temperature and density), which affect both the trap height and the potential for hydrate formation. Other factors such as duration of the blowout and ambient currents are also included but are less important.

The OILMAP Deep blowout model implementation is done in two parts; the first is the plume model described in the previous section, based on the McDougall bubble plume model; the second is the oil droplet size distribution and volume fraction calculation. Both are based on the same scenario blowout specifications (e.g., oil type and flow rate, gas oil ratio and depth), but the model predictions are treated separately and do not interact. The two parts of the model predictions only come together at the collapse of the near field plume, at the trap height, where the depth and droplet distribution predictions are used for initialization of the far field particle model simulation.

The blowout plume model solves equations for conservation of water mass, momentum, buoyancy, and gas mass as described in Section 2.1 of the OILMAP Deep Technical Documentation, using integral plume theory. An additional equation for the conservation of oil at the plume centerline is also solved.

The plume model prediction is defined externally by a small set of parameters including:

- Blowout release depth
- Oil discharge rate
- Oil density
- Gas: oil ratio (GOR) at the surface
- Atmospheric pressure
- Ambient seawater density profile
- Plume spreading coefficient
- Entrainment parameter (α)
- Slip velocity of gas bubbles in the oil plume
- Ambient current velocity
- Water column profile of temperature and density

The blowout plume models the evolution of the plume within the water column, solving for the position, radius, velocity and oil and gas concentrations along the centerline. The blowout droplet model solves for the distribution of mass within droplet sizes associated with the turbulence of the release. Typically, the near-field model is on the timescale of seconds and length scale of hundreds of meters, where the far-field model is on the scales of hours/days and kilometers. The details of the near field modelling that are passed along to the far field model include the distribution of the release mass in different droplet sizes at the appropriate initial position in the water column.

2.3 References

Chen, F.H. and P.D. Yapa. 2007. Estimating the Oil Droplet Size Distributions in Deepwater Oil Spills. Journal of Hydraulic Engineering, Vol. 133, No. 2, pp. 197-207.

Fanneløp, T.K. and K. Sjoen , 1980a. Hydrodynamics of underwater blowouts, AIAA 8th Aerospace Sciences Meeting, January 14-16, Pasadena, California, AIAA paper, pp. 80- 0219.

Fanneløp, T. K. and K. Sjoen, 1980b. Hydrodynamics of underwater blowouts, Norwegian Maritime Research, No. 4, pp. 17-33.

Hinze, J. O. 1955 Fundamentals of the hydrodynamics mechanisms of splitting in dispersion process. AIChE J. 1, 289–295.

Kolluru, V., M.L. Spaulding and E. Anderson, 1994. A three dimensional subsurface oil dispersion model using a particle based approach. In Proceedings of 17th Arctic and Marine Oil Spill Program (AMOP) Technical Seminar, Vancouver, British Columbia, June 8-10, 1994, Emergencies Science Division, Environment Canada, Ottawa, ON, Canada, pp. 867-893.

McDougall, T.J., 1978. Bubble plumes in stratified environments, Journal of Fluid Mechanics, Vol. 85, Part 4, pp. 655-672.

Rosin, P. and E. Rammler, 1933. The Laws Governing the Fineness of Powdered Coal, Journal of the Institute of Fuel 7: 29–36Seo, I.W. and K.O. Baek, 2004. Estimation of the Longitudinal Dispersion Coefficient Using the Velocity Profile in Natural Streams. Journal of Hydraulic Engineering. March 2004.

Spaulding, M.L., 1982. User's manual for a simple gas blowout plume model, Continental Shelf Institute, Trondheim, Norway.

Spaulding, M.L., 1984. A vertically averaged circulation model using boundary-fitted coordinates. Journal of Physical Oceanography 14: 973-982.

Spaulding, M.L., P.R. Bishnoi, E. Anderson, and T. Isaji, 2000, An Integrated Model for Prediction of Oil Transport from a Deep Water Blowout.

Yapa, P. D., Zheng, L., and Chen, F. H. 2001a. A model for deepwater oil/gas blowouts. Mar. Pollution Bull., 43, 234–241.

Yapa, P. D., Zheng, L., and Chen, F. H. 2001b. Clarkson deepwater oil & gas ~CDOG model. Rep. No. 01–10, Dept. of Civil and Environmental Engineering, Clarkson Univ., Potsdam, N.Y.

Zheng, L. and Yapa, P.D., 2002. Modelling Gas Dissolution in Deepwater Oil/Gas Spills, Journal of Marine Systems, Elsevier, the Netherlands, March, 299-309

Zheng, L., Yapa, P.D. and Chen, F.H., 2003. A Model for Simulating Deepwater Oil and Gas Blowouts - Part I: Theory and Model Formulation, Journal of Hydraulic Research, IAHR, August, Vol. 41(4), 339-351